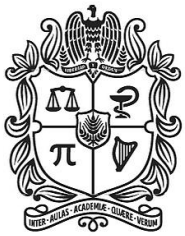

UNIVERSIDAD
NACIONAL
DE COLOMBIA

New Analogs of Tariquidar: Synthesis, Characterization and Evaluation of their Inhibitory Activity against Breast Cancer Resistance Protein (ABCG2)

Diana Catherine Peña Solórzano

Universidad Nacional de Colombia

Facultad de Ciencias

Departamento de Química

Bogotá, Colombia

2016

New Analogs of Tariquidar: Synthesis, Characterization and Evaluation of their Inhibitory Activity against Breast Cancer Resistance Protein (ABCG2)

Diana Catherine Peña Solórzano

Thesis presented as partial fulfillment of the requirement for the degree of:

Doctor en Ciencias-Química

PhD Advisor:

Dr. rer. nat. Cristian Ochoa Puentes

Macromolecules Research Group

Universidad Nacional de Colombia

Facultad de Ciencias

Departamento de Química

Bogotá, Colombia

2016

New Analogs of Tariquidar: Synthesis, Characterization and Evaluation of their Inhibitory Activity against Breast Cancer Resistance Protein (ABCG2)

Diana Catherine Peña Solórzano

Thesis presented as partial fulfillment of the requirement for the degree of:
Doktor der Naturwissenschaften (Dr. rer. nat.)

PhD Advisor (Cotutelle):
Prof. Dr. Burkhard König

Regensburg University
Faculty of Chemistry and Pharmacy
Institute of Organic Chemistry
Regensburg, Germany
2016

Dedicated to Ludi,

Carlos, Dres

Acknowledgements

I would like to express my sincere gratitude

- My research supervisor Prof. Dr. Cristian Ochoa Puentes for the guidance and assistance
- Prof. Dr. Cesar Sierra for his help and support
- Prof. Dr. Burkhard König for his support, and for give the opportunity to know another world
- Financial support COLCIENCIAS
- Prof. Dr. Armin Buschauer and Matthias Scholler for his help with the biological investigations
- All members of the Macromolecules Research Group for their support, Meli, Brian, JC, Sandra, William, Camilo, Lau, Tats, Pipe, Karen, Lorena, Pacos, Fredy, Yeimy
- All members of the König-group for their help, ideas and support, especially Simone and Manuel
- All my friends in Germany, specially Leyre, Ada, Riz, Yeimy for making my stay in Regensburg wonderful and exciting
- My parents Carlos and Ludivia who support and accompany with me any time through all of my study
- My brother for his help, constant motivation, friendship and love
- All my family for their love and support
- My friends in Colombia, Ali, Liliam, Cata, Adri
- Luna for getting me out of the routine
- Oscar for his love, patience, encouragement and understanding

Table of contents

List of figures

List of tables

List of Abbreviations

ABC	ATP-Binding Cassette
ABCB1	ATP-binding cassette sub-family B member 1
ABCC1	ATP-binding cassette sub-family C member 1
ABCG2	ATP-binding cassette sub-family G member 2
ADME	Absorption, Distribution, Metabolism, Excretion
ART	Antiretroviral therapy
ATP	Adenosine triphosphate
ATRA	All-trans retinoic acid
AZT	Zidothymidine
BBB	Blood brain barrier
BCRP	Breast Cancer Resistance Protein
Boc_2O	Di-tert-butyl dicarbonate
CsA	Cyclosporine A
DCM	Dichloromethane
EGFR	Epidermal Growth Factor Receptor
EMEM	Eagle's Minimum Essential Medium
FLT3	Fms-like tyrosine kinase 3
FTC	Fumitremorgin C
HAART	Highly Active Antiretroviral Therapy
HEK293-R482	Cell line
HEK293-T482	Cell line
HIV	Human Immunodeficiency Virus
HPLC	High Performance Liquid Chromatography
HR-MS	High Resolution Mass Spectrometry
IC_{50}	Half Maximal Inhibitory Concentration
ICZ	Indolocarbazole
I_{max}	Maximun inhibition
IR	Infrared spectroscopy
Kb-V1	Cell line
Log P	Partition coefficient
LRP	Lung-resistance Protein
MCF-7	Cell line
MDCKII	Cell line
MDR	Multidrug resistance
mRNA	Messenger Ribonucleic Acid
MRP1	Multidrug Resistance-associated Protein-1

MSD	Membrane Spanning Domain
MTX	Methotrexate
MX	Mitoxantrone
NBD	Nucleotide Binding Domain
NMR	Nuclear Magnetic Resonance
NNRTIs	Non-Nucleoside Reverse Transcriptase Inhibitors
NRTIs	Nucleoside Reverse Transcriptase Inhibitors
NtRTIs	Nucleotide Reverse Transcriptase Inhibitors
P-gp	P-glycoprotein
PhA	Pheophorbide A
QSAR	Quantitative Structure-Activity Relationship
Quinol	Quinolina
rt	room temperature
TCBZ	Triclabendazole
TCBZSO	Triclabendazole sulfoxide
$TCBZSO_2$	Triclabendazole sulfone
TEA	Triethylamine
THIQ	Tetrahydroisoquinoline
TKIs	Tyrosine Kinase inhibitors
TPS-A	Tryprostatin A
TsCl	*p*-toluensulfonyl chloride
VEGFR2	Vascular Endothelial Growth Factor

1 General Introduction[1]

Multidrug resistance (MDR) in cancer cells is the development of resistance to a variety of structurally and functionally non-related anticancer drugs. This phenomenon has become a major obstacle to cancer chemotherapy seriously affecting the clinical outcome. MDR is associated with increased drug efflux from cells mediated by an energy-dependent mechanism involving the ATP-binding cassette (ABC) transporters, mainly P-glycoprotein (P-gp, ABCB1), the multidrug resistance-associated protein-1 (MRP1, ABCC1) and the breast cancer resistance protein (BCRP, ABCG2). The first two transporters have been widely studied already and ABCG2 is subject of intense study since its discovery as its overexpression has been detected in resistant cell lines in numerous types of human cancers. To date, a long list of modulators of ABCG2 exists and continues to increase. However, little is known about the clinical consequences of ABCG2 modulation. This fact makes the design of novel, potent and non-toxic modulators of this efflux protein a major challenge to reverse multidrug resistance and thereby increase the success of chemotherapy. The aim of the present chapter is to describe and highlight specific ABCG2 modulators reported to date based on the selectivity of the compounds, as many of them are effective against one or more ABC transport proteins.

---

[1]Diana Peña-Solórzano[ŧ], Simone Alexandra Stark[ŧ], Burkhard König, Cesar Augusto Sierra, Cristian Ochoa-Puentes. ABCG2/BCRP: Specific and Non-Specific Modulators. Medicinal Research Reviews. ([ŧ]These authors (D.P-S and S.A.S) contributed equally to this work. Doi: 10.1002/med.21428

1.1 Multidrug resistance phenomenon

Chemotherapy is one of the most important cancer treatments. Unfortunately, most cancers are either resistant to chemotherapy or acquire resistance during treatment,[1] these phenomenon is known as multidrug resistance (MDR), defined as the cross-resistance or insensitivity of cancer cells to numerous drugs which are often structurally or functionally unrelated (Figure 1-1).[2,3] MDR is often the ultimate cause of failure of cytotoxic drugs in cancer chemotherapy. Many mechanisms of drug resistance, such as activation of detoxifying systems, evasion of the apoptotic control, changes in cellular repair mechanisms or activation of drug efflux pumps have been identified.[4] Based on this knowledge, strategies to overcome drug resistance and to increase the efficacy of cancer chemotherapy have been developed. Thereby, the inhibition or modulation of cellular efflux pumps to reverse drug resistance has been subject of research for decades.

Stimulated by the identification of the MDR1 gene,[5] initially many clinical trials in cancer therapy focused on the ABCB1 transporter. P-gp expression was considered to be solely responsible for the phenomenon of MDR. However, during the last two decades it became clear that ABCB1 is not the only member of the ABC transporter family which is involved in the resistance against clinically relevant chemotherapeutics. After the discovery of MRP1 (ABCC1) and its affiliation to the ABC transporter family,[6] additional proteins contributing to chemoresistance were identified, including the Breast Cancer Resistance Protein.

MDR in cancer is caused by multiple mechanisms that operate either independently or in unison. Overexpression of drug transporters is just one of the many ways that cancer cells have adapted in order to survive the diversity of agents used in cancer chemotherapy.[7]

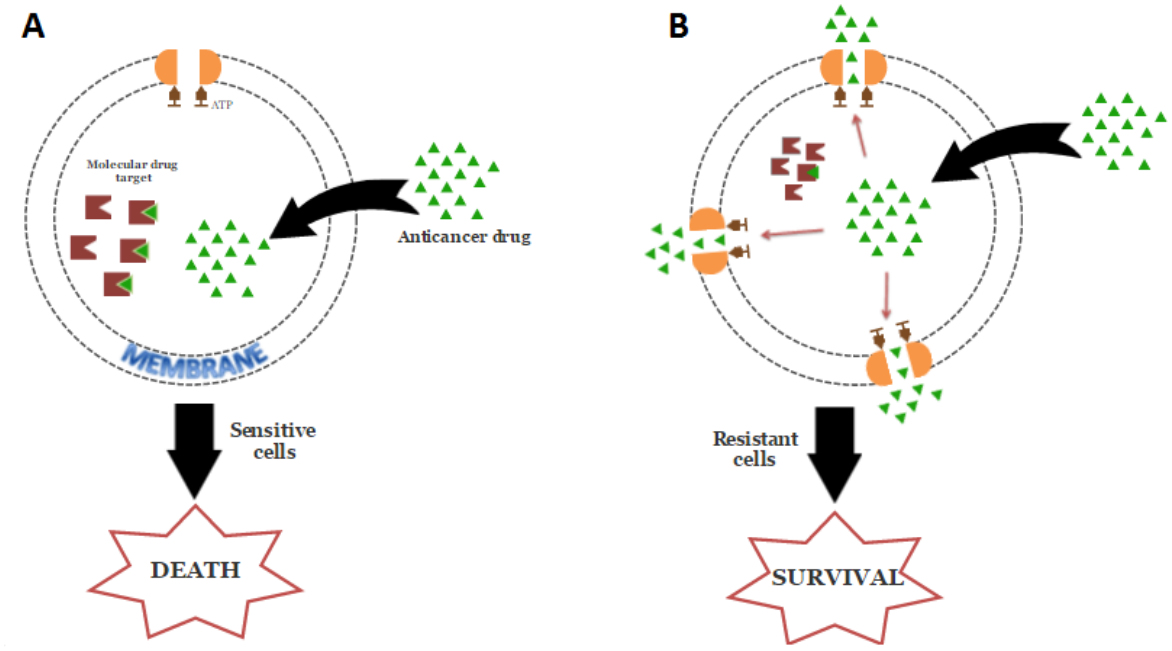

Figure 1-1 Multidrug Resistance Phenomenon. **A**. Schematic presentation of anticancer drug entry into a cancer cell via membrane. **B** Schematic presentation of the phenomenon of MDR in cancer cells (Adapted from Ullah, M. 2008[3])

1.2 ABC transporter superfamily

The ATP-binding cassette (ABC) transporter superfamily contains membrane-embedded proteins that are involved in the transport of a wide variety of substrates, such as cholesterol, peptides, drugs, toxins, bile salt, organic anions, nucleosides, iron, chloride ion and sterols across extra- and intracellular membranes.[8,9] The intracellular concentration of endo- and exogenous substrates is limited by their active efflux through ATP binding and hydrolysis as supplier of energy. To date, 49 human ABC transporter members are known and classified into seven subfamilies (ABC-A to ABC-G).

The ABC efflux pumps use the energy of ATP hydrolysis to transport a huge variety of molecules against the concentration gradient across biological membranes.[10] In our cellular defense system, the location of ABC transporters in the gastrointestinal tract represents the first defense mechanism against numerous ingested xenobiotics. As this also includes numerous orally administered drugs, ABC proteins, especially P-gp, play a

major role in limiting the uptake and, thus, the bioavailability of drugs.[11] ABC transporters are furthermore involved in limiting the access of various compounds to sensitive tissues like the testes, the placenta or the brain, thereby protecting these organs from toxic agents. Classically exemplified by ABCB1, ABCC1 and ABCG2, respectively, it became clear that these plasma membrane proteins are key players in protecting the organism from xenobiotics and toxins by preventing their uptake and procuring their elimination.

From all the identified transporters, three are associated with multidrug resistance (MDR): P-glycoprotein (P-gp, ABCB1), the multidrug resistance-associated protein-1 (MRP-1, ABCC1) and the breast cancer resistance protein (BCRP, ABCG2) (Figure 1-2). [12-14]

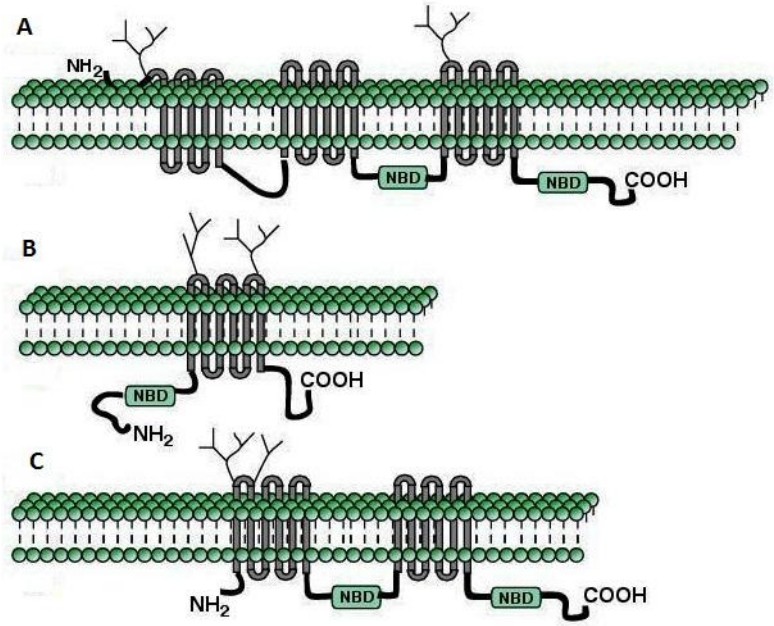

Figure 1-2 Topology and domain arrangement of the ABC transporters ABCC1 (**A**), ABCG2 (**B**) and ABCB1 (**C**) (Adapted from Vautier *et al.*[15])

ABC transporters are considered as therapeutic targets to overcome MDR in tumor therapy[16] and many efforts have been made to identify and develop modulators. Several reviews concerning the biochemical, and pharmacological aspects,[14,17-20] as well as computational methods and models used to predict substrate properties of drug-like compounds[21] and the discovery of reversal agents[22-26] for ABCB1 and ABCC1 proteins have been published. In the last decade ABCG2/BCRP emerged as an important protein involved in multidrug resistance and the focus of MDR studies shifted to this protein.

1.3 Breast Cancer Resistance Protein (ABCG2)

ABCG2 (ATP-binding cassette sub-family G member 2) was simultaneously discovered by three different groups in 1998, and is therefore known as ABCP for its identification in human placenta, BCRP for its isolation from the breast cancer cell line MCF-7/AdrVp and MXR for its identification in the mitoxantrone-resistant colon carcinoma cell line S1-M1-80.[12] The human ABCG2 protein is a half-transporter composed of 665 amino acids with a molecular weight of 72 kDa. Unlike other ABC transporters, ABCG2 is a half-transporter with a single nucleotide binding domain (NBD) and one membrane spanning domain (MSD) containing six transmembrane segments, which is supposed to form homodimers or homomultimers to become functional. Despite intensive research a high-resolution crystal structure has not been reported limiting a deeper insight into precise transport mechanisms.[13,27-29]

Multiple physiological functions have been considered for ABCG2, but in general its tissue localization appears to play a protective role against various xenobiotics limiting their oral absorption.[30-32] Studies have indicated that ABCG2 is a key player in preventing the absorption of toxic compounds from the gut, increase their hepatobiliary clearance, and protect the maternal–fetus, blood–brain and blood–testis barriers.[33] High ABCG2 expression has been found especially in the placenta and intestine, but also in the brain endothelium, prostate, testes, ovaries, liver, adrenal gland, uterus, and central nervous system.[34]

Several evidences suggest that when the ABCG2 is overexpressed in cancer lines, contains a mutation in the glicine482 and this is a dominant factor for the resistance to various cytostatic agents, as many studies have demonstrated that this position is critical for the recognition of substrates by protein.[35,1]

Functional characterization has demonstrated that ABCG2 transports a highly diverse range of substrates including methotrexate (MTX), mitoxantrone (MX) and many tyrosine kinase modulators, which were reported both as substrates and inhibitors of ABCG2. Furthermore, ABCG2 recognizes a broad variety of positively and negatively charged substances and is resistant to most topoisomerase I or II inhibitors such as topotecan or doxorubicin explaining failures of cancer therapy (Figure 1-3).[36,37]

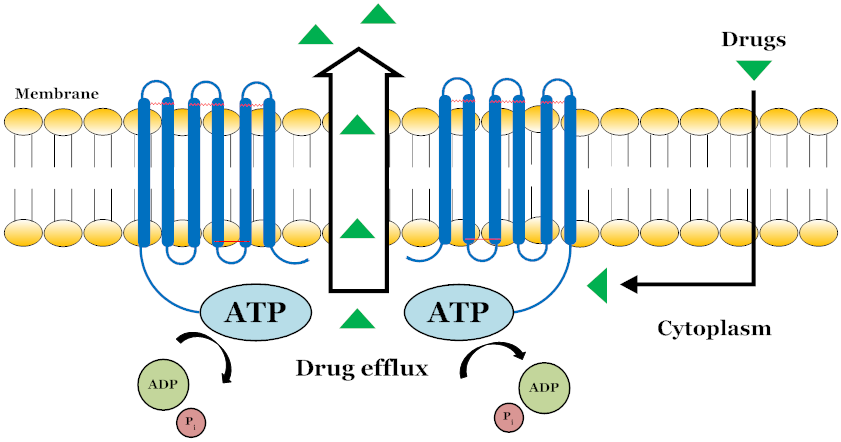

Figure 1-3 Schematic molecular mechanism of substrate binding and ATP hydrolysis by ABC transporters

1.4 ABCG2 modulators

A modulator may be a compound that can act as an activator/substrate, an inhibitor, or both. Therefore, the term modulator will be used throughout the text instead of the term inhibitor, even though in some publications the term inhibitor was used. The term inhibitor should only be used when a compound was proven by a suitable assay, such as ATPase assay to act as a real inhibitor and is not transported itself.

High overexpression of ABCG2 is observed in many tumor types, e.g. in melanoma, making it one of the major obstacles in the treatment of cancer.[38] One of the main approaches avoiding MDR during chemotherapy is blocking of the functions of this ABC transporter. Suitable modulators for the transporter have been developed.[32,39] However, it should be kept in mind that the mutual blocking of ABCG2 transporter function in malignant cells and of endogenous ABCG2 in healthy cells can lead to side effects such as increased toxicity caused by ABCG2 substrates.[30,40] In addition, as ABC transporters play a major role as a detoxification and protection system for the human body, blocking of the efflux function has the risk of provoking serious side effects, as the inhibition will not only occur in cancer cells but also in tissues where a normal ABC function is desired. In severe diseases like glioblastoma side effects of an effective therapy may be acceptable, in other cases however, the use and risks must be considered carefully. Moreover, inhibition of an ABC transporter will not only impede the efflux of its substrate drugs, but also alter their distribution. This may cause drug-drug interactions.

The main clinical implications of specific ABCG2 modulators are their potential to act as multidrug reversal agents affecting the ADME (absorption, distribution, metabolism, excretion) properties of its substrates.[41] The ideal ABCG2 modulator should antagonize the drug efflux activity even at nanomolar concentrations, be completely selective for ABCG2 with no or little inherent toxicity. Furthermore, selective modulators are of importance as pharmacological tools to identify possible binding sites and examine the ABCG2 mediated MDR at a molecular level. The mechanism of transport is not completely understood until now. Modulators may alter the efflux activity in many different ways, e.g. through specific interactions with the protein or by behaving as a "poor", very slowly transported substrate blocking the efflux function for other substrates. Other possibilities are the interaction with the ATP-binding site affecting the binding of ATP depending on intracellular ATP levels. Interaction with the the membrane phospholipids can increase the membrane permeability for ions reducing the activity of the transporter.

Several types of ABCG2 modulators, such as chemotherapy drugs, tyrosine kinase inhibitors, antivirals, carcinogens and flavonoids were reported recently. Unfortunately, very few compounds have shown promising results in preclinical trials.[28,42-45] The aim of the present chapter is to describe and highlight specific ABCG2 modulators reported to date based on the selectivity of the compounds, as many of them are effective against one or more ABC transport proteins.

1.4.1 Acrylonitriles

In 2011, two acrylonitriles, YHO-13177 (**1**) and its water-soluble diethylaminoacetate prodrug YHO-13351 (**2**) were reported as reversal agents of ABCG2-mediated drug resistance, both *in vitro* (**1**) and *in vivo* (**2**, Figure 1-4).[46] Acrylonitrile **1** was able to reverse resistance to the ABCG2 substrates SN-38, which is the active metabolite of irinotecan, mitoxantrone (MX) and topotecan in ABCG2-transduced cells HCT116/ABCG2 and cells that acquired resistance to SN-38 mediated by ABCG2 (A549/SN4), whereas little or no effect was observed in the parental cells. The concentration of **1** producing a half-maximal reversal of the drug resistance was within a range of 0.01 to 0.1 µM. No effect on ABCB1-mediated resistance to paclitaxel in ABCB1-transduced K562 cells and ABCC1-mediated resistance to doxorubicin in ABCC1-transfected KB-3-1 cells was observed. Also, a

cytotoxic effect of **1** itself on the cancer cells was not observed. The authors investigated the underlying mechanism of reversal of drug resistance and suggested that **1** is involved in a posttranscriptional downregulation of ABCG2 and inhibits the drug transport function. However, further studies are needed for elucidating the exact mode of action. The water-soluble prodrug **2** was used for *in vivo* studies in mice. Co-administration of irinotecan (30 mg/kg) with 100 or 200 mg/kg of **2** significantly increased the survival time in a dose-dependent manner. In a pharmacokinetic study, co-administration of 30 mg/kg of **2** (i.v.) in mice increased $AUC_{0-\infty}$ (total drug exposure over time) values of irinotecan in 1.4-fold and for SN-38 in 1.6-fold compared with 45 mg/kg irinotecan (in vivo) alone.

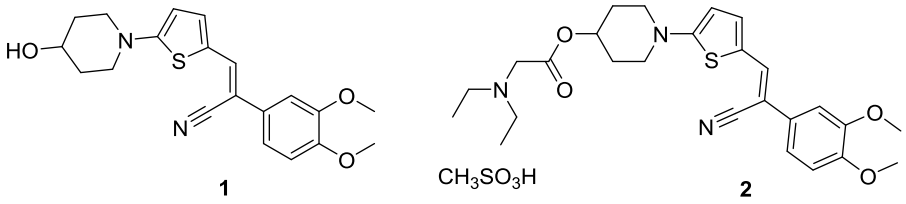

Figure 1-4 Acrylonitriles

1.4.2 Anti HIV-Based Modulators

Human immunodeficiency virus (HIV) can be controlled by the administration of three to four antiretroviral drugs from different classes acting on different viral targets. This is known as highly active antiretroviral therapy (HAART). The antiretroviral agents are HIV-protease inhibitors (PIs), non-nucleoside reverse transcriptase inhibitors (NNRTIs), nucleoside reverse transcriptase inhibitors (NRTIs) and nucleotide reverse transcriptase inhibitors (NtRTIs).[47] Some investigations indicated that drugs used for the treatment of human immunodeficiency virus (HIV) might also interact with ABCG2[48,49] as shown by Kis et al.[50] This study, performed with HIV-negative healthy volunteers, ART-naïve HIV+, and HIV+ subjects receiving ART, showed that a lower expression of ABCC2 was found in ART-naïve subjects compared to control, while CYP3A4 and ABCG2 showed a trend towards decreased expression. In addition, the protein expression of ABCC2 and ABCG2 was also significantly lower in HIV+ naïve group compared to control and was partially restored to baseline levels in HIV+ subjects receiving ART.

In 2007, Weiss et al. evaluated the influence of several anti-HIV drugs on ABCG2 activity *in vitro*. ABCG2 inhibition was estimated by measuring the increase of the ABCG2 substrate pheophorbide A (PhA) accumulation in MDCKII-ABCG2 cells using fumitremorgin C (FTC, **82**, 10 µM) as reference compound (IC_{50} 0.47 µM). The PIs lopinavir (**3**), nelfinavir (**4**), delavirdine (**5**), efavirenz (**6**) and saquinavir (**7**, Figure 1-5) showed potent ABCG2 inhibitory activity with values of 7.66 µM, 13.5 µM, 18.7 µM, 20.6 µM and 27.4 µM, respectively. The NNRTI nevirapine and NRTI/NtRTI zidovudine showed low inhibition whereas PI indinavir and NRTIs/NtRTIs didanosine, emtricitabine, lamivudine, stavudine, tenofovir and zalcitabine had no inhibitory effect.[47] Also, Peroni et al. investigated how the intestinal permeability of efavirenz (**6**) was modulated by ABCG2. Antiretroviral **6** was shown to be transported by ABCG2, but not by ABCB1. Moreover, after repeated oral administration increasing protein levels of ABCG2 were found in the intestinal epithelium.[49] A study by Neumanova et al. in 2016 investigated the influence of MDR-associated transporters on the distribution of zidovudine and lamuvidine by an *in vitro* bidirectional transport study and concentration equilibrium assays on cell monolayers.[51] The established MDCKII cell line was used with overexpressing ABCG2, ABCB1, ABCC2 or ABCC5. Consistent with the study performed by Weiss et al., lamuvidine was found to have zero interactions with these transporters. In contrast to the previous study, zidovudine (**8**, Figure 1-5), also known as zidothymidine (AZT), was reported to be a substrate of both ABCB1 and ABCG2, but not ABCC2 or ABCC5 and its transport was shown to be blocked upon addition of the dual ABCB1/ABCG2 modulator elacridar (**129**, 2 µM).

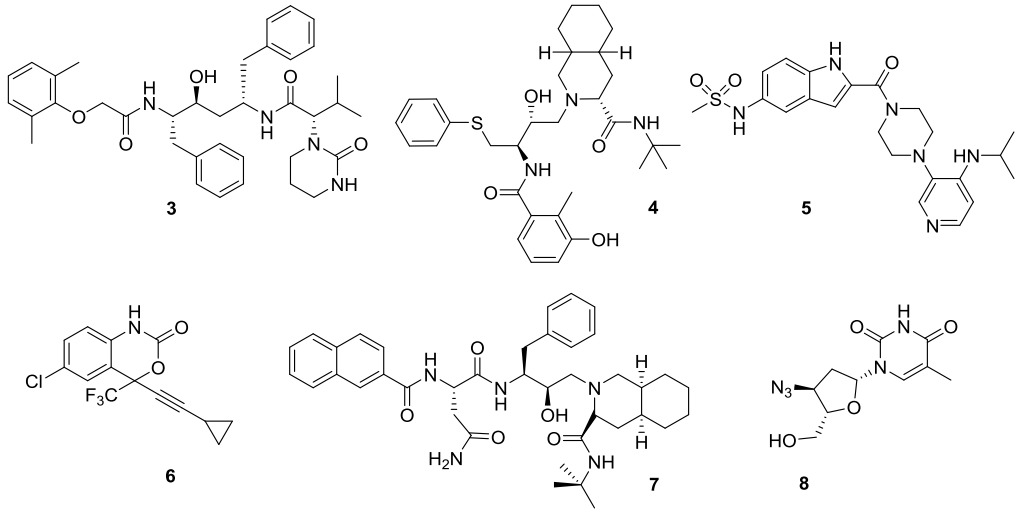

Figure 1-5 Anti HIV-based modulators

1.4.3 Flavonoids and Chromone Derivatives

Flavonoids comprise a large class of polyphenolic compounds, and are integral components in our common diet as they are ubiquitously present in plants. Several studies have indicated that flavonoids may play a protective role in the prevention of cancer, coronary heart diseases, bone loss and also have anti-allergic, antioxidant,[52,53] antibacterial,[54] antiviral[55] and anti-inflammatory[56] properties.[57] Due to the health beneficial activities and low toxicity, hundreds of herbal preparations containing flavonoids are available as dietary supplements. The consumption of these products is becoming more and more widespread, along with the burgeoning public interest in alternative medicine and in disease prevention. Therefore, their interaction with ABCG2 has to be taken into consideration as pharmacokinetics of drugs being ABCG2 substrates may be drastically altered. On the other hand, flavonoids may have potential as multidrug reversal agents.

1.4.3.1 Aurones

Aurones are flavonoid-type heterocyclic compounds found in plants and contribute to the pigmentation of some flowers and fruits. As aurones are structurally related to flavones it does not come as a surprise that this compound class is now increasingly investigated by researchers for their therapeutic values.[58,59]

A series of 4,6-dimethoxyaurones was evaluated for their potential to modulate ABCG2 by increasing the accumulation of mitoxantrone in MDA-MB-231 cells transfected with ABCG2. Ten aurones (**9**–**18**, Figure 1-6) were effective at a concentration of 0.5 µM compared to the reference compound FTC (**82**) at 10 µM. The effect of the same compounds at higher concentration (10 µM) on the accumulation of calcein-AM in MDCKII/ABCB1 cells was also investigated and none of the aurones were considerably better than the ABCB1 modulator verapamil, which shows a preference of the studied compounds for ABCG2 inhibition.[60,61] In a more recent report the same authors identified three new derivatives: trimethoxyaurone (**19**), indanone (**20**), and azaaurone (**21**, Figure 1-6), which were clearly selective for ABCG2. These compounds exhibited EC_{50PhA} values (test compound concentration required to increase the accumulation of PhA to 50% of maximum levels obtained with 10 µM FTC, **82**) of 5.42 ± 0.24 µM, 1.76±0.19 µM and

4.61±0.25 µM, respectively in the PhA accumulation assay using ABCG2-overexpressing MDA-MB-231 cells.[62]

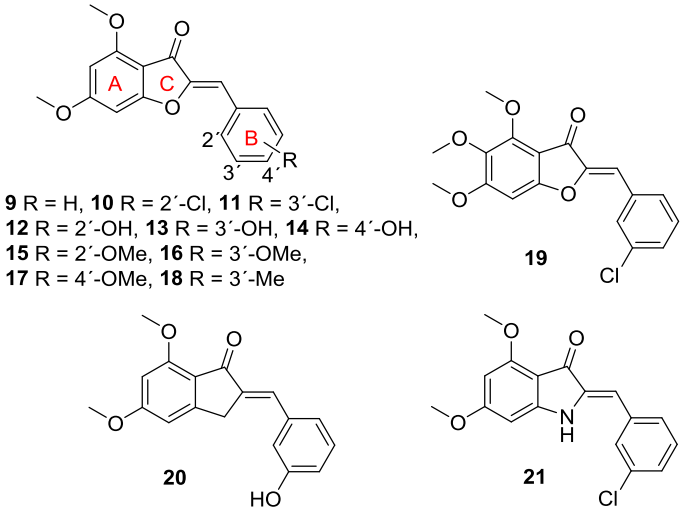

Figure 1-6 Aurones

1.4.3.2 Chalcones

Different types of chalcones, which are intermediates of flavonoid biosynthesis in plants, are modulators of the multidrug resistance-associated transporter ABCB1.[63,64] Han et al. investigated 17 non-basic chalcone analogues for their ABCG2-modulating properties.[65] Chalcones **22**–**24** (Figure 1-7) with 2,4-dimethoxy groups or 2,4-dihydroxyl groups on ring A were found to increase mitoxantrone accumulation to a greater extent than FTC (**82**, 10 µM) at a concentration of 5 µM with no significant effect on ABCB1. However, the authors stated that ABCC1 and ABCC2 may be possible targets of these compound classes, which has to be further investigated. It was clearly observed that among all chalcones, compounds with 2,4-dimethoxy substituents at ring A were most active. Different substituents on the A-ring appeared to be required for inhibiting ABCG2, but the inhibition was rather low due to inadequate substitutions in both rings A and B.

In 2012 a series of 44 chalcones and 1,3-diarylpropenones was investigated for inhibition of ABCG2-mediated mitoxantrone transport. Elacridar (**129**, 5 µM) was used as a control (100% inhibition). The best compounds were **25** (2 µM, 130.7%) and **26** (2 µM, 103.5%, Figure 1-7), showing potent inhibition of ABCG2 and low toxicity. In general, methoxy groups at positions 3, 4, and 5 of the ring B increase the cytotoxicity markedly and should

be therefore avoided. Chalcones and indoylphenylpropenones are promising leads as modulators of ABCG2. The easy chemical syntheis of such compounds and their high activity and specificity are important prerequisites for preclinical trials.[66] Wiese et al. investigated in 2012 chalcones and benzochalcones with different substituents on ring A and B using the Hoechst 33342 accumulation assay. The inhibitory activity was tested in MCF-7/MX and MDCK/ABCG2-expressing cells. The authors also tested the compounds for inhibition of ABCB1 and ABCC1. Substituents at position 2´ and 4´ on ring A were found to be crucial for the activity, whereas substituents on ring B were changing the activity. 3,4-Dimethoxy substitution on ring B and to a smaller extent, 2-and 4-chloro substitution improve ABCG2 inhibition. Compounds **27** (IC_{50} 0.85 µM) and **28** (IC_{50} 0.53 µM, Figure 1-7) were found to be most potent with an activity threefold smaller compared to the reference compound Ko143 (**85**, IC_{50} 0.26 µM).[67]

Two years later, a series of quinoxaline-substituted chalcones as modulators of ABCG2-mediated mitoxantrone efflux was designed, synthesized and evaluated. The IC_{50} values were determined comparing each quinoxaline-containing compound with the corresponding compounds containing either a 2-naphthyl or a 3,4-methylenedioxyphenyl moiety. Compounds **29**–**34** (Figure 1-7) have a quinoxaline attached to ring B of the chalcone and showed the smallest IC_{50} values, 1.7, 1.9, 1.4, 2.2, 1.4, 2.1 µM, respectively, in comparison to compounds **35**–**40** (Figure 1-7) with 2-naphtyl attached to ring B (IC_{50} 17.0, 4.1, 11.2, 2.5, 23.3 µM, respectively) and compounds **41**–**46** (Figure 1-7) with 3,4-methylenedioxyphenyl substituent (IC_{50} 5.6, 3.5, 6.1, 0.94 µM, respectively). This allowed the identification of three characteristic structure–activity relationship (SAR) parameters for ABCG2 drug-efflux activity. First, the high efficiency of the new quinoxaline- and 1-naphthyl derivatives compared to that of 3,4-methylenedioxyphenyl- and 2-naphthyl-containing chalcones at the B-ring position; second, at least two methoxy groups on the phenyl A-ring (through both electrostatic and steric contributions) are required, while a bicyclic unit occupying the B-ring position provides maximal inhibition and third, a higher potency can be reached by shifting the bicyclic unit to the A-ring and methoxy substituents to the phenyl B-ring.[68,69]

In 2016 Wiese et al. reported heterodimeric modulators of ABCG2 by combining chalcone and quinazoline scaffolds, which were both found to be inhibitors of ABCG2. A series of 22 compounds was synthesized and tested for inhibition, specificity and cytotoxicity.[70] The most potent compound of the series (**47**, Figure 1-7) has a IC_{50} value of 0.19 µM, low

cytotoxicity and is almost ABCG2 selective, whereas other compounds were dual ABCB1/ABCG2 modulators or even less active at ABCG2 than ABCB1.[70]

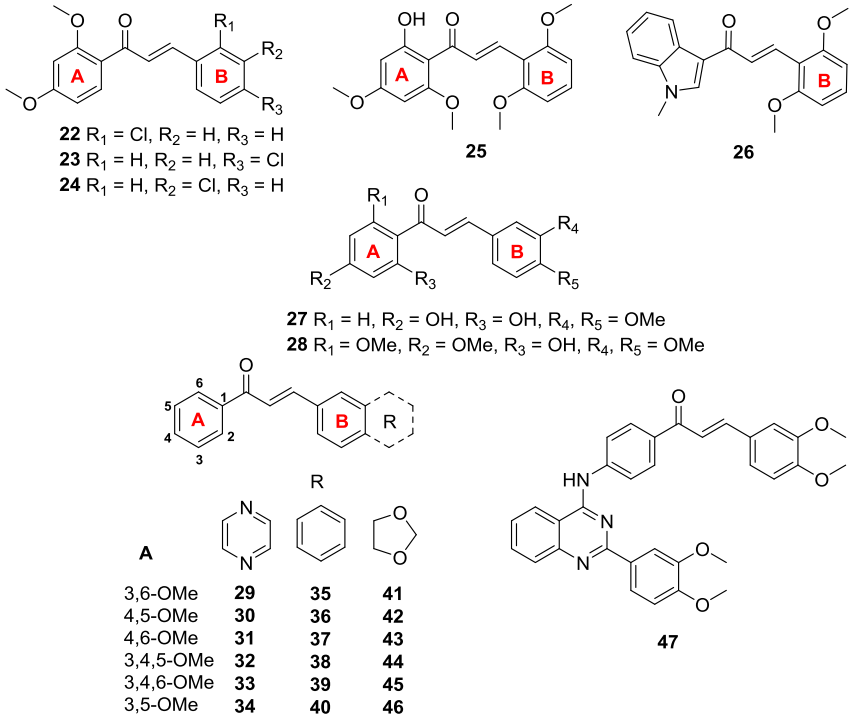

Figure 1-7 Chalcones

1.4.3.3 Chromones

Chromones (1,4-benzopyrones) are natural compounds with a partial structure of flavonoids. Since flavonoids were earlier described as modulators with poor selectivity toward ABCG2, it was hypothesized that higher potency and selectivity could be achieved by maintaining the chromone skeleton and replacing the B-ring of flavonoids with a chemical motif found in other ABCG2 modulators.[28]

In 2005, 14 benzopyrane (chromone) derivatives were evaluated for their effect on the accumulation and the cytotoxicity of the anticancer drug mitoxantrone. At 10 µM, phenylalkylamine linked chromones **48** and **49** (Figure 1-8) increased both intracellular accumulation and cytotoxicity of mitoxantrone in HCT116/R cells with a comparable rate as FTC (**82**) and imatinib mesylate (**160**) used as reference compounds. Lack of cytotoxicity as well as their interesting chemosensitizing properties make these compounds good candidates for *in vivo* studies.[71]

In 2012, Valdameri et al. synthesized a series of 13 substituted chromones and analyzed them for their ability to inhibit ABCG2-mediated mitoxantrone efflux from transfected HEK293 cells. The percentage of inhibition was determined by flow cytometry, relative to elacridar (**129**, 5 µM) as a control. The best compounds of this series were compound **50** (IC_{50} 0.11 µM, Figure 1-8), **51** (IC_{50} 0.16 µM, Figure 1-8) and **52** (IC_{50} 0.17 µM, Figure 1-8).[72,73] Compound **52** was also synthesized by another group as a reference compound due to its structural similarity to flavonoid derivatives being selective ABCC1 modulators.[74] Interestingly, the potency of compound **52** determined with MCF-7/Topo cells (IC_{50} 1.8 µM, I_{max} 108%, Hoechst 33342 assay, FTC, **82** was used as reference at 10 µM) was tenfold lower than reported for the transfected HEK293 cells. The authors stated that the compound is selective for ABCG2, but mentioned that compound **52** stimulates ABCB1 mediated drug efflux activity at high concentrations. The results demonstrate that the data for potency of some modulators may dependent on the assay system and the reference compounds used, complicating direct comparison.

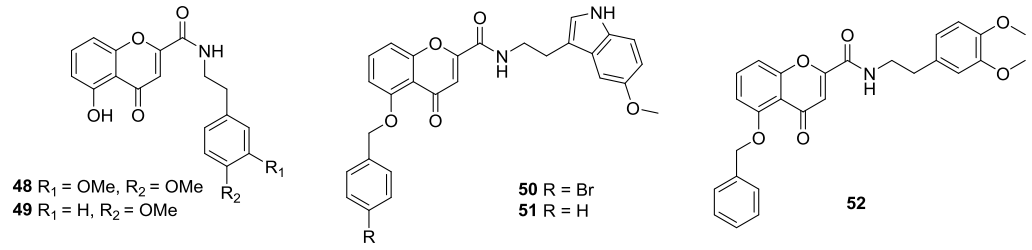

Figure 1-8 Chromones

1.4.3.4 Flavones, Isoflavones, Flavanones, Flavonols and Rotenoids

A first study on the ABCG2-mediated transport performed with five flavonoids (quercetin, hesperetin, silymarin and daidzein, and the stilbenoid resveratrol) showed that all polyphenols (each at 30 µM) significantly increased the accumulation of the ABCG2 substrates mitoxantrone and bodipy-FL-prazosin in the ABCG2-overexpressing cell lines MCF7/MR and K562/BCRP as measured by flow cytometry. Hesperetin (**69**) exhibited the highest ABCG2 inhibitory activity (30 µM, Figure 1-9), and was comparable to that produced by the reference ABCG2 modulator Ko143 (**85**) at 10 µM.[57] In the same year, the effect of 20 flavonoids on the accumulation and cytotoxicity of mitoxantrone in ABCG2-overexpressing human breast cancer cells (MCF-7/MX100) and large cell lung

carcinoma cells (NCI-H460 MX20) were investigated. The flavonoids apigenin (**53**), biochanin A (**65**), chrysin (**55**), genistein (**64**), hesperetin (**69**), kaempferol (**72**), naringenin (**67**), and silymarin (each at 50 µM, Figure 1-9) were shown to modulate ABCG2 in such a manner, that a threefold increase in accumulation of mitoxantrone was observed in both cell lines. The effect was similar to FTC (**82**) at 10 µM. The flavonoids daidzein (**66**), fisetin (**70**, Figure 1-9), phloretin, quercetin and silibin were able to produce a twofold increase. Chrysin (**55**) and biochanin A (**65**) were the most potent modulators producing significant increases in mitoxantrone accumulation at concentrations as low as 0.5 or 1.0 µM and in mitoxantrone cytotoxicity at a concentration as low as 2.5 µM.[75] However, oral co-administration of neither chrysin nor 7,8-benzoflavone had a significant effect on the accumulation of the ABCG2 substrate topotecan in rats or in mdr1a/1b (–/–) mice. The authors attributed this *in vitro - in vivo* discrepancy to the poor inhibition activity of the investigated flavonoids against mouse or rat ABCG2 (Abcg2).[76]

The analysis of the combined effects of apigenin (**53**), biochanin A (**65**), chrysin (**55**), genistein (**64**), kaempferol (**72**), hesperetin (**69**), naringenin (**67**), and silymarin on the mitoxantrone accumulation in MCF-7/MX100 cells overexpressing ABCG2 indicated that the ABCG2 inhibition is additive when different flavonoid combinations with equimolar concentrations are given.[77] Imai et al. evaluated the effects of phytoestrogens, which are similar to estrogen in their structure and/or function and other flavonoids in ABCG2-mediated MDR.[78] It was found that genistein (**64**) and naringenin (**67**, Figure 1-9) are potent ABCG2 modulators at a concentration of 3 µM on drug resistant K562/ABCG2 cells and the cytotoxicity of anticancer drugs SN-38 and mitoxantrone was potentiated. This effect was also observed with acacetin (**54**) and kaempferol (**72**) while some glycosylated flavonoids displayed moderate reversal activity. Naringenin-7-glucoside (**68**) and luteolin-4'-*O*-glucoside (**59**, Figure 1-9) were the most potent glycosylated flavonoids and might be useful due to their high water solubility. Studies of transcellular transport of [^{3}H]-genistein using LLC/ABCG2 cells suggest that the inhibition by genistein (**64**) is caused by competitive transport of this compound by ABCG2.

Structure–activity relationship (SAR) and quantitative–structure activity relationship (QSAR) studies of 25 flavonoids were performed by Zhang and co-workers in order to derive a model for flavonoid-ABCG2 interaction.[79] The presence of a 2,3-double bond in ring C, attachment of ring B to position 2, hydroxylation at position 5, lack of hydroxylation at position 3 and hydrophobic substituents at positions 6, 7, 8 or 4´ appear to be the

structural requirements for inhibiting ABCG2. A planar conformation may improve the binding of the respective flavonoid to ABCG2. In the same year a flavonoid SAR study led to the identification of 6-prenylchrysin (**60**) and tectochrysin (**61**, Figure 1-9) as potent and specific modulators of ABCG2.[80] Comparison between flavonoids containing three hydroxyl groups using ABCG2-transfected wild-type HEK293-R482 and mutant HEK293-T482 cells indicated that the flavone apigenin (**53**) was more efficient (IC_{50} 16 µM) than the flavonol galangin (**71**, IC_{50} 19 µM) and isoflavone genistein (**64**, IC_{50} 24 µM). The least efficient compound was the flavanone naringenin (**63**, IC_{50} 37 µM). As apigenin (**53**) was the most active compound, the effect produced by the position of hydroxyl groups and hydrophobic substituents on the flavone skeleton was evaluated An OH group at position 5 and C-isoprenylation at position 6 yields the most active compound. The potency of 6-prenylchrysin was comparable with that of GF120918/elacridar (**129**, IC_{50} 0.3 µM).

In a more recent study the interactions between ABCG2 and 56 dietary phytochemicals, including 33 flavonoids were examined using cell- and membrane-based methods. In the first assay, test compounds at a concentration of 50 µM were investigated for their ability to diminish the efflux of mitoxantrone using HEK293/ABCG2 cells, and except for anthocyanins (cyanidin 3-glucoside, cyanidin 3-rutinoside, delphinidin 3-glucoside, delphinidin 3-rutinoside), flavanols (+)-catechin and (–)-epicatechin, hesperidin, morin, myricetin and tricetin, all of the tested flavonoids showed increased values of mitoxantrone accumulation. Next, the effect of the phytochemicals on the transport of the tritiated ABCG2 substrate methotrexate (MTX-^{3}H) into Sf9/ABCG2 membrane vesicles at 5 and 50 µM was evaluated. Consistent with the cell-based mitoxantrone accumulation assay most flavonoids inhibited the transport of methotrexate at both concentrations. (+)-Catechin showed no effect at both concentrations, while the anthocyanins and (–)-epicatechin were only effective at 50 µM. The effect of many flavonoids at 50 µM was comparable to 1 µM Ko143 (**85**). IC_{50} values were determined for compounds exhibiting a significant inhibition of methotrexate transport, and seven flavonoids (apigenin (**53**), chrysoeriol (**56**), diosmetin (**57**), kaempferol (**72**), myricetin 3',4',5'-trimethylether (**76**), tamarixetin (**78**) and tricetin 3',4',5'-trimethylether (**63**, Figure 1-9), were found to have IC_{50} values below 0.1 µM and in the same range as the reference compound Ko143 (0.026 ± 0.003 µM). Compounds acacetin (**54**), chrysin (**55**), kaempferide (**73**), laricitrin (**74**), luteolin (**58**), myricetin (**75**), quercetin (**77**), tricetin (**62**, Figure 1-9) showed IC_{50} values below 0.5 µM.[81]

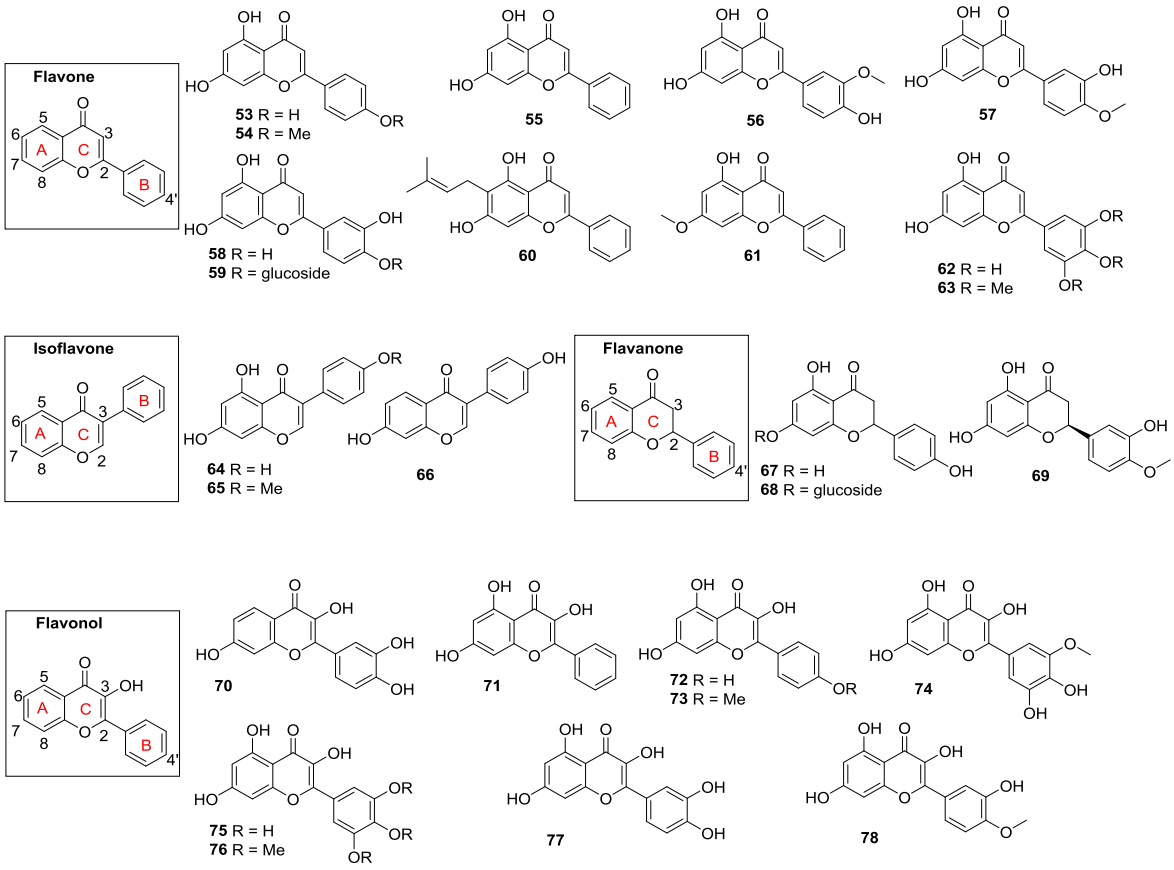

Figure 1-9 Flavonoids

Inhibition of the ABCG2-mediated efflux by rotenoids isolated from roots of *Boerhaavia diffusa* (Nyctaginaceae) was investigated by flow cytometry using ABCG2-transfected HEK293-R482 cells.[82] From the eleven isoflavonoid derivatives studied, boeravinones G (**79**) and H (**80**, Figure 1-10) efficiently inhibit the efflux of mitoxantrone at a concentration of 5 µM with IC_{50} values of 0.7 ± 0.07 µM and 2.5 ± 0.47 µM, respectively. The effect of boeravinone G was comparable to elacridar (**129**, 5 µM). The other nine rotenoid derivatives were less effective and higher concentrations were needed to achieve inhibition. A SAR study performed with these compounds showed the positive effect of a methoxy group at position 6, a double bond between ring B and C (6a and 12a positions) and the absence of substituents at position 10. Tetrasubstitution of ring D and contraction of ring B are unfavourable.

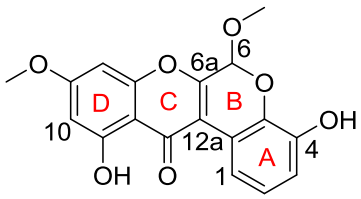

79

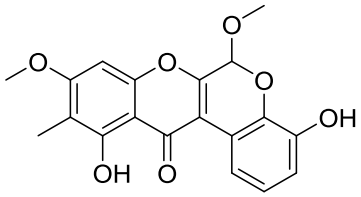

80

Figure 1-10 Rotenoids

In 2011 Pick et al. analyzed a structurally diverse set of flavonoids.[83] The activities of 31 compounds were evaluated by structure–activity relationships based on 2D and 3D-QSAR analyses revealing the influence of the different substituents at the various positions. The authors were able to identify some structural features positively contributing to the inhibition of ABCG2: a hydroxyl group in position 5, a double bond between 2 and 3 and a methoxy moiety in position 3, whereas an OH-group in the same position diminished the inhibitory activity, which indicates the importance of a hydrogen bond acceptor in this position (Figure 1-11).

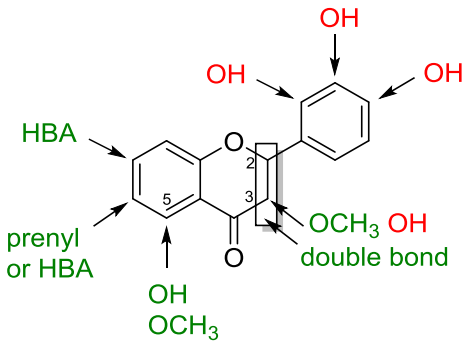

Figure 1-11 Overview of structural features influencing the inhibition of ABCG2 by flavonoids (green illustrates a positive contribution, red a negative contribution to the inhibitory potency)

Two years later, Juvale et al. synthesized a series of flavones, 7,8-benzoflavones and 5,6 benzoflavones with varying substituents at positions 3,3′ and 4′.[84] The synthesized (benzo)flavones were evaluated for their ABCG2 inhibition properties in both Hoechst 33342 and PhA accumulation assays and further screened for their inhibitory activity towards ABCB1 and ABCB1 by a calcein AM accumulation assay. Compound **81** was found to be the most potent of this series (Figure 1-12).

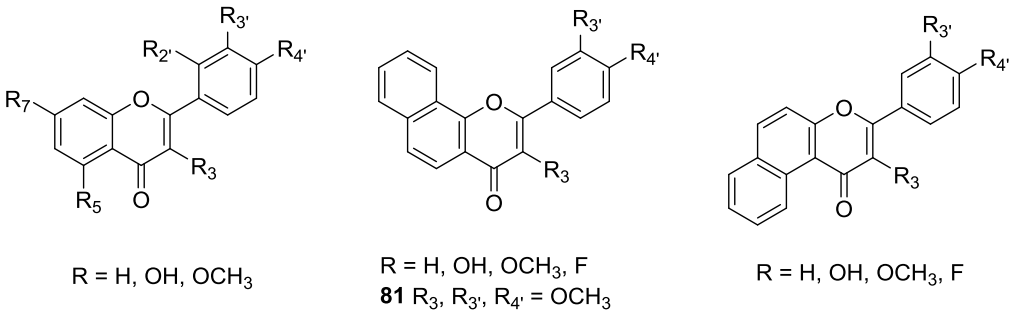

Figure 1-12 Flavones, 7,8-benzoflavones and 5,6-benzoflavones

1.4.4 Fumitremorgin C (FTC) Analogues

Fumitremorgin C (FTC, **82**, Figure 1-13) is a prenylated indole alkaloid isolated from *Aspergillus fumigates,* which has been described as a potent and selective ABCG2 modulator. However, its adverse neurotoxic effects including tremors and convulsion in mice, prevent its safe use in patients.[85-87]

To improve the specificity and selectivity of **82** while eliminating the potential for toxicity, a panel of 42 mixtures of diastereoisomers was screened for ABCG2 inhibitory activity on mitoxantrone accumulation and compared with elacridar (**129**). To demonstrate the functional comparability of human ABCG2 and mouse homologue Abcg2, assays were performed on the T6400 mouse as well as the human T8 cell line. The purified diastereoisomers (3*S*, 6*S* configuration) Ko132 (**83**) and Ko134 (**84**, Figure 1-13) showed a mitoxantrone accumulation (at a concentration of 1 µM) in T6400 cell line comparable to elacridar (**129**) and therefore constitute interesting leads for further development.[88]

In 2002, Schinkel et al. evaluated a new tetracyclic analogue of FTC (Ko143, **85**, **Figure 1-13**) as a modulator of ABCG2. The diketopiperazine analogue was compared with two FTC derivatives (**83** and **84**) and elacridar (**129**) by increased cellular mitoxantrone accumulation in the mouse MEF3.8/T6400 fibroblast cell line. Ko143 (EC_{90} 23 nM) is a more specific inhibitor of ABCG2 than other known inhibitors of ABCG2 such as elacridar (**129**, EC_{90} 51 nM). More importantly, Ko143 is nontoxic at effective *in vitro* and *in vivo* concentrations, which makes it one of the most promising compounds for the development of clinical modulators of ABCG2-mediated efflux and appears to be the most potent ABCG2 inhibitor known thus far.[89,90] However, it was recently reported that Ko143 is also targeting ABCB1 and ABCC1 at concentrations higher than 1 µM. An ATPase

assay was used to monitor the activity of ABCG2 and ABCB1 ATPase in the presence of Ko143. The ATPase activity of ABCG2 was found to be lower in presence of Ko143, while the ATPase activity of ABCB1 was stimulated. Moreover, the compound lacks stability in rat plasma due to the rapid hydrolysis of the *tert*-butyl ester moiety. When Ko143 was incubated together with NaF acting as an esterase inhibitor, no metabolism product was detected. The authors also investigated the inhibition properties of the synthesized hydrolysis product of Ko143 (**86**, Figure 1-13) showing that the inhibitory effect is only induced by Ko143 and not by its hydrolytic metabolite. [91]

In 2007, Wu et al. reported a new class of FTC analogues with simplified structure. Doxorubicin was used as ABCG2 substrate to evaluate the effect of the compounds on the chemosensitivity in ABCG2-overexpressing MES-SA/Dx5 cells. Compared with doxorubicin (IC_{50} 1.55 µM), compounds **87**–**91** (IC_{50} 0.86, 0.75, 0.80, 0.82 and 0.66 µM, respectively, Figure 1-13) significantly reversed the ABCG2-mediated resistance to doxorubicin. Compared with the native pentacyclic FTC (**82**), the new simplified FTC analogues developed in these studies retain the tetracyclic core of **82**, but were accessible in only four steps with high purity of the diastereomers and good yields.[90,92]

In 2016, Wiese et al. synthesized and tested 37 tricyclic tetrahydro-*ß*-carboline derivatives. Ko143 (**85**), FTC (**82**) and harmine (**106**) are modulators of ABCG2 and also contain a tetrahydro-*ß*-carboline or *ß*-carboline moiety.[93] Two compounds (**92** and **93**, Figure 1-13) of this series have a comparable inhibitory activity to Ko143 (**85**) .[94] The inhibitory effect was investigated in a Hoechst 33342 and a PhA accumulation assay using the MDCKII/ABCG2 cell line. Compound **92** had an IC_{50} value of 0.233 ± 0.044 µM in the Hoechst 33342 assay and an IC_{50} value of 0.237 ± 0.080 µM in the PhA assay, respectively. Shifting the methoxy moiety from the 4 to the 3-position (**93**) resulted in IC_{50} values of 0.238 ± 0.044 µM (Hoechst 33342 assay) and 0.206 ± 0.025 µM (PhA assay), respectively. Ko143 (**85**) was used as positive control (IC_{50} 0.221 ± 0.024 µM, Hoechst 33342 assay). Both compounds were selective for ABCG2 and compared to Ko143 (**85**) easily accessible in a two-step synthesis starting from tryptamine.

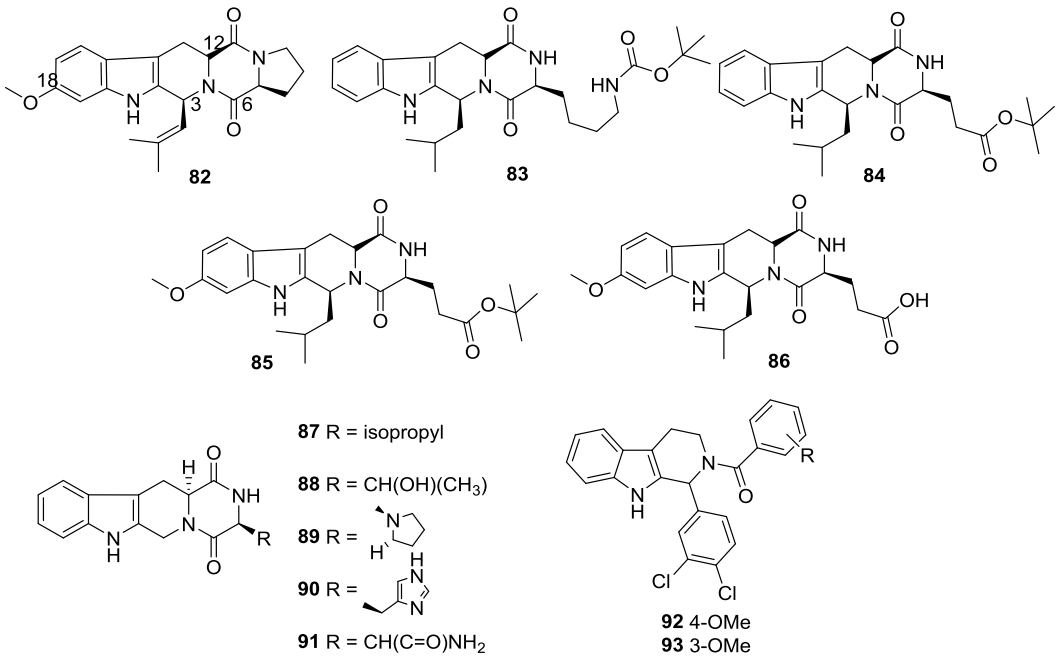

Figure 1-13 FTC analogues

1.4.5 Natural Product Derivatives

Natural products and their derivatives are a rich sources of novel therapeutics. The majority of current cancer chemotherapeutics was derived from natural products. Many of the reported ABCG2 modulators are natural products or natural product related compounds.[95,96]

1.4.5.1 Antibiotics

Novobiocin (**94**, Figure 1-14) is an aminocoumarin prokaryotic enzyme gyrase inhibitor produced by the actinomycete *Streptomyces niveus*.[97] In 2004 it was shown that antibiotic **94** was effective in the reversal of drug resistance in cancer cells with various levels of ABCG2 mRNA expression and increased the intracellular accumulation of the ABCG2 substrate topotecan in non-cytotoxic concentrations. For example, at a concentration of 60 µM, **94** decreased the degree of topotecan resistance (from 141- to 5.42-fold in PC-6/SN2-5H2 cells), SN-38 resistance (from 173-to 4-fold) and of mitoxantrone resistance (from 57.2- to 1.63-fold). Shiozawa et al. identified **94** as a competitive inhibitor by

studying topotecan transport using plasma membrane vesicles derived from ABCG2-overexpressing cancer cells.[97]

Three years later, Sinko et al. demonstrated that **94** significantly inhibits the activity of ABCG2, but not of ABCB1.[98] They also investigated the influence of **94** (50 mg/kg) on the orally-dosed topotecan (2 mg/kg) *in vivo* pharmacokinetic in rats. Co-administration significantly increased the peak plasma concentration of topotecan by 3-fold.

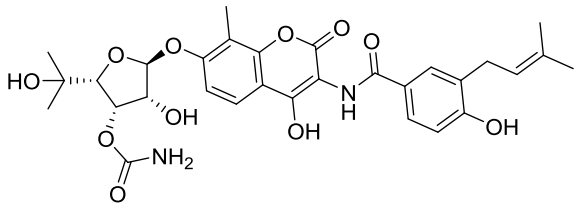

94

Figure 1-14 Antibiotics

1.4.5.2 Curcuminoids

Curcumin (or diferuloylmethane) is a polyphenol found in the rhizomes of the plant *Curcuma longa* (turmeric) and known for its antitumor, antioxidant, antiarthritic, anti-amyloid and anti-inflammatory properties.[99] Curcumin was shown to interact with the transporter with very high affinity and reverses ABCG2-mediated drug resistance.[100]

Ambudkar et al. evaluated the ability to modulate the function of the ABCG2 transporter in the cellular mitoxantrone accumulation of three purified curcuminoids found in turmeric powder, which are curcumin (curcumin I, **95**), demethoxycurcumin (curcumin II, **96**), and bisdemethoxycurcumin (curcumin III, **97**). The curcuminoids **95-97** (Curcumin I; IC_{50} 2.2 nM, II IC_{50} 2.5 nM and III IC_{50} 1.9 nM, Figure 1-15) inhibited the transport of the substrates from ABCG2-expressing cells and the maximal inhibition was comparable with 5 µM FTC (**82**, IC_{50} 2.1 nM). These findings suggest that curcuminoids may play an important role in clinical therapy and the simultaneous administration of recommended therapeutic doses of curcuminoids with anticancer drugs would probably result in an increased bioavailability of the drugs inside the cells. Thus, these curcuminoids (or curcumin mixture) might be used as modulators offering clinical benefits to improve the effectiveness of chemotherapy in cancer patients.[101,102]

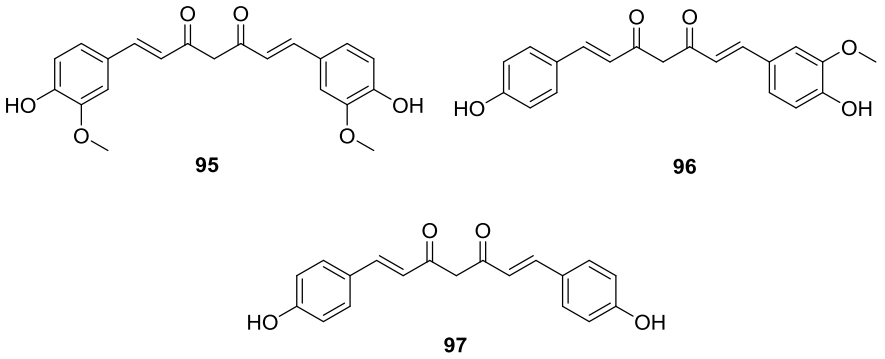

Figure 1-15 Curcuminoids

1.4.5.3 Fungal Metabolites

Fungi inhabit a wide range of environments, including extreme environments such as hypersaline waters, tropical forests, and deserts. A wide variety of fungal derived bioactive compounds have been described, including, a number of antibacterial agents (cephalosporins), immunosuppressive drugs (cyclosporins), and anticancer candidates (plinabulin and fumagillin).[103]

Interactions between immunosuppressants such as cyclosporine A (CsA, **98**) and ABCG2 substrate chemotherapy drugs have already been reported. Mao et al. investigated the effect of the immunosuppressants **98**, tacrolimus (**99**, FK-506, fujimycin) and sirolimus (**100**, rapamycin, Figure 1-16) as possible inhibitors of ABCG2.[104] The EC_{50} values for inhibition of ABCG2-mediated PhA efflux were 4.3 ± 1.9 µM (**98**), 3.6 ± 1.8 µM (**99**) and 1.9 ± 0.4 µM (**100**). The reversal capability of CsA, tacrolimus and sirolimus to ABCG2-mediated topotecan and MX resistance was studied at 2 and 5 µM at which the three immunosuppressants showed no apparent toxicity (CsA and tacrolimus) or low toxicity (sirolimus) to HEK cells. Upon addition of 2 and 5 µM CsA, the relative resistance (RR) values of topotecan were reduced from 16.7 to 5.6 and 3.6 in HEK/482R cells, respectively, whereas the reversal capability of tacrolimus and sirolimus to topotecan resistance was even greater than that of CsA as topotecan resistance was nearly completely reversed. Direct efflux studies performed with immunosuppressants **189–191** revealed that the intracellular levels of [^{3}H]-CsA, tacrolimus or sirolimus in HEK/482R and HEK/vector cells were not significantly different and that the addition of the ABCG2 modulator FTC (**82**) did not affect the efflux, suggesting a non-substrate behavior.[104]

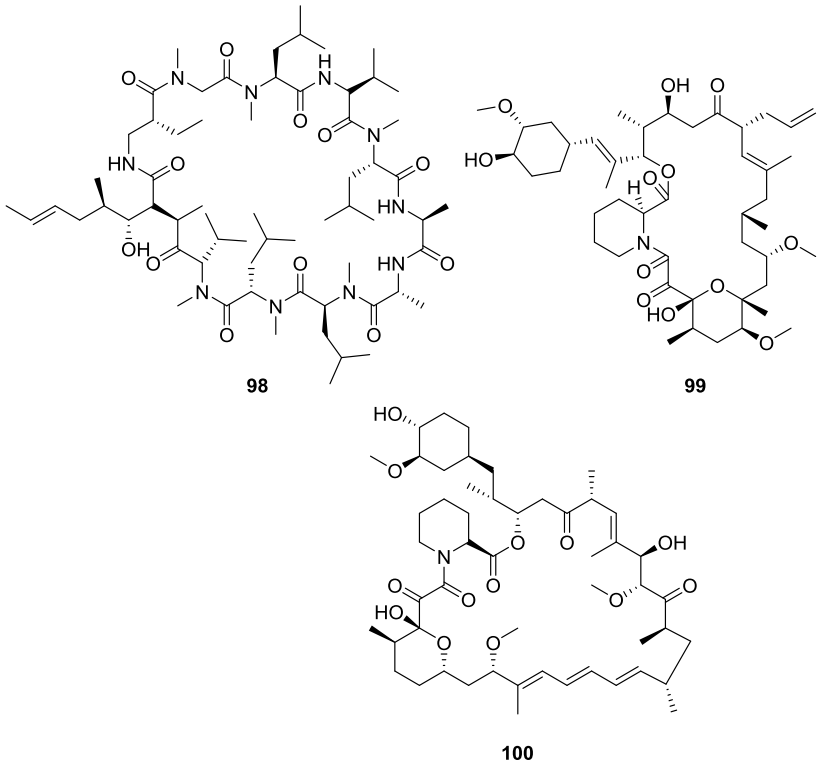

Figure 1-16 Fungal metabolites

1.4.5.4 Miscellaneous Natural Products and their derivatives

Many unique natural products from marine habitats are used for pharmaceutical and biotechnological applications.[105] Compounds isolated from marine sources are evalated in clinical trials or serve as prototypes for the design and synthesis of new therapeutic agents, like vidarabine (for the treatment of a recurrent epithelial keratitis caused by herpes simplex virus type 1 and 2 and superficial keratitis), cytarabine (for cancer), ziconotide (for the treatment of severe chronic pain in patients with cancer or AIDS), trabectedin (for use as an anticancer agent against soft tissue sarcoma) and halaven (for metastatic breast cancer).[44,106]

The indolocarbazole (ICZ) family of natural products is a source of lead compounds with potential therapeutic applications in the treatment of cancer and other diseases. The compounds have been isolated from different organisms; from prokaryotes (actinomycetes, cyanobacteria, b-proteobacteria) to eukaryotes (myxomycetes, basidiomycetes,marine invertebrates).[107] Robey et al. examined the ability of

indolocarbazole to inhibit ABCG2. At a concentration of 10 µM, all of the tested compounds increased the intracellular fluorescence of the ABCG2-specific substrate PhA in ABCG2-transfected HEK-293 cells by 1.3 to 6-fold as measured by flow cytometry; whereas FTC (**82**) increased intracellular fluorescence by 6.6-fold. K252c (**101**, Figure 1-17) and arcyriaflavin A (**102**, Figure 1-17) were the most potent compounds, with IC_{50} values for inhibition of [^{125}I]-iodoarylazidoprazosin (IAAP) labeling of 0.37 and 0.23 µM, respectively. The results show that indolocarbazoles interact with the ABCG2 protein and may increase the oral bioavailability of ABCG2 substrates.[108]

Tryprostatin A (TPS-A, **103**, Figure 1-17) is an *Aspergillus fumigatus* secondary metabolite with a diketopiperazine scaffold structurally similar to FTC (**82**). This compound was evaluated for its ability to reverse of ABCG2-mediated drug resistance in MCF-7 cells. At a concentration of 1 µM, **103** gave a dose-dependent sensitization of ABCG2-expressing cells to mitoxantrone (IC_{50} for mitoxantrone without **103**: 0.013 ± 0.006 µM, IC_{50} for mitoxantrone with **103**: 0.021 ± 0.005 µM) while the positive control elacridar (**129**) gave an IC_{50} of 0.034 ± 0.009 µM at the same concentration. TPS-A (**103**) is of interest as a pharmacologic tool for *in vivo* studies as well as in functional assays of ABCG2-dependent drug efflux activity for individual tailoring of chemotherapeutic regiments.[38,109]

In 2009, extracts from the marine ascidian *Botryllus tyreus* were found to be active when tested for inhibition of ABCG2-mediated PhA transport. After purification of the extract, ten botryllamides (known botryllamides A-H and new botryllamide I and botryllamide J) were obtained and evaluated in a PhA accumulation assay with FTC (**82**, 1 µM, IC_{50} 0.79 µM) as reference compound in NCI-H460/MX20 cells. Except botryllamides C and H the maximal activity was at least 60% compared to FTC (**82**). Botryllamide G (**104**, IC_{50} 6.9 µM, I_{max} 123.7%, Figure 1-17) was the most potent botryllamide of this series. The activity as modulators of ABCG2 was further confirmed in a flow-cytometry-based assay. Inhibition of ABCG2-mediated BODIPY-prazosin efflux from ABCG2-transfected HEK293 cells was investigated with either 10 µM FTC (**82**) or 10 µM botryllamide. In presence of FTC (**82**) a 3.4-fold increase of intracellular BODIPY-prazosin fluorescence compared to the absence of any modulator was observed. Except botryllamides H and J, all botryllamides were able to increase the intracellular fluorescence of the substrate 2.3 to 3.3-fold. Furthermore, the authors studied the competition of the botryllamides with [^{125}I]-iodoarylazidoprazosin (IAAP) labelling of the ABCG2 protein and the stimulation of the

ATPase activity of ABCG2. Botryllamide G (**104**) is the most potent and ABCG2-specific compound of this series.[96]

To explore a SAR study among the botryllamides with regard to ABCG2, additional twelve structural analogues were synthesized. ABCG2 inhibitory activity was evaluated by the cellular accumulation of the ABCG2 specific substrate PhA in ABCG2-overexpressing cells using FTC (**82**, IC_{50} 0.79 µM) as positive control. Synthetic botryllamide **105** (IC_{50} 6.4 µM, Figure 1-17) was the most potent and specific ABCG2 modulator of this series. The biological activity of synthetic botryllamide analogues implied that the 2-methoxy-*p*-coumaric acid portion (C1-C9), and the degree of double bond conjugation within this group, were critical for inhibition of ABCG2. This structural studies provide the basis for the continued preclinical evaluation of the botryllamides and it may lead to the development of more potent and selective ABCG2 modulators as potential therapeutic agents.[110]

Harmine (7-methoxy-1-methyl-9*H*-pyrido[3, 4-*b*]indole, **106**, Figure 1-17) is a tricyclic *ß*-carboline alkaloid and a monoamine oxidase inhibitor (MAOI) widely distributed in nature. This alkaloid was isolated from marine brown alga, some cyanobacteria and marine animals. It shows antimicrobial, antiplasmodial, antifungal, antioxidative, antitumor, antimutagenic, cytotoxic and hallucinogenic properties.[111] In 2010, harmine was identified in a screening program as a novel ABCG2 reversal agent; it inhibited ABCG2-mediated drug efflux and increased the cytotoxicity of mitoxantrone (1 µM **106**, IC_{50} 2.71 µM) and camptothecin (5 µM **106**, IC_{50} 1.15 µM) in the cancer cell line MDA-MB-231. Moreover, harmine did not inhibit ABCB1-mediated drug efflux.[93] Similar to FTC (**82**), the neurotoxicity and cytotoxicity of **106** led to an exclusion of this compound from further studies.

A series of naphthopyrones isolated by Mckee et al. from marine crinoids of the Comasteridae family were evaluated for their ability to inhibit the multidrug transporter ABCG2 by measuring the accumulation of the ABCG2 specific substrate PhA in ABCG2-overexpressing NCI-H460 MX20 cells. Authors found that in comparison to the positive control FTC (**82**, 1 µM, 100% inhibition), six angular naphthopyrones (**107**–**112**, Figure 1-17) showed moderate activity (I_{max} 59.3, 46.3, 31.0, 54.3, 27.5, 44.0%, IC_{50} 11.9, 5.9, 12.8, 9.0, >20, 16.6 µM respectively) while none of the tested linear naphthopyrones inhibited ABCG2-mediated transport.[112]

Liao et al. identified a novel nor-neolignan, asperjinone (**113**, Figure 1-17) isolated from *Aspergillus terreus*, and twelve known compounds from thermophilic *A. terreus*. Among them, terrein (**114,** Figure 1-17) was 100-fold more cytotoxic against breast cancer MCF-7 cells than paclitaxel, which is an antimicrotubule agent. The IC_{50} value of **114** against breast cancer MCF-7 cells was 1.1 nM, whereas for paclitaxel it was 0.1 µM. A reduction of the growth rate by 70% was observed upon incubation of MCF-7 cells with **114** (1 nM). This suppressive effect was achieved by introducing apoptosis via activation of the caspase-7 pathway and inhibition of the Akt signaling pathwayin ABCG2-expressing cells. The findings suggest that terrein may serve as a potential ABCG2 modulator for the treatment of drug-resistant breast cancer cells.[103]

The lamellarins are a group of over 30 naturally occurring pyrrole alkaloids isolated from several marine invertebrates such as sponges which show interesting anticancer and antiviral activities.[44] Their name comes from *Lamellaria sp.*, a prosobranch mollusc (family Lamellariidae).[113,114] In 2014, Lamellarin O (**115**, Figure 1-17) was identified as a selective modulator of ABCG2 in a flow cytometry based mitoxantrone efflux assay in NCI-H460/MX20 cells. It was found that compound **115** exhibited an increase in intracellular concentration of mitoxantrone (3.05-fold, 94.5%, 20 µM) which was comparable to that of FTC (**82**, 3.17-fold, 100%, 10 µM), indicating **115** as a promising ABCG2 modulator.[115]

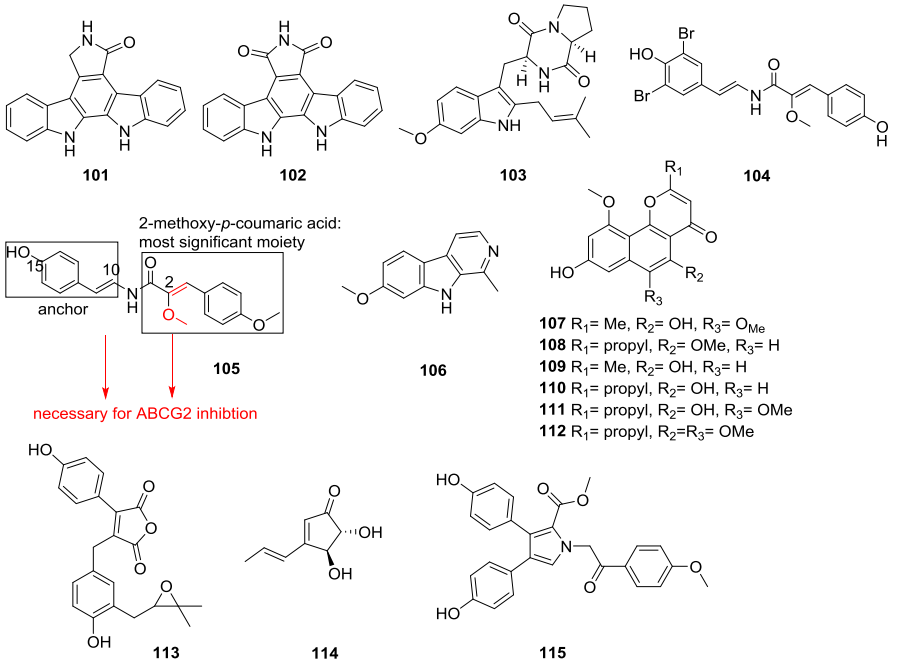

Figure 1-17 Miscellaneous Natural Products and their derivatives

1.4.5.5 Metabolites and others

Ginsenosides are among the active ingredients of Ginseng, a slow-growing perennial plant which has been used in traditional herbal remedies/medicine in Eastern Asia for over 2000 years.[116] In 2006, ginsenosides derived from Panax ginseng were examined as potential modulators of ABCG2 on cellular mitoxantrone accumulation using reserpine as positive control (5 µM, IC_{50} 1.95 µM). Metabolites PPD (**116**, IC_{50} 1.13 µM), PPT (**117**, IC_{50} 3.50 µM) and Rh2 (**118**, IC_{50} 1.62 µM, Figure 1-18) at a concentration of 20 µM enhanced MX associated cytotoxicity in MCF-7/MX cells overexpressing ABCG2 and inhibited MX efflux in the same cell line. PPD additionally stimulated ATPase activity.[117]

All-*trans* retinoic acid (ATRA, **119**, Figure 1-18) is a bioactive metabolite of vitamin A involved in many biological functions, e.g. reproduction, vision and immune response. In 2010, Matsuzaki et al. investigated ATRA as a modulator of ABCG2 by flow cytometry with doxorubicin as substrate. KSL cells treated with doxorubicin and ATRA (50 µM) or with doxorubicin and reserpine (7 µM) as a reference displayed higher fluorescence than without any modulator.[118] These results show that ATRA has a novel function as modulator of the ABCG2 transporter.

Falcarinol type polyacetylenes are present in vegetables such as carrots and parsley. They display interesting bioactivities and have the potential being health-promoting and therapeutic agents.[119] In a recent study, falcarinol (**120**, IC_{50} 41.7 µM), falcarindiol (**121**, IC_{50} 29.7 µM), falcarindiol 3-acetate (**122**, IC_{50} 36.5 µM, Figure 1-18) and the non-natural falcarindiol 3,8-diacetate (**123**, IC_{50} 19.7 µM, Figure 1-18) were examined for their ABCG2-modulating properties using three *in vivo* models, namely accumulation of the ABCG2 substrate MX in HEK293 cells overexpressing ABCG2, a vesicular transport assay and an ATPase assay. The mitoxantrone accumulation assay was performed with Ko143 (**85**) as reference compound at a concentration of 5 µM whereby a 1.9-fold MX accumulation was observed. Compound **121** (20 µM) was able to produce an 1.5-fold accumulation, while the other three polyacetylenes were in the range of 1.2 to 1.3-fold accumulation indicating a moderate inhibition effect. In the vesicular transport assay all polyacetylenes show a concentration-dependent inhibition of the tritiated methotrexate ([^{3}H]-MTX) transport. Compound **123** had the lowest IC_{50} value of 19.7 µM (Ko143, **85**, 0.026 µM). The results indicate a possible role of ABCG2 in the absorption and

disposition of the polyacetylenes and suggest a potential application as MDR reversal agents.[120]

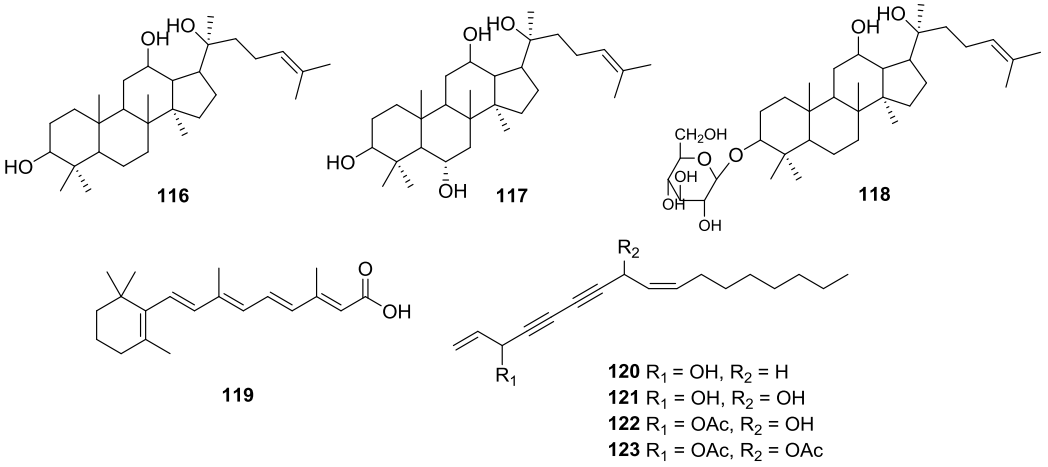

Figure 1-18 Metabolites and others

1.4.5.6 Stilbenes

The tubers of *Bletilla striata* (Orchidaceae) have been used as traditional medicine to treat pulmonary tuberculosis and as hemostatic agent. In 2005, Morita et al. examined the potential of reversal of ABCG2-mediated drug resistance with eight stilbenoids isolated from *B. striata*. Three stilbenoids (compounds **124-126**, Figure 1-19) were able to increase the cytotoxicity of the ABCG2 substrate SN-38 in K562/ABCG2 cells but not in K562 cells. Reversal indices for SN-38 (given as the ratio of IC_{50} measurements in the absence of the reversal agent to levels in the presence of the reversal agent) were 1.7, 1.8 and 3.0, for compounds **124**, **125** and **126**, respectively.[121,122]

In 2011, a series of eleven methoxylated resveratrol analogues were evaluated as ABCG2 modulators. The best compound of this series (**127**, IC_{50} 0.16 µM, Figure 1-19) showed a maximal inhibition of mitoxantrone efflux of 75% measured by flow cytometry, using elacridar (**129**, IC_{50} 0.16 µM) as reference (100% inhibition). Methoxy stilbenes were found effective for inhibition without inducing cytotoxicity, suggesting that these molecules could be used in combination with other modulators to block ABCG2 drug-efflux activity and appear to be good candidates for *in vivo* experiments.[123]

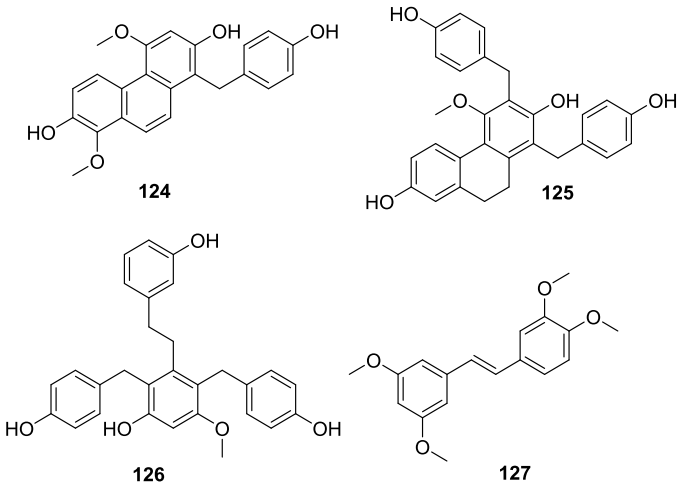

Figure 1-19 Stilbenes

1.4.6 Other Types of Modulators

1.4.6.1 Acridones

Natural and synthetic acridones are well known heterocyclic compounds that exhibit a broad spectrum of biological activities and found applications in oncology.[124] In 2007, a series of acridone derivatives was synthesized and their ABCG2 modulatory activity was investigated using human wild-type (R482) ABCG2-transfected cells. One of the acridones, namely MBLI-87 (**128**, IC_{50} 0.56 µM, 112.3% inhibition, Figure 1-20) was as potent as the reference compound elacridar, which is an acridone-derived compound (**129**, IC_{50} 0.41 µM, 100% inhibition, Figure 1-20) inhibiting mitoxantrone efflux. The camptothecin analogue irinotecan and its active metabolite SN-38 are both substrates of ABCG2. By addition of MBLI-87 (**128**) a significant sensitization to irinotecan and SN-38 was observed, although the doses remained below the maximum tolerated dose due to the limited solubility of **128**.[125-127]

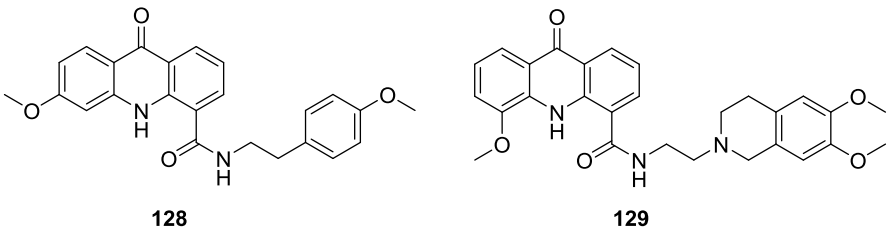

Figure 1-20 Acridones

1.4.6.2 Anthelmintics

Barrera et al. identified the anthelmintic triclabendazole (TCBZ, **130**, Figure 1-21) and its main plasma metabolites triclabendazole sulfoxide (TCBZSO, **131**, Figure 1-21) and triclabendazole sulfone ($TCBZSO_2$, **132**, Figure 1-21) as modulators of ABCG2 *in vitro* and *in vivo* with different assays and substrates. For example, an accumulation assays with mitoxantrone as substrate and murine Abcg2- and human ABCG2-transduced MDCKII cells confirmed that TCBZSO and $TCBZSO_2$ are ABCG2 modulators. TCBZ as parent drug is not detected in plasma, and in mitoxantrone accumulation assays with a concentration range from 5 to 25 µM, both metabolites (TCBZSO and $TCBZSO_2$) showed inhibitory potencies between 40 and 55% for murine Abcg2/human ABCG2. These results support the potential of TCBZSO and $TCBZSO_2$ to participate in drug interactions and modulate ABCG2-mediated pharmacokinetic processes.[128-130]

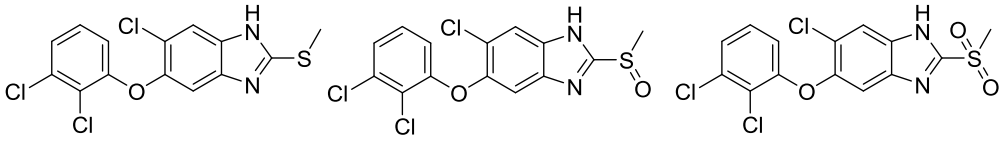

130 **131** **132**

Figure 1-21 Anthelmintics

1.4.6.3 Hormones

New strategies to circumvent ABCG2 mediated MDR in the central nervous system (CNS) are required. One major approach to increase brain drug levels is to manipulate signaling mechanisms that control transporter expression and function. In 2010 the long-term effect of 17*β*-estradiol on ABCG2 was investigated in an *ex vivo* model for the blood-brain barrier (BBB).[131] Concomitantly, levels of ABCG2 mRNA were reduced by 17*β*-estradiol (**133**) suggesting a down-regulation of the ABCG2 transporter via a genomic pathway. Mahringer et al. identified the estrogen receptor beta (ER *β*) being linked to the function of ABCG2 upon stimulation with **133**.[132]

Masereeuw et al. investigated the interaction between ABCG2 activity and twelve steroid hormones using membrane vesicles of HEK293/ABCG2 cells. Estradiol (**133**, 40.4%, Figure 1-22), testosterone (**134**, 20.1%, Figure 1-22), progesterone (28.7%) and

androstenedione (**135**, 42.4%, Figure 1-22) were the most efficient compounds of this series inhibiting tritiated estrone-sulphate (E_1S) uptake in a concentration-dependent manner. The vesicular E_1S uptake is expressed as a percentage of maximum uptake after incubation with 250 nM E_1S with or without 50 µM of the steroid. The efficient inhibition implies a clear interaction between the steroids and the efflux pump.[133]

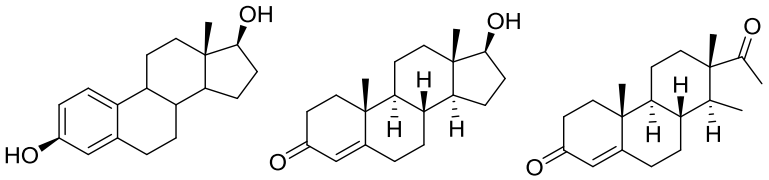

133 **134** **135**

Figure 1-22 Hormones

1.4.6.4 Kinases

Cyclin-dependent kinases (CDKs) are protein kinases, which are involved in many diverse biological processes. Their regulation by small-molecule inhibitors, e.g. purine cyclin-dependent kinase inhibitors (CDKi), opens an opportunity for the treatment of cancer. In 2012, five purine CDKi were investigated for their inhibitory effect on ABCG2 transport activity *in vitro* using accumulation assays in ABCG2-transduced MCDKII cells and Hoechst 33342, glyburide as substrate and FTC (**82**) as reference. Four of the five CDKi inhibited ABCG2 significantly in the following order: purvalanol A (**136**, Figure 1-23) > olomoucine II (**137**, Figure 1-23) ≈ FTC > roscovitine (**138**, Figure 1-23) ≈ bohemine (**139**, Figure 1-23). Compounds **136** and **137** are comparable to FTC (**82**). The same order of potency was found in dually perfused rat placenta expressing Abcg2, but the associated mechanism is not clear.[134,135]

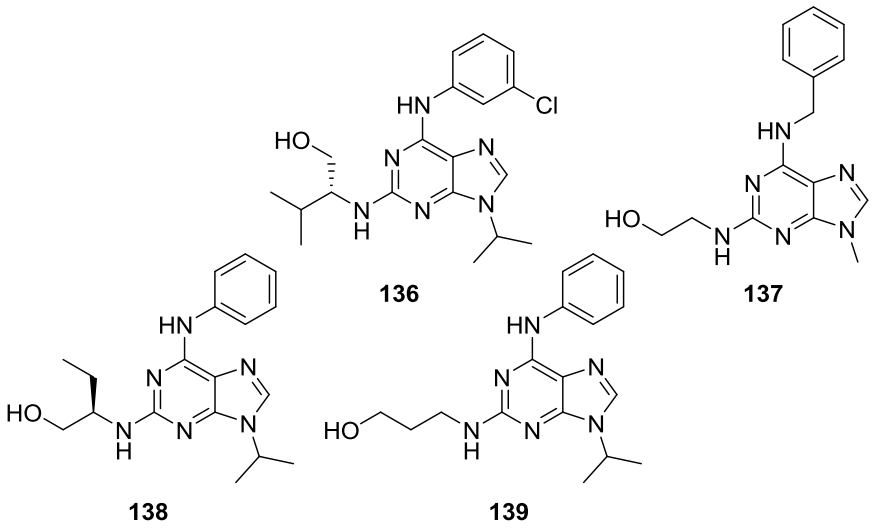

Figure 1-23 Kinases

1.4.6.5 Xanthines

Methylxanthines and other xanthine derivatives are adenosine receptor (AR) antagonists, which are used for treatment of asthma, chronic bronchitis, emphysema and neural degenerative diseases.[136] Furthermore, the AR antagonist 1,3,7-metyxanthine (**140**, also known as caffeine, Figure 1-24) has been shown to downregulate the expression of ABCG2 in cancer cell lines in a time- and dose-dependent and reversible way.[137]

Also theophylline and dyphylline decreased ABCG2 expression significantly in MCF-7/MX100 cells in a time-dependent, dose-dependent and reversible manner. Caffeine treatment was shown to increase the retention of mitoxantrone. Combination treatment with MX and **140** (IC_{50} 81.4 µM) decreased the IC_{50} of MX tenfold and induced a greater degree of apoptotic cell death than MX treatment alone (IC_{50} 946.5 µM). These results unveil xanthines as potential chemosensitizers.[137,138]

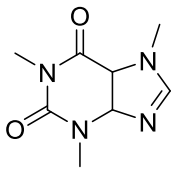

140

Figure 1-24 Caffeine

1.4.7 Tariquidar-like Compounds

Compound XR9576 (**141**, tariquidar, Figure 1-25) is an anthranilamide derivative, which was developed as a modulator of ABCB1 undergoing clinical trial III studies. Unfortunately, the outcome of the clinical trials was disappointing due to inefficiency and toxic effects. However, appropriate dosing, considering altered pharmacokinetics and a proper selection of the patient cohort may had produced different results.[139] Later, it has been shown that **141** inhibits both ABCB1 and ABCG2 transport function similarly to elacridar (**129**), and was now used as a scaffold for designing ABCG2-specific modulators by structural modifications.[140]

Wiese et al. investigated 30 compounds, which are structurally related to **141** *in vitro* and also with 3D-QSAR models in order to identify the main structural features determining the interaction with ABCB1 or ABCG2. Elimination of the methoxy groups in positions 6 and 7 of the tetrahydroisoquinoline substructure, the addition of a second amide linker, a shift of the hetarylcarboxamido group from the ortho to the meta position and the introduction of an ester group to the central aromatic core were shown to increase the interaction with ABCG2.[141,142]

Kühnle et al. synthesized a series of selective ABCG2 modulators by minimal structural modification, replacing the 3,4-dimethoxy-2-(quinoline-3-carbonylamino)benzoyl moiety in tariquidar (**141**) with a 4-methoxycarbonylbenzoyl moiety bearing a hetarylcarboxamide group in 3-position. This resulted in a drastic shift in favor of ABCG2 inhibition. A quinoline-3-carboxamide (**142**, IC_{50} 0.119 µM, Figure 1-25) or quinoline-2-carboxamide group (**143**, IC_{50} 0.060 µM, flow cytometric mitoxantrone efflux assay, topotecan-resistant MCF7 breast cancer cells, using Ko143 (**85**) as positive control with an IC_{50} value of 0.225 µM, Figure 1-25) gave the most potent compounds of the series. Furthermore, the selectivity for ABCG2 over ABCB1 was about 100 to 500-fold and the compounds were inactive at ABCC2. Chemosensitivity assays against MCF-7/Topo cells revealed that the non-toxic modulator **143** completely reverted ABCG2-mediated topotecan resistance at concentrations higher than 100 nM, whereas **142** showed ABCG2 independent cytotoxicity.[143]

Interestingly, compounds bearing triethylene glycol ether groups at the tetrahydroisoquinoline moiety (**144** and **145**, Figure 1-25) were comparable to compound **143** in potency, but considerably more efficient (I_{max} 83% and 88% vs 60%, FTC, **82**, as

reference was set to 100%). These results support the hypothesis that solubility of the new ABCG2 modulators and of the reference compounds tariquidar (**141**) and elacridar (**129**) is the efficacy limiting factor in aqueous media. Unfortunately, the compounds were unstable in mouse plasma due to rapid enzymatic cleavage of the benzamide bond. Replacing of the labile benzanilide core was considered as a promising bioisosteric approach to solve the stability problem.[144]

In search for more stable analogues, according to a bioisosteric approach, a series of *N*-(biphenyl-3-yl)quinoline carboxamides were prepared both by solid phase and solution phase synthesis. Inhibition of ABCG2 was determined in a Hoechst 33342 accumulation assay. Most synthesized compounds inhibited the ABCG2 transporter selectively at submicromolar concentrations with a maximal inhibitory effect (I_{max}) over 90%, (compound **146**, IC_{50} 0.591 µM, I_{max} 109%; **147**, IC_{50} 0.544 µM, I_{max} 112%, Figure 1-25). The biphenyl analogues **146** and **147** are considerably more stable and show that the benzanilide core is not a crucial structural element of quinoline carboxamide-type ABCG2 modulators.[145]

In modulators **148** and **149** (Figure 1-25) the labile benzamide unit was replaced by quinolyl (**148**) and indolyl moieties (**149**). The compounds were investigated together with the reference compounds FTC (**82**, IC_{50} 731 ± 92 nM, 10 µM as 100% ABCG2 inhibition), Ko143 (**85**, IC_{50} 117 ± 53 nM) and tariquidar (**141**, 1 µM as 100% ABCB1 inhibition, ABCB1: IC_{50} 223 ± 8 nM, I_{max} 103 ± 2%, ABCG2: IC_{50} 526 ± 85 nM, I_{max} 69 ± 5%) in a calcein-AM and a Hoechst 33342 microplate assay using ABCB1-overexpressing Kb-V1 and ABCG2-overexpressing MCF-7/Topo cells. The quinoline analogue **148** (IC_{50} 602 ± 44 nM, I_{max} 60%) was inactive at ABCB1 and ABCG2. However, the compound is poorly soluble and therefore inferior to compound **149** (ABCG2: IC_{50} 46 ± 1 nM, I_{max} 111 ± 9%, ABCB1: IC_{50} 3570 ± 640 nM, I_{max} 36 ± 4%), which is superior to tariquidar (**141**), FTC (**82**) and even Ko143 (**85**). Moreover, compound **149** had no effect on the cell proliferation even at a high concentration of 1 µM, whereas a strong cytostatic effect was observed in combination with topotecan (100 nM).[146]

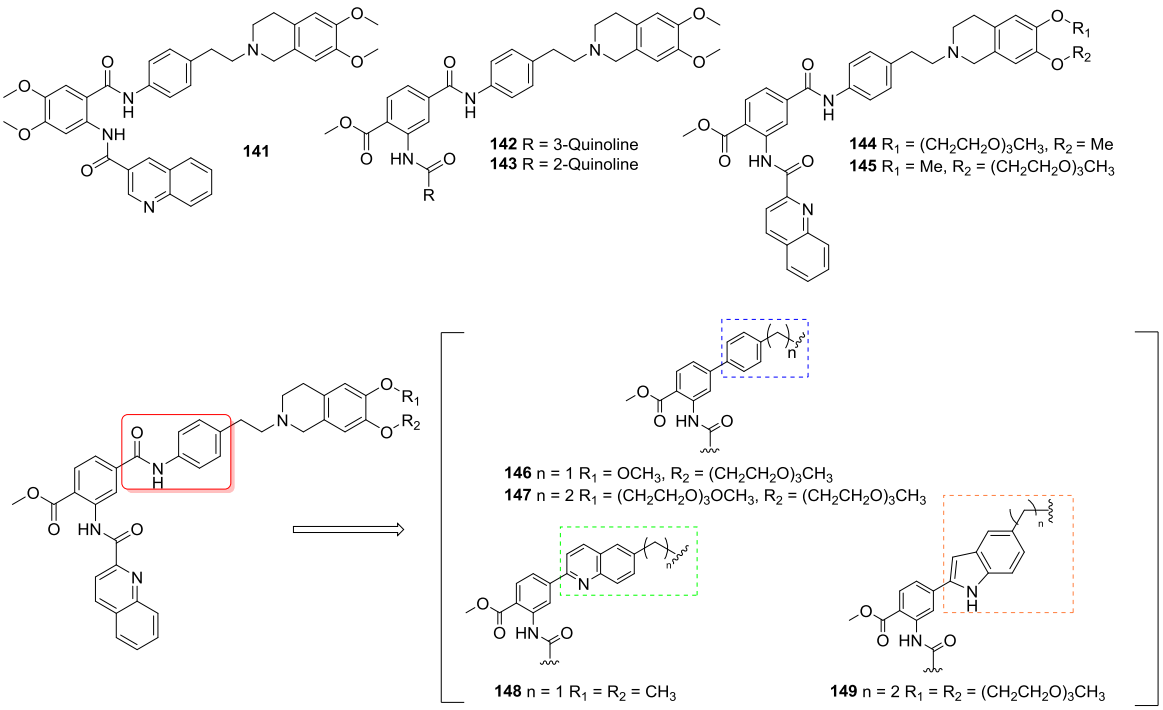

Figure 1-25 Tariquidar analogues

Subsequently, the labile amide and ester groups were replaced by a triazole and a ketone moiety in a bioisosteric approach[147,148] resulting in a 24 h plasma-stable, ABCG2-selective quinoline-carboxamide type series of very potent modulators. Compound **150** (Figure 1-26) inhibited the ABCG2 transporter to 95% with an IC_{50} value of 64 nM without affecting ABCB1 or ABCC1 (FTC, **82**, as reference for 100% ABCG2 inhibition, IC_{50} 731 nM). Combining selective and potent ABCG2 modulation with high plasma stability, the modulators are promising candidates for *in vivo* investigations. Studies on the bio-distribution of the modulators and their effect on the pharmacokinetics and enhancement of cytostatic concentration of co-administered topotecan are subject of ongoing work (unpublished data).

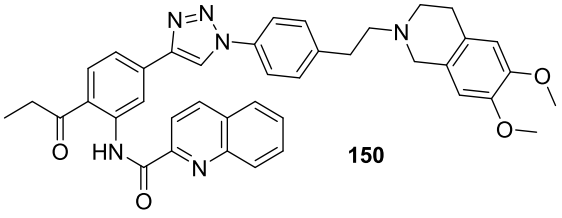

Figure 1-26 Triazolic tariquidar analogue

1.4.8 Tyrosine Kinase Inhibitor-Based Compounds

Various tyrosine kinase inhibitors (TKIs) were designed as anticancer agents with high specificity and selectivity. However, as most TKIs are targeting intracellular parts and therefore have to cross cell membranes, their therapeutic potential may be drastically affected by certain ABC membrane transporters. Recently, it was demonstrated that several human multidrug transporter ABC proteins interact with specific TKIs. In particular, the ABCG2 transporter has a high affinity for some of the TKIs.[149] In the following, we discus first TKIs as inhibitors of epidermal growth factor receptor (EGFR) and followed by other TKIs.

1.4.8.1 Epidermal Growth Factor Receptor (EGFR) Inhibitors

Mutations of the epidermal growth factor receptor (EGFR) are correlated with tumor proliferation. Inhibition of EGFR by small molecule inhibitors, such as gefitinib (**151**), pelitinib (**152**), neratinib (**153**), vandetanib (**154**) and telatinib (**155**) is therefore a promising therapeutic option.[9]

Gefitinib (**151**, “Iressa”, ZD1839, Figure 1-27) is an orally active, selective EGFR-TKI used for the treatment of certain cancer types. Gefitinib was already reported to act as chemosensitizer combined with various cytotoxic agents *in vitro*. However, the underlying mechanism was not described. In 2005, Nakamura et al. investigated the mode of action of gefitinib (**151**) in multidrug-resistant MCF-7 cells overexpressing ABCG2 by monitoring the intracellular topotecan accumulation. No effects of **151** were observed in the parental cells. Reversal of drug resistance in MCF-7/MX cells was observed with gefitinib (**151**, 2 µM) in combination with topotecan (IC_{50} 716 ± 118 nM), SN-38 (IC_{50} 116 ± 18.2 nM), and mitoxantrone resistance (IC_{50} 178 ± 16.3 nM) in comparison to topotecan (4143 ± 161 nM), SN-38 (1139 ± 79.3 nM) and mitoxantrone (1210 ± 289 nM) alone. The results show that gefitinib (**151**) effectively reversed drug resistance through inhibition of drug efflux in three multidrug-resistant cancer cell lines overexpressing ABCG2 and was not transported itself.[150]

If local drug concentrations are low, ABCG2 can confer gefitinib (**151**) or pelitinib (**152**, Figure 1-27) resistance. However, anti-cancer efficiency of neratinib (**153**, Figure 1-27) and vandetanib (**154**, “Caprelsa”, Figure 1-27) will most probably not be restricted.

Conformational changes of ABCG2 can be monitored with the anti-ABCG2 5D3 antibody, and drugs, which increase 5D3 immunoreactivity of ABCG2 similar to 1 µM Ko143 (**85**, 100% 5D3 binding) are likely to inhibit ABCG2 function as well. The most pronounced increase in 5D3 binding was obtained when 10 µM EGFR inhibitors were applied. 5D3 binding in A431/ABCG2 cells was observed for gefitinib (71.3%), pelitinib (41.9%), vandetanib (9.3%) and neratinib (26.0%) relative to Ko143 (**85**). The finding that these EGFR inhibitors efficiently block ABCG2 function may help to design novel therapeutic drug-combination strategies.[9]

Telatinib (**155**, Figure 1-27) is a small molecule TKI inhibiting vascular endothelial growth factor receptor (VEGFR), platelet-derived growth factor receptor-ß (PDGFR-ß) and stem cell growth factor receptor (c-KIT). Chen et al. examined telatinib in 2014 as a reversal agent for ABCG2-mediated MDR in H460/MX20 and HEK293 cells overexpressing ABCG2 *in vitro* and *in vivo*. In the cell viability assay the cytotoxicity of ABCG2 substrate anticancer drugs was enhanced in ABCG2-transfected cells and drug selected ABCG2-overexpressing cancer cells, whereas it has no effect on the parental cells lacking the ABCG2 transporter. Also, no effect was observed on ABCB1-, ABCC1- and ABCC10-mediated MDR. Compound **155** at 1 µM (IC_{50} 0.0468 µM) significantly enhanced the intracellular accumulation of mitoxantrone (MX) in ABCG2-overexpressing cell lines (FTC, **82**, IC_{50} 0.0442 µM as positive control). These results showed that telatinib (**155**) selectively inhibits ABCG2, potentiates the ABCG2 substrate anticancer drugs and induces cell cytotoxicity in cells overexpressing ABCG2 *in vitro* and *in vivo* at clinically achievable concentrations. The ATPase activity of ABCG2 was stimulated by telatinib in a concentration-dependent manner, indicating a substrate behavior. Co-administration of telatinib and doxorubicin significantly decreased the size of ABCG2-expressing tumor xenografts compared to the vehicle control or the group treated with doxorubicin only. The results indicate that telatinib has the potential to be used in combination with conventional ABCG2 substrate anticancer drugs to reduce the MDR-mediated by ABCG2. Nevertheless, further clinical studies are required to prove its usefulness.[151]

The same year, the EGFR inhibitor AST1306 (**156**, Figure 1-27) was evaluated on the reversal of ABCG2-mediated MDR. A significant increase of intracellular accumulation of tritiated mitoxantrone (1 µM **156**, IC_{50} 15.03 nM, FTC, **82**, 15.41 µM as positive control) in ABCG2-overexpressing HEK293 cells was observed. AST1306 (**156**) was shown to directly inhibit the function of the ABCG2 protein at non-toxic concentrations, thus

increasing the intracellular concentration of substrate anti-cancer drugs without affecting the expression or localization of ABCG2. AST1306 (**156**) might be considered as a novel reversal agent of the ABCG2 transporter with a potential to improve the clinical response when combined with conventional chemotherapeutic agents.[152]

In 2012, Pick et al. determined the inhibitory potencies of seven TKIs against ABCB1, ABCC1 and ABCG2 with different fluorescence based accumulation assays. Among them, AG1428 (**157**) and PD158780 (**158**) (Figure 1-27), were found to be selective for ABCG2 as determined by a Hoechst 33342 assay (**157**: IC_{50} 5.50 ± 0.38 µM, **158**: IC_{50} 0.36 ± 0.07 µM) and a pheophorbide A assay using MDCK/ABCG2 cells (**157**: IC_{50} 2.40 ± 0.85 µM, **158**: IC_{50} 0.25 ± 0.09 µM). However, no effect up to 10 µM was observed in the calcein-AM assay using MDCK/MDR1 cells for ABCB1 and 2008/MRP1 cells for ABCC1.[153]

The quinazolinic alpha-adrenergic blocker prazosin has been found to be a substrate of ABCG2.[154] Also the ABCG2 inhibitory potential of quinazoline based TKIs such as PD153035 (**159**, Figure 1-27) has been reported.[155]

Imatinib mesylate (**160**, “Gleevec”, STI571, Figure 1-27), is a potent kinase inhibitor used in the treatment of various cancers. The ATP competitor acts similar as many other 4-anilinoquinazolinic TKIs. The compounds potently reverse ABCG2-mediated resistance and significantly increase the accumulation of topotecan in the human osteosarcoma cell line Saos2. With an increasing concentration of **160**, the concentration of topotecan required to inhibit cell growth by half decreased from 257 nM to 10 nM. Reversal of topotecan resistance by half was achieved at a concentration of 170 nM of compound **160**. However, overexpression of ABCG2 does not confer resistance to **160**. These results suggest that **160** is a potent inhibitor, but not a substrate of the ABCG2 transporter.[156,157]

Juvale et al. investigated several 4-substituted analogues of 2-phenylquinazoline for their ABCG2 inhibition, using the Hoechst 33342 assay with MDCK/ABCG2-overexpressing cells. It was observed that quinazoline compounds bearing a phenyl substitution at position 2 of the quinazoline moiety were potent modulators. From the SAR analysis, it was observed that a meta-substituted aniline group at position 4 of the quinazoline produced higher inhibitory effects in comparison to an ortho- or para-substituted aniline

ring. Nitro, nitrile or trifluoromethyl substituents on the aniline ring were most suitable for the inhibition of the ABCG2 transporter. Compounds **161** (IC_{50} 0.130 µM, Figure 1-27) and **162** (IC_{50} 0.076 µM, Figure 1-27), both bearing an NO_2-substituent were the most active compounds among all investigated quinazolines, having even lower IC_{50} values than Ko143 (**85**, 0.25 µM) as reference. After investigating the compounds for their intrinsic cytotoxicity, it was found that compound **161** has twice the therapeutic ratio of **162**, indicating its higher usability in future *in vivo* studies. These findings can be the basis for further development of quinazolines as potent ABCG2 modulators.[155,158]

Varlitinib/ARRY-334543 (**163**) is a small molecule ATP-competitive TKI, which was studied for its ability to interact with ABC transporters to enhance the efficacy of conventional anticancer drugs. NCI-H460 ABCG2-overexpressing cells were used for the reversal study. Compound **163** (1.0 µM, IC_{50} 0.0272 µM; FTC, **82**, 5 µM, IC_{50} 0.0243 µM as positive control, Figure 1-27) directly inhibited the drug efflux transporter, thereby elevating the intracellular amount of the ABCG2 substrate mitoxantrone. The cytotoxicity of **167** was screened by an MTT assay and the IC_{50} value of **163** alone was shown to be > 10 µM. At a concentration of 1 µM **163** only slightly reversed ABCB1- and partially reversed ABCC10-mediated MDR is observed. Moreover, **163** did not affect the expression of the ABCG2 protein or cause its translocation. The TKI **163** inhibited the photoaffinity labeling of ABCG2 with [^{125}I]-IAAP and is therefore directly interacting with ABCG2 at the drug-binding pocket, which is consistent with findings for other TKIs.[159]

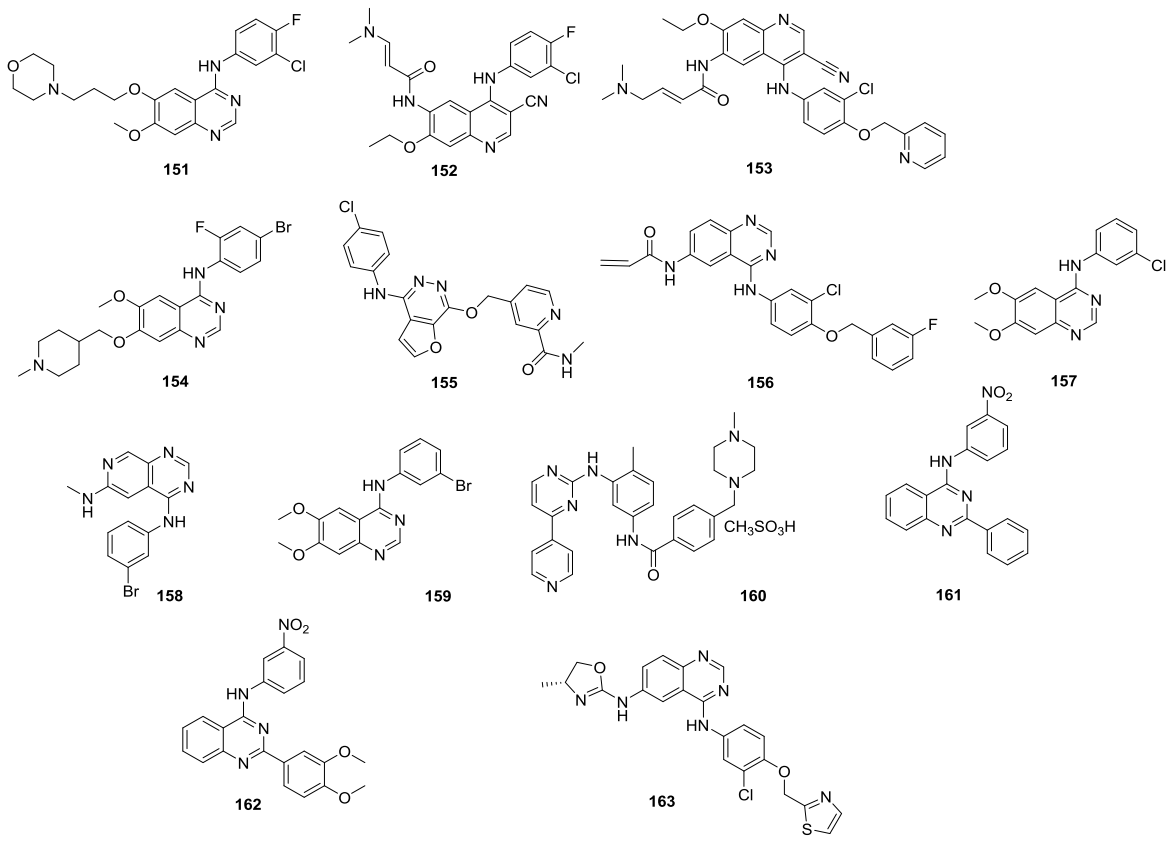

Figure 1-27 EGFR inhibitors

1.4.8.2 Other TKIs

Tyrosine kinase inhibitors (TKIs) compete with ATP for the binding at the catalytic domain of tyrosine kinases. *In vitro* studies with biochemical and cell-based assays showed that TKIs also interact as substrates or as modulators with the function of the ABC transporters such as ABCG2, ABCB1 and ABCC1.[160]

Sunitinib (**164**, "Sutent", Figure 1-28) is an ATP-competitive multi-targeted small molecule TKI of platelet-derived growth factor (PDGFRß), vascular endothelial growth factor (VEGFR2) and Fms-like tyrosine kinase 3 (FLT3). In 2009 the possible interaction of sunitinib (**164**) with ABCB1, ABCC1, ABCG2 and lung-resistance protein (LRP) was evaluated *in vitro*. The effect of sunitinib on the ABCG2 reversal is given as the ratio of the IC_{50} for S1-M1-80 cells with the anticancer drug (topotecan and doxorubicin, respectively) in the absence of **164** to the IC_{50} value obtained in the presence of **164**. The results showed that **164** gave a 56.4-fold MDR reversal for topotecan at a non-toxic

concentration of 2.5 µM of **164** (IC_{50} for topotecan with 2.5 µM **164**: 0.091 µM, IC_{50} for topotecan: 5.132 µM) and a 37.8-fold reversal for doxorubicin (IC_{50} for doxorubicin with 2.5 µM **164**: 0.181 µM, IC_{50} for doxorubicin: 6.845 µM). No significant reversal effect of **164** on ABCB1-, ABCC1- and LRP-mediated drug resistance was observed.[160]

Although the ABCG2 transporter appears to be a promising target to overcome MDR, to date no modulator has successfully passed through the clinical trials. Toxicity and safety issues are major obstacles in testing novel chemical structures. An appealing strategy is the use of already described compounds (where sudden side effects are unlikely) as ABCG2 modulators. This might be the case for sorafenib (**165**, "Nexavar"), an orally active multikinase inhibitor, which was found to induce ABCG2 degradation in lysosome in addition to act as modulator of ABCG2. The study may facilitate the rediscovery of new functions of structurally diverse FDA-approved compounds, which are ready for clinical testing and provide a safe way of reversing MDR in cancer chemotherapy. Sorafenib (**165**, Figure 1-28) serves as a substrate of the ABCG2 transporter at a low concentration. While saturating all binding sites, it can inhibit the transporter at high concentrations (2.5 µM, IC_{50} 1.31 µM, 2.1 µM MX accumulation) producing a significant increase of mitoxantrone accumulation in HEK293/ABCG2 cells (Ko143, **85**, 2.9 µM MX accumulation). The successful identification of sorafenib (**165**) as ABCG2 modulator through a pharmacophore-based evaluation process indicates that this is a valuable approach to rediscover novel uses for known drugs in the reversal of ABCG2-mediated drug transport and resistance.[161-163]

Tandutinib (**166**, Figure 1-28) is a novel small molecule multi-targeted TKI. In 2013 the capability of tandutinib to reverse ABC transporter-mediated multidrug resistance was investigated. Tandutinib potentiated the cytotoxicity of ABCG2 substrate drugs, such as topotecan (3 µM, IC_{50} 5.175 µM; FTC, **82**, 2.5 µM, IC_{50} 1.041 µM as positive control) in the S1-M1-80 ABCG2-overexpressing cell line. Tandutinib significantly reverses ABCG2-mediated drug resistance by inhibiting the drug efflux function of ABCG2 and increasing intracellular accumulation of cytotoxic agents in ABCG2-overexpressing cells. Moreover, tandutinib (**166**) was able to restore the sensitivity of side population (SP) cells to chemotherapeutic agents and exerts a positive effect on reversing ABCG2-mediated MDR.[164]

OSI-930 (**167**, Figure 1-28) is a heterocyclic anthranilamide analogue currently used as a potent multikinase inhibitor. The quinoline core of **167** was modified with either pyridyl or phenyl substituents to obtain a series of fifteen compounds, from which the nitropyridyl and ortho-nitrophenyl analogues (**168**, VKJP1 and **169**, VKJP3, Figure 1-28) were effective in the reversal of MDR mediated by ABCG2, but unable to reverse ABCB1- or ABCC1-mediated MDR indicating a selectivity for ABCG2. At a concentration of 1, 3 and 10 mM, the two OSI-930 analogues **168** and **169** decreased the IC_{50} values of ABCG2 substrates mitoxantrone, SN-38 and doxorubicin in transfected wild-type (R2) or mutant (T7) ABCG2-overexpressing cells. The IC_{50} value for the non-ABCG2 substrate cisplatin was not affected. As an example, in the ABCG2-482-R2 cell line the IC_{50} value for mitoxantrone was 278 nM and significantly lowered to 17 nM in presence of 10 µM **168** or to 53 nM in presence of **169**, respectively (positive control FTC, **82** at a concentration of 2.5 µM, IC_{50} for mitoxantrone 9.03 nM). The sensitization of cells treated with **168** (10 µM) was the same as with FTC (**82**, 2.5 µM). These results suggest that the compounds specifically inhibit the function of ABCG2 through direct interaction with its substrate binding site.[165]

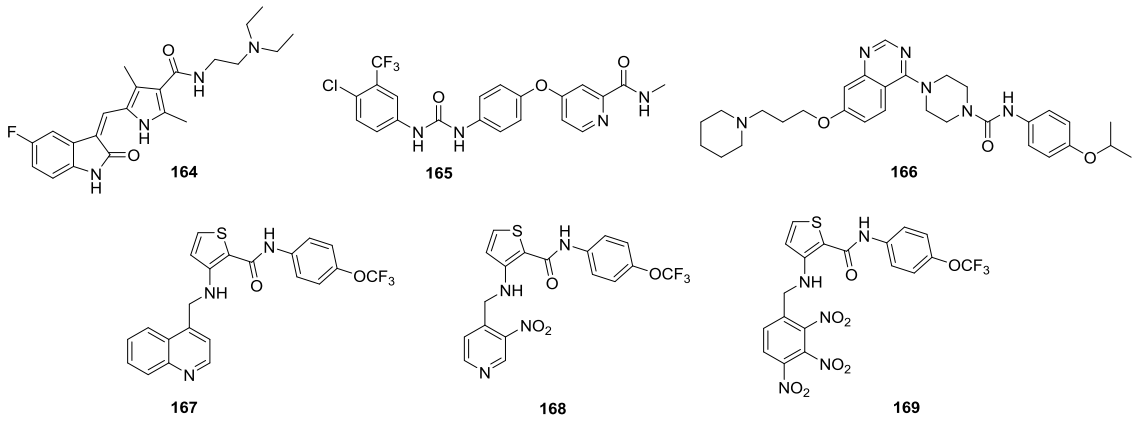

Figure 1-28 Other TKIs

1.4.9 Conclusion

In contrast to the prominent P-glycoprotein (ABCB1) very few suitable inhibitors for ABCG2/BCRP have been reported, possibly due to its recent discovery in the late 90s. The most remarkable modulator is the non-toxic FTC derivative Ko143, but recently

published data reported that this compound is unstable in rat plasma and even unspecific at higher concentrations. This inevitably will require further investigations before Ko143 can be clinically applied.

The second promising class of ABCG2 modulators is based on the chromone skeleton. The most active compound of the series was shown to be highly potent, selective for ABCG2 and not cytotoxic. The compound is a good candidate for future *in vivo* studies.

Literature research reveals an increasing number of reports on certain phytochemicals being ABC modulators, substrates and inhibitors – depending on their structure. However, the authors are aware that polyhydroxylated compounds like curcumin as well as their analogues and similar natural products are typical pan-assay interference compounds (PAINS).[166-169] PAINS are frequent hitters in high throughput assays, which may be artifacts as the compounds show unspecific binding to various proteins. Moreover, recent findings[170,171] indicate the interaction of certain phytochemicals, which were also reported as modulators of ABC transporters, with membranes causing a promiscuous behavior.

The last highly active class of compounds is comprised of the anthranilic acid core. The structural element is found in tariquidar (XR9576), an ABCB1 modulator, which reached clinical trial phase III. Minimal structural modifications resulted in a series of highly active and non-toxic modulators selective for ABCG2. However, to the best of knowledge, clinical trials to prove reversal of ABCG2-mediated MDR *in vivo* have not been published.

Well characterized and clinically useful ABCG2 modulators are highly desired and will constitute an active field of research in the future. It will be important to assess the performance of the most promising candidates in comprehensive clinical trials. Even if a translation into the clinical oncology remains challenging due to several reasons,[172] the development of potent, specific and non-toxic modulators offers the possibility to study the ABCG2 transporter at a molecular level and to gain detailed knowledge of its regulation, function and its role in certain diseases. Therefore, the investigation and development of compounds acting as modulators is not only of importance for clinical use, but is also useful for basic research serving as molecular tools for studying transporter function. Apart from that, the research focus may be extended from generating novel modulators in the laboratory to proofing their usefulness for drug accumulation *in vivo*.

1.5 Aims and Scope

ABCG2 overexpression causes resistance to treatment in two types of cancer with high incidence and mortality around the world. Prostate cancer (second most common in men in Colombia) reported 9564 cases in Colombia on 2012, of which over 30% were fatal and it is estimated that by 2017 the incidence will increase more than three times. Breast cancer (fifth leading cause of death in the country) claimed the lives of 31% of 8686 cases reported on 2012 in Colombia, and it is estimated that in 2017 the incidence would increase almost fourfold (Figure 1-29).[173,174] With these elements we decided to start a pioneering study in our country related to the ABCG2.

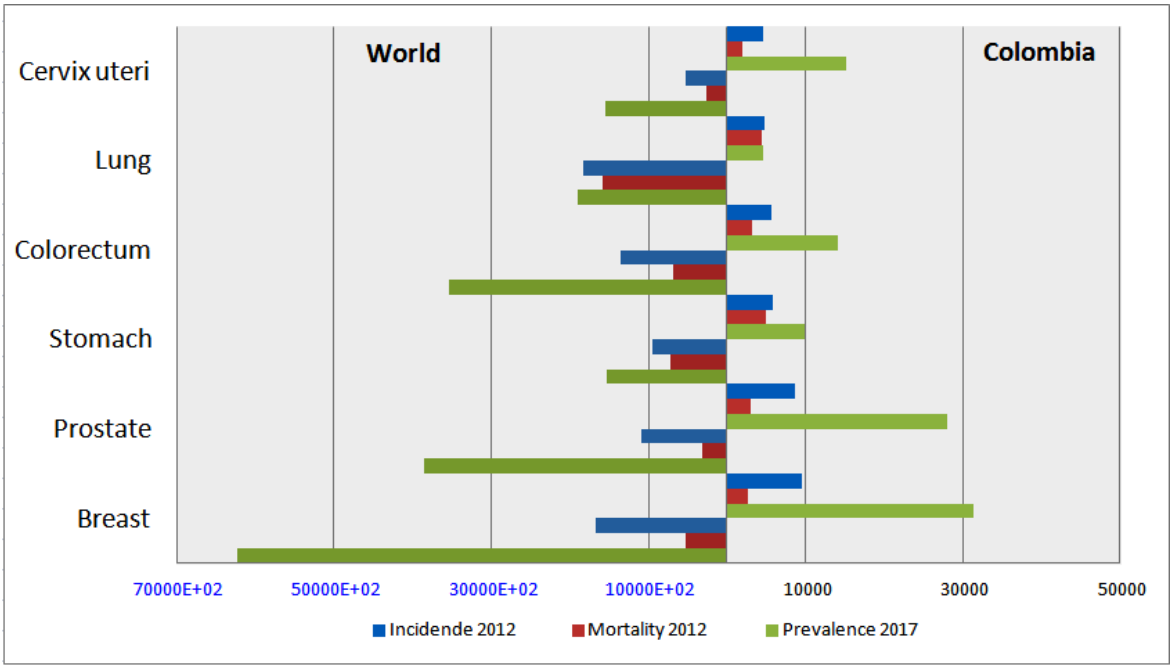

Figure 1-29 Main types of Cancer in Colombia and in the world

Previously, a series of new tariquidar analogs was synthesized (Figure 1-30, compounds **143** and **145**), which were identified as a new class of potents and selectives ABCG2 modulators, compound UR-ME22-1 was the most promising representative.[143] Further studies tried to improve water solubility of these compounds by adding triethylenglycol chains (UR-COP78),[144] the maximal inhibitory effect of these new modulators class clearly increased, but unfortunately, in mouse plasma the compounds were enzymatically cleaved at the central core structure within 10 minutes.

In continuation with these previous works, a bioisosteric approach of the amide bond located in the central core of the structure is proposed to increase the stability against enzymatic hydrolysis. Also, the addition of ethylene and triethylene glycol chains in the tetrahydroisoquinoline moiety would improve the hydrophilicity of the synthesized compounds.

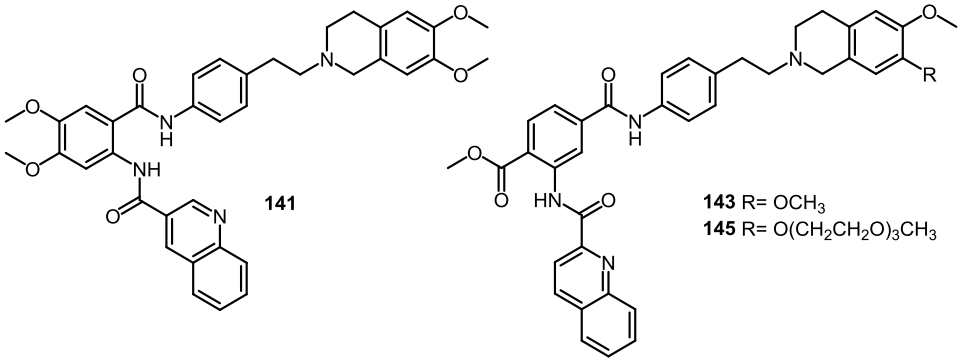

Figure 1-30 Some ABCG2 modulators. Tariquidar (**141**), UR-ME22-1 (**143**), UR-COP78 (**145**)

General objective

Synthesize and characterize new tariquidar analogs with improved stability against enzymatic hydrolysis and evaluate their inhibitory activity against breast cancer resistance protein (ABCG2).

Specific objectives

- ✓ Synthesize and characterize two series of new compounds with possible inhibitory activity against ABCG2, in which a rigid fragment is included to increase the stability of the compounds against enzymatic hydrolysis.

- ✓ Evaluate the biological activity of the synthesized compounds determining the half maximal inhibitory concentration (IC_{50}) as well as their percentage of maximum inhibition (I_{max}).

- ✓ Evaluate the stability of the compounds with highest activity against enzymatic degradation.

1.6 References

1. Mao Q. Role of the breast cancer resistance protein (ABCG2) in drug transport. The AAPS journal 2005;7(1):E118-E133.
2. Boumendjel A, Boutonnat J, Robert J. ABC transporters and multidrug resistance. New Jersey: John Wiley & Sons; 2009. 83-118 p.
3. Ullah MF. Cancer multidrug resistance (MDR): a major impediment to effective chemotherapy. Asian Pac J Cancer Prev 2008;9(1):1-6.
4. Gillet J-P, Gottesman MM. Mechanisms of Multidrug Resistance in Cancer. In: Zhou J, editor. Multi-Drug Resistance in Cancer. Totowa, NJ: Humana Press; 2010. pp 47-76.
5. Juliano RL, Ling V. A surface glycoprotein modulating drug permeability in Chinese hamster ovary cell mutants. BBA Biomembranes 1976;455(1):152-162.
6. Cole S, Bhardwaj G, Gerlach J, Mackie J, Grant C, Almquist K, Stewart A, Kurz E, Duncan A, Deeley R. Overexpression of a transporter gene in a multidrug-resistant human lung cancer cell line. Science 1992;258:1650-1650.
7. Wu C-P, Hsieh C-H, Wu Y-S. The emergence of drug transporter-mediated multidrug resistance to cancer chemotherapy. Mol Pharmaceutics 2011;8(6):1996-2011.
8. Glavinas H, Krajcsi P, Cserepes J, Sarkadi B. The role of ABC transporters in drug resistance, metabolism and toxicity. Curr Drug Delivery 2004;1:27-42.
9. Hegedüs C, Truta-Feles K, Antalffy G, Várady G, Német K, Özvegy-Laczka C, Kéri G, Őrfi L, Szakács G, Settleman J. Interaction of the EGFR inhibitors gefitinib, vandetanib, pelitinib and neratinib with the ABCG2 multidrug transporter: implications for the emergence and reversal of cancer drug resistance. Biochem Pharmacol 2012;84(3):260-267.
10. Deeley RG, Westlake C, Cole SP. Transmembrane transport of endo-and xenobiotics by mammalian ATP-binding cassette multidrug resistance proteins. Physiol Rev 2006;86(3):849-899.
11. Sarkadi B, Homolya L, Szakács G, Váradi A. Human multidrug resistance ABCB and ABCG transporters: participation in a chemoimmunity defense system. Physiol rev 2006;86(4):1179-1236.
12. Staud F, Pavek P. Breast cancer resistance protein (BCRP/ABCG2). Int J Biochem Cell Biol 2005;37:720-725.
13. Robey RW, To KKK, Polgar O, Dohse M, Fetsch P, Dean M, Bates SE. ABCG2: a perspective. Adv Drug Delivery Rev 2009;61(1):3-13.
14. Choudhuri S, Klaassen CD. Structure, function, expression, genomic organization, and single nucleotide polymorphisms of Human ABCB1 (MDR1), ABCC (MRP), and ABCG2 (BCRP) efflux transporters. Int J Toxicol 2006;25(4):231-259.
15. Vautier S, Fernandez C, Milane A, Lacomblez L, Davrinche C, Farinotti R. ABCB 1 (P-glycoprotein) and blood-brain barrier: role in neurological diseases and their treatments. J Pharm Clin 2006;25(4):225.
16. Gatti L, Beretta GL, Cossa G, Zunino F, Perego P. ABC transporters as potential targets for modulation of drug resistance. Mini Rev Med Chem 2009;9:1102-1112.
17. Ambudkar SV, Dey S, Hrycyna CA, Ramachandra M, Pastan I, Gottesman MM. Biochemical, cellular, and pharmacological aspects of the multidrug transporter. Annu Rev Pharmacol Toxicol 1999;39:361-398.
18. Cole SPC. Multidrug resistance protein 1 (MRP1, ABCC1), a “multitasking” ATP-binding cassette (ABC) transporter. J Biol Chem 2014;289(45):30880-30888.

19. Kruh GD, Belinsky MG. The MRP family of drug efflux pumps. Oncogene 2003;22(47):7537-7552.
20. Ambudkar SV, Kimchi-Sarfaty C, Sauna ZE, Gottesman MM. P-glycoprotein: from genomics to mechanism. Oncogene 2003;22(47):7468-7485.
21. Demel MA, Schwaha R, Krämer O, Ettmayer P, Haaksma EJ, Ecker GF. In silico prediction of substrate properties for ABC-multidrug transporters. Expert Opin Drug Metab Toxicol 2008;4:1167-1180.
22. Baumert C, Hilgeroth A. Recent advances in the development of p-gp inhibitors. Anti-Cancer Agents Med Chem 2009;9:46-436.
23. Seelig A, Gatlik-Landwojtowicz E. Inhibitors of multidrug efflux transporters: their membrane and protein interactions. Mini Rev Med Chem 2005;5:135-151.
24. Pleban K, Ecker GF. Inhibitors of p-glycoprotein - lead identification and pptimisation. Mini Rev Med Chem 2005;5:153-163.
25. Boumendjel A, Baubichon-Cortay H, Trompier D, Perrotton T, Di Pietro A. Anticancer multidrug resistance mediated by MRP1: Recent advances in the discovery of reversal agents. Med Res Rev 2005;25(4):453-472.
26. Nobili S, Landini I, Mazzei T, Mini E. Overcoming tumor multidrug resistance using drugs able to evade P-glycoprotein or to exploit its expression. Med Res Rev 2012;32(6):1220-1262.
27. Stacy AE, Jansson PJ, Richardson DR. Molecular pharmacology of ABCG2 and its role in chemoresistance. Mol Pharmacol 2013;84(5):655-669.
28. Lecerf-Schmidt F, Peres B, Valdameri G, Gauthier C, Winter E, Payen L, Di Pietro A, Boumendjel A. ABCG2: recent discovery of potent and highly selective inhibitors. Future Med Chem 2013;5(9):1037-1045.
29. Ni Z, Bikadi Z, Rosenberg MF, Mao Q. Structure and function of the human breast cancer resistance protein (BCRP/ABCG2). Curr Drug Metab 2010;11:603-617.
30. Jonker JW, Buitelaar M, Wagenaar E, van der Valk MA, Scheffer GL, Scheper RJ, Plösch T, Kuipers F, Elferink RPO, Rosing H. The breast cancer resistance protein protects against a major chlorophyll-derived dietary phototoxin and protoporphyria. Proc Natl Acad Sci 2002;99(24):15649-15654.
31. Robey R, Polgar O, Deeken J, To K, Bates S. ABCG2: determining its relevance in clinical drug resistance. Cancer Metastasis Rev 2007;26(1):39-57.
32. Shukla S, Robey RW, Bates SE, Ambudkar SV. The calcium channel blockers, 1, 4-dihydropyridines, are substrates of the multidrug resistance-linked ABC drug transporter, ABCG2. Biochemistry 2006;45(29):8940-8951.
33. Doyle LA, Ross DD. Multidrug resistance mediated by the breast cancer resistance protein BCRP (ABCG2). Oncogene 2003;22(47):7340-7358.
34. Xu J, Peng H, Zhang JT. Human Multidrug Transporter ABCG2, a Target for Sensitizing Drug Resistance in Cancer Chemotherapy. Curr Med Chem 2007;14:689-701.
35. Shafran A, Ifergan I, Bram E, Jansen G, Kathmann I, Peters GJ, Robey RW, Bates SE, Assaraf YG. ABCG2 harboring the Gly482 mutation confers high-level resistance to various hydrophilic antifolates. Cancer res 2005;65(18):8414-8422.
36. Lee CA, O'Connor MA, Ritchie TK, Galetin A, Cook JA, Ragueneau-Majlessi I, Ellens H, Feng B, Taub ME, Paine MF, Polli JW, Ware JA, Zamek-Gliszczynski MJ. Breast cancer resistance protein (ABCG2) in clinical pharmacokinetics and drug interactions: practical recommendations for clinical victim and perpetrator drug-drug interaction study design. Drug Metab Dispos 2015;43(4):490-509.
37. Noguchi K, Katayama K, Mitsuhashi J, Sugimoto Y. Functions of the breast cancer resistance protein (BCRP/ABCG2) in chemotherapy. Adv Drug Delivery Rev 2009;61(1):26-33.

38. Jain HD, Zhang C, Zhou S, Zhou H, Ma J, Liu X, Liao X, Deveau AM, Dieckhaus CM, Johnson MA. Synthesis and structure–activity relationship studies on tryprostatin A, an inhibitor of breast cancer resistance protein. Bioorg Med Chem 2008;16(8):4626-4651.
39. Shukla S, Ohnuma S, Ambudkar SV. Improving cancer chemotherapy with modulators of ABC drug transporters. Current drug targets 2011;12(5):621-630.
40. Hardwick LJ, Velamakanni S, van Veen HW. The emerging pharmacotherapeutic significance of the breast cancer resistance protein (ABCG2). Br J Pharmacol 2007;151(2):163-174.
41. Yanase K, Tsukahara S, Mitsuhashi J, Sugimoto Y. Functional SNPs of the breast cancer resistance protein-therapeutic effects and inhibitor development. Cancer lett 2006;234(1):73-80.
42. Ahmed-Belkacem A, Pozza A, Macalou S, Pe`rez-Victoria JM, Boumendjel An, Di Pietro A. Inhibitors of cancer cell multidrug resistance mediated by breast cancer resistance protein (BCRP/ABCG2). Anti-Cancer Drugs 2006;17(3):239-243.
43. Wiese M. BCRP/ABCG2 inhibitors: a patent review (2009–present). Expert Opin Ther Pat 2015;25(11):1229-1237.
44. Cherigo L, Lopez D, Martinez-Luis S. Marine natural products as breast cancer resistance protein inhibitors. Mar Drugs 2015;13(4):2010.
45. Juvale K, Wiese M. Design of inhibitors of BCRP/ABCG2. Future Med Chem 2015;7(12):1521-1527.
46. Yamazaki R, Nishiyama Y, Furuta T, Hatano H, Igarashi Y, Asakawa N, Kodaira H, Takahashi H, Aiyama R, Matsuzaki T, Yagi N, Sugimoto Y. Novel acrylonitrile derivatives, YHO-13177 and YHO-13351, reverse BCRP/ABCG2-mediated drug resistance in vitro and in vivo. Mol Cancer Ther 2011;10:1252-1263.
47. Weiss J, Rose J, Storch C, Ketabi N, Sauer A, Haefeli W, Efferth T. Modulation of human BCRP (ABCG2) activity by anti-HIV drugs. J Antimicrob Chemother 2007;59:238-245.
48. Gupta A, Zhang Y, Unadkat JD, Mao Q. HIV protease inhibitors are inhibitors but not substrates of the human breast cancer resistance protein (BCRP/ABCG2). J Pharmacol Exp Ther 2004;310(1):334-341.
49. Peroni RN, Di Gennaro SS, Hocht C, Chiappetta DA, Rubio MC, Sosnik A, Bramuglia GF. Efavirenz is a substrate and in turn modulates the expression of the efflux transporter ABCG2/BCRP in the gastrointestinal tract of the rat. Biochem Pharmacol 2011;82(9):1227-1233.
50. Kis O, Sankaran-Walters S, Hoque MT, Walmsley SL, Dandekar S, Bendayan R. HIV-1 Alters Intestinal Expression of Drug Transporters and Metabolic Enzymes: Implications for Antiretroviral Drug Disposition. Antimicrob Agents Chemother 2016;60(5):2771-2781.
51. Neumanova Z, Cerveny L, Ceckova M, Staud F. Role of ABCB1, ABCG2, ABCC2 and ABCC5 transporters in placental passage of zidovudine. Biopharm Drug Dispos 2016;37(1):28-38.
52. Heim KE, Tagliaferro AR, Bobilya DJ. Flavonoid antioxidants: chemistry, metabolism and structure-activity relationships. J Nutr Biochem 2002;13(10):572-584.
53. Rice-Evans CA, Miller NJ, Paganga G. Structure-antioxidant activity relationships of flavonoids and phenolic acids. Free Radicals Biol Med 1996;20(7):933-956.
54. Cushnie TPT, Lamb AJ. Antimicrobial activity of flavonoids. Int J Antimicrob Agents 2005;26(5):343-356.

55. Li BQ, Fu T, Dongyan Y, Mikovits JA, Ruscetti FW, Wang JM. Flavonoid baicalin inhibits HIV-1 infection at the level of viral entry. Biochem Biophys Res Commun 2000;276(2):534-538.
56. Tunon MJ, Garcia-Mediavilla MV, Sanchez-Campos S, Gonzalez-Gallego J. Potential of flavonoids as anti-inflammatory agents: modulation of pro-inflammatory gene expression and signal transduction pathways. Curr Drug Metab 2009;10:256-271.
57. Cooray HC, Janvilisri T, van Veen HW, Hladky SB, Barrand MA. Interaction of the breast cancer resistance protein with plant polyphenols. Biochem Biophys Res Commun 2004;317(1):269-275.
58. Boumendjel A. Aurones: a subclass of flavones with promising biological potential. Curr Med Chem 2003;10(23):2621-2630.
59. Zwergel C, Gaascht F, S. V, Diederich M, Bagrel D, Kirsch G. Aurones: Interesting Natural and Synthetic Compounds with Emerging Biological Potential. Nat Prod Commun 2012;7(3):389-394.
60. Sim HM, Lee CY, Ee PLR, Go ML. Dimethoxyaurones: potent inhibitors of ABCG2 (breast cancer resistance protein). Eur J Pharm Sci 2008;35:293-306.
61. Haudecoeur R, Boumendjel A. Recent advances in the medicinal chemistry of aurones. Curr Med Chem 2012;19(18):2861-2875.
62. Sim HM, Loh KY, Yeo WK, Lee CY, Go ML. Aurones as modulators of ABCG2 and ABCB1: synthesis and structure–activity relationships. ChemMedChem 2011;6(4):713-724.
63. Bois F, Beney C, Boumendjel A, Mariotte A-M, Conseil G, Di Pietro A. Halogenated chalcones with high-affinity binding to p-glycoprotein: potential modulators of multidrug resistance. J Med Chem 1998;41(21):4161-4164.
64. Gu X, Ren Z, Tang X, Peng H, Ma Y, Lai Y, Peng S, Zhang Y. Synthesis and biological evaluation of bifendate–chalcone hybrids as a new class of potential P-glycoprotein inhibitors. Bioorg Med Chem 2012;20(8):2540-2548.
65. Han Y, Riwanto M, Go M-L, Rachel Ee PL. Modulation of breast cancer resistance protein (BCRP/ABCG2) by non-basic chalcone analogues. Eur J Pharm Sci 2008;35(1–2):30-41.
66. Valdameri G, Gauthier C, Terreux Rl, Kachadourian Rm, Day BJ, Winnischofer SM, Rocha ME, Frachet Vr, Ronot X, Di Pietro A. Investigation of chalcones as selective inhibitors of the breast cancer resistance protein: critical role of methoxylation in both inhibition potency and cytotoxicity. J Med Chem 2012;55(7):3193-3200.
67. Juvale K, Pape VF, Wiese M. Investigation of chalcones and benzochalcones as inhibitors of breast cancer resistance protein. Bioorg Med Chem 2012;20(1):346-355.
68. Rangel LP, Winter E, Gauthier C, Terreux R, Chiaradia-Delatorre LD, Mascarello A, Nunes RJ, Yunes RA, Creczynski-Pasa TB, Macalou S. New structure–activity relationships of chalcone inhibitors of breast cancer resistance protein: polyspecificity toward inhibition and critical substitutions against cytotoxicity. Drug Des, Dev Ther 2013;7:1043-1052.
69. Winter E, Gozzi GJ, Chiaradia-Delatorre LD, Daflon-Yunes N, Terreux R, Gauthier C, Mascarello A, Leal PC, Cadena SM, Yunes RA. Quinoxaline-substituted chalcones as new inhibitors of breast cancer resistance protein ABCG2: polyspecificity at B-ring position. Drug Des, Dev Ther 2014;8:609-619.
70. Kraege S, Stefan K, Juvale K, Ross T, Willmes T, Wiese M. The combination of quinazoline and chalcone moieties leads to novel potent heterodimeric modulators

of breast cancer resistance protein (BCRP/ABCG2). Eur J Med Chem 2016;117:212-229.
71. Boumendjel A, Nicolle E, Moraux T, Gerby B, Blanc M, Ronot X, Boutonnat J. Piperazinobenzopyranones and Phenalkylaminobenzopyranones: Potent Inhibitors of Breast Cancer Resistance Protein (ABCG2). J Med Chem 2005;48(23):7275-7281.
72. Valdameri G, Genoux-Bastide E, Peres B, Gauthier C, Guitton Jrm, Terreux Rl, Winnischofer SM, Rocha ME, Boumendjel An, Di Pietro A. Substituted chromones as highly potent nontoxic inhibitors, specific for the breast cancer resistance protein. J Med Chem 2012;55(2):966-970.
73. Winter E, Lecerf-Schmidt F, Gozzi G, Peres B, Lightbody M, Gauthier C, Ozvegy-Laczka C, Szakacs G, Sarkadi B, Creczynski-Pasa TB, Boumendjel A, Di Pietro A. Structure–activity relationships of chromone derivatives toward the mechanism of interaction with and inhibition of breast cancer resistance protein ABCG2. J Med Chem 2013;56(24):9849-9860.
74. Obreque-Balboa JE, Sun Q, Bernhardt G, König B, Buschauer A. Flavonoid derivatives as selective ABCC1 modulators: synthesis and functional characterization. Eur J Med Chem 2016;109:124-133.
75. Zhang S, Yang X, Morris ME. Flavonoids are inhibitors of breast cancer resistance protein (ABCG2)-mediated transport. Mol Pharmacol 2004;65(5):1208-1216.
76. Zhang S, Wang X, Sagawa K, Morris ME. Flavonoids chrysin and benzoflavone, potent breast cancer resistance protein Inhibitors, have no significant effect on topotecan pharmacokinetics in rats or MDR1A/1B(-/-) mice. Drug Metab Dispos 2005;33(3):341-348.
77. Zhang S, Yang X, Morris ME. Combined effects of multiple flavonoids on breast cancer resistance protein (ABCG2)-mediated transport. Pharm Res 2004;21(7):1263-1273.
78. Imai Y, Tsukahara S, Asada S, Sugimoto Y. Phytoestrogens/flavonoids reverse breast cancer resistance protein/ABCG2-mediated multidrug resistance. Cancer Res 2004;64(12):4346-4352.
79. Zhang S, Yang X, Coburn R, Morris M. Structure activity relationships and quantitative structure activity relationships for the flavonoid-mediated inhibition of breast cancer resistance protein. Biochem Pharmacol 2005;70(4):627-639.
80. Ahmed-Belkacem A, Pozza A, Munoz-Martinez F, Bates SE, Castanys S, Gamarro F, Di PA, Perez-Victoria JM. Flavonoid structure-activity studies identify 6-prenylchrysin and tectochrysin as potent and specific inhibitors of breast cancer resistance protein ABCG2. Cancer Res 2005;65:4852-4860.
81. Tan KW, Li Y, Paxton JW, Birch NP, Scheepens A. Identification of novel dietary phytochemicals inhibiting the efflux transporter breast cancer resistance protein (BCRP/ABCG2). Food Chem 2013;138(4):2267-2274.
82. Ahmed-Belkacem A, Macalou S, Borrelli F, Capasso R, Fattorusso E, Taglialatela-Scafati O, Di Pietro A. Nonprenylated rotenoids, a new class of potent breast cancer resistance protein inhibitors. J Med Chem 2007;50(8):1933-1938.
83. Pick A, Müller H, Mayer R, Haenisch B, Pajeva IK, Weigt M, Bönisch H, Müller CE, Wiese M. Structure–activity relationships of flavonoids as inhibitors of breast cancer resistance protein (BCRP). Bioorg Med Chem 2011;19(6):2090-2102.
84. Juvale K, Stefan K, Wiese M. Synthesis and biological evaluation of flavones and benzoflavones as inhibitors of BCRP/ABCG2. Eur J Med Chem 2013;67(0):115-126.

85. Rabindran SK, He H, Singh M, Brown E, Collins KI, Annable T, Greenberger LM. Reversal of a novel multidrug resistance mechanism in human colon carcinoma cells by fumitremorgin C. Cancer Res 1998;58(24):5850-5858.
86. Rabindran SK, Ross DD, Doyle LA, Yang W, Greenberger LM. Fumitremorgin C reverses multidrug resistance in cells transfected with the breast cancer resistance protein. Cancer Res 2000;60(1):47-50.
87. Nishiyama M, Kuga T. Central effects of the neurotropic mycotoxin fumitremorgin A in the rabbit (I) effects on the spinal cord. Jpn J Pharmacol 1989;50(2):167-173.
88. Loevezijn AV, Allen JD, Schinkel AH, Koomen GJ. Inhibition of BCRP-mediated drug efflux by fumitremorgin-type indolyl diketopiperazines. Bioorg Med Chem Lett 2001;11(1):29-32.
89. Li Y, Hayman E, Plesescu M, Prakash SR. Synthesis of potent BCRP inhibitor—Ko143. Tetrahedron Lett 2008;49(9):1480-1483.
90. Allen JD, van Loevezijn A, Lakhai JM, van der Valk M, van Tellingen O, Reid G, Schellens JHM, Koomen GJ, Schinkel AH. Potent and specific inhibition of the breast cancer resistance protein multidrug transporter in vitro and in mouse intestine by a novel analogue of fumitremorgin C. Mol Cancer Ther 2002;1:417-425.
91. Weidner LD, Zoghbi SS, Lu S, Shukla S, Ambudkar SV, Pike VW, Mulder J, Gottesman MM, Innis RB, Hall MD. The inhibitor Ko143 is not specific for ABCG2. J Pharmacol Exp Ther 2015;354(3):384-393.
92. Wu G, Liu J, Bi L, Zhao M, Wang C, Baudy-Floc'h M, Ju J, Peng S. Toward breast cancer resistance protein (BCRP) inhibitors: design, synthesis of a series of new simplified fumitremorgin C analogues. Tetrahedron 2007;63(25):5510-5528.
93. Ma Y, Wink M. The beta-carboline alkaloid harmine inhibits BCRP and can reverse resistance to the anticancer drugs mitoxantrone and camptothecin in breast cancer cells. Phytother Res 2010;24(1):146-149.
94. Spindler A, Stefan K, Wiese M. Synthesis and investigation of tetrahydro-β-carboline derivatives as inhibitors of the breast cancer resistance protein (ABCG2). J Med Chem 2016;59(13):6121-6135.
95. Tan KW, Cooney J, Jensen D, Li Y, Paxton JW, Birch NP, Scheepens A. Hop-derived prenylflavonoids are substrates and inhibitors of the efflux transporter breast cancer resistance protein (BCRP/ABCG2). Mol Nutr Food Res 2014;58(11):2099-2110.
96. Henrich CJ, Robey RW, Takada K, Bokesch HR, Bates SE, Shukla S, Ambudkar SV, McMahon JB, Gustafson KR. Botryllamides: natural product inhibitors of ABCG2. ACS Chem Biol 2009;4(8):637-647.
97. Shiozawa K, Oka M, Soda H, Yoshikawa M, Ikegami Y, Tsurutani J, Nakatomi K, Nakamura Y, Doi S, Kitazaki T, Mizuta Y, Murase K, Yoshida H, Ross DD, Kohno S. Reversal of breast cancer resistance protein (BCRP/ABCG2)-mediated drug resistance by novobiocin, a coumermycin antibiotic. Int J Cancer 2004;108(1):146-151.
98. Su Y, Hu P, Lee S-H, Sinko PJ. Using novobiocin as a specific inhibitor of breast cancer resistant protein to assess the role of transporter in the absorption and disposition of topotecan. J Pharm Pharm Sci 2007;10(4):519-536.
99. Shishodia S, Chaturvedi MM, Aggarwal BB. Role of curcumin in cancer therapy. Curr Probl Cancer 2007;31(4):243-305.
100. Aggarwal BB, Kumar A, Bharti AC. Anticancer potential of curcumin: preclinical and clinical studies. Anticancer Res 2003;23(1A):363-398.

101. Chearwae W, Shukla S, Limtrakul P, Ambudkar SV. Modulation of the function of the multidrug resistance–linked ATP-binding cassette transporter ABCG2 by the cancer chemopreventive agent curcumin. Mol Cancer Ther 2006;5(8):1995-2006.
102. Shukla S, Zaher H, Hartz A, Bauer B, Ware JA, Ambudkar SV. Curcumin inhibits the activity of ABCG2/BCRP1, a multidrug resistance-linked ABC drug transporter in mice. Pharm Res 2009;26(2):480-487.
103. Liao W-Y, Shen C-N, Lin L-H, Yang Y-L, Han H-Y, Chen J-W, Kuo S-C, Wu S-H, Liaw C-C. Asperjinone, a nor-neolignan, and terrein, a suppressor of ABCG2-expressing breast cancer cells, from thermophilic Aspergillus terreus. J Nat Prod 2012;75(4):630-635.
104. Gupta A, Dai Y, Vethanayagam RR, Hebert MF, Thummel KE, Unadkat JD, Ross DD, Mao Q. Cyclosporin A, tacrolimus and sirolimus are potent inhibitors of the human breast cancer resistance protein (ABCG2) and reverse resistance to mitoxantrone and topotecan. Cancer Chemother Pharmacol 2006;58:374-383.
105. Rocha-Martin J, Harrington C, Dobson AD, O'Gara F. Emerging strategies and integrated systems microbiology technologies for biodiscovery of marine bioactive compounds. Mar Drugs 2014;12(6):3516-3559.
106. Lopez D, Martinez-Luis S. Marine natural products with P-glycoprotein inhibitor properties. Mar Drugs 2014;12(1):525-546.
107. Sánchez C, Méndez C, Salas JA. Indolocarbazole natural products: occurrence, biosynthesis, and biological activity. Nat Prod Rep 2006;23(6):1007-1045.
108. Robey RW, Shukla S, Steadman K, Obrzut T, Finley EM, Ambudkar SV, Bates SE. Inhibition of ABCG2-mediated transport by protein kinase inhibitors with a bisindolylmaleimide or indolocarbazole structure. Mol Cancer Ther 2007;6(6):1877-1885.
109. Woehlecke H, Osada H, Herrmann A, Lage H. Reversal of breast cancer resistance protein–mediated drug resistance by tryprostatin A. Int J Cancer 2003;107(5):721-728.
110. Takada K, Imamura N, Gustafson KR, Henrich CJ. Synthesis and structure–activity relationship of botryllamides that block the ABCG2 multidrug transporter. Bioorg Med Chem Lett 2010;20(4):1330-1333.
111. Patel K, Gadewar M, Tripathi R, Prasad S, Patel DK. A review on medicinal importance, pharmacological activity and bioanalytical aspects of beta-carboline alkaloid “Harmine”. Asian Pac J Trop Biomed 2012;2(8):660-664.
112. Bokesch HR, Cartner LK, Fuller RW, Wilson JA, Henrich CJ, Kelley JA, Gustafson KR, McMahon JB, McKee TC. Inhibition of ABCG2-mediated drug efflux by naphthopyrones from marine crinoids. Bioorg Med Chem Lett 2010;20(13):3848-3850.
113. Davis RA, Carroll AR, Pierens GK, Quinn RJ. New lamellarin alkaloids from the Australian ascidian, Didemnum chartaceum. J Nat Prod 1999;62(3):419-424.
114. Bailly C. Lamellarins, from A to Z: a family of anticancer marine pyrrole alkaloids. Curr Med Chem Anti-Cancer Agents 2004;4(4):363-378.
115. Huang X-C, Xiao X, Zhang Y-K, Talele TT, Salim AA, Chen Z-S, Capon RJ. Lamellarin O, a pyrrole alkaloid from an australian marine sponge, *ianthella sp*., reverses BCRP mediated drug resistance in cancer cells. Mar Drugs 2014;12(7):3818-3837.
116. Christensen LP. Ginsenosides: chemistry, biosynthesis, analysis, and potential health effects. Adv Food Nutr Res 2008;55:1-99.
117. Jin J, Shahi S, Kang HK, van Veen HW, Fan T-P. Metabolites of ginsenosides as novel BCRP inhibitors. Biochem Biophys Res Commun 2006;345(4):1308-1314.

118. Lawrence Lein YN, Yo Mabuchi, Sadafumi Suzuki, Satoru Morikawa, Yumi Matsuzaki. Inhibition of Abcg2 transporter on primitive hematopoietic stem cells by All-trans retinoic acid increases sensitivity to anthracycline. Inflammation Regener 2010;30(1):55-62.
119. Hansen SL, Purup S, Christensen LP. Bioactivity of falcarinol and the influenceof processing and storage on its content in carrots (Daucus carota L). J Sci Food Agric 2003;83(10):1010-1017.
120. Tan KW, Killeen DP, Li Y, Paxton JW, Birch NP, Scheepens A. Dietary polyacetylenes of the falcarinol type are inhibitors of breast cancer resistance protein (BCRP/ABCG2). Eur J Pharmacol 2014;723(0):346-352.
121. Morita H, Koyama K, Sugimoto Y, Kobayashi J. Antimitotic activity and reversal of breast cancer resistance protein-mediated drug resistance by stilbenoids from Bletilla striata. Bioorg Med Chem Lett 2005;15(4):1051-1054.
122. Wesolowska O, Wisniewski J, Bielawska-Pohl A, Paprocka M, Duarte N, Ferreira M-JU, Dus D, Michalak K. Stilbenes as multidrug resistance modulators and apoptosis inducers in human adenocarcinoma cells. Anticancer Res 2010;30(11):4587-4593.
123. Valdameri G, Pereira Rangel L, Spatafora C, Guitton Jrm, Gauthier C, Arnaud Ol, Ferreira-Pereira A, Falson P, Winnischofer SM, Rocha ME. Methoxy stilbenes as potent, specific, untransported, and noncytotoxic inhibitors of breast cancer resistance protein. ACS Chem Biol 2011;7(2):322-330.
124. Belmont P, Dorange I. Acridine/acridone: a simple scaffold with a wide range of application in oncology. Expert Opin Ther Pat 2008;18(11):1211-1224.
125. Boumendjel A, Macalou S, Ahmed-Belkacem A, Blanc M, Di Pietro A. Acridone derivatives: Design, synthesis, and inhibition of breast cancer resistance protein ABCG2. Bioorg Med Chem 2007;15(8):2892-2897.
126. Arnaud O, Boumendjel A, Gèze A, Honorat M, Matera E, Guitton J, Stein W, Bates S, Falson P, Dumontet C. The acridone derivative MBLI-87 sensitizes breast cancer resistance protein-expressing xenografts to irinotecan. Eur J Cancer 2011;47(4):640-648.
127. Sostelly A, Payen L, Guitton J, Pietro AD, Falson P, Honorat M, Valdameri G, Geze A, Boumendjel A, Freyer G. A template model for studying anticancer drug efflux transporter inhibitors in vitro. Fundam Clin Pharmacol 2013;27(5):544-556.
128. Breedveld P, Zelcer N, Pluim D, Sönmezer Ö, Tibben MM, Beijnen JH, Schinkel AH, van Tellingen O, Borst P, Schellens JH. Mechanism of the pharmacokinetic interaction between methotrexate and benzimidazoles potential role for breast cancer resistance protein in clinical drug-drug interactions. Cancer res 2004;64(16):5804-5811.
129. Merino G, Jonker JW, Wagenaar E, Pulido MM, Molina AJ, Alvarez AI, Schinkel AH. Transport of anthelmintic benzimidazole drugs by breast cancer resistance protein (BCRP/ABCG2). Drug Metab Dispos 2005;33(5):614-618.
130. Barrera B, Otero JA, Egido E, Prieto JG, Seelig A, Álvarez AI, Merino G. The anthelmintic triclabendazole and its metabolites inhibit the membrane transporter ABCG2/BCRP. Antimicrob Agents Chemother 2012;56(7):3535-3543.
131. Hartz AMS, Mahringer A, Miller DS, Bauer B. 17-[beta]-Estradiol: a powerful modulator of blood-brain barrier BCRP activity. J Cereb Blood Flow Metab 2010;30(10):1742-1755.
132. Mahringer A, Fricker G. BCRP at the blood−brain barrier: genomic regulation by 17β-estradiol. Mol Pharmaceutics 2010;7(5):1835-1847.
133. Dankers AC, Sweep FC, Pertijs JC, Verweij V, van den Heuvel JJ, Koenderink JB, Russel FG, Masereeuw R. Localization of breast cancer resistance protein (Bcrp)

in endocrine organs and inhibition of its transport activity by steroid hormones. Cell Tissue Res 2012;349(2):551-563.
134. Hofman J, Ahmadimoghaddam D, Hahnova L, Pavek P, Ceckova M, Staud F. Olomoucine II and purvalanol A inhibit ABCG2 transporter *in vitro* and *in situ* and synergistically potentiate cytostatic effect of mitoxantrone. Pharmacol Res 2012;65(3):312-319.
135. An R, Hagiya Y, Tamura A, Li S, Saito H, Tokushima D, Ishikawa T. Cellular phototoxicity evoked through the inhibition of human ABC transporter ABCG2 by cyclin-dependent kinase inhibitors in vitro. Pharmacol Res 2009;26(2):449-458.
136. Chen J-F, Chern Y. Impacts of methylxanthines and adenosine receptors on neurodegeneration: human and experimental studies. Methylxanthines. Berlin Heidelberg: Springer; 2011. pp 267-310.
137. Ding R, Shi J, Pabon K, Scotto KW. Xanthines down-regulate the drug transporter ABCG2 and reverse multidrug resistance. Mol Pharmacol 2012;81(3):328-337.
138. Ding R, Shi J, Scotto KW. Modulation of ABCG2 mediated multidrug resistance by xanthine derivatives. Cancer Res 2011;71(8 Supplement):1746-1746.
139. Efferth T. Resistance to targeted ABC transporters in cancer. Switzerland: Springer International Publishing; 2014. 53-88 p.
140. Mistry P, Stewart AJ, Dangerfield W, Okiji S, Liddle C, Bootle D, Plumb JA, Templeton D, Charlton P. In vitro and in vivo reversal of p-glycoprotein-mediated multidrug resistance by a novel potent modulator, XR9576. Cancer res 2001;61:749-758.
141. Pick A, Müller H, Wiese M. Novel lead for potent inhibitors of breast cancer resistance protein (BCRP). Bioorg Med Chem Lett 2010;20(1):180-183.
142. Pick A, Müller H, Wiese M. Structure–activity relationships of new inhibitors of breast cancer resistance protein (ABCG2). Bioorg Med Chem 2008;16(17):8224-8236.
143. Kühnle M, Egger M, Müller C, Mahringer A, Bernhardt G, Fricker G, König B, Buschauer A. Potent and selective inhibitors of breast cancer resistance protein (ABCG2) derived from the p-glycoprotein (ABCB1) modulator tariquidar. J Med Chem 2009;52:1190-1197.
144. Puentes CO, Höcherl P, Kühnle M, Bauer S, Bürger K, Bernhardt G, Buschauer A, König B. Solid phase synthesis of tariquidar-related modulators of ABC transporters preferring breast cancer resistance protein (ABCG2). Bioorg Med Chem Lett 2011;21(12):3654-3657.
145. Ochoa-Puentes C, Bauer S, Kühnle M, Bernhardt Gn, Buschauer A, König B. Benzanilide–biphenyl replacement: a bioisosteric approach to quinoline carboxamide-type ABCG2 modulators. ACS Med Chem Lett 2013;4(4):393-396.
146. Bauer S, Ochoa-Puentes C, Sun Q, Bause M, Bernhardt G, König B, Buschauer A. Quinoline Carboxamide-Type ABCG2 Modulators: Indole and Quinoline Moieties as Anilide Replacements. ChemMedChem 2013;8(11):1773-1778.
147. Bause M. Synthesis of melanoma inhibitory activity protein inhibitors, ABCG2 transporter modulators, and neurotensin mimetics [Dissertation]. Universität Regensburg: University of Regensburg; 2015.
148. Bauer S. Quinoline carboxamides as modulators of Breast Cancer Resistance Protein (ABCG2): Investigations on potency, selectivity, mechanism of action, cytotoxicity, stability and drug-like properties [Dissertation]. Universität Regensburg: University of Regensburg; 2014.

149. Özvegy-Laczka C, Cserepes J, Elkind NB, Sarkadi B. Tyrosine kinase inhibitor resistance in cancer: role of ABC multidrug transporters. Drug Resist Updates 2005;8(1):15-26.
150. Nakamura Y, Oka M, Soda H, Shiozawa K, Yoshikawa M, Itoh A, Ikegami Y, Tsurutani J, Nakatomi K, Kitazaki T. Gefitinib ("Iressa", ZD1839), an epidermal growth factor receptor tyrosine kinase inhibitor, reverses breast cancer resistance protein/ABCG2–mediated drug resistance. Cancer res 2005;65(4):1541-1546.
151. Sodani K, Patel A, Anreddy N, Singh S, Yang D-H, Kathawala RJ, Kumar P, Talele TT, Chen Z-S. Telatinib reverses chemotherapeutic multidrug resistance mediated by ABCG2 efflux transporter in vitro and in vivo. Biochem pharmacol 2014;89(1):52-61.
152. Zhang H, Wang Y-J, Zhang Y-K, Wang D-S, Kathawala RJ, Patel A, Talele TT, Chen Z-S, Fu L-W. AST1306, a potent EGFR inhibitor, antagonizes ATP-binding cassette subfamily G member 2-mediated multidrug resistance. Cancer letters 2014;350(1–2):61-68.
153. Pick A, Wiese M. Tyrosine Kinase Inhibitors Influence ABCG2 Expression in EGFR-Positive MDCK BCRP Cells via the PI3K/Akt Signaling Pathway. ChemMedChem 2012;7(4):650-662.
154. Zhou L, Schmidt K, Nelson FR, Zelesky V, Troutman MD, Feng B. The effect of breast cancer resistance protein and P-glycoprotein on the brain penetration of flavopiridol, imatinib mesylate (Gleevec), prazosin, and 2-methoxy-3-(4-(2-(5-methyl-2-phenyloxazol-4-yl) ethoxy) phenyl) propanoic acid (PF-407288) in mice. Drug Metab Dispos 2009;37(5):946-955.
155. Juvale K, Wiese M. 4-Substituted-2-phenylquinazolines as inhibitors of BCRP. Bioorg Med Chem Lett 2012;22(21):6766-6769.
156. Houghton PJ, Germain GS, Harwood FC, Schuetz JD, Stewart CF, Buchdunger E, Traxler P. Imatinib mesylate is a potent inhibitor of the ABCG2 (BCRP) transporter and reverses resistance to topotecan and SN-38 in vitro. Cancer res 2004;64(7):2333-2337.
157. Jordanides NE, Jorgensen HG, Holyoake TL, Mountford JC. Functional ABCG2 is overexpressed on primary CML CD34+ cells and is inhibited by imatinib mesylate. Blood 2006;108:1370-1373.
158. Juvale K, Gallus J, Wiese M. Investigation of quinazolines as inhibitors of breast cancer resistance protein (ABCG2). Bioorg Med Chem 2013;21(24):7858-7873.
159. Wang DS, Patel A, Sim HM, Zhang YK, Wang YJ, Kathawala RJ, Zhang H, Talele TT, Ambudkar SV, Xu RH. ARRY-334543 reverses multidrug resistance by antagonizing the activity of ATP-binding cassette subfamily g member 2. J Cell Biochem 2014;115(8):1381-1391.
160. Dai C-l, Liang Y-j, Wang Y-s, Tiwari AK, Yan Y-y, Wang F, Chen Z-s, Tong X-z, Fu L-w. Sensitization of ABCG2-overexpressing cells to conventional chemotherapeutic agent by sunitinib was associated with inhibiting the function of ABCG2. Cancer lett 2009;279(1):74-83.
161. Wei Y, Ma Y, Zhao Q, Ren Z, Li Y, Hou T, Peng H. New Use for an Old Drug: Inhibiting ABCG2 with Sorafenib. Mol Cancer Ther 2012;11(8):1693-1702.
162. Agarwal S, Sane R, Ohlfest JR, Elmquist WF. The role of the breast cancer resistance protein (ABCG2) in the distribution of sorafenib to the brain. J Pharmacol Exp Ther 2011;336(1):223-233.
163. Mazard T, Causse A, Simony J, Leconet W, Vezzio-Vie N, Torro A, Jarlier M, Evrard A, Del Rio M, Assenat E. Sorafenib overcomes irinotecan resistance in colorectal cancer by inhibiting the ABCG2 drug-efflux pump. Mol Cancer Ther 2013;12(10):2121-2134.

164. Zhao X-q, Dai C-l, Ohnuma S, Liang Y-j, Deng W, Chen J-J, Zeng M-S, Ambudkar SV, Chen Z-S, Fu L-W. Tandutinib (MLN518/CT53518) targeted to stem-like cells by inhibiting the function of ATP-binding cassette subfamily G member 2. Eur J Pharm Sci 2013;49(3):441-450.
165. Kuang Y-H, Patel JP, Sodani K, Wu C-P, Liao L-Q, Patel A, Tiwari AK, Dai C-L, Chen X, Fu L-W. OSI-930 analogues as novel reversal agents for ABCG2-mediated multidrug resistance. Biochem Pharmacol 2012;84(6):766-774.
166. Baell J, Walters M. Chemistry: chemical con artists foil drug discovery. Nature 2014;513(7519):481-483.
167. Bisson J, McAlpine JB, Friesen JB, Chen S-N, Graham J, Pauli GF. Can invalid bioactives undermine natural product-based drug discovery? J Med Chem 2015;59(5):1671-1690.
168. dos Santos JL CC. Pan-assay interference compounds (PAINS): warning signs in biochemical-pharmacological evaluations. Biochem Pharmacol 2015;4(2):2.
169. Baell JB. Feeling nature's PAINS: natural products, natural product drugs, and pan assay interference compounds (PAINS). J Nat Prod 2016;79(3):616-628.
170. Tsuchiya H. Membrane interactions of phytochemicals as their molecular mechanism applicable to the discovery of drug leads from plants. Molecules 2015;20(10):18923-18966.
171. Ingólfsson HI, Thakur P, Herold KF, Hobart EA, Ramsey NB, Periole X, de Jong DH, Zwama M, Yilmaz D, Hall K, Maretzky T, Hemmings HC, Blobel C, Marrink SJ, Koçer A, Sack JT, Andersen OS. Phytochemicals perturb membranes and promiscuously alter protein function. ACS Chem Biol 2014;9(8):1788-1798.
172. W Robey R, Ierano C, Zhan Z, E Bates S. The challenge of exploiting ABCG2 in the clinic. Curr Pharm Biotechnol 2011;12(4):595-608.
173. Ferlay J SI, Ervik M, Dikshit R, Eser S, Mathers C, Rebelo M, Parkin DM, Forman D, Bray, F. GLOBOCAN 2012 v1.0, Cancer Incidence and Mortality Worldwide: IARC CancerBase No. 11 [Internet]. Lyon, France: International Agency for Research on Cancer; 2013 Available from: http://globocaniarcfr 2013.
174. Bray F RJ, Masuyer E, Ferlay J. Estimates of global cancer prevalence for 27 sites in the adult population in 2008. Int J Cancer 201;132(5):1133-45 2012.

2 Tariquidar-like Ketones as Breast Cancer Resistance Protein (ABCG2) modulators[2]

Some studies have identified selective tariquidar analogs as ABCG2 inhibitors, which were among the most potent representatives reported so far, but these compounds were seriously affected by enzymatic hydrolysis which limited any further testing. In search for more stable tariquidar analogues a new series of Tariquidar-like ketones were investigated, fully characterized and tested for their ABCG2 inhibitory activity; in addition their selectivity and stability against enzymatic hydrolysis were determinated. The synthesized ketones were active against ABC transporters and exhibited selectivity over ABCG2. Some compounds of the series exhibited a maximum inhibition between 85-110% based on fumitremorgin C as reference compound (100%), and with a remarkable chemical stability against the hydrolysis after incubation for 24 hours at 37°C.

[2]All synthesis, purification and characterization of the compounds were carried out by Diana Catherine Peña. Inhibition assays (ABCG2, ABCB1, ABCC1), stability and solubility tests were carried out by Diana Catherine Peña at the University of Regensburg, Germany. Cell cultures, chemosensitive assay and reference compounds were provided by Matthias Scholler, a doctoral student at the University of Regensburg.

2.1 Introduction

ATP-binding cassette transporters use the energy of ATP-hydrolysis to transport a broad variety of substrates across the cell membrane. Under physiological conditions, these efflux pumps, including ABCB1 (p-glycoprotein, P-gp), ABCC1 (multidrug resistance related protein 1) and ABCG2 (ABCP, BCRP, MXR), appear to play a protective role in several tissues.[1] ABC transporters play also an important role in conjunction with multi-drug resistance (MDR). According to estimations, multi-drug resistant tumors account for up to half of all cancer-related deaths. Hence, in many respects, the manipulation of the ABCG2 transporter might be a promising approach in cancer chemotherapy. Predominantly, inhibition of the efflux pump by potent and selective modulators might be a conceivable application to reverse ABCG2-mediated multidrug resistance or to specifically target the cancer-stem cells. Long-term survival of these cells, due to resistance against cytostatics, that are ABCG2 substrates, might be overcome by a specific ABCG2 inhibitor in combination with the pharmacologically active compound.[2]

In search for more stable analogs, the replacement of the labile benzanilide moiety in UR-ME22-1 and UR-COP78 (Figure 1-30) by ketones and the substitution of the hydrolysis-sensitive ester by hydrogen and methyl group may improve their chemical stability. It is known that several aromatic and aliphatic ketones possess antibacterial, antimicrobial activity and antifungal properties.[3-6] Considering the different properties of the ketones; we designed and synthesized a new series derived from tariquidar. All compounds were fully characterized and tested for their ABCG2 inhibitory activity and ABC transporters selectivity. In addition, the solubility and stability against enzymatic hydrolysis was also evaluated. The synthesized ketones showed activity against ABC transporters and exhibited a marked preference for ABCG2 inhibition.

2.2 Results and discussion

2.2.1 Synthesis. Synthesis of compounds **176a-f** is shown in scheme 2-1.

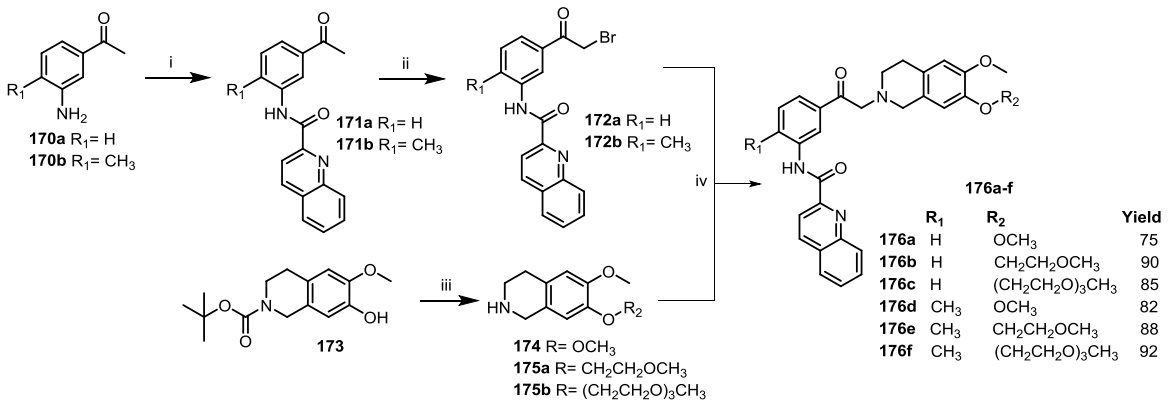

Scheme 2-1 Synthesis of compounds 176a-f. Reagents and conditions: (i) Quinaldic acid, Ts-Cl, TEA, 50ºC, overnight; (ii) NBS, MeOH, reflux; (iii) 2-methoxyethyl 4-methylbenzenesulfonate or 2-(2-(2-methoxyethoxy)ethoxy)ethyl 4-methylbenzenesulfonate, KOH, THF, N_2, 6h; (iv) K_2CO_3, acetonitrile, 90°C, overnight

Amines **170a-b** were prepared from commercially available acetophenone and 4-methylacetophenone through an electrophilic aromatic substitution with a HNO_3/H_2SO_4 mixture, followed by a Bechamp reduction with iron powder and a catalytic amount of concentrated hydrochloric acid. The amides **171a-b** were obtained by reaction between quinaldic acid, p-toluenesulfonyl chloride (Ts-Cl) and the amines **(170a-b)** in presence of triethylamine (TEA), using DCM as solvent. Compounds **172a-b** were obtained by a bromination with *N*-bromosuccinimide. Tetrahydroisoquinoline **174** is commercially available as a hydrochloride salt. The protected tetrahydroisoquinoline **173** reacted with 2-methoxyethyl 4-methylbenzenesulfonate or 2-(2-(2-methoxyethoxy)ethoxy)ethyl 4-methylbenzenesulfonate in presence of potassium hydroxide, subsequently they were deprotected with trifluoroacetic acid to produce the desired compounds as a trifluoroacetic salts **(175a-b)**. Finally, a nucleophilic substitution between the brominated compounds (**172a-b**) and the respective tetrahydroisoquinolines (**174, 175a-b**) in presence of

potassium carbonate and using acetonitrile as solvent led the target ketones (**176a-f,** Scheme 2-1) in good yields (75-92%, Scheme 3-1). All synthesized compounds were characterized by nuclear magnetic resonance (NMR), infrared spectroscopy (IR), high resolution mass spectrometry (HR-MS) and the purity was confirmed by analytical high performance liquid chromatography (HPLC).

2.2.2 Inhibitory activity evaluation

2.2.2.1 Inhibitory activity evaluation on breast cancer resistance protein (ABCG2)

Synthesized ketones **176a-f** and reference compounds fumitremorgin C (FTC) nd tariquidar were investigated for inhibition of ABCG2 in a Hoechst 33342 microplate assay using ABCG2-overexpressing MCF-7/Topo cells, obtaining inhibitory effects and IC_{50} values as summarized in Table 2.1. Concentration response curves of selected compounds obtained in the Hoechst 33342 assay are shown in Figure 2-1.

All ketones exhibited maximal inhibitory activities between 46-103%, which means that they were active against ABCG2 transporter. Compounds **176d-f**, had the best maximal inhibitory effect of the whole series (90%, 103% and 95% respectively) in comparison with Tariquidar (69%) as reference compound, compound **176e** was even superior to FTC (100%).

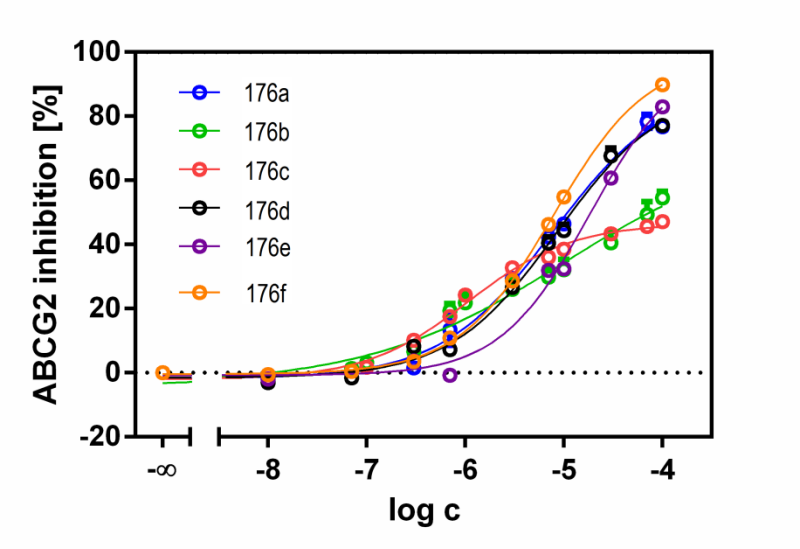

Figure 2-1 Concentration dependent inhibition of the ABCG2 transporter in MCF-7/Topo cells (Hoechst 33342 assay) by ketones **176a-f**. The inhibition is expressed as % relative to the maximal inhibition of ABCG2 by 10 μM of fumitremorgin C (100%)

Compound **176c** (IC_{50} 1.13 μM,) was comparable in potency to reference compound (FTC, IC_{50} 0.731 μM) and the efficacy was improved with the incorporation of a methyl group (R_1 in the structure, Table 2-1) at the amino ketone moiety in case of **176e** and **176f** (Imax 103 and 95% respectively, Table 2-1), but at the same time these compounds had IC_{50} values that exceeded 31 and 9 times the IC_{50} value of FTC and 44 and 13 times for Tariquidar respectively (Table 2-1).

Table 2-1 Inhibitory activity evaluation on ABCG2 by reference compound and ketones 176a-f

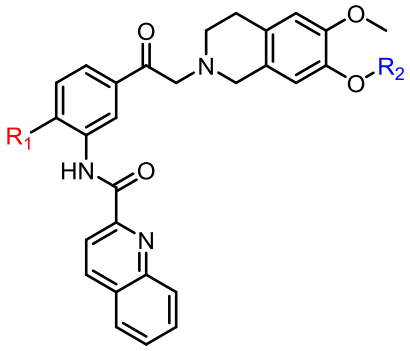

			ABCG2[a]		
Compound	**R_1**	**R_2**	**IC_{50} (μM)[b]**	**I_{max} (%)[c]**	**Log P**
Fumitremorgin C			0.731 ± 0.092	100	
Tariquidar			0.526± 0.085	69 ± 5	
176a	H	CH_3	6.73 ± 1.02	88 ± 6	4.45
176b	H	$CH_2CH_2OCH_3$	14.39 ±11.8	73 ± 4	4.12
176c	H	$(CH_2CH_2O)_3CH_3$	1.13 ± 0.27	46 ± 2	3.40
176d	CH_3	CH_3	8.76 ± 1.59	90 ± 1	4.91
176e	CH_3	$CH_2CH_2OCH_3$	23.24 ± 4.36	103 ± 6	4.58
176f	CH_3	$(CH_2CH_2O)_3CH_3$	6.65 ± 1.27	95 ± 6	3.86

[a]Hoechst 33342 microplate assay using ABCG2-overexpressing MCF-7/Topo cells. [b]Mean values ± SEM from three independent experiments performed in triplicate. [c]Maximal inhibitory effects [%] are expressed as inhibition caused by the highest concentration of the compound tested relative to the inhibitory effect caused by 10 μM FTC (100% inhibition). [d] Calculated values using ACD/Labs I-Lab 2.0 ilab.acdlabs.com, Algorithm Version: v5.0.0.184

Synthesized ketones were more hydrophilic than the chalcone series (Chapter 3, Table 3-1). Calculated partition coefficients for the ketones serie were between 3.40 and 4.91 (lipinski rules, Log P < 5), while this value for the chalcone series was between 5.92 and 6.97. As shown in the Table 2-1, ketone 176**d** has the largest partition coefficient (Log P) among all the synthesized compounds and its potency was comparable with the FTC (100%) and higher than Tariquidar (69%). Compounds **176d** and **176e** have a large value of Log P for the whole series and the highest maximum inhibition (90 and 103% respectively, Table 2-1). Compound **176e** showed a considerable increase in the maximal inhibitory effect (103%) in comparison with compound **176b** (73%).

2.2.2.2 Selectivity evaluation. Inhibitory activity evaluation on ABCB1 and ABCC1

All synthesized compounds were additionally screened for their inhibition of ABCB1 and ABCC1 utilizing the calcein accumulation assay. The screening was conducted at a fixed concentration of 1 and 10 μM using Kb-V1 cells (ABCB1) and MDCKII (ABCC1) cell lines. Tariquidar (10 μM) was used as standard inhibitor for ABCB1 and Reversan (30 μM) was used as standard inhibitor for ABCC1. Figure 2-2 illustrates the effects of the 6 ketones on the accumulation of calcein and it exemplifies that the studied substances possess low affinity for ABCB1 (Figure 2-2A) and ABCC1 (Figure 2-2B).

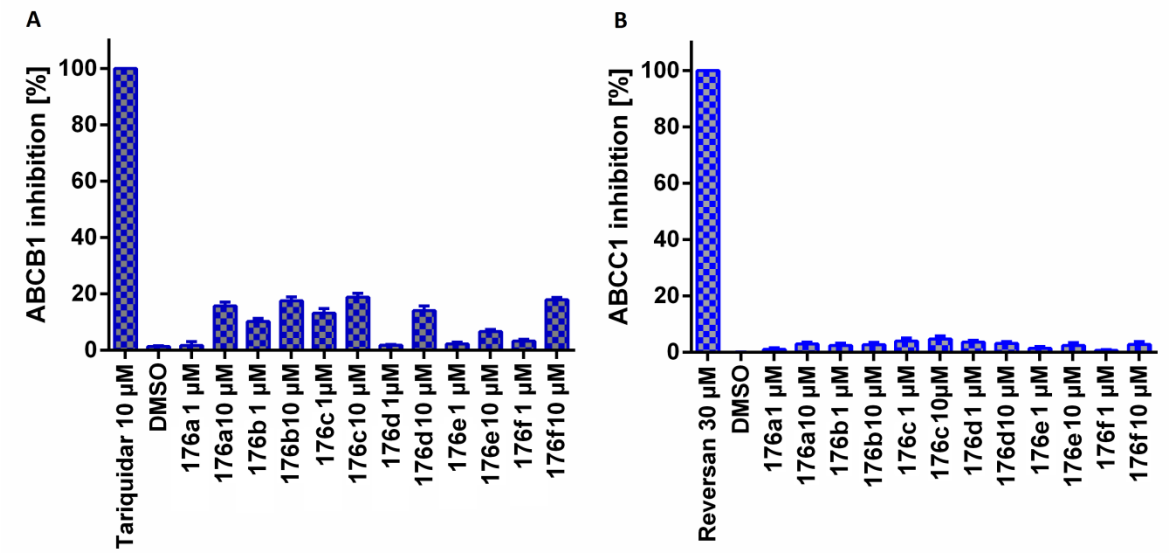

Figure 2-2 Effects of ketones **176a-f** at 1 and 10 μM concentration on the accumulation of calcein in ABCB1 (A) and ABCC1 (B) overexpressing Kb-V1 and MDCKII cells respectively. Data were normalized by defining the inhibition caused by 10 μM Tariquidar and of 30 μM Reversan as 100 % and are presented as mean ± SD of two independent experiments

All compounds showed lowest affinity at ABCC1, but some compounds presented inhibitory activity against ABCB1 above 15%, as compounds **176b, 176c** and **176f.** Concentration-response curves were not generated for the synthesized ketones since none of them showed more than 25% inhibition at 10 μM (Table 2-2).

Compounds did not show a clear trend based on the substituents (Table 2-2), either the presence of methyl in R_1, but as shown in Table 2-2, the results for the ABCB1 transporter the first three compounds showed an increase in the maximal inhibitory effect when was added ethylene and triethylenglicol chains in substituent R_2 (Table 2-2**¡Error! No se encuentra el origen de la referencia.**).

Table 2-2 Inhibitory activity evaluation on ABCB1 and ABCC1 by reference compounds and ketones 176a-f

	ABCB1[a]	**ABCC1**[b]
Compound	**I_{max} (%)**[c]	**I_{max} (%)**[d]
Tariquidar	100	n.d[e]
Reversan	n.d[e]	100
176a	16 ± 1	3± 1
176b	18± 1	3± 1
176c	19± 1	5± 1
176d	14± 2	3± 1
176e	7± 1	2± 1
176f	18± 1	3± 1

[a]Calcein-AM microplate assay using ABCB1-overexpressing Kb-V1 cells. [b]Calcein-AM microplate assay using ABCC1-overexpressing MDCKII cells. [c]Maximal inhibitory effect (Imax) relative to the response to tariquidar at a concentration of 10 μM (100% inhibition). [d]Maximal inhibitory effect (Imax) relative to the response to reversan at a concentration of 30 μM (100% inhibition). [e]n.d.: not determinated

The maximal inhibitory effect values for the ketones **176a-f** over ABCB1 and ABCC1 were not significant for these transporters, but, according to what is shown in the Table 2-2, all compounds show a preference for ABCB1 than for ABCC1.

According to the results obtained, the synthesized ketones were selective against ABCG2 instead of the other transporters here studied.

2.2.3 Chemical stability test in Eagle's Minimum Essential Medium (EMEM)

The metabolism of drugs occurs through basic chemical reactions as soon as the administered compound comes into contact with enzymes that are capable of altering its chemical structure. Conversely, a drug's stability after administration is due mainly to its lack of transformation by the body's enzymes. However, many drugs are susceptible to some form of chemical decomposition, be it through the interaction with enzymes or through improper storage and use, and such degradation often leads to a loss of potency. Hydrolysis is the more common pathway for drug breakdown and is the mechanism that we will concentrate on here with regard to both chemical stability and metabolism. Hydrolysis means the reaction of a molecule with water resulting in the cleavage of a chemical bond within that molecule. Although there are a large number of functional groups that are susceptible to hydrolysis, esters and amides are the most common ones found in drugs prone to hydrolysis.[7]

The bioisosteric approach and the replacement of the hydrolysis-sensitive amide bond bearing the phenethyl tetrahydroisoquinoline fragment (previously reported ABCG2 modulators, Figure 1-30, compounds **143** and **145**), by ketones moieties resulted in stable compounds after incubation in EMEM. As shown in Figure 2-3, synthesized chalcones were incubated in EMEM at a temperature of 37°C and aliquots were analyzed by HPLC over a period of 24 hours, products of cleavage or degradation of compounds were not detected, compounds were not affected by the components present in the incubation medium (EMEM) during the assay.

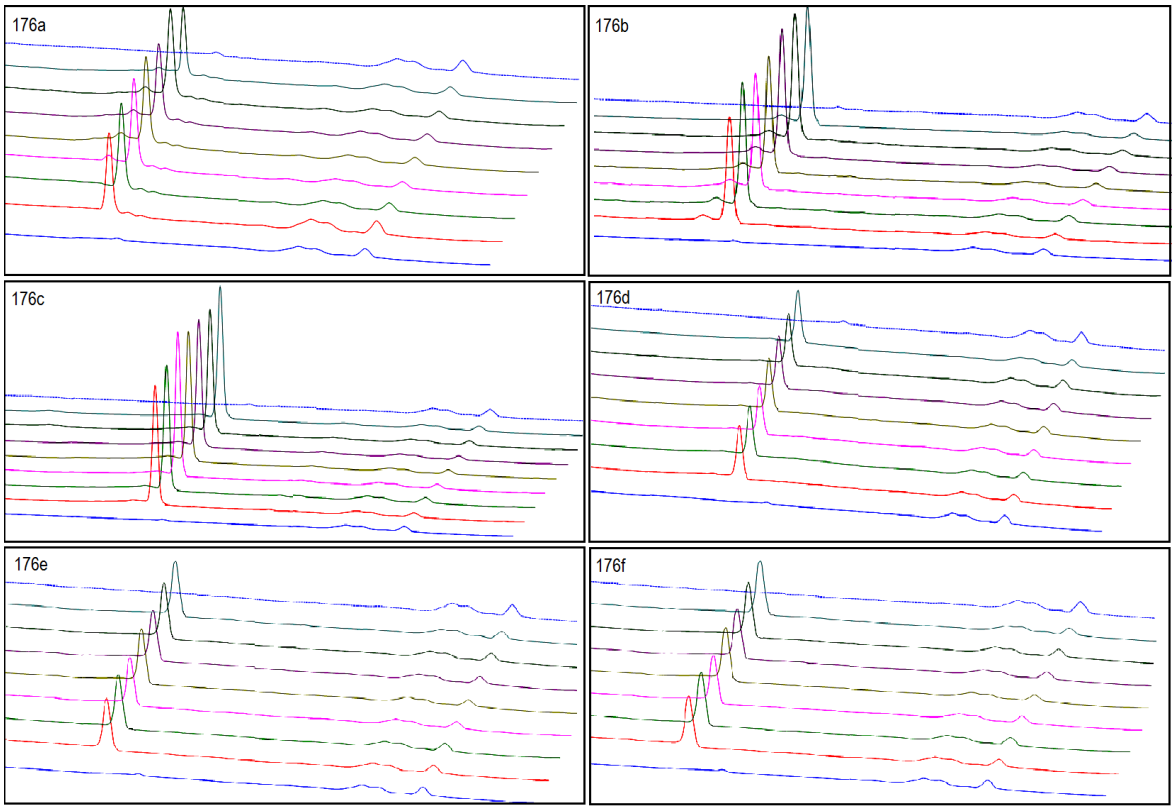

Figure 2-3 Chemical stability of compounds 176a-f incubated in EMEM for 24 h (HPLC analysis, UV detection at 220 nm).

2.2.4 Solubility in Eagle's Minimum Essential Medium (EMEM)

The solubility in EMEM for ketones was evaluated; aliquots were taken for three different concentrations for each compound at three times, the results showed that all chalcones were soluble. As shown in Figure 2-4, the concentration found for ketones **176a-f** was similar in all analyzed aliquots, which means that after 2 h of incubation all compound was acting in the assay, and these were not affected by the physiological pH, temperature or the substances present in the medium (salts, amino acids or vitamins). Then, the results for the inhibition correspond to the entire concentration used in the assay.

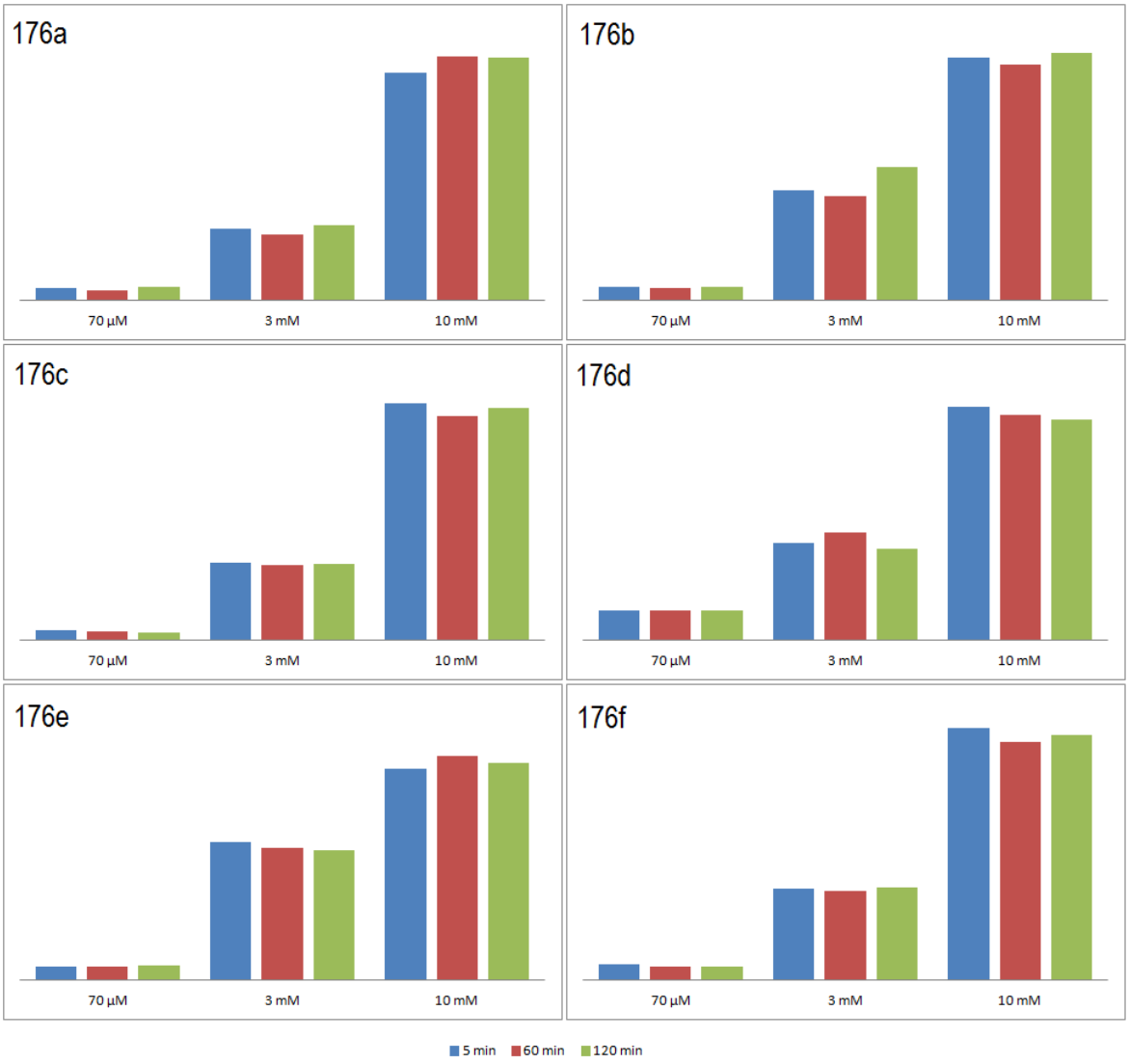

Figure 2-4 Solubility for ketones in Eagle's Minimum Essential Medium (EMEM)

2.2.5 Chemosensitivity assay

To confirm ABCG2 transporter inhibition, resulting in a reversal of ABCG2 mediated drug resistance; the effect of the compound **176a** on the proliferation of one cell line was investigated using a kinetic crystal violet chemosensitivity assay (Figure 2-5). ABCG2-overexpressing MCF-7/Topo cells show resistance against the cytostatic drug topotecan, a known ABCG2 substrate. The cells were incubated with topotecan alone and in combination with different concentrations of the new modulator and the cytostatic drug

vinblastine as positive control.[8] The modulator was well tolerated up to a concentration of 3 µM.

The combination of topotecan at a nontoxic concentration of 100 nM with compound **176a**, resulted in a cytotoxic drug effect, even at a low modulator concentration of 1 µM. A higher concentration of the modulator the cyctotoxicity increases.

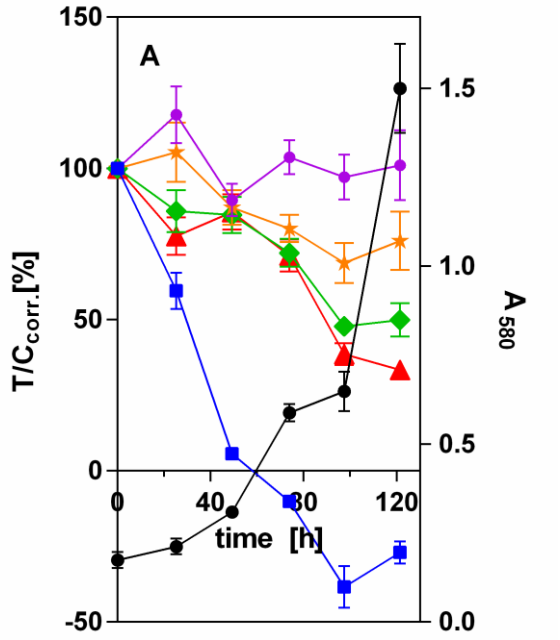

Figure 2-5 Effect of compound **176a** in combination with topotecan on proliferating MCF-7/Topo cells: vehicle (filled black circles, untreated cells), positive control vinblastine [100 nM] (filled blue squares), **176a** at concentrations of 10 µM (filled red triangles), 3 µM (filled green diamonds), 1 µM (filled orange stars) and topotecan alone at 100 nM (filled purple circles)

2.3 Conclusion

In summary, we presented the synthesis and characterization of a series of ketones combining quinoline and isoquinoline moieties as ABCG2 modulators. All tested compounds showed weak inhibitory activity over ABCB1 and ABCC1 transporter but good inhibitory activity towards ABCG2. Compounds with methyl group as substituent in R_1 (**176d-f**) has the best results for maximal inhibitory effect (I_{max}) in comparison with

reference compound and tariquidar. Compound **176c** was the most potent ABCG2 modulator; with the best IC_{50} value (1.13 µM) in the Hoechst assay, compound **176e** had the higher maximal inhibitory effect (103 %) compared to the standard ABCG2 modulator Fumitremorgin C and Tariquidar. The unstable benzamide moiety was replaced in a bioisosteric approach with a ketone system as central core structure; chemical stability tests in EMEM revealed that these compounds (**176a-f)** are stable to degradation over a period of 24 hours of incubation. The hidrophilicity was improved with the addition of ethylene and ethylene glycol chains in substituent R_2 (Scheme 3-1) as shown in the calculated partition coefficient (Table 3-1), in addition, the efficacy for compounds increased (I_{max} 90-103%). The synthesized ketones were more hydrophilic than the chalcones series, as can be seen in the calculated partition coefficient, but their IC_{50} is higher that the value for the reference compound, even when their maximal inhibitory effect was much higher than the synthesized chalcones and the reference compound.

2.4 Experimental section

2.4.1 Synthesis and characterization

General procedure for the preparation of nitro compounds: compounds were prepared according to known procedures**.**[9]

1-(3-Nitrophenyl)ethan-1-one

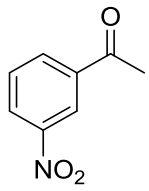

Light yellow solid (1.8 g, yield 50%, R_f PE/EA 1:1 0.67). mp 75-78°C (76-78ºC lit).[9] **^{1}H NMR ($CDCl_3$, 400 MHz): δ**= 8.81 (d, ^4J=1.9 Hz, 1H, ArH), 8.46 (ddd, ^3J=8.2, ^4J=2.2, ^4J=1.1 Hz, 1H, ArH), 8.32 (d, ^3J=7.8 Hz, 1H, ArH), 7.72 (s, 1H, ArH), 2.72 (s, 3H, CH_3CO). **^{13}C NMR ($CDCl_3$, 100 MHz): δ**= 195.8 (C_{quat}), 147.0 (C_{quat}), 138.4 (C_{quat}), 133.7 (+), 129.9

(+), 127.4 (+), 123.2 (+), 26.7 (+). **IR (KBr) [cm^{-1}]: v** = 3237, 3090, 1691, 1520, 1428, 1348, 1250, 970, 821, 587.

1-(4-methyl-3-nitrophenyl)ethan-1-one

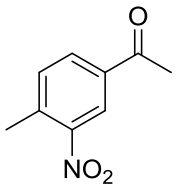

Yellow solid (1.5 g, yield 65%, R_f PE/EA 7:3 0.43). mp 60-62°C (60-61 lit).[10] **^{1}H NMR (400 MHz, $CDCl_3$): δ** 8.52 (d, ^3J=1.5 Hz, 1H, ArH), 8.08 (dd, ^3J=8.0, ^4J=1.5 Hz, 1H, ArH), 7.47 (s, 1H, ArH), 2.67 (s, 3H, CH_3CO), 2.65 (s, 3H, CH_3). **^{13}C NMR (100 MHz, $CDCl_3$): δ** 195.5 (C_{quat}), 149.2 (C_{quat}), 138.6 C_{quat}), 136.1 (C_{quat}), 133.3 (+), 131.9 (+), 124.6 (+), 26.5 (+), 20.6 (+). **IR [cm^{-1}]: v** = 1692, 1617, 1531, 1348, 1282, 1251, 833, 803.

General procedure for the preparation of amino compounds (170a-b): The respective nitro derivative (1 equiv) was dissolved in a mixture of ethanol and water (2:1), iron powder (10 equiv) and conc. HCl (0.05 mL) were added and the mixture was refluxed for 90 min. Ethyl acetate was added and the mixture was filtered over celite, dried over sodium sulfate, filtered again and the solvent evaporated, resulted the corresponding amino compound.

1-(3-aminophenyl)ethan-1-one (170a)

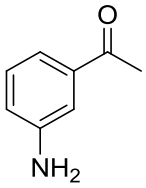

Light brown solid (1.2 g, yield 85%, R_f Pentane:EA 1:1 0.55). mp 93-95°C (94-98ºC).[11] **^{1}H NMR ($CDCl_3$, 400 MHz)**: **δ=** 6.97 (t, ^3J=7.7 Hz, 1H, ArH), 6.90 (m, 1H, ArH), 6.85 (m, 1H, ArH) 6.50 (dd, ^3J=7.8, ^4J=1.7 Hz, 1H, ArH), 2.19 (s, 3H, CH_3CO). **^{13}C NMR ($CDCl_3$, 100 MHz)**: **δ=** 198.6 (C_{quat}), 146.7 (C_{quat}), 138.1 (C_{quat}), 129.4 (+), 119.7 (+), 118.9 (+), 114.0 (+), 26.7 (+). **IR (KBr) [cm^{-1}]: v =**3550, 3473, 3415, 3236, 2925, 2810, 1639, 1618, 1458, 1384, 1358, 1323, 1238, 870, 621.

1-(3-amino-4-methylphenyl)ethan-1-one (170b)

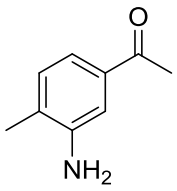

Brown solid (1.4 g, yield 93%, R_f Hex/EA 4:1 0.24). mp 78-80ºC (80-81ºC lit).[10] **^{1}H NMR (400 MHz, $CDCl_3$): δ** 7.28 (dd, ^3J=7.5, ^4J=2.0 Hz, 1H, ArH), 7.27 (d, ^3J=7.3, 1H, ArH), 7.12 (d, ^3J=7.5, 1H, ArH), 2.54 (s, 3H, $COCH_3$), 2.21 (s, 3H, CH_3). **^{13}C NMR (100 MHz, $CDCl_3$): δ** 198.3 (C_{quat}), 144.8 (C_{quat}), 136.2 (C_{quat}), 130.4 (C_{quat}), 128.0 (+), 119.1 (+), 113.8 (+), 26.5 (+), 17.5 (+). **IR [cm^{-1}]: v** = 3367, 1672, 1573, 1422, 1356, 1291, 1237, 1199.

General procedure for the amide formation (171a-b)[12]: TsCl (1.2 equiv) and amine (**170a-b**) were added, in that order, at 0 °C under N_2 to a flask containing quinaldic acid (1.2 equiv), triethylamine (2 equiv), and CH_2Cl_2, and the mixture was stirred at 40-50°C overnight. AcOH (5% aq.) was added to quench the reaction, the organic phase was separated and washed three times with water, dried over sodium sulfate, filtered again and the solvent evaporated.The obtained solid was washed with ether furnishing the desired product.

***N*-(3-Acetylphenyl)quinoline-2-carboxamide (171a)**

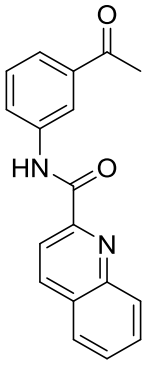

White solid (0.500 g, yield quant, R_f PE:EA 2:1 0.40).**^{1}H NMR ($CDCl_3$, 400 MHz)**: **δ=** 8.43 (s, 2H, quinol), 8.39 (t, ^3J=1.9 Hz, 1H, quinol), 8.25 (m, 2H, ArH), 7.96 (d, ^3J=8.2 Hz, 1H,

quinol), 7.87 (t, ^{3}J=8.3 Hz, 1H, ArH), 7.79 (d, ^{3}J=7.9 Hz, 1H, ArH), 7.71 (t, ^{3}J=7.5 Hz, 1H, quinol), 7.56 (t, ^{3}J=7.9 Hz, 1H, quinol), 2.70 (s, 3H, CH_3). **^{13}C NMR ($CDCl_3$, 100 MHz)**: **δ=** 197.8 (C_{quat}), 162.3 (C_{quat}), 149.1 (C_{quat}), 146.1 (C_{quat}), 138.3 (C_{quat}), 138.1 (C_{quat}), 137.9 (C_{quat}), 130.5 (+), 129.5 (+), 129.5 (+), 129.4 (+), 128.4 (+), 127.8 (+), 124.2 (+), 124.1 (+), 119.3 (+), 118.7 (+), 26.7 (+). **IR (KBr) [cm^{-1}]: ν =**3483, 3416, 3341, 3082, 2923, 1687, 1591, 1530, 1504, 1442, 1365, 1295, 1126, 955, 846, 774, 686, 584. **HRMS (EI-MS)** calcd. For $C_{18}H_{15}N_2O_2$ $[M+H]^+$: 291.1089; found $[M+H]^+$: 291.1128.

***N*-(5-Acetyl-2-methylphenyl)quinoline-2-carboxamide (171b)**

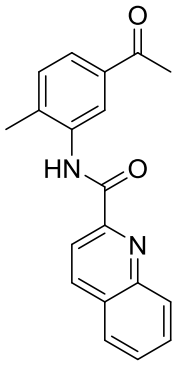

Light yellow solid (0.700 g, yield quant, R_f PE/EA 2:1 0.52). **^{1}H NMR (400 MHz, $CDCl_3$): δ** 8.95 (d, ^{3}J=7.7 Hz, 1H, quinol), 8.40 (s, 2H, ArH quinol), 8.17 (d, ^{3}J=8.5 Hz, 1H, ArH), 7.93 (d, ^{3}J=9.0 Hz, 1H, quinol), 7.82 (ddd, ^{3}J=8.4, ^{3}J=6.9 Hz, 1H, quinol), 7.73 (dd, ^{3}J=7.9, 1H, ArH), 7.67 (ddd, ^{3}J= 8.1, ^{3}J=6.9 Hz, 1H, quinol), 7.35 (d, ^{3}J=7.9 Hz, 1H, quinol), 2.65 (s, 3H, CH_3), 2.55 (s, 3H, $COCH_3$). **^{13}C NMR (100 MHz, $CDCl_3$): δ**= 197.8 (C_{quat}), 162.2 (C_{quat}), 149.5 (C_{quat}), 146.2 (C_{quat}), 138.0 (C_{quat}), 136.2 (C_{quat}), 133.5 (C_{quat}), 130.7 (C_{quat}), 130.4 (+), 129.8 (+), 129.5 (+), 128.3 (+), 127.8 (+), 124.1 (+), 121.5 (+), 118.6 (+), 26.7 (+), 18.0 (+). **IR [cm^{-1}]: ν =** 3420, 3050, 2910, 1670, 1580, 1410, 1350, 1220, 1080, 760. **HRMS (EI-MS)** calcd. For $C_{19}H_{17}N_2O_2$ $[M+H]^+$: 305.1245; found $[M+H]^+$: 305.1285.

General procedure for the bromination of ketones 172a-b:[13] To a solution of acetophenone (10 mmol) in methanol at reflux conditions were added 10% (w/w) silica gel and slowly *N*-bromosuccinimide (12 mmol), the progress of the reaction was monitored by TLC until the disappearance of the substrate. The reaction was filtered after the completion of the reaction. The filtrate was concentrated under vacuum and the solid was

washed twice with distilled water, then aqueous sodium thiosulfate was added to quench the reaction and the product was extracted with dichloromethane, organic layers were collected and washed thrice with water, dried over anhydrous Na_2SO_4, filtered and concentrated to give the desired product.

***N*-(3-(2-Bromoacetyl)phenyl)quinoline-2-carboxamide (172a)**

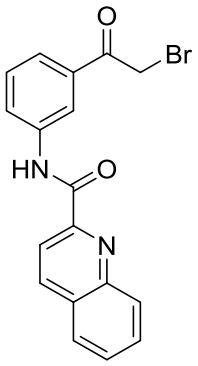

White solid (0.500 g, yield 84%, R_f PE:EA 2:1 0.67). **^{1}H NMR ($CDCl_3$, 400 MHz): δ** 8.46 (t, ^3J=7.9 Hz, 1H, quinol), 8.42 (s, 1H, quinol), 8.27 (d, ^3J=8.5 Hz, 1H, ArH), 8.22 (d, ^3J=7.7 Hz, 1H, quinol), 7.95 (d, ^3J=8.2 Hz, 1H, quinol), 7.86 (ddd, ^3J=8.4, ^3J=6.9 Hz, 1H, ArH), 7.81 (m, 1H, quinol), 7.72 (m, 2H, ArH), 7.56 (t, ^3J=7.9 Hz, 1H, quinol), 4.54 (s, 2H, CH_2Br).**^{13}C NMR ($CDCl_3$, 100 MHz): δ** 191.0 (C_{quat}), 162.2 (C_{quat}), 148.9 (C_{quat}), 145.9 (C_{quat}), 138.5 (C_{quat}), 138.4 (C_{quat}), 134.8 (+), 130.8 (+), 129.7 (+), 128.6 (+), 127.9 (+), 125.0 (+), 124.7 (+), 119.8 (+), 118.8 (+), 31.1 (-). **IR (KBr) [cm^{-1}]: ν** =3483, 3416, 3341, 3082, 2923, 1687, 1591, 1530, 1504, 1442, 1365, 1295, 1126, 955, 846, 774, 686, 584. **HRMS (EI-MS)** calcd. For $C_{18}H_{14}BrN_2O_2$ $[M+H]^+$: 369.0194; found $[M+H]^+$: 369.0233.

***N*-(5-(2-Bromoacetyl)-2-methylphenyl)quinoline-2-carboxamide (172b)**

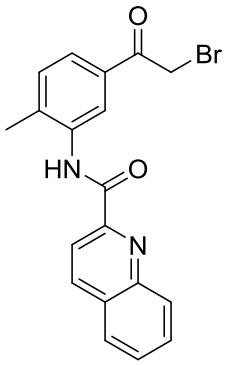

Light yellow solid (0.720 g, yield 77%, R_f PE:EA 2:1 0.59). **^{1}H NMR ($CDCl_3$, 400 MHz): δ** 9.02 (d, ^3J=1.7 Hz, 1H, quinol), 8.41 (s, 1H, quinol), 8.18 (d, ^3J=8.5 Hz, 1H, ArH), 7.94 (d, ^3J=8.2 Hz, 1H, quinol), 7.86 (m, 1H, quinol), 7.77 (d, ^3J=7.9 Hz, 2H, ArH), 7.68 (dd, ^3J=8.1, ^3J=7.0 Hz, 1H, quinol), 7.39 (d, ^3J=7.9 Hz, 1H, quinol), 4.54 (s, 2H, CH_2Br), 2.57 (s, 3H, CH_3). **^{13}C NMR ($CDCl_3$, 100 MHz): δ** 192.6 (C_{quat}), 162.3 (C_{quat}), 149.6 (C_{quat}), 146.6 (C_{quat}), 138.1 (C_{quat}), 136.4 (C_{quat}), 134.8 (C_{quat}), 133.3 (+), 131.1 (+), 130.5 (+), 129.8 (+), 129.6 (+), 128.4 (+), 127.9 (+), 124.8 (+), 121.9 (+), 118.7 (+), 31.4 (-), 20.6 (+). **IR (KBr) [cm^{-1}]: ν** 3483, 3416, 3341, 3082, 2923, 1687, 1591, 1530, 1504, 1442, 1365, 1295, 1126, 955, 846, 774, 686, 584. **HRMS (EI-MS)** calcd. For $C_{19}H_{16}BrN_2O_2$ $[M+H]^+$: 383.0350; found $[M+H]^+$: 383.0396.

tert-Butyl 7-hydroxy-6-methoxy-3,4-dihydroisoquinoline-2(1H)-carboxylate (173)

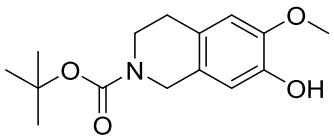

6-Methoxy-1,2,3,4-tetrahydroisoquinolin-7-ol hydrochloride (1 mmol) and triethylamine (2.5 equiv) were dissolved in 10 mL of dry DCM, the mixture was cooled in an ice bath and di-*tert*-butyl dicarbonate (1 equiv) was added slowly. The mixture was stirred at room temperature overnight, and then washed with water and brine, dried over magnesium sulphate, filtered and the solvent evaporated. The compound was purified by column chromatography (PE:EA 2:1), white solid (3.0 g, yield 89%, R_f PE:EA 1:1 0.55). mp 124-126 ºC (123.6-124.2ºC lit).[14] **^{1}H NMR ($CDCl_3$, 400 MHz): δ**= 6.85 (s, 1H, ArH), 6.70 (s, 1H, ArH), 4.47 (s, 2H, NCH_2), 3.81 (s, 3H, OCH_3), 3.60 (m, 2H, NCH_2CH_2), 2.75 (t, ^3J=5.6 Hz, 2H, NCH_2CH_2), 1.48 (s, 9H, $C(CH_3)_3$). **^{13}C NMR ($CDCl_3$, 100 MHz): δ**= 154.8 (C_{quat}), 151.7 (C_{quat}), 149.5 (C_{quat}), 138.5 (C_{quat}), 133.1 (C_{quat}), 120.1 (+), 112.5 (+), 83.4 (C_{quat}), 56.0 (+), 45.1 (-), 40.4 (-), 28.9 (-), 28.4 (+). **IR (KBr) [cm^{-1}]: ν** = 3024, 2976, 1685.

2-Methoxyethyl 4-methylbenzenesulfonate[15]

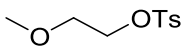

A solution of 4-toluenesulfonyl chloride (0.06 mol) in dichloromethane was added drop-wise to a solution of (2-methoxyethoxy)ethanol (0.057 mol) and triethylamine (0.114 mol) in dichloromethane at 0°C under a nitrogen atmosphere. The formation of a white precipitate was observed. The reaction mixture was stirred at room temperature for 18h and then poured into water (50 mL). The aqueous layer was extracted with dichloromethane. The organic layers were combined and washed with 3M HCl (50 mL), saturated solution of sodium bicarbonate (50 mL), and water (50 mL). The organic phase was dried over magnesium sulfate, filtered and the solvent was removed in vacuo. Pale yellow oil (1.45 g, yield 100%). **^{1}H NMR (CD_3OD, 400 MHz)**: **δ=** 7.82 (d, ^{3}J=8.3 Hz, 2H, ArH), 7.36 (d, ^{3}J=8.0 Hz, 2H, ArH), 4.17 (d, ^{3}J=1.2 Hz, 2H, OCH_2CH_2), 3.60 (s, 2H, CH_2OCH_3), 3.32 (s, 3H, CH_3), 2.46 (s, 3H, OCH_3).**^{13}C NMR (CD_3OD, 100 MHz)**: **δ=** 140.87 (C_{quat}), 129.12 (C_{quat}), 125.87 (+), 124.03 (+), 65.99 (-), 65.11 (-), 55.06 (+), 17.68 (+). **IR (KBr) [cm^{-1}]: ν =**3070, 2928, 2822, 1598, 1495, 1356, 1311, 1018, 817, 689.

2-(2-(2-Methoxyethoxy)ethoxy)ethyl 4-methylbenzenesulfonate

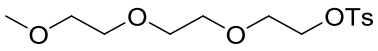

2-(2-(2-methoxyethoxy)ethoxy)ethyl 4-methylbenzenesulfonate was prepared according to known procedures.[15] Pale yellow oil (2.0 g, yield 100%). **^{1}H NMR (CD_3OD, 400 MHz)**: **δ=** 7.77 (d, ^{3}J=8.3, 2H, tosyl), 7.32 (d, ^{3}J=8.2, 2H, tosyl), 4.13 (t, ^{3}J=4.8, 2H, CH_2 PEG), 3.66 (t, ^{4}J=4.8, 2H, CH_2 PEG), 3.55 (m, 6H, $3CH_2$ PEG), 3.48 (m, 2H, CH_2 PEG), 3.36 (s, 3H, OCH_3), 2.43 (s, 3H, CH_3 tosyl).

6-Methoxy-7-(2-methoxyethoxy)-1,2,3,4-tetrahydroisoquinoline-2,2,2-trifluoroacetate (175a)

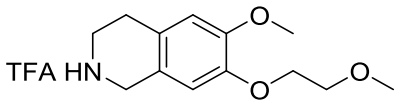

Compound **175a** was prepared according to known procedures with slight modifications.[14] (quantitative yield, R_f DCM:MeOH 19:1 0.50). **^{1}H NMR (CD_3OD, 400 MHz): δ=** 6.81 (s, 1H, ArH), 6.79 (s, 1H, ArH), 4.25 (s, 2H, CH_2), 4.12 (m, 2H, CH_2), 3.82 (s, 3H, CH_3), 3.76 (m, 2H, CH_2), 3.46 (t, ^3J=6.4 Hz, 2H, CH_2), 3.41 (s, 3H, CH_3), 3.04 (t, ^3J=6.3 Hz, 2H, CH_2). **^{13}C NMR (CD_3OD, 100 MHz): δ=** 149.6 (C_{quat}), 147.6 (C_{quat}), 124.0 (C_{quat}), 119.6 (C_{quat}), 111.6 (+), 70.7 (-), 68.4 (-), 57.8 (+), 55.0 (+), 44.0 (-), 41.5 (-), 24.2 (-).**HRMS (EI-MS)** calcd. For $C_{15}H_{21}F_3NO_5$ $[M+H]^+$: 352.1327; found $[M+H]^+$: 352.1347.

6-Methoxy-7-(2-(2-(2-methoxyethoxy)ethoxy)ethoxy)-1,2,3,4-tetrahydroisoquinoline-2,2,2-trifluoroacetate (175b)

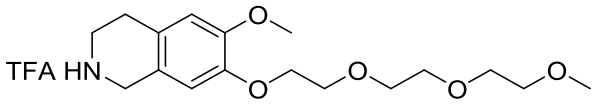

Compound **175b** was prepared according to known procedures with slight modifications.[14] Sticky brown solid (Yield 79%, R_f DCM:MeOH 19:1 0.46). **^{1}H NMR ($CDCl_3$, 400 MHz): δ**= 6.60 (s, 1H, CH THIQ), 6.57 (s, 1H, CH THIQ), 4.39 (s, 2H, NCH_2 THIQ), 4.06 (t, ^3J=5.04 Hz, 4H, CH_2 PEG), 3.77 (t, ^3J=5.1 Hz, 4H, $2CH_2$ PEG), 3.65 (m, 4H, $2CH_2$ PEG), 3.56 (m, 8H, $4CH_2$ PEG), 3.51 (m, 2H, CH_2 THIQ), 3.46 (m, 4H, CH_2 PEG), 3.30 (s, 6H, $2OCH_3$), 2.65 (t, ^3J=5.3 Hz, 2H, CH_2 THIQ). **^{13}C NMR ($CDCl_3$, 100 MHz): δ**= 154.8 (+), 147.5 (C_{quat}), 147.4 (C_{quat}), 127.5 (C_{quat}), 126.2 (C_{quat}), 115.0 (+), 112.7 (+), 79.7 (C_{quat}), 71.9 (-),70.78 (-), 70.6 (-), 70.5 (-), 69.6 (-), 69.0 (-), 69.0 (-), 59.0 (+), 45.5 (-), 44.8 (+), 41.9 (-), 40.6 (-), 28.4 (+), 28.4 (-). **IR (KBr) [cm-1]: v** = 2920, 2875, 1670.

General procedure for the synthesis of compounds 176a-f A mixture of the tretrahydroisoquinoline derivative **174**, **175a-b** (1 equiv), **172a-b** (1 mol) and potassium carbonate (3 equiv) was refluxed during 18 h in CH_3CN, the solvent was evaporated, the residue taken up in water and extracted with DCM. The solution was dried over $MgSO_4$, filtered and concentrated to give the crude product. Compounds were purified by column chromatography (PE:EA) and reverse column chromatography or preparative HPLC.

***N*-(3-(2-(6,7-Dimethoxy-3,4-dihydroisoquinolin-2(1*H*)-yl)acetyl)phenyl)quinoline-2-carboxamide (176a)**

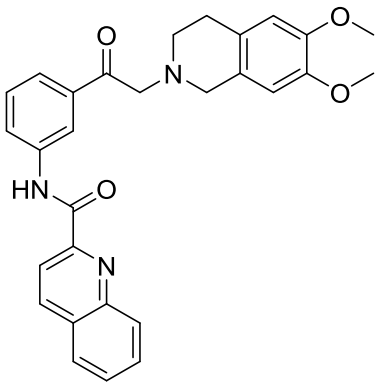

Light yellow solid. (0.025 g, yield 75%, R_f PE:EA 2 : 1 0.36). **^{1}H-NMR (400 MHz, $CDCl_3$): δ** 8.38 (m, 1H, quinol), 8.30 (dd, ^3J=7.6, ^3J=8.4 Hz, 2H, quinol), 8.12 (dd, ^3J=8.3, ^3J=7.9 Hz, 2H, ArH), 7.87 (d, ^3J=8.1 Hz, 1H, quinol), 7.78 (t, ^3J=7.4 Hz, 1H, quinol), 7.69 (m, 2H, ArH), 7.47 (t, ^3J=6.2 Hz, 1H, quinol), 6.62 (s, 1H, CH THIQ), 6.52 (s, 1H, CH THIQ), 4.90 (s, 2H, $COCH_2$), 4.56 (m, 2H, CH_2 THIQ), 3.83 (s, 3H, OCH_3), 3.80 (s, 3H, OCH_3), 3.13 (m, 4H, $2CH_2$ THIQ). **^{13}C-NMR (100 MHz, $CDCl_3$): δ** 194.5 (C_{quat}), 169.7 (C_{quat}), 149.2 (C_{quat}), 148.8 (C_{quat}), 148.5 (C_{quat}), 146.6 (C_{quat}), 138.6 (C_{quat}), 138.0 (C_{quat}), 136.2 (C_{quat}), 134.4 (C_{quat}), 130.5 (+), 129.9 (+), 129.7 (+), 128.4 (+), 127.8 (+), 125.8 (+), 123.7 (+), 122.3 (+), 118.5 (+), 111.2 (+), 55.9 (-), 52.8 (+), 50.0 (-), 45.7 (-), 24.1 (-). **IR (KBr) [cm^{-1}]: v =** 2880, 1689, 1635, 1425, 1150, 753, 726. **HRMS (EI-MS)** calcd. For $C_{29}H_{28}N_3O_4$ $[M+H]^+$: 482.2035; found $[M+H]^+$: 482.2048

_N_-(3-(2-(6-Methoxy-7-(2-methoxyethoxy)-3,4-dihydroisoquinolin-2(1_H_)-yl)acetyl)phenyl)quinoline-2-carboxamide (176b)

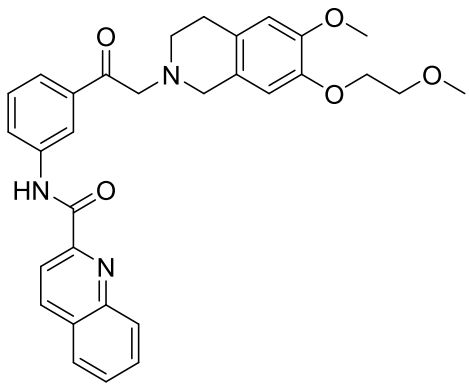

Light yellow solid. (0.030 g, yield 90%, R_f PE:EA 2:1 0.31). **^{1}H-NMR (400 MHz, $CDCl_3$): δ** 8.38 (m, 2H, quinol), 8.33 (s, 2H, quinol), 8.21 (d, ^3J=8.5 Hz, 2H, ArH), 7.93 (d, ^3J=8.3 Hz, 2H, quinol), 7.83 (dd, ^3J=8.4, ^3J=7.0 Hz, 2H, ArH), 7.67 (t, ^3J=7.9 Hz, 2H, quinol), 6.80 (s, 1H, CH THIQ), 6.62 (s, 1H, CH THIQ), 5.28 (s, 2H, $COCH_2$), 4.19 (s, 2H, CH_2 THIQ), 3.87 (d, ^3J=5.4 Hz, 2H, CH_2 PEG), 3.83 (s, 3H, OCH_3), 3.80 (d, ^3J=4.7 Hz, 2H, CH_2 PEG), 3.47 (s, 3H, CH_2OCH_3), 3.14 (m, 2H, CH_2 THIQ), 2.86 (t, ^3J=5.7 Hz, 2H, CH_2 THIQ). **^{13}C-NMR (100 MHz, $CDCl_3$): δ** 187.0 (C_{quat}), 163.4 (C_{quat}), 146.3 (C_{quat}), 138.6 (C_{quat}), 138.0 (C_{quat}), 134.3 (C_{quat}), 130.5 (C_{quat}), 129.8 (C_{quat}), 129.7 (C_{quat}), 129.5 (+), 128.4 (+), 127.8 (+), 125.8 (+), 125.6 (+), 125.6 (+), 122.8 (+), 120.6 (+), 118.7 (+), 111.8 (+), 111.6 (+), 71.0 (-), 68.7 (-), 59.6 (-), 55.8 (+), 49.5 (+), 49.3 (-), 45.8 (-), 29.7 (-). **IR (KBr) [cm^{-1}]: ν =** 2903, 1673, 1645, 1402, 1189, 764, 731. **HRMS (EI-MS)** calcd. For $C_{31}H_{32}N_3O_5$ $[M+H]^+$: 526.2297; found $[M+H]^+$: 526.2315

***N*-(3-(2-(6,7-*bis*(2-(2-(2-Methoxyethoxy)ethoxy)ethoxy)-3,4-dihydroisoquinolin-2(1*H*)-yl)acetyl)phenyl)quinoline-2-carboxamide (176c)**

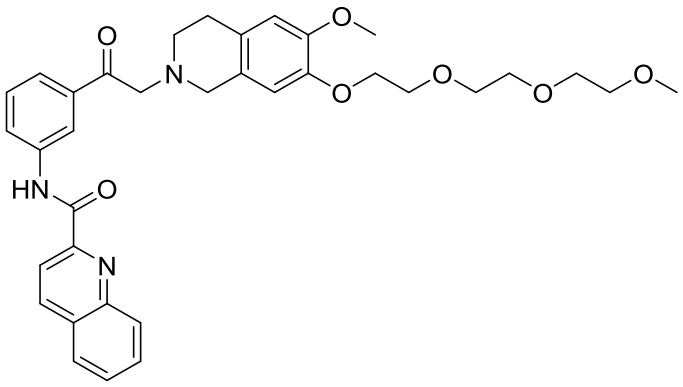

Light yellow solid. (0.026 g, yield 85%, R_f PE:EA 2:1 0.20). **^{1}H-NMR (400 MHz, $CDCl_3$): δ** 8.38 (m, 2H, quinol), 8.33 (s, 2H, quinol), 8.20 (d, ^3J=8.5 Hz, 1H, ArH), 7.91 (s, 1H, ArH quinol), 7.84 (m, 1H, quinol), 7.67 (t, ^3J=7.2 Hz, 1H, ArH), 7.53 (m, 2H, ArH), 6.81 (s, 1H, CH THIQ), 6.62 (s, 1H, CH THIQ), 5.27 (s, 2H, $COCH_2$), 4.21 (s, 2H, CH_2 THIQ), 3.91 (dd, ^3J=5.7, 4.3 Hz, 2H, CH_2 THIQ), 3.82 (s, 3H, OCH_3), 3.81 (s, 4H, CH_2 PEG), 3.78 (m, 4H, CH_2 PEG), 3.59 (m, 4H, CH_2 PEG), 3.39 (s, 3H, CH_2OCH_3), 3.32 (d, ^3J=3.6 Hz, 2H, CH_2 THIQ). **^{13}C-NMR (100 MHz, $CDCl_3$): δ** 195.0 (C_{quat}), 162.3 (C_{quat}), 149.0 (C_{quat}), 148.6 (C_{quat}), 146.3 (C_{quat}), 138.3 (C_{quat}), 137.8 (C_{quat}), 134.1 (C_{quat}), 130.5 (C_{quat}), 129.8 (C_{quat}), 129.7 (C_{quat}), 129.6 (+), 128.3 (+), 127.6 (+), 125.8 (+), 125.6 (+), 122.7 (+), 120.6 (+), 118.6 (+), 111.7 (+), 111.6 (+), 71.9 (-), 70.6 (-), 70.5 (-), 69.4 (-), 68.7 (-), 68.5 (-), 58.8 (+), 55.8 (+), 49.6 (-), 49.2 (-), 28.6 (-). **IR (KBr) [cm^{-1}]: v =** 2892, 1705, 1687, 1412, 1126, 749, 731. **HRMS (EI-MS)** calcd. For $C_{35}H_{40}N_3O_7$ $[M+H]^+$: 614.2822; found $[M+H]^+$: 614.2851

_N_-(5-(2-(6,7-Dimethoxy-3,4-dihydroisoquinolin-2(1_H_)-yl)acetyl)-2-methylphenyl)quinoline-2-carboxamide (176d)

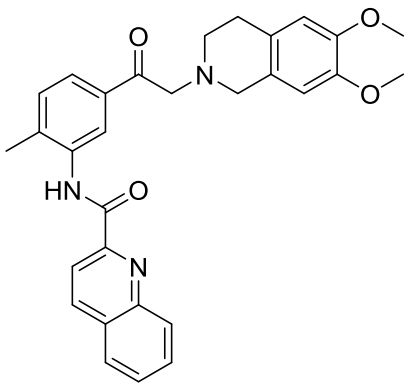

Light yellow solid. (0.024 g, yield 82%, R_f PE:EA 2:1 0.40). **^{1}H-NMR (400 MHz, $CDCl_3$): δ** 8.61 (m, 2H, quinol), 8.32 (t, ^3J=7.5 Hz, 2H, quinol), 8.16 (m, 1H, ArH), 7.87 (s, 1H, ArH), 7.75 (t, ^3J=8.4 Hz, 1H, ArH), 7.61 (t, ^3J=7.0 Hz, 1H, quinol), 7.46 (d, ^3J=8.3 Hz, 1H, quinol), 6.51 (s, 1H, CH THIQ), 6.44 (s, 1H, CH THIQ), 5.23 (s, 2H, $COCH_2$), 3.91 (s, 2H, CH_2 THIQ), 3.78 (s, 3H, OCH_3), 3.77 (s, 3H, OCH_3), 3.09 (t, ^3J=5.5 Hz, 2H, CH_2 THIQ), 2.68 (t, ^3J=5.7 Hz, 2H, CH_2 THIQ). **^{13}C-NMR (100 MHz, $CDCl_3$): δ** 200.2 (C_{quat}), 162.2 (C_{quat}), 149.2 (C_{quat}), 146.2 (C_{quat}), 138.9 (C_{quat}), 138.1 (C_{quat}), 135.6 (C_{quat}), 132.2 (C_{quat}), 130.5 (C_{quat}), 129.7 (C_{quat}), 128.4 (+), 127.8 (+), 121.4 (+), 119.6 (+), 118.6 (+), 113.6 (+), 111.9 (+), 110.4 (+), 109.1 (+), 56.0 (+), 55.2 (-), 53.4 (-), 47.2 (-), 29.7 (-), 17.3 (+). **IR (KBr) [cm^{-1}]: ν =** 2873, 1712, 1696, 1402, 1127, 762, 734. **HRMS (EI-MS)** calcd. For $C_{30}H_{30}N_3O_4$ $[M+H]^+$: 496.2192; found $[M+H]^+$: 496.2224

***N*-(3-(2-(6-Methoxy-7-(2-methoxyethoxy)-3,4-dihydroisoquinolin-2(1*H*)-yl)acetyl)phenyl)quinoline-2-carboxamide (176e)**

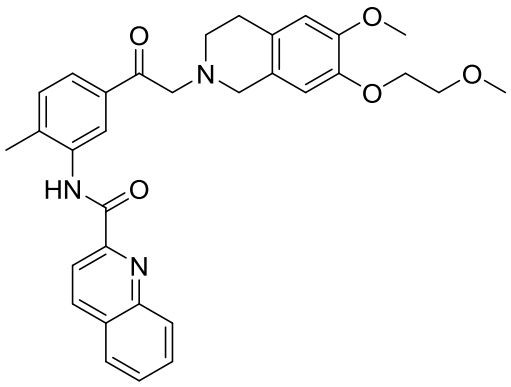

Light yellow solid. (0.032 g, yield 88%, R_f PE:EA 2:1 0.33). **^{1}H-NMR (400 MHz, $CDCl_3$): δ** 8.95 (d, ^{3}J=7.7 Hz, 1H, quinol), 8.40 (s, 1H, quinol), 8.16 (d, ^{3}J=8.4 Hz, 1H, ArH), 7.93 (d, ^{3}J=8.2 Hz, 1H, quinol), 7.84 (m, 1H, quinol), 7.73 (d, ^{3}J=9.7 Hz, 2H, ArH), 7.67 (t, ^{3}J=7.5 Hz, 1H, quinol), 7.35 (d, ^{3}J=8.0 Hz, 1H, quinol), 6.57 (s, 1H, CH THIQ), 6.55 (s, 1H, CH THIQ), 4.94 (s, 2H, $COCH_2$) 4.12 (s, 2H, CH_2 THIQ), 3.88 (s, 3H, OCH_3), 3.60 (t, ^{3}J=5.6 Hz, 2H, CH_2 THIQ), 3.37 (s, 3H, CH_2OCH_3), 2.76 (t, ^{3}J=5.6 Hz, 2H, CH_2 THIQ), 2.55 (s, 3H, CH_3). **^{13}C-NMR (100 MHz, $CDCl_3$): δ** 200.2 (C_{quat}), 162.19 (C_{quat}), 149.2 (C_{quat}), 146.2 (C_{quat}), 138.9 (C_{quat}), 138.1 (C_{quat}), 135.6 (C_{quat}), 135.5 (C_{quat}), 132.2 (C_{quat}), 130.5 (C_{quat}), 129.8 (C_{quat}), 129.6 (C_{quat}), 128.4 (+), 127.8 (+), 127.6 (+), 127.0 (+), 121.4 (+), 118.5 (+), 113.6 (+), 76.7 (-), 70.9 (-), 68.6 (-), 59.1 (+), 56.0 (+), 55.6 (-), 51.2 (-), 30.9 (-), 17.3 (+). **IR (KBr) [cm^{-1}]: ν =** 2905, 1652, 1624, 1423, 1151, 739, 725. **HRMS (EI-MS)** calcd. For $C_{32}H_{34}N_3O_5$ $[M+H]^+$: 540.2454; found $[M+H]^+$: 540.2487

***N*-(5-(2-(6,7-*bis*(2-(2-(2-Methoxyethoxy)ethoxy)ethoxy)-3,4-dihydroisoquinolin-2(1*H*)-yl)acetyl)-2-methylphenyl)quinoline-2-carboxamide (176f)**

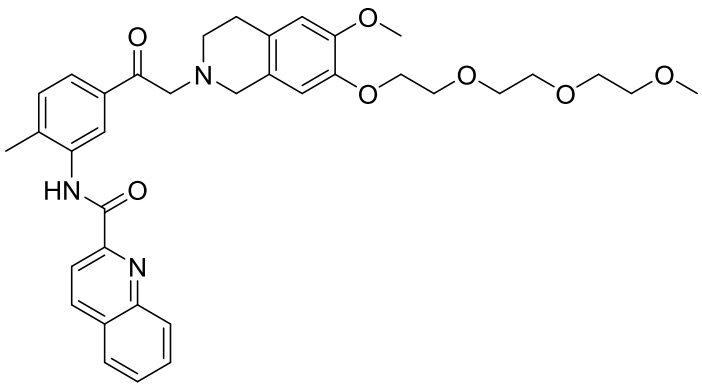

Light yellow solid. (0.031 g, yield 82%, R_f PE:EA 2:1 0.28). **^{1}H-NMR (400 MHz, $CDCl_3$): δ** 8.67 (m, 1H, quinol), 8.38 (d, ^{3}J=3.9 Hz, 1H, quinol), 8.15 (d, ^{3}J=8.5 Hz, 2H, ArH), 7.93 (d, ^{3}J=8.1 Hz, 1H, quinol), 7.74 (m, 1H, ArH), 7.84 (m, 1H, quinol), 7.69 (m, 1H, quinol), 7.52 (s, 1H, quinol), 6.87 (s, 1H, CH THIQ), 6.65 (s, 1H, CH THIQ), 5.29 (s, 2H, $COCH_2$), 4.20 (s, 2H, CH_2 THIQ), 4.14 (m, 16H, $4CH_2$ PEG), 3.87 (s, 3H, OCH_3), 3.72 (t, ^{3}J=5.2 Hz, 4H, $2CH_2$ PEG), 3.65 (d, ^{3}J=4.8 Hz, 4H, $2CH_2$ PEG), 3.55 (s, 3H, CH_2OCH_3), 2.50 (s, 3H, CH_3). **^{13}C-NMR (100 MHz, $CDCl_3$): δ** 199.7 (C_{quat}), 161.6 (C_{quat}), 148.7 (C_{quat}), 147.6 (C_{quat}), 146.1 (C_{quat}), 145.7 (C_{quat}), 138.4 (C_{quat}), 137.6 (C_{quat}), 136.4 (C_{quat}), 135.1 (C_{quat}), 131.7 (C_{quat}), 130.0 (C_{quat}), 129.2 (+), 127.9 (+), 127.3 (+), 120.9 (+), 118.1 (+), 113.1 (+), 112.8 (+), 112.0 (+), 111.4 (+), 110.2 (+), 71.4 (-), 70.3 (-), 70.1 (-), 70.0 (-), 69.1 (-), 68.4 (-), 68.2 (-), 58.5 (+), 55.5 (+), 46.7 (-), 29.2 (-), 16.8 (+). **IR (KBr) [cm^{-1}]: v =** 2873, 1675, 1649, 1392, 1129, 741, 716. **HRMS (EI-MS)** calcd. For $C_{36}H_{42}N_3O_7$ $[M+H]^+$: 628.2978; found $[M+H]^+$: 628.2994.

2.4.2 Biological investigations

2.4.2.1 Drugs and Chemicals

Hoechst 33342 (Invitrogen, Karlsruhe, Germany) was dissolved in sterile water to produce a 0.8 mM working solution. Calcein-AM (4 mM in anhydrous DMSO) and pluronic F127 were obtained from Biotium (Hayward, CA, USA) and diluted to 100 µM. Bovine serum albumin (BSA) was purchased from Serva (Heidelberg, Germany). Fumitremorgin C (FTC; Merck, Darmstadt, Germany) was also dissolved in DMSO and diluted to a concentration of 1 mM. Reversan was purchased from Tocris Bioscience (Bristol, UK) and diluted to a 3 mM working solution in DMSO. Topotecan and vinblastine for cell culture supplementation were purchased from Sigma (Munich, Germany). Loading buffer (calcein-AM assay) was made of 120 mM NaCl, 5 mM KCl, 2 mM $MgCl_2.6H_2O$, 1.5 mM $CaCl_2.2H_2O$, 25 mM HEPES, 10 mM glucose, pH 7.4. PBS (phosphate buffered saline) was made of 8.0 g/L NaCl, 1.0 g/L $Na_2HPO_4.2H_2O$, 0.20 g/L KCl, 0.20 g/L KH_2PO_4 and 0.15 g/L $NaH_2PO_4.H_2O$. The pH value was adjusted to 7.3 - 7.4. A solution of 4% (m/m) paraformaldeyde (PFA) in PBS was made by stirring 2 g of PFA per 50 g total solution while heating on a magnetic stirrer for approximately 30 min. The test compounds were dissolved in DMSO at a concentration of 10 mM if possible, depending on the solubility of the compounds. All stock solutions were stored at −20 °C. If not otherwise stated, chemicals (p.a. quality) were obtained from Merck (Darmstadt, Germany). Purified water (Milli-Q system, Millipore, Eschborn, Germany) was used throughout.

2.4.2.2 Cell lines and culture conditions

MCF-7/Topo cells, an ABCG2-overexpressing subclone of MCF-7 cells (ATCC® HTB-22™, American Type Culture Collection, Manassas, VA), were obtained as described[16] and cultured in water-saturated atmosphere (95% air, 5% CO_2) at 37 °C in 75 cm^2 culture flasks from Nunc (Wiesbaden,Germany) in Eagle's minimum essential medium (EMEM; Sigma, Munich, Germany) containing l-glutamine, 2.2 g/L $NaHCO_3$ and 110 mg/L sodium pyruvate supplemented with 10% fetal calf serum (FCS; Biochrom, Berlin, Germany) and 550 nm topotecan to induce overexpression of the ABCG2 transporter. Human Kb-V1 cells, an ABCB1-overexpressing subclone of Kb cells (ATCC® CCL-17™), were obtained and cultured as described.[16] MDCKII-MRP1 cells: MDCKII cells (Madin-Darby Canine

Kidney cells, strain II; a dog epithelial cell line; ATCC® CRL-2936™), transfected with human ABCC1, [17,18] were a kind gift from Prof. Dr. P. Borst from the Netherland Cancer Institute (Amsterdam, NL). The cells were cultured in DMEM supplemented with 10% FCS, 3.7 g/L $NaHCO_3$ and 110 mg/L sodium pyruvate. Trypsinization was performed at 37 °C (95% air, 5% CO_2) for 20-30 min using 0.1% trypsin / 0.04% EDTA. All cells were routinely monitored for mycoplasma contamination by PCR (Venor GeM, Minerva Biolabs, Berlin, Germany) and only mycoplasma-negative cultures were used.

2.4.2.3 Calcelin-AM microplate assay for the determination of ABCB1 inhibition

Kb-V1 cells were seeded into flat-bottomed 96-well plates (Greiner, Frickenhausen, Germany) at a density of 20,000 cells per well. On the following day, cells were washed with loading buffer (120 mM NaCl, 5 mM KCl, 2 mM $MgCl_2.6H_2O$, 1.5 mM $CaCl_2.2H_2O$, 25 mM HEPES, 10 mM glucose, pH 7.4) in order to remove unspecific serum esterases. Afterwards, cells were incubated with loading suspension (loading buffer, 5 mg/mL BSA, 1.25 µL/mL pluronic F127 (20% in DMSO)) containing 0.5 µM calcein-AM and the test compounds at increasing concentrations (10 nM – 100 µM) for 10 min (37 °C / 5% CO2) to construct concentration-response curves. Tariquidar served as positive control at a final concentration of 1 µM corresponding to 100% 3 inhibition of calcein-AM efflux. Subsequently, the loading suspension was discarded and cells were fixed with 4% PFA solution in PBS for 30 min. After three washing steps, fixed cells were overlaid with loading buffer and relative fluorescence intensities were determined with a GENios Pro microplate reader (Tecan Deutschland, Crailsheim, Germany). Measurement mode: fluorescence top; excitation filter (calcein-AM): 485/20; emission filter (calcein-AM): 535/25; number of reads: 10; integration time: 40 µs; lag time: 0 µs; mirror selection: Dichroic 3; plate definition file: GRE96ft.pdf; multiple reads per well (Circle): 3x3; time between move and flash: 100 ms. On each plate, the optimal gain was calculated by determination of the fluorescence intensity in the presence of the reference substance, tariquidar. IC_{50} values were calculated using SIGMA PLOT 11.0 (Systat Software, Erkrath, Germany), “Four parameter logistic curve” fitting. Errors were expressed as standard error of the mean (SEM).

2.4.2.4 Calcelin-AM microplate assay for the determination of ABCC1 inhibition

MDCKII cells were seeded into flat-bottomed 96-well plates at a density of about 20,000 cells/well. On the following day, cells were washed with loading buffer in order to remove unspecific serum esterases. Afterwards, cells were incubated with loading suspension (loading buffer, 5 mg/mL BSA, 1.25 µL/mL pluronic F127 (20% (m/v) in DMSO)) containing 0.5 µM calcein-AM and the test compound at increasing concentrations (10 nM-100 µM) for 60 min (37 °C / 5% CO2). Reversan served as positive control at a final concentration of 30 µM corresponding to 100% ABCC1 inhibition. In general, test compounds were investigated as triplicates, controls as sextuplicates, respectively. Subsequently, the loading suspension was discarded, and the cells were fixed with 4% PFA solution for 30 min. After three washing circles (loading buffer), fixed cells were overlaid with loading buffer, and relative fluorescence intensities were determined at 535/25 nm at the GENios Pro microplate reader after excitation at 485/20 nm. The following cell quantification procedure was performed by analogy with the H33342 assay. The obtained mean fluorescence intensities were related to the controls and plotted against the various concentrations of test compounds. TECAN instrument settings: Measurement mode: fluorescence top; number of reads: 10; integration time: 40 µs; lag time: 0 µs; mirror selection: Dichroic 3 (e.g. Fl.); plate definition file: GRE96ft.pdf; multiple reads per well (Circle): 3x3; time between move and flash: 100 ms.

2.4.2.5 Hoechst 33342 microplate assay for the determination of ABCG2 inhibition

Optimal conditions of the assay were systematically determined as described elsewhere[19] with slight modifications. MCF-7/Topo cells were seeded into 96-well plates at a density of 20,000 cells/well (total volume: 100 mL) and allowed to attach to the surface of the microplates overnight in a water-saturated atmosphere (95% air, 5% CO2) at 37 °C. The next day, the culture medium was removed, and the cells were incubated with loading suspension (EMEM, supplemented as described above, and 0.8 µM Hoechst 33342) in combination with the test compound at increasing concentrations (10 nM-100 µM) for 2 h (37 °C, 5% CO_2). FTC at a final concentration of 10 µM served as reference compound;

under these conditions the response was defined as 100% inhibition of Hoechst 33342 efflux. The supernatants were drained and the cells were fixed for 30 min under light protection using 100 mL per well of a 4% PFA solution. Finally, MCF-7/Topo cells were washed with PBS (2x250 mL per well) to remove residual dye. Cells were overlaid with PBS (100 mL), and the fluorescence intensities were determined using a GENios Pro microplate reader (TECAN Deutschland GmbH, Crailsheim, Germany). Measurement mode: fluorescence top; excitation filter: 340/35 nm; emission filter: 485/20 nm; number of reads: 10; integration time: 40 ms; lag time: 0 ms; mirror selection: automatic; plate definition file: GRE96ft.pdf; multiple reads per well (circle, 3x3); time between move and flash: 50 ms. On each plate, the optimal gain was calculated by determination of the fluorescence intensity in the presence of the reference compound FTC. IC_{50} values were calculated using SIGMA PLOT 11.0, “four parameter logistic curve” fitting. Errors are expressed as standard error of the mean (SEM).

2.4.2.6 Chemical Stability in Eagle’s minimum essential medium (EMEM)

Stock solutions of the test compounds (3 mM) were prepared in DMSO. A 1:50 dilution of the substances in EMEM was prepared in 1.5-mL polypropylene reaction vessels (Eppendorf, Hamburg, Germany). The samples were shortly vortexed and incubated at 37 °C. At different periods of time, aliquots were taken, and the samples were mixing with two parts of ice-cold acetonitrile. For quantitative precipitation, the samples were vortexed and stored at 4 °C for 30 min. Finally, samples were centrifuged for 5 min at 14,000 g, using an Eppendorf MiniSpin plus centrifuge, and the supernatants were transferred into new reaction vessels. Prior to HPLC analysis, the samples were diluted (1:1) with acetonitrile and stored at -80 °C. Subsequent RP-HPLC analysis was performed with a analytical HPLC (1220 Infinity LC System from Agilent) with a reverse phase Phenomenex Luna® 3µ C18(2) 100A column (150 × 2.0 mm, 100 Å) at 30°C. HPLC conditions were the following: solvent A = water (Millipore)/TFA (0.05% v/v), solvent B = MeCN (Merck, gradient grade); flow rate = 0.3 mL/min; injection volume 100 µL, elution with a gradient of 10% to 95% MeCN in 30 min. UV-detection at 220 nm.

2.4.2.7 Solubility

A calibration curve for each compound was made, using solutions 1µM-10nM in DMSO and using the analytical HPLC (1220 Infinity LC System from Agilent) with a reverse phase Phenomenex Luna® 3µ C18(2) 100A column (150 × 2.0 mm, 100 Å) at 30°C. HPLC conditions were the following: solvent A = water (Millipore)/TFA (0.05% v/v), solvent B = MeCN (Merck, gradient grade); flow rate = 0.3 mL/min; injection volume 0.2 µL, elution with a gradient of 10% to 95% MeCN in 30 min. UV-detection at 220 nm. Stock solutions of the test compounds (70 µM, 3 mM and 10 mM) were used for this assay, aliquots at 5, 60 and 120 minutes were taken and processed with the same protocol used in the stability assay. The area found in the HPLC chromatogram for each aliquot was introduced in the calibration curve equation and compared with the areas found in different periods of time.

2.4.2.8 Chemosensitivity assay

The assays were performed as described previously[8] with slight modifications. Briefly, 100 mL/well of a tumor cell suspension, yielding a density of 10-20 cells per microscopic field (Olympus, CK2, 320x), were seeded into 96-well plates and incubated overnight at 37 °C and 5% CO_2. The next day, 100 mL/well of fresh medium was added containing the test compounds in various concentrations or vehicle. In general, test compounds were added as 1000-fold concentrated feed solutions (16 wells per drug concentration). On every plate, untreated cells (solvent DMSO in a dilution of 1:1000) served as growth control (vehicle), cells treated with a reference cytostatic (vinblastine) as a positive control. Incubation of the cells was stopped after different periods of time by removal of medium and fixation with a solution of 2% glutardialdehyde (in PBS). All plates were stored at 4 °C until the end of the experiment and afterwards simultaneously stained with 100 mL/well of a 0.02% aq crystal violet solution for 20 min. The trays were rinsed with H_2O for 20 min in order to remove residual dye. Crystal violet bound by the fixed cells was extracted with 70% EtOH (180 mL/well) while shaking the microplates for 2-3 h. Absorbance (a parameter proportional to cell mass) was measured at 580 nm using the GENios Pro microplate reader.

2.5 References

1. Cervenak J, Andrikovics H, Özvegy-Laczka C, Tordai A, Német K, Váradi A, Sarkadi B. The role of the human ABCG2 multidrug transporter and its variants in cancer therapy and toxicology. Cancer lett 2006;234(1):62-72.
2. Doyle LA, Yang W, Abruzzo LV, Krogmann T, Gao Y, Rishi AK, Ross DD. A multidrug resistance transporter from human MCF-7 breast cancer cells. PNAS 1998;95(26):15665-15670.
3. Fukumaru T, Awata H, Hamma N, Komatsu T. Synthesis and bioactivity of novel acetylenic compounds. Agric Biol Chem 1975;39(2):519-527.
4. Germinara GS, De Cristofaro A, Rotundo G. Bioactivity of short-chain aliphatic ketones against adults of the granary weevil, Sitophilus granarius (L.). Pest Manag Sci 2012;68(3):371-377.
5. Zhang Y, Byun Y, Ren YR, Liu JO, Laterra J, Pomper MG. Identification of Inhibitors of ABCG2 by a Bioluminescence Imaging–Based High-Throughput Assay. Cancer Res 2009;69(14):5867-5875.
6. Herrera JM, Zunino MP, Dambolena JS, Pizzolitto RP, Gañan NA, Lucini EI, Zygadlo JA. Terpene ketones as natural insecticides against Sitophilus zeamais. Ind Crops Prod 2015;70:435-442.
7. Snape TJ, Astles AM, Davies J. Understanding the chemical basis of drug stability and degradation. Pharm J 2010;285(7622):416-417.
8. Bernhardt G, Reile H, Birnböck H, Spruß T, Schönenberger H. Standardized kinetic microassay to quantify differential chemosensitivity on the basis of proliferative activity. J Cancer Res Clin Oncol 1992;118(1):35-43.
9. Corson B, Hazen R. m-Nitroacetophenone. Org Synth 1930(10):74-74.
10. Montiel LE, Zepeda LG, Tamariz J. Efficient total synthesis of racemic bisabolane sesquiterpenes curcuphenol and xanthorrhizol starting from substituted acetophenones. Helv Chim Acta 2010;93(7):1261-1273.
11. Chang F, Kim H, Lee B, Park S, Park J. Highly efficient solvent-free catalytic hydrogenation of solid alkenes and nitro-aromatics using Pd nanoparticles entrapped in aluminum oxy-hydroxide. Tetrahedron Lett 2010;51(32):4250-4252.
12. Ueki H, Ellis TK, Martin CH, Soloshonok VA. Efficient Large-Scale Synthesis of Picolinic Acid-Derived Nickel (II) Complexes of Glycine. Eur J Org Chem 2003;2003(10):1954-1957.
13. Reddy BM, Kumar VVR, Reddy NCG, Rao SM. Silica gel catalyzed α-bromination of ketones using N-bromosuccinimide: An easy and rapid method. Chin Chem Lett 2014;25(1):179-182.
14. Ochoa-Puentes C, Bauer S, Kühnle M, Bernhardt Gn, Buschauer A, König B. Benzanilide–Biphenyl Replacement: A Bioisosteric Approach to Quinoline Carboxamide-Type ABCG2 Modulators. ACS Med Chem Lett 2013;4(4):393-396.
15. Hao J, Servello J, Sista P, Biewer MC, Stefan MC. Temperature-sensitive aliphatic polyesters: synthesis and characterization of γ-substituted caprolactone monomers and polymers. J Mater Chem 2011;21(29):10623-10628.
16. Glavinas H, Kis E, Pal A, Kovacs R, Jani M, Vagi E, Molnar E, Bánsághi S, Kele Z, Janáky T. ABCG2 (breast cancer resistance protein/mitoxantrone resistance-associated protein) ATPase assay: a useful tool to detect drug-transporter interactions. Drug Metab Dispos 2007;35(9):1533-1542.

17. Bakos E, Evers R, Szakács G, Tusnády GE, Welker E, Szabó K, de Haas M, van Deemter L, Borst P, Váradi A. Functional multidrug resistance protein (MRP1) lacking the N-terminal transmembrane domain. J Biol Chem 1998;273(48):32167-32175.
18. Evers R, Kool M, van Deemter L, Janssen H, Calafat J, Oomen L, Paulusma CC, Elferink RO, Baas F, Schinkel AH. Drug export activity of the human canalicular multispecific organic anion transporter in polarized kidney MDCK cells expressing cMOAT (MRP2) cDNA. J Clin Invest 1998;101(7):1310.
19. Kühnle M. Experimental therapy and detection of glioblastoma: investigation of nanoparticles, ABCG2 modulators and optical imaging of intracerebral xenografts [Doctoral thesis]. Regensburg: Regensburg University; 2010.

3 Synthesis and characterization of ABCG2 modulators combining chalcone, quinoline and isoquinoline moieties[3]

ABC transporters such as ABCG2 have been associated with the resistance of cancer cells to a variety of structurally and functionally non-related anticancer drugs. To date, several ABCG2 modulators including acridone derivatives, chalcones and benzochalcones, indoles and quinolines, among others have been reported in the literature. However, the efficiency of these modulators varies regarding potency, selectivity profile, interaction with the transporter as substrate or inhibitor, toxicity and physicochemical properties. Some studies have shown several tariquidar analogs as a new class of potent and selective inhibitors of ABCG2, but the structural stability of these compounds is seriously affected by enzymatic hydrolysis of the amide bond attached to the anthranilic ring in the structure. In search for more stable tariquidar analogues, a new series of chalcones combined with quinoline and isoquinoline moieties were investigated, fully characterized and tested for their ABCG2 inhibitory activity, ABC transporters selectivity and stability against enzymatic hydrolysis. The synthesized chalcones were active against ABC transporters and showed preference over ABCG2. Some compounds of the series exhibited a maximum inhibition between 85-110% based on fumitremorgin C as reference compound (100% inhibition), and have a remarkable chemical stability against the enzymatic hydrolysis after incubation for 24 hours at 37°C.

---

[3] All synthesis, purification and characterization of the compounds were carried out by Diana Catherine Peña. Inhibition assays (ABCG2, ABCB1, ABCC1), stability and solubility tests were carried out by Diana Catherine Peña at Regensburg University, Germany. Cell cultures, reference compounds and chemosensitive assay were provided by Matthias Scholler, a doctoral student at Regensburg University.

3.1 Introduction

Natural products such as flavonoids are becoming interesting in anticancer therapy. More than 6000 naturally occurring flavonoids have been identified to date.[1] Chalcone or (*E*)-1,3-diphenyl-2-propene-1-one, the synthetic precursor of flavonoids and isoflavonoids and the open chain intermediates in aurones synthesis of flavones,[2] is an important chemotype that has attracted great research interest for decades due to the high natural abundance of chalcone compounds, their easy synthesis, and most importantly, their diverse biological activities. Indeed, many natural chalcones demonstrated a wide variety of bioactivities, including anti-cancer, anti-inflammatory, anti-diabetic, cancer chemopreventive, anti-oxidant, and anti-microbial activities (Figure 3-1).[3,4] Effective drug development will depend on multidisciplinary collaboration embracing natural product lead discovery and optimization through the application of total and diversity oriented synthesis.[5]

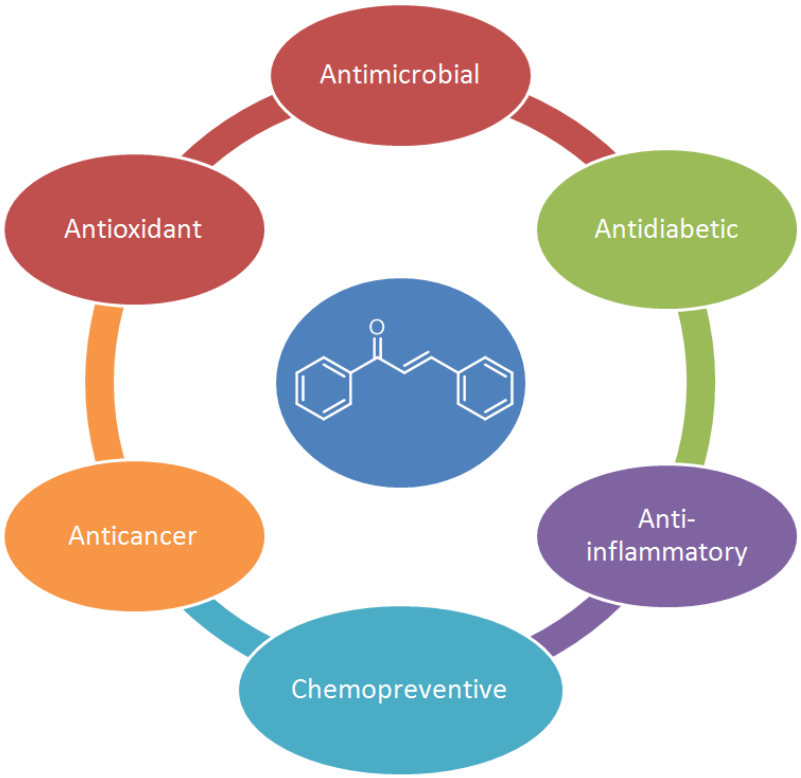

Figure 3-1 Structure scaffold of chalcone and bioactivities (adapted from Zhou *et.al*[3])

Taking into account the broad spectrum of action of chalcones, we designed and synthesized a new series based on that structure. All compounds were fully characterized and tested for their ABCG2 inhibitory activity and ABC transporters selectivity, solubility and stability against enzymatic hydrolysis. The synthesized chalcones were active against ABC transporters and showed a marked preference for ABCG2 inhibition.

3.2 Results and discussion

3.2.1 Synthesis. Synthesis of compounds **179a-f** is shown in Scheme 3-1

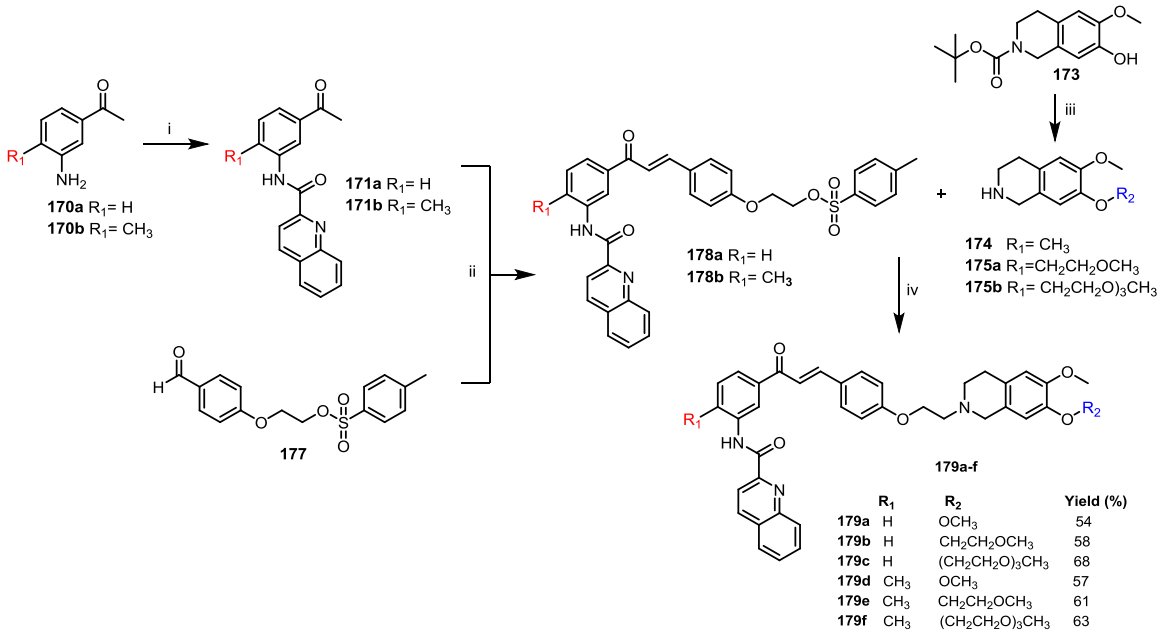

Scheme 3-1 Synthesis of compounds 179**a-f. Reagents and conditions:** (i) Quinaldic acid, Ts-Cl, TEA, 50ºC, overnight; (ii) NaOH 30%, rt, 24h; (iii) a) 2-methoxyethyl 4-methylbenzenesulfonate or 2-(2-(2-methoxyethoxy)ethoxy)ethyl 4-methylbenzenesulfonate, KOH, THF, N_2, 6h; b) DCM, trifluoroacetic acid, rt, overnight; (iv) K_2CO_3, acetonitrile, 90°C, overnight

The syntheses of compounds **170a-b**, **171a-b** and tetrahydroisoquinolines **174**, **175a-b** were already explained in chapter 2. Compound **177** was prepared according to known procedures,[6,7] A Claisen-Schmidt condensation of the ketones **171a-b** with the aldehyde

177 with NaOH 30% resulted in the desired chalcones **178a**-**b**. Finally, a nucleophilic substitution between the tosylated compounds (**178a-b**) and the respective tetrahydroisoquinolines (**174, 175a-b**) in presence of potassium carbonate and using acetonitrile as solvent led the target chalcones (**179a-f,** Scheme 3-1) in moderate yields (54-68%, Scheme 3-1). All synthesized compounds were characterized by nuclear magnetic resonance (NMR), infrared spectroscopy (IR), high resolution mass spectrometry (HR-MS) and the purity was confirmed by analytical high performance liquid chromatography (HPLC).

3.2.2 Inhibitory activity evaluation

3.2.2.1 Inhibitory activity evaluation on breast cancer resistance protein (ABCG2)

The synthesized chalcones **179a-f** and reference compounds fumitremorgin C (FTC) and tariquidar were investigated for inhibition of ABCG2 in a Hoechst 33342 microplate assay using ABCG2-overexpressing MCF-7/Topo cells, obtaining inhibitory effects and IC_{50} values as summarized in Table 3-1. Concentration response curves of selected compounds obtained in the Hoechst 33342 assay are shown in Figure 3-2.

All chalcones exhibited maximal inhibitory activities between 72-111%, which means that they were active against ABCG2 transporter. Compounds bearing a methyl substituent at the amino chalcone core (**179d**-**f**) were most active in the series with the lowest IC_{50} values and they are superior with respect to the maximal inhibitory effect. Compound **179d** was almost equipotent with the reference compound FTC while compounds **179e** and **179f** were two to four fold less potent. However, the maximal inhibitory effects (86%, 97% and 111% respectively) were significantly higher to that of tariquidar or even surpassing that of FTC (Figure 3-2, compound **179f**).

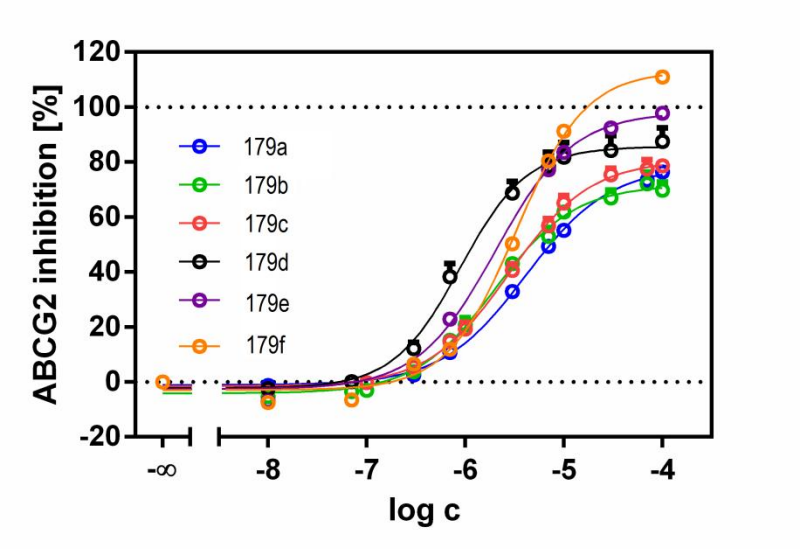

Figure 3-2 Concentration dependent inhibition of the ABCG2 transporter in MCF-7/Topo cells (Hoechst 33342 assay) by chalcones **179a-f**. The inhibition is expressed as % relative to the maximal inhibition of ABCG2 by 10 μM of fumitremorgin C (100%)

The addition of ethylene and triethylene glycol chains (R_2 in the structure, Scheme 3-1) at the tetrahydroisoquinoline moiety in compounds **179a-c** did not have a tendency in the IC_{50} values or I_{max} effect (Table 3-1). On the other hand the maximal inhibitory effect in compounds **179d-f** increased from 86 until 111% (Table 3-1).

Table 3-1 Inhibitory activity evaluation on ABCG2 by reference compound and chalcones **179a-f**

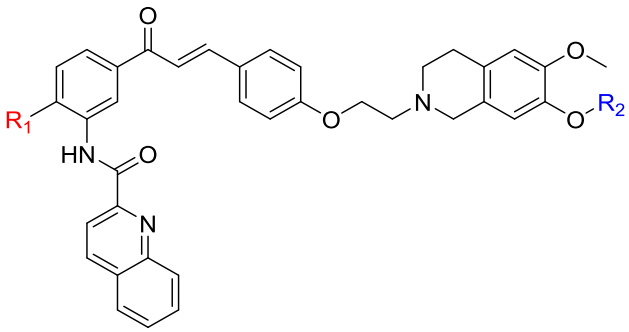

			ABCG2[a]		
Compound	**R_1**	**R_2**	**IC_{50} (μM)[b]**	**I_{max} (%)[c]**	**Log P[d]**
FTC			0.731 ± 0.092	100	
Tariquidar			0.526 ± 0.085	69 ± 5	
179a	H	CH_3	4.08 ± 0.29	79 ± 4	6.51
179b	H	$CH_2CH_2OCH_3$	2.13 ± 0.47	72 ± 8	6.18
179c	H	$(CH_2CH_2O)_3CH_3$	2.83 ± 0.30	81 ± 5	5.46
179d	CH_3	CH_3	0.88 ± 0.02	86 ± 10	6.97
179e	CH_3	$CH_2CH_2OCH_3$	1.55 ± 0.36	97 ± 3	6.64
179f	CH_3	$(CH_2CH_2O)_3CH_3$	2.72 ± 0.54	111 ± 4	5.92

[a]Hoechst 33342 microplate assay using ABCG2-overexpressing MCF-7/Topo cells. [b]Mean values ± SEM from three independent experiments performed in triplicate. [c]Maximal inhibitory effects [%] are expressed as inhibition caused by the highest concentration of the compound tested relative to the inhibitory effect caused by 10 μM FTC (100% inhibition). [d]Calculated values using ACD/Labs I-Lab 2.0 ilab.acdlabs, Algorithm Version: v5.0.0.184

The partition coefficient (Log P) is a measure of differential solubility of a compound in a hydrophobic solvent (octanol) and a hydrophilic solvent (water). The logarithm of these two values enables compounds to be ranked in terms of hydrophilicity (or hydrophobicity).[8] As shown in Table 3-1, chalcone **179d** has the largest partition coefficient (Log P) among all the synthesized compounds and it is the most potent and similar to the reference compound in the series.

Compounds bearing a methyl substituent at the amino chalcone core (**179d-f**) exhibited a higher calculated partition coefficient in comparison to compounds with hydrogen as substituent at the amino chalcone core (**179a-c,** Table 3-1). These differences were clearer as follows, compounds **179a** and **179d** differ in substituent R_1 (Scheme 3-1), the

maximal inhibition was better for most lipophilic compound (**179d**, 86%) and also the IC_{50} values was more than 5 times less (**179a** 4.08 μM, **179d** 0.88 μM, Table 3-1). Compounds with ethylene glycol in position R_2 (**179b** and **179e,** Scheme 3-1), differ in the presence of the methyl group in R_1, compound **179e** showed a considerable increase in the maximal inhibitory effect (97%) in comparison with compound **179b** (72%) and also the IC_{50} value is lower (**179b** 2.13 μM, **179e** 1.55 μM, Table 3-1). Compounds **179c** and **179f** were the most hydrophilic compounds of the series, but between them two compound **179f** showed the best maximal inhibitory effect of the whole series (Table 3-1), the IC_{50} is similar in this case for both compounds (**179c** 2.83 μM, **179f** 2.72 μM, Table 3-1).

3.2.2.2 Selectivity evaluation. Inhibitory activity evaluation on ABCB1 and ABCC1

Tariquidar is an anthranilic acid derivative and have been reported as a potent and specific inhibitor of ABCB1 (P-gp), therefore, it is commonly used as a reference compound for these transporter inhibition assays.[9,10] Reversan is a lead compound found in a pyrazolopyrimidines librarie as a prominent structural class of potent ABCC1 modulators, has been demonstrated that this compound increase the toxicity of chemotherapeutic drug exposure.[11,12,13]

All synthesized compounds were additionally screened for their inhibition of ABCB1 and ABCC1 with the calcein accumulation assay, Tariquidar and Reversan were used as reference compounds. The screening was conducted at a fixed concentration of 1 and 10 μM using Kb-V1 cells (ABCB1) and MDCKII (ABCC1) cell lines. Tariquidar (10 μM) was used as standard inhibitor for ABCB1 and Reversan (30 μM) for ABCC1. Figure 3-3 illustrates the effects of the 6 synthesized chalcones on the accumulation of calcein and it exemplifies that the studied substances possess low affinity for ABCB1 (Figure 3-3A) and ABCC1 (Figure 3-3B).

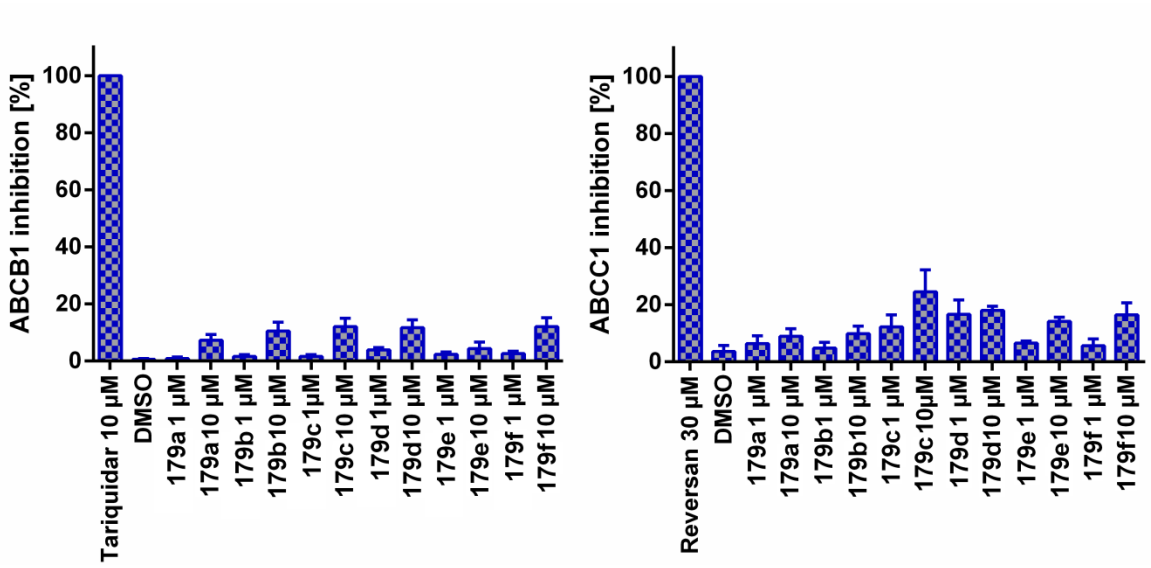

Figure 3-3 Effects of chalcones **179a-f** at 1 and 10 µM concentration on the accumulation of calcein in ABCB1 (A) and ABCC1 (B) overexpressing Kb-V1 and MDCKII cells respectively. Data were normalized by defining the inhibition caused by 10 µM Tariquidar and of 30 µM Reversan as 100% and are presented as mean ± SD of two independent experiments.

Chalcone **179a** showed the lowest affinity at both transporters contrary to compound **179c** which has the largest inhibitory activity against ABCC1, although the only difference between these two compounds is a triethylenglycol chain in the tetrahydrisoquinoline fragment. When a methyl group to one side of the molecule was added, compounds **179d** and **179f** showed almost the same inhibitory effect against both transporters. Compounds **179b** and **179e** contain an ethylenglycol chain in the tetrahydroisoquinoline moiety and showed less affinity for both transporters than the compounds with similar characteristics. Concentration-response curves were not generated for the synthesized chalcones since none of them showed more than 25% inhibition at 10 µM (Table 3-2).

Compounds did not show a clear trend based on the substituents (Table 3-2), either the presence of methyl in R_1 (Scheme 3-1) or methoxy substituents, ethylene or triethylene glycol chains in R_2 (Scheme 3-1).

Table 3-2 Inhibitory activity evaluation on ABCB1 and ABCC1 by reference compounds and chalcones **179a-f**

	ABCB1[a]	**ABCC1[b]**
Compound	**I_{max} (%)[c]**	**I_{max} (%)[d]**
Tariquidar	100	n.d[e]
Reversan	n.d[e]	100
179a	7 ± 2	8 ± 1
179b	10 ± 3	10 ± 6
179c	12 ± 3	24 ± 7
179d	12 ± 3	18 ± 2
179e	4 ± 2	14 ± 4
179f	12 ± 3	16 ± 4

[a]Calcein-AM microplate assay using ABCB1-overexpressing Kb-V1 cells. [b]Calcein-AM microplate assay using ABCC1-overexpressing MDCKII cells. [c]Maximal inhibitory effect (Imax) relative to the response to tariquidar at a concentration of 10 μM (100% inhibition). [d]Maximal inhibitory effect (Imax) relative to the response to reversan at a concentration of 30 μM (100% inhibition). [e]n.d.: not determinated

The maximal inhibitory effect values for the chalcones **179a-f** over ABCB1 and ABCC1 were not significant for these transporters, but, according to the data shown in the Table 3-2, all compounds showed more affinity for ABCC1 than for ABCB1.

According to the results presented in the Table 3-2 for the ABCB1 and ABCC1 transporters inhibition, we can conclude that the synthesized chalcones showed selectivity for the ABCG2 transporter.

3.2.3 Chemical stability test in Eagle's Minimum Essential Medium (EMEM)

In aqueous solutions almost all of the drugs are subject to some form of chemical degradation and, frequently, the therapeutic activity is impaired by the drug instability, for that reason the stability assay is a prerequisite for *in vivo* studies. The most common

consequence of the drug's degradation is the loss of potency but in some cases harmful degradation products may be formed.[14]

The bioisosteric approach and the replacement of the hydrolysis-sensitive amide bond bearing the phenethyl tetrahydroisoquinoline fragment (previously reported ABCG2 modulators, Figure 1-30, compounds **143** and **145**), by chalcones moieties resulted in stable compounds after incubation in EMEM. As shown in Figure 3-4, synthesized chalcones were incubated in EMEM at a temperature of 37°C and aliquots were analyzed by HPLC over a period of 24 hours, products of cleavage or degradation of compounds were not detected, compounds were not affected by the components present in the incubation medium (EMEM) during the assay.

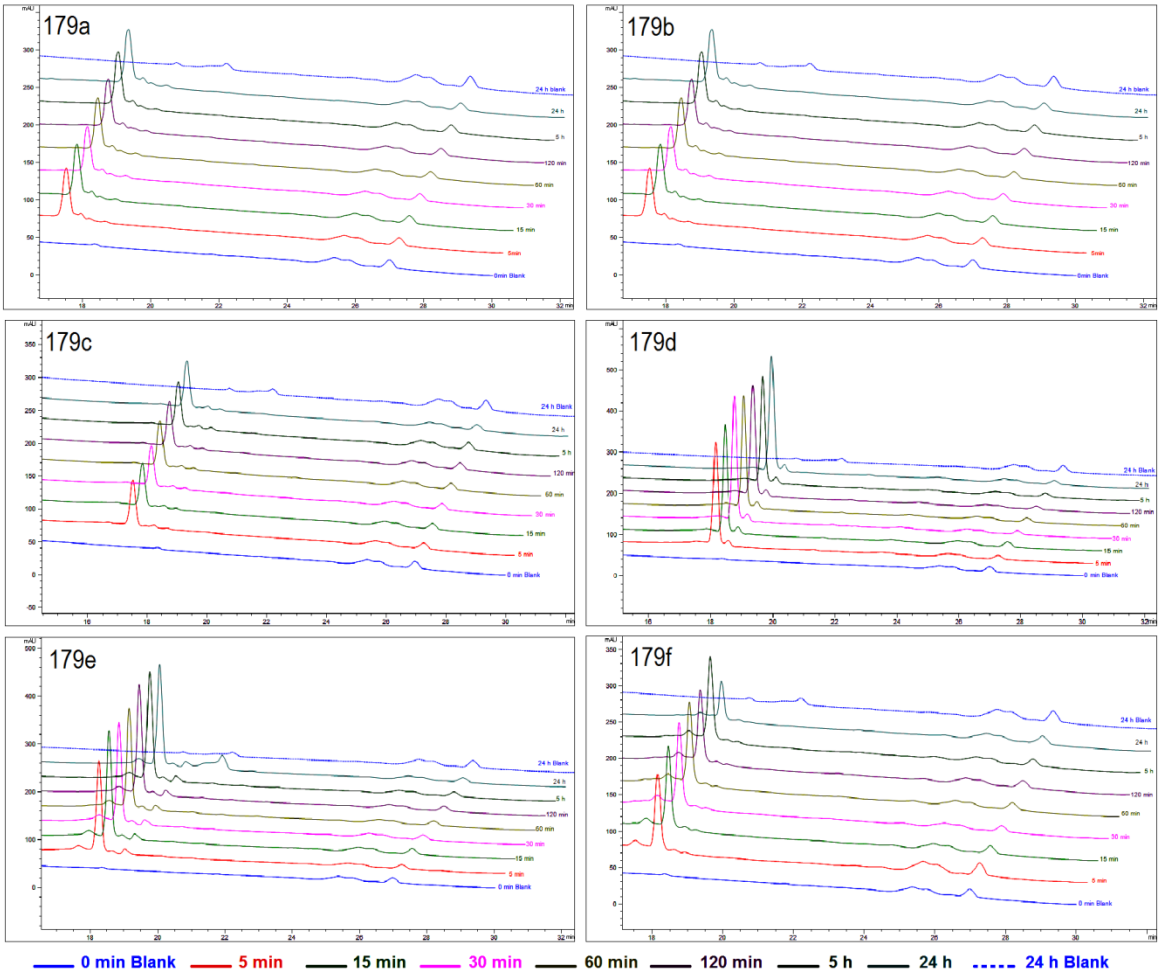

Figure 3-4 Chemical stability of compounds **179a-f** incubated in EMEM for 24 h (HPLC analysis, UV detection at 220 nm).

3.2.4 Solubility in Eagle's Minimum Essential Medium (EMEM)

Solubility, the phenomenon of dissolution of solute in solvent to give a homogenous system, is one of the important parameters to achieve desired concentration of drug in systemic circulation for desired (anticipated) pharmacological response. The most frequent causes of low oral bioavailability are attributed to poor solubility and low permeability. Poorly water soluble drugs often require high doses in order to reach therapeutic plasma concentrations after oral administration. Low aqueous solubility is the major problem encountered with formulation development of new chemical entities as well as generic development. Any drug to be absorbed must be present in the form of an aqueous solution at the site of absorption. Water is the solvent of choice for liquid

pharmaceutical formulations. Most of the drugs are either weakly acidic or weakly basic having poor aqueous solubility.[8]

The improvement of drug solubility thereby its oral bioavailability remains one of the most challenging aspects of drug development process especially for oral-drug delivery system. There are numerous approaches available and reported in literature to enhance the solubility of poorly water-soluble drugs.[15] Solubility improvement techniques can be categorized in to physical modification: particle size reduction,[16] modification of the crystal habit,[17] cocrystallization,[18] solid dispersions,[19] solid solutions and cryogenic techniques; chemical modifications: change of pH, use of buffer, derivatization,[20] complexation,[21] and salt formation;[22] and miscellaneous methods: supercritical fluid process,[23] use of adjuvant[24] and novel excipients.[25]

Compound **143** (Figure 1-30) is a tariquidar analog (Figure 1-30, compound **141**), in which the quinoline-carboxamide residue was shifted to the *meta*-position at the benzamide core and the two methoxy groups were replaced by a methyl carboxylate, was highly selective for ABCG2, but when one of the methoxy groups on the tetrahydroisoquinoline moiety was replaced by a triethylenglycol chain the maximal response increased to about 90% (Figure 1-30, compound **145**), indicating that water solubility was limiting the efficacy in this class of compounds.

The solubility in EMEM for all compounds was evaluated; the results showed that all chalcones were soluble. As shown in Figure 3-5, the concentration found for chalcones **179a-e** was very similar in all analyzed aliquots at different times, which means that after 5 h of incubation we will find the same amount of the compound in the assay, and these were not affected by the physiological pH, temperature or the substances present in the medium (salts, amino acids or vitamins). Then, inhibition results for the transporters corresponded to the entire concentration used in the assay.

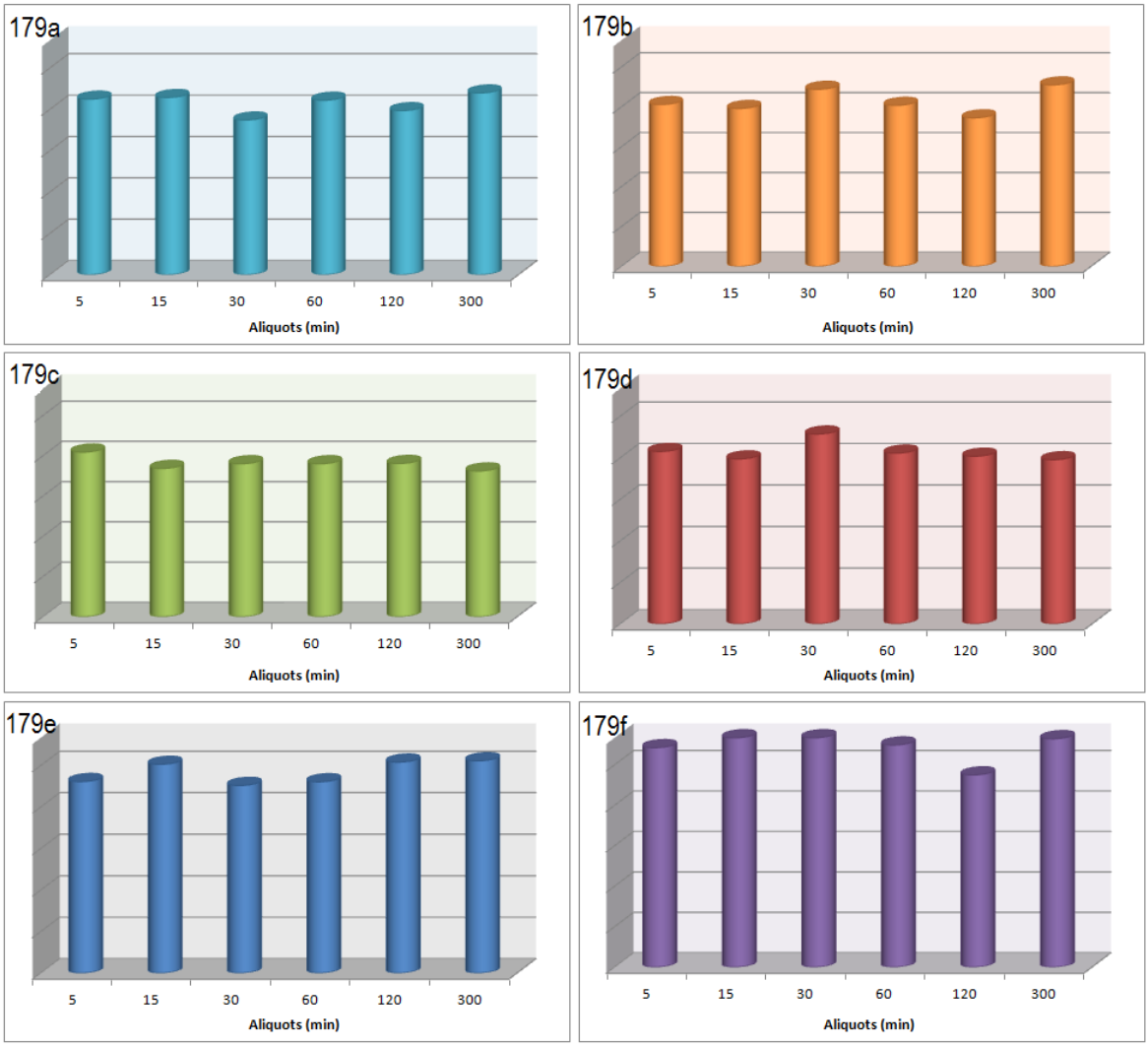

Figure 3-5 Solubility for chalcones **179a-f** in Eagle's Minimum Essential Medium (EMEM)

3.2.5 Chemosensitivity assay

Cytotoxicity assays are widely used by the pharmaceutical industry to screen for cytotoxicity in compound libraries. Researchers can either look for cytotoxic compounds, if they are interested in developing a therapeutic that targets rapidly dividing cancer cells, for instance; or they can screen "hits" from initial high-throughput drug screens for unwanted cytotoxic effects before investing in their development as a pharmaceutical.[26]

The effect of the most potent modulator (**179d**) on the proliferation of ABCG2-overexpressing MCF-7/Topo cells was investigated by means of a kinetic chemosensitivity assay,[26] using the modulators in combination with topotecan (known ABCG2 substrate) and the cytostatic drug vinblastine as a positive control (Figure 3-6). The modulator was well tolerated up to a concentration of 1 µM. The combination of topotecan at a nontoxic concentration of 100 nM with compound **179**d resulted in a strong cytotoxic drug effect and thus reversal of ABCG2-mediated drug resistance.

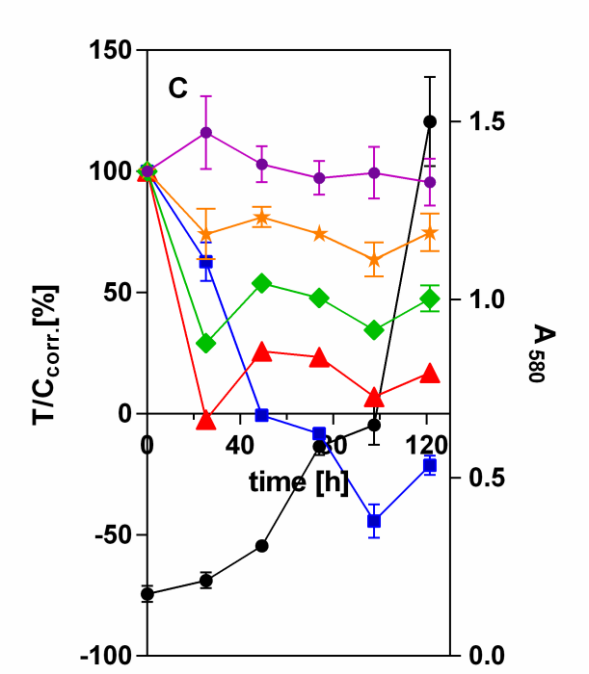

Figure 3-6 Effect of compound **179d** in combination with topotecan on proliferating MCF-7/Topo cells: vehicle (filled black circles, untreated cells), positive control vinblastine [100 nM] (filled blue squares), **179d** at concentrations of 10 µM (filled red triangles), 3 µM (filled green diamonds), 1 µM (filled orange stars) and topotecan alone at 100 nM (filled purple circles)

3.3 Conclusion

In summary, we presented the synthesis and characterization of a series of chalcones combining quinoline and isoquinoline moieties as ABCG2 modulators. All tested compounds showed a marked preference for ABCG2 inhibition, because the maximal inhibitory effect values for the chalcones over ABCB1 and ABCC1 were not significant.

Compounds bearing a methyl substituent at the amino chalcone core (**179d-f**) were most active in the series with the lowest IC_{50} values and were superior with respect to the maximal inhibitory effect (86%, 97% and 111% respectively) to that tariquidar or even surpassing that of FTC (compound **179f**). Compound **179d** was almost equipotent with the referente compound (FTC) with IC_{50} value of 0.880 µM in the Hoechst assay and maximal inhibitory effect of 86%. The replacement of one methoxy group for glycol chains in the tetrahydroisoquinoline moiety increased the water solubility of the compounds and efficacy as ABCG2 modulators (I_{max} 72-111%). The unstable benzamide moiety in compound **145** (Figure 1-30) was replaced in a bioisosteric approach with a chalcone system as central core structure, the stability tests in EMEM revealed that the chalcones were stables to degradation after 24 hours of incubation and solubility tests showed that the inhibition results corresponded to the entire concentration used in the assay. Additionally, chemosensitivity assay showed that compound **179d** had a strong cytotoxic drug effect in combination with topotecan (chemotherapeutic agent) and thus reversal of ABCG2-mediated drug resistance.

3.4 Experimental section

3.4.1 Synthesis and characterization

4-(2-Hydroxyethoxy)benzaldehyde

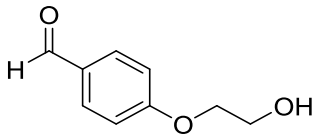

4-(2-hydroxyethoxy)benzaldehyde has already been described.[6] Colorless oil (1.2 g, yield 85%, R_f Hex:EA 1:1 0.20), **^{1}H NMR ($CDCl_3$, 400 MHz): δ**= 7.45 (d, ^3J=8.9 Hz, 2H, OCH_2CH_2), 6.64 (d, ^3J=8.7 Hz, 2H, OCH_2CH_2), 3.79 (t, ^3J=9.0 Hz, 2H, OCH_2), 3.73 (t, ^3J=9.3 Hz, 2H, CH_2OH). **^{13}C NMR ($CDCl_3$, 100 MHz): δ**= 190.99 (C_{quat}), 163.72 (C_{quat}), 131.80 (C_{quat}), 130.10 (+), 114.82 (+), 69.55 (-), 61.21 (-). **IR [cm^{-1}]: v** = 3443, 3274, 2873, 2842, 2747, 1690, 1580, 1427, 1044, 916, 653.

2-(4-Formylphenoxy)ethyl 4-methylbenzenesulfonate (177)

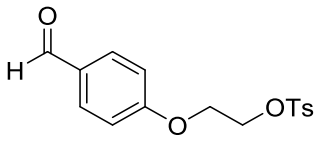

Compound 177 has already been described.[7] Light pink solid (0.700 g, yield 84%, R_f Pen: EA 1:1 0.62). mp: 102-104ºC (103-105ºC lit).[7] **^{1}H NMR ($CDCl_3$, 400 MHz)**: **δ=** 7.83 (d, ^3J=2.5 Hz, 2H, ArH), 7.81 (d, ^3J=7.0 Hz, 2H, ArH), 7.36 (d, ^3J=8.1 Hz, 2H, ArH), 6.91 (d, ^3J=8.7 Hz, 2H, ArH), 4,42 (m, 2H, OCH_2), 4,25 (m, 2H, CH_2OSO_2), 2.46 (s, 3H, CH_3). **^{13}C NMR ($CDCl_3$, 100 MHz)**: **δ=** 190.6 (C_{quat}), 162.8 (C_{quat}), 145.1 (C_{quat}), 127.9 (C_{quat}), 128.0 (C_{quat}), 129.9 (+), 129.9 (+), 130.4 (+), 131.8 (+), 131.9 (+), 132.8 (+), 114.7 (+), 114.7 (+), 67.6 (-), 65.6 (-), 21.6 (+). **IR (KBr) [cm^{-1}]: v =**3254, 2830, 2750, 1698, 1603, 1508, 1271, 1015, 915, 665.

General procedure for the chalcone formation (178a-b): Chalcones were obtained by a Claisen-Schmidt condensation. The ketone **171a-b** (1equiv) and aldehyde **177** (1.3 equiv) were mixed and heated for 2 hours at 80ºC, then the mixture was allowed to reach room temperature and at 0ºC and 1 mL of NaOH 30% was added slowly. After 24 h at room temperature, ice was added to the mixture; the product was filtered and dried.

(*E*)-2-(4-(3-*oxo*-3-(3-(Quinoline-2-carboxamido)phenyl)prop-1-en-1-yl)phenoxy)ethyl 4-methylbenzenesulfonate (178a)

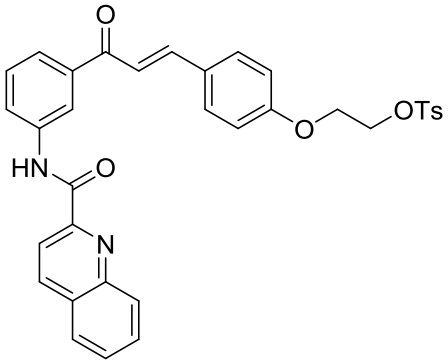

Pale yellow solid (0.400 g, yield 72%, R_f Hex:EA 2:1 0.47). **^{1}H NMR (400 MHz, $CDCl_3$): δ** 8.40 (d, ^{3}J=8.3 Hz, 2H, ArH), 8.23 (t, ^{3}J=9.0 Hz, 2H, ArH), 7.93 (d, ^{3}J=8.2 Hz, 1H, ArH), 7.84 (m, 5H, ArH), 7.67 (t, ^{3}J=7.5 Hz, 1H, quinol), 7.60 (m, 2H, ArH), 7.55 (s, 1H, ArH), 7.47 (d, ^{3}J=15.6 Hz, 1H, COCH), 7.35 (d, ^{3}J=8.0 Hz, 2H, tosyl), 6.83 (d, ^{3}J=7.7 Hz, 2H, ArH), 4.44 (t, ^{3}J=4.0 Hz, 2H, $ArOCH_2$), 4.37 (t, ^{3}J=4.1 Hz, 2H, CH_2OSO_2), 2.45 (s, 3H, CH_3 Tosyl). **^{13}C NMR (100 MHz, $CDCl_3$): δ** 190.0 (C_{quat}), 162.4 (C_{quat}), 160.0 (+), 158.3 (C_{quat}) 154.7 (C_{quat}), 147.6 (C_{quat}), 145.0 (+), 143.8 (C_{quat}), 142.1 (C_{quat}), 141.6 (C_{quat}), 139.3 (C_{quat}), 138.9 (C_{quat}), 137.8 (+), 132.9 (+), 131.5 (C_{quat}), 130.5 (+), 130.3 (+), 129.9 (+), 129.7 (+), 129.5 (+), 128.3 (+), 127.9 (+), 124.4 (+), 114.9 (+), 67.8 (-), 65.5 (-), 21.6 (+). **IR (KBr) [cm-1]: v** = 1640, 1710, 730. **HRMS (EI-MS)** calcd. For $C_{34}H_{29}N_2O_6S$ $[M+H]^+$: 593.1702; found $[M+H]^+$: 593.1729.

(*E*)-2-(4-(3-(4-Methyl-3-(quinoline-2-carboxamido)phenyl)-3-oxoprop-1-en-1-yl)phenoxy)ethyl 4-methylbenzenesulfonate (178b)

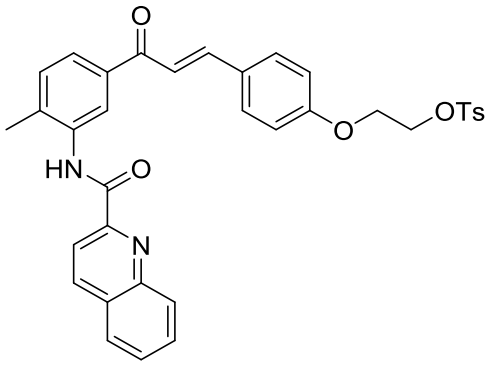

Yellow solid. (0.600 g, yield 80%, R_f Hex:EA 2:1 0.50). **^{1}H-NMR (400 MHz, $CDCl_3$): δ** 9.00 (s, 1H, quinol), 8.42 (m, 2H, quinol), 8.18 (d, ^3J=8.4 Hz, 1H, ArH), 7.94 (d, ^3J=8.2 Hz, 1H, quinol), 7.89 (m, 2H, ArH), 7.68 (t, ^3J=7.6 Hz, 2H, quinol), 7.60 (d, ^3J=8.7 Hz, 2H, ArH), 7.50 (d, ^3J=15.6 Hz, 1H, COCH), 7.35 (d, ^3J=8.1 Hz, 2H, tosyl), 6.81 (d, ^3J=8.7 Hz, 2H, ArH), 4.39 (t, ^3J=5.5 Hz, 2H, OCH_2CH_2), 4.20 (t, ^3J=5.6 Hz, 2H, CH_2OSO_2), 2.58 (s, 3H, CH_3 tosyl), 2.45 (s, 3H, CH_3). **^{13}C-NMR (101 MHz, $CDCl_3$): δ** 190.6 (C_{quat}), 162.3 (C_{quat}), 146.3 (C_{quat}), 138.0 (C_{quat}), 136.2 (C_{quat}), 133.6 (C_{quat}), 131.9 (C_{quat}), 130.7 (C_{quat}), 130.4 (C_{quat}), 129.9 (+), 129.8 (C_{quat}), 129.6 (C_{quat}), 129.4 (+), 128.3 (+), 128.0 (+), 127.8 (+), 127.9 (+), 124.1 (+), 121.6 (+), 118.7 (+), 114.7 (+), 67.6 (-), 65.6 (-), 26.7 (+), 21.6 (+). **IR (KBr) [cm-1]: v** = 1635, 1693, 735. **HRMS (EI-MS)** calcd. For $C_{34}H_{29}N_2O_6S$ $[M+H]^+$: 607.1858; found $[M+H]^+$: 607.1906.

General procedure for the preparation of compounds 179a-f: A mixture of **178a-b** (1 mol), 1,2,3,4-tetrahydroisoquinoline **174**, **175a**-**b** (1.3 equiv) and K_2CO_3 (3 equiv) was refluxed in CH_3CN overnight. The solvent was evaporated, water was added and the compound was extracted with DCM, organic layer was separated, dried with Na_2SO_4, filtered and the solvent evaporated to give the crude product. Compounds were purified, first, with a flash column chromatography (DCM:MeOH) and second, reverse column chromatography and in some cases a preparative HPLC.

(*E*)-*N*-(3-(3-(4-(2-(6,7-Dimethoxy-3,4-dihydroisoquinolin-2(1*H*)-yl)ethoxy)phenyl)acryloyl)phenyl)quinoline-2-carboxamide (179a)

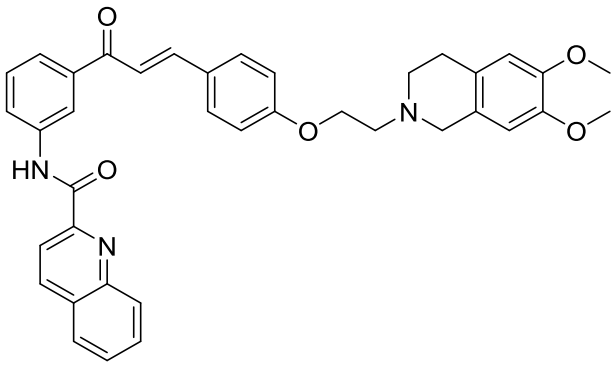

Yellow solid (0.030 g, yield 54%, R_f DCM:MeOH 20:1 0.42). **^{1}H-NMR (400 MHz, $CDCl_3$): δ** 8.38 (m, 3H, quinol), 8.24 (m, 2H, ArH), 7.93 (m, 2H, quinol), 7.80 (m, 2H, ArH), 7.69 (m, 1H, quinol), 7.52 (d, ^3J=15.5 Hz, 1H, C_qCOCH), 6.96 (d, ^3J=8.5 Hz, 2H, ArH), 6.65 (s, 1H, CH THIQ), 6.54 (s, 1H, CH THIQ), 4.53 (s, 2H, CH_2 THIQ), 3.87 (s, 3H, OCH_3), 3.85 (s, 3H, OCH_3), 3.81 (s, 2H, CH_2 THIQ), 3.65 (m, 2H, CH_2 THIQ), 3.42 (m, 2H, OCH_2CH_2), 2.65 (m, 2H, CH_2 THIQ). **^{13}C-NMR (100 MHz, $CDCl_3$): δ** 190.0 (C_{quat}), 162.5 (C_{quat}), 159.1 (C_{quat}), 149.2 (C_{quat}), 148.6 (C_{quat}), 146.3 (C_{quat}), 144.4 (+), 139.1 (C_{quat}), 138.3 (C_{quat}), 138.0 (C_{quat}), 130.5 (+), 129.6 (+), 129.0 (+), 128.3 (C_{quat}), 127.8 (+), 124.3 (+), 123.9 (C_{quat}), 122.2 (+), 120.5 (+), 119.5 (+), 118.4 (+), 118.2 (+), 115.0 (+), 109.2 (+), 63.2 (-), 56.0 (+), 53.0 (-), 49.6 (-), 23.8 (-). **IR (KBr) [cm-1]: v** = 3137, 2810, 1642, 1689, 1660, 1140, 693. **HRMS (EI-MS)** calcd. For $C_{38}H_{36}N_3O_5$ $[M+H]^+$:614.2610; found $[M+H]^+$: 614.2657.

(*E*)-*N*-(3-(3-(4-(2-(6-Methoxy-7-(2-methoxyethoxy)-3,4-dihydroisoquinolin-2(1*H*)-yl)ethoxy)phenyl)acryloyl)phenyl)quinoline-2-carboxamide (179b)

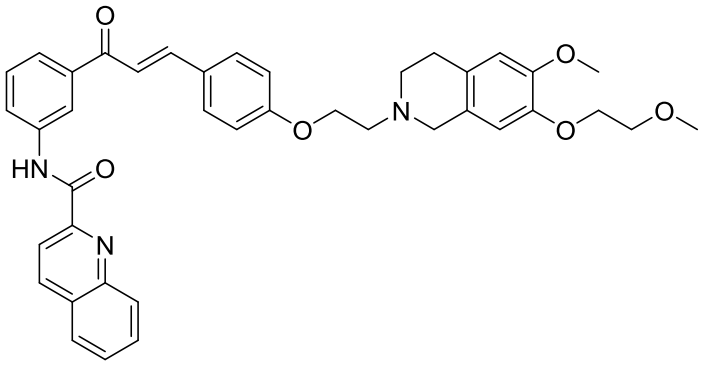

Pale yellow solid. (0.032 g, yield 63%, R_f DCM:MeOH 20:1 0.39). **^{1}H NMR (400 MHz, $CDCl_3$): δ** 8.43 (m, 2H, quinol), 8.22 (d, ^3J=8.4 Hz, 2H, ArH), 7.92 (d, ^3J=8.5 Hz, 1H, quinol), 7.87 (m, 2H, ArH), 7.63 (s, 2H, quinol), 7.55 (d, ^3J=15.7 Hz, 1H, COCH), 7.46 (t, ^3J=7.5 Hz, 1H, ArH), 6.96 (s, 1H, CH THIQ), 6.58 (s, 1H, CH THIQ), 4.28 (m, 2H, CH_2 PEG), 4.17 (m, 2H, CH_2 THIQ), 4.02 (m, 2H, OCH_2CH_2), 3.80 (s, 3H, OCH_3), 3.73 (m, 2H, CH_2CH_2O), 3.60 (m, 2H, CH_2 THIQ), 3.44 (s, 3H, CH_2OCH_3), 2.86 (m, 2H, CH_2 PEG), 2.44 (d, ^3J=3.8 Hz, 2H, CH_2 THIQ).**^{13}C NMR (100 MHz, $CDCl_3$): δ** 190.1 (C_{quat}), 162.5 (C_{quat}), 159.3 (C_{quat}), 154.5 (C_{quat}), 149.3 (C_{quat}), 146.3 (C_{quat}), 144.9 (+), 140.0 (C_{quat}), 139.3 (C_{quat}), 138.3 (C_{quat}), 138.0 (+), 132.0 (+), 130.4 (+), 130.2 (C_{quat}), 128.3 (+), 128.0 (+), 124.2 (C_{quat}), 119.8 (+), 119.4 (+), 118.7 (+), 115.0 (+), 71.0 (-), 68.6 (-), 65.7 (-), 59.1 (+), 58.9 (+), 55.9 (-), 51.3 (-), 29.7 (+). **IR (KBr) [cm-1]: v** = 3185, 2836, 1617, 1676, 1660, 1260, 710. **HRMS (EI-MS)** calcd. For $C_{40}H_{40}N_3O_6$ $[M+H]^+$: 658.2872; found $[M+H]^+$: 658.2920.

(*E*)-*N*-(3-(3-(4-(2-(6,7-bis(2-(2-(2-Methoxyethoxy)ethoxy)ethoxy)-3,4-dihydroisoquinolin-2(1*H*)-yl)ethoxy)phenyl)acryloyl)phenyl)quinoline-2-carboxamide (179c)

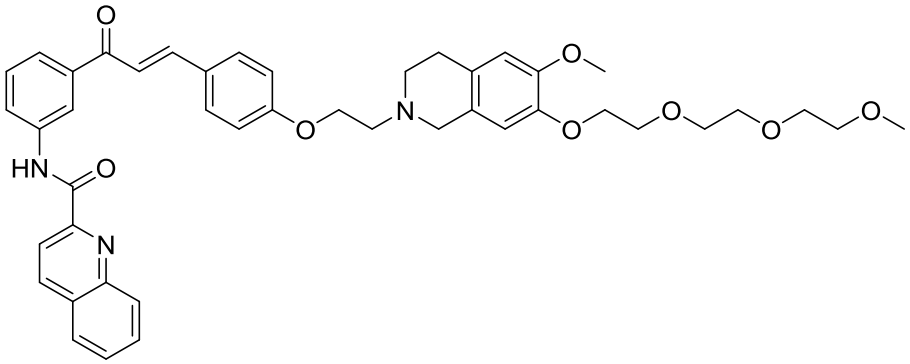

Pale yellow solid. (0.025 g, yield 58%, R_f DCM:MeOH 20:1 0.35). **^{1}H NMR (400 MHz, $CDCl_3$): δ** 8.43 (m, 3H, quinol), 8.27 (m, 1H, ArH), 7.94 (d, ^3J=8.2 Hz, 1H, quinol), 7.84 (dd, ^3J=8.2, ^3J=6.9, 3H, ArH), 7.68 (t, ^3J=7.2 Hz, 2H, quinol), 7.50 (d, ^3J=15.6 Hz, 1H, COCH), 6.98 (s,1H, CH THIQ), 6.66 (s,1H, CH THIQ), 4.52 (s, 2H, CH_2 THIQ), 4.17 (m, 2H, CH_2 THIQ), 3.94 (m, 2H, CH_2 THIQ), 3.87 (s, 3H, OCH_3), 3.73 (dd, ^3J=5.8, ^3J=3.1 Hz, 4H, $2CH_2$ PEG), 3.70 (m, 4H, $2CH_2$ PEG), 3.55 (dd, ^3J=5.7, ^3J=3.5 Hz, 4H, $2CH_2$ PEG), 3.36 (m, 2H, CH_2OCH_3), 3.14 (m, 2H, CH_2CH_2N). **^{13}C NMR (100 MHz, $CDCl_3$): δ** 190.1 (C_{quat}), 162.4 (C_{quat}), 161.0 (C_{quat}), 149.3 (C_{quat}), 148.3 (C_{quat}), 146.8 (C_{quat}), 145.0 (+), 139.3 (C_{quat}), 138.3 (C_{quat}), 138.0 (C_{quat}), 132.0 (+), 130.4 (+), 129.6 (+), 128.3 (C_{quat}), 127.8 (+), 126.8 (+), 124.2 (C_{quat}), 119.4 (+), 118.7 (+), 115.0 (+), 112.5 (+), 111.9 (+), 71.9 (-), 70.9 (-), 70.3 (-), 69.6 (+), 68.7 (-), 59.0 (+), 56.6 (-), 56.0 (-), 28.5 (-). **IR (KBr) [cm-1]: v** = 3156, 2891, 1672, 1661, 1646, 1040, 682. **HRMS (EI-MS)** calcd. For $C_{44}H_{48}N_3O_8$ $[M+H]^+$: 746.3397; found $[M+H]^+$: 746.3444.

(*E*)-*N*-(5-(3-(4-(2-(6,7-Dimethoxy-3,4-dihydroisoquinolin-2(1*H*)-yl)ethoxy)phenyl)acryloyl)-2-methylphenyl)quinoline-2-carboxamide (179d)

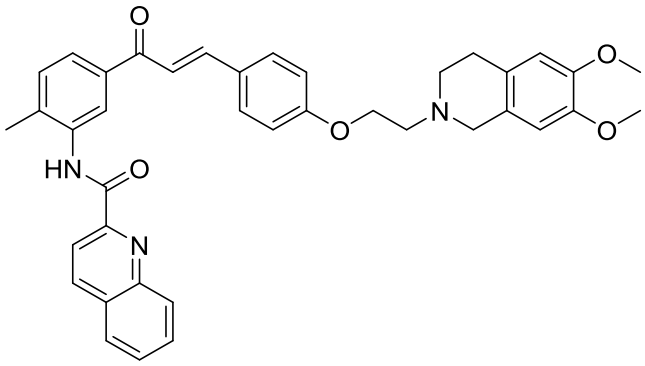

Brown yellow solid. (0.042 g, yield 68%, R_f DCM:MeOH 20:1 0.47). **^{1}H NMR (400 MHz, $CDCl_3$): δ** 8.99 (s, 2H, quinol), 8.41 (s, 2H, ArH), 8.18 (d, ^3J=8.4 Hz, 1H, ArH), 7.93 (d, ^3J=13.6 Hz, 1H, quinol), 7.83 (m, 1H, ArH), 7.65 (d, ^3J=8.7 Hz, 3H, quinol), 7.50 (d, ^3J=15.6 Hz, 1H, COCH), 7.38 (d, ^3J=8.0 Hz, 1H, ArH), 6.96 (d, ^3J=8.7 Hz, 2H, ArH), 6.61 (s, 1H, CH THIQ), 6.53 (s, 1H, CH THIQ), 4.31 (s, 2H, CH_2 THIQ), 3.85 (s, 3H, OCH_3), 3.84 (s, 3H, OCH_3), 3.66 (m, 2H, CH_2 THIQ), 3.16 (m, 2H, CH_2 THIQ), 2.58 (s, 3H, CH_3). **^{13}C NMR (100 MHz, $CDCl_3$): δ** 189.9 (C_{quat}), 162.3 (C_{quat}), 159.8 (C_{quat}), 154.6 (C_{quat}), 149.6 (C_{quat}), 146.3 (C_{quat}), 144.4 (C_{quat}), 142.4 (C_{quat}), 138.0 (C_{quat}), 137.4 (C_{quat}), 136.1 (+), 133.3 (+), 130.9 (+), 130.4 (+), 129.8 (+), 129.5 (+), 128.3 (C_{quat}), 127.8 (C_{quat}), 126.4 (C_{quat}) 124.7 (+), 121.4 (+), 118.7 (+), 115.0 (+), 111.3 (+), 109.4 (+), 68.0 (-), 58.1 (+), 55.9 (-), 51.0 (-), 27.2 (-), 18.0 (+). **IR (KBr) [cm-1]: v** = 3185, 2824, 1583, 1653, 1660, 1047, 698. **HRMS (EI-MS)** calcd. For $C_{39}H_{38}N_3O_5$ $[M+H]^+$: 628.2767; found $[M+H]^+$: 628.2814.

(*E*)-*N*-(5-(3-(4-(2-(6,7-bis(2-Methoxyethoxy)-3,4-dihydroisoquinolin-2(1*H*)-yl)ethoxy)phenyl)acryloyl)-2-methylphenyl)quinoline-2-carboxamide (179e)

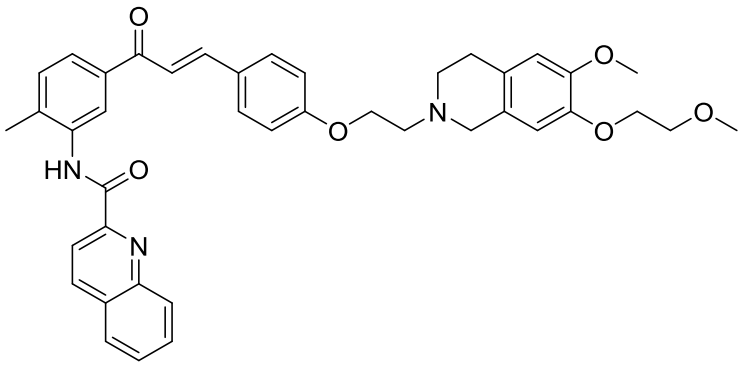

Yellow solid. (0.036 g, yield 57%, R_f DCM:MeOH 20:1 0.45). **^{1}H NMR (400 MHz, $CDCl_3$): δ** 8.43 (m, 2H, ArH quinol), 8.21 (m, 2H, ArH), 7.93 (d, ^3J=8.1 Hz, 2H, ArH quinol), 7.81 (t, ^3J=7.2 Hz, 4H), 7.71 (m, 2H, ArH quinol), 7.57 (m, 1H, ArH), 7.36 (d, ^3J=8.3 Hz, 1H, COCH), 6.57 (s, 1H, CH THIQ), 6.56 (s, 1H, CH THIQ), 4.13 (m, 4H, OCH_2CH_2), 3.80 (s, 3H, OCH_3), 3.76 (t, ^3J=7.0 Hz, 2H, CH_2 PEG), 3.74 (d, ^3J=4.9 Hz, 2H, CH_2 PEG), 3.61 (m, 2H, CH_2 THIQ), 3.52 (m, 2H, CH_2 THIQ), 3.41 (m, 2H, CH_2 THIQ), 3.38 (s, 3H, CH_2OCH_3), 2.57 (s, 3H, CH_3). **^{13}C NMR (101 MHz, $CDCl_3$): δ** 191.5 (C_{quat}), 163.5 (C_{quat}), 149.9 (C_{quat}), 148.3 (C_{quat}), 146.8 (C_{quat}), 144.6 (+), 143.5 (+), 141,5 (C_{quat}), 138.0 (C_{quat}), 130.9 (+) 130.4 (+), 129.7 (+), 128.3 (C_{quat}), 127.9 (+), 126.9 (C_{quat}), 126.3 (C_{quat}), 125.3 (+), 115.0 (+), 112.4 (+), 111.8 (+), 71.0 (-), 70.6 (-), 68.6 (-), 59.1 (+), 58.9 (-), 57.4 (+), 55.9 (-), 51.3 (-), 29.7 (-), 28.4 (+). **IR (KBr) [cm-1]: v** = 3158, 2823, 1631, 1596, 1632, 976, 683. **HRMS (EI-MS)** calcd. For $C_{41}H_{42}N_3O_6$ $[M+H]^+$: 672.3029; found $[M+H]^+$: 672.3072.

(*E*)-*N*-(5-(3-(4-(2-(6,7-bis(2-(2-(2-Methoxyethoxy)ethoxy)ethoxy)-3,4-dihydroisoquinolin-2(1*H*)-yl)ethoxy)phenyl)acryloyl)-2-methylphenyl)quinoline-2-carboxamide (179f)

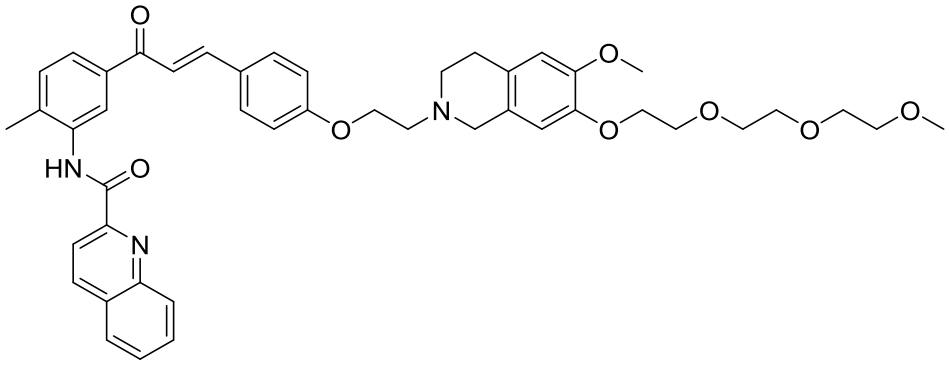

Yellow solid. (0.023 g, yield 61%, R_f DCM:MeOH 20:1 0.44). **^{1}H NMR (400 MHz, $CDCl_3$): δ** 8.41 (m, 2H, ArH quinol), 8.24 (m, 1H, ArH), 8.05 (s, 1H, ArH), 7.93 (d, ^{3}J=8.2 Hz, 2H, ArH quinol), 7.82 (t, ^{3}J=9.8 Hz, 1H, ArH), 7.66 (m, 2H, ArH quinol), 7.51 (d, ^{3}J=15.6 Hz, 1H, COCH), 7.35 (d, ^{3}J=8.1 Hz, 2H, ArH), 6.92 (d, ^{3}J=6.0 Hz, 1H, ArH), 6.57 (s, 1H, CH THIQ), 6.55 (s, 1H, CH THIQ), 4.19 (m, 4H, $2CH_2$ PEG), 3.90 (m, 2H, CH_2 THIQ), 3.87 (m, 2H, CH_2 PEG), 3.81 (s, 3H, OCH_3), 3.68 (m, 2H, CH_2 PEG), 3.55 (d, ^{3}J=5.0 Hz, 2H, CH_2 PEG), 3.37 (m, 4H, $2CH_2$ PEG), 3.09 (t, ^{3}J=5.9 Hz, 2H, CH_2 THIQ), 2.69 (t, ^{3}J=5.8 Hz, 2H, CH_2 THIQ). **^{13}C NMR (100 MHz, $CDCl_3$): δ** 170.7 (C_{quat}), 162.3 (C_{quat}), 154.6 (C_{quat}), 153.6 (C_{quat}), 148.0 (C_{quat}), 146.4 (C_{quat}), 139.0 (C_{quat}), 138.0 (C_{quat}), 128.2 (C_{quat}), 127.9 (C_{quat}), 127.3 (C_{quat}), 118.7 (+), 115.0 (+), 112.6 (+), 111.9 (+), 71.9 (-), 70.7 (-), 70.6 (-), 70.5 (-), 69.6 (+), 68.7 (-), 59.0 (+), 56.0 (-), 43.9 (-), 28.7 (-), 18.0 (+). **IR (KBr) [cm-1]: ν** = 3217, 2913, 1702, 1692, 1589, 984, 714. **HRMS (EI-MS)** calcd. For $C_{45}H_{50}N_3O_8$ $[M+H]^+$: 760.3553; found $[M+H]^+$: 760.3606.

3.4.2 Biological investigations

3.4.2.1 Drugs and Chemicals

Hoechst 33342 (Invitrogen, Karlsruhe, Germany) was dissolved in sterile water to produce a 0.8 mM working solution. Calcein-AM (4 mM in anhydrous DMSO) and pluronic F127 were obtained from Biotium (Hayward, CA, USA) and diluted to 100 µM. Bovine serum albumin (BSA) was purchased from Serva (Heidelberg, Germany). Fumitremorgin C (FTC; Merck, Darmstadt, Germany) was also dissolved in DMSO and diluted to a concentration of 1 mM. Reversan was purchased from Tocris Bioscience (Bristol, UK) and diluted to a 3 mM working solution in DMSO. Topotecan and vinblastine for cell culture supplementation were purchased from Sigma (Munich, Germany). Loading buffer (calcein-AM assay) was made of 120 mM NaCl, 5 mM KCl, 2 mM $MgCl_2.6H_2O$, 1.5 mM $CaCl_2.2H_2O$, 25 mM HEPES, 10 mM glucose, pH 7.4. PBS (phosphate buffered saline) was made of 8.0 g/L NaCl, 1.0 g/L $Na_2HPO_4.2H_2O$, 0.20 g/L KCl, 0.20 g/L KH_2PO_4 and 0.15 g/L $NaH_2PO_4.H_2O$. The pH value was adjusted to 7.3 - 7.4. A solution of 4% (m/m) paraformaldeyde (PFA) in PBS was made by stirring 2 g of PFA per 50 g total solution while heating on a magnetic stirrer for approximately 30 min. The test compounds were dissolved in DMSO at a concentration of 10 mM if possible, depending on the solubility of the compounds. All stock solutions were stored at −20 °C. If not otherwise stated, chemicals (p.a. quality) were obtained from Merck (Darmstadt, Germany). Purified water (Milli-Q system, Millipore, Eschborn, Germany) was used throughout.

3.4.2.2 Cell lines and culture conditions

MCF-7/Topo cells, an ABCG2-overexpressing subclone of MCF-7 cells (ATCC® HTB-22™, American Type Culture Collection, Manassas, VA), were obtained as described[27] and cultured in water-saturated atmosphere (95% air, 5% CO_2) at 37 °C in 75 cm^2 culture flasks from Nunc (Wiesbaden,Germany) in Eagle's minimum essential medium (EMEM; Sigma, Munich, Germany) containing l-glutamine, 2.2 g/L $NaHCO_3$ and 110 mg/L sodium pyruvate supplemented with 10% fetal calf serum (FCS; Biochrom, Berlin, Germany) and 550 nm topotecan to induce overexpression of the ABCG2 transporter. Human Kb-V1 cells, an ABCB1-overexpressing subclone of Kb cells (ATCC® CCL-17™), were obtained and cultured as described.[27] MDCKII-MRP1 cells: MDCKII cells (Madin-Darby Canine

Kidney cells, strain II; a dog epithelial cell line; ATCC® CRL-2936™), transfected with human ABCC1,[28,29] were a kind gift from Prof. Dr. P. Borst from the Netherland Cancer Institute (Amsterdam, NL). The cells were cultured in DMEM supplemented with 10% FCS, 3.7 g/L $NaHCO_3$ and 110 mg/L sodium pyruvate. Trypsinization was performed at 37 °C (95% air, 5% CO_2) for 20-30 min using 0.1% trypsin / 0.04% EDTA. All cells were routinely monitored for mycoplasma contamination by PCR (Venor GeM, Minerva Biolabs, Berlin, Germany) and only mycoplasma-negative cultures were used.

3.4.2.3 Calcein-AM microplate assay for the determination of ABCB1 inhibition

Kb-V1 cells were seeded into flat-bottomed 96-well plates (Greiner, Frickenhausen, Germany) at a density of 20,000 cells per well. On the following day, cells were washed with loading buffer (120 mM NaCl, 5 mM KCl, 2 mM $MgCl_2.6H_2O$, 1.5 mM $CaCl_2.2H_2O$, 25 mM HEPES, 10 mM glucose, pH 7.4) in order to remove unspecific serum esterases. Afterwards, cells were incubated with loading suspension (loading buffer, 5 mg/mL BSA, 1.25 µL/mL pluronic F127 (20% in DMSO)) containing 0.5 µM calcein-AM and the test compounds at increasing concentrations (10 nM – 100 µM) for 10 min (37 °C / 5% CO2) to construct concentration-response curves. Tariquidar served as positive control at a final concentration of 1 µM corresponding to 100% 3 inhibition of calcein-AM efflux. Subsequently, the loading suspension was discarded and cells were fixed with 4% PFA solution in PBS for 30 min. After three washing steps, fixed cells were overlaid with loading buffer and relative fluorescence intensities were determined with a GENios Pro microplate reader (Tecan Deutschland, Crailsheim, Germany). Measurement mode: fluorescence top; excitation filter (calcein-AM): 485/20; emission filter (calcein-AM): 535/25; number of reads: 10; integration time: 40 µs; lag time: 0 µs; mirror selection: Dichroic 3; plate definition file: GRE96ft.pdf; multiple reads per well (Circle): 3x3; time between move and flash: 100 ms. On each plate, the optimal gain was calculated by determination of the fluorescence intensity in the presence of the reference substance, tariquidar. IC_{50} values were calculated using SIGMA PLOT 11.0 (Systat Software, Erkrath, Germany), “Four parameter logistic curve” fitting. Errors were expressed as standard error of the mean (SEM).

3.4.2.4 Calcein-AM microplate assay for the determination of ABCC1 inhibition

MDCKII cells were seeded into flat-bottomed 96-well plates at a density of about 20,000 cells/well. On the following day, cells were washed with loading buffer in order to remove unspecific serum esterases. Afterwards, cells were incubated with loading suspension (loading buffer, 5 mg/mL BSA, 1.25 µL/mL pluronic F127 (20% (m/v) in DMSO)) containing 0.5 µM calcein-AM and the test compound at increasing concentrations (10 nM-100 µM) for 60 min (37 °C / 5% CO2). Reversan served as positive control at a final concentration of 30 µM corresponding to 100% ABCC1 inhibition. In general, test compounds were investigated as triplicates, controls as sextuplicates, respectively. Subsequently, the loading suspension was discarded, and the cells were fixed with 4% PFA solution for 30 min. After three washing circles (loading buffer), fixed cells were overlaid with loading buffer, and relative fluorescence intensities were determined at 535/25 nm at the GENios Pro microplate reader after excitation at 485/20 nm. The following cell quantification procedure was performed by analogy with the H33342 assay. The obtained mean fluorescence intensities were related to the controls and plotted against the various concentrations of test compounds. TECAN instrument settings: Measurement mode: fluorescence top; number of reads: 10; integration time: 40 µs; lag time: 0 µs; mirror selection: Dichroic 3 (e.g. Fl.); plate definition file: GRE96ft.pdf; multiple reads per well (Circle): 3x3; time between move and flash: 100 ms.

3.4.2.5 Hoechst 33342 microplate assay for the determination of ABCG2 inhibition

Optimal conditions of the assay were systematically determined as described elsewhere[30] with slight modifications. MCF-7/Topo cells were seeded into 96-well plates at a density of 20,000 cells/well (total volume: 100 mL) and allowed to attach to the surface of the microplates overnight in a water-saturated atmosphere (95% air, 5% CO2) at 37 °C. The next day, the culture medium was removed, and the cells were incubated with loading suspension (EMEM, supplemented as described above, and 0.8 µM Hoechst 33342) in combination with the test compound at increasing concentrations (10 nM-100 µM) for 2 h (37 °C, 5% CO_2). FTC at a final concentration of 10 µM served as reference compound;

under these conditions the response was defined as 100% inhibition of Hoechst 33342 efflux. The supernatants were drained and the cells were fixed for 30 min under light protection using 100 mL per well of a 4% PFA solution. Finally, MCF-7/Topo cells were washed with PBS (2x250 mL per well) to remove residual dye. Cells were overlaid with PBS (100 mL), and the fluorescence intensities were determined using a GENios Pro microplate reader (TECAN Deutschland GmbH, Crailsheim, Germany). Measurement mode: fluorescence top; excitation filter: 340/35 nm; emission filter: 485/20 nm; number of reads: 10; integration time: 40 ms; lag time: 0 ms; mirror selection: automatic; plate definition file: GRE96ft.pdf; multiple reads per well (circle, 3x3); time between move and flash: 50 ms. On each plate, the optimal gain was calculated by determination of the fluorescence intensity in the presence of the reference compound FTC. IC_{50} values were calculated using SIGMA PLOT 11.0, “four parameter logistic curve” fitting. Errors are expressed as standard error of the mean (SEM).

3.4.2.6 Chemical Stability in Eagle’s minimum essential medium (EMEM)

Stock solutions of the test compounds (3 mM) were prepared in DMSO. A 1:50 dilution of the substances in EMEM was prepared in 1.5-mL polypropylene reaction vessels (Eppendorf, Hamburg, Germany). The samples were shortly vortexed and incubated at 37 °C. At different periods of time, aliquots were taken, and the samples were mixing with two parts of ice-cold acetonitrile. For quantitative precipitation, the samples were vortexed and stored at 4 °C for 30 min. Finally, samples were centrifuged for 5 min at 14,000 g, using an Eppendorf MiniSpin plus centrifuge, and the supernatants were transferred into new reaction vessels. Prior to HPLC analysis, the samples were diluted (1:1) with acetonitrile and stored at -80 °C. Subsequent RP-HPLC analysis was performed with a analytical HPLC (1220 Infinity LC System from Agilent) with a reverse phase Phenomenex Luna® 3µ C18(2) 100A column (150 × 2.0 mm, 100 Å) at 30°C. HPLC conditions were the following: solvent A = water (Millipore)/TFA (0.05% v/v), solvent B = MeCN (Merck, gradient grade); flow rate = 0.3 mL/min; injection volume 100 µL, elution with a gradient of 10% to 95% MeCN in 30 min. UV-detection at 220 nm.

3.4.2.7 Solubility tests

A calibration curve for each compound was made using five concentrations solutions (1µM-10nM in DMSO) in the analytical HPLC (1220 Infinity LC System from Agilent) with a reverse phase Phenomenex Luna® 3µ C18(2) 100A column (150 × 2.0 mm, 100 Å) at 30°C. HPLC conditions were the following: solvent A = water (Millipore)/TFA (0.05% v/v), solvent B = MeCN (Merck, gradient grade); flow rate = 0.3 mL/min; injection volume 0.2 µL, elution with a gradient of 10% to 95% MeCN in 30 min. UV-detection at 220 nm. Stock solution of the test compounds (3 mM) for the stability assay was used for the measumerement of the solubility also the results for this solution. The area found in the HPLC chromatogram for each aliquot was introduced in the calibration curve equation and compared with the areas found in different periods of time.

3.4.2.8 Chemosensitivity assay

The assays were performed as described previously[26] with slight modifications. Briefly, 100 mL/well of a tumor cell suspension, yielding a density of 10-20 cells per microscopic field (Olympus, CK2, 320x), were seeded into 96-well plates and incubated overnight at 37 °C and 5% CO_2. The next day, 100 mL/well of fresh medium was added containing the test compounds in various concentrations or vehicle. In general, test compounds were added as 1000-fold concentrated feed solutions (16 wells per drug concentration). On every plate, untreated cells (solvent DMSO in a dilution of 1:1000) served as growth control (vehicle), cells treated with a reference cytostatic (vinblastine) as a positive control. Incubation of the cells was stopped after different periods of time by removal of medium and fixation with a solution of 2% glutardialdehyde (in PBS). All plates were stored at 4 °C until the end of the experiment and afterwards simultaneously stained with 100 mL/well of a 0.02% aq crystal violet solution for 20 min. The trays were rinsed with H_2O for 20 min in order to remove residual dye. Crystal violet bound by the fixed cells was extracted with 70% EtOH (180 mL/well) while shaking the microplates for 2-3 h. Absorbance (a parameter proportional to cell mass) was measured at 580 nm using the GENios Pro microplate reader.

3.5 References

.

1. Kraege S, Köhler SC, Wiese M. Acryloylphenylcarboxamides: A New Class of Breast Cancer Resistance Protein (ABCG2) Modulators. ChemMedChem 2016;11(21):2422-2435.
2. Mahapatra DK, Bharti SK, Asati V. Anti-cancer chalcones: Structural and molecular target perspectives. Eur J Med Chem 2015;98:69-114.
3. Zhou B, Xing C. Diverse Molecular Targets for Chalcones with Varied Bioactivities. Med Chem 2015;5(8):388.
4. Asif M. A review on recent advances and potential pharmacological activities of versatile chalchone molecule. Chem Int 2016;2(1):1-18.
5. Kakati D. Studies on new synthetic strategies towards the synthesis of some novel bioactive chalcone and derivatives [Doctoral thesis]. India: Dibrugarh University; 2012. 205 p.
6. Watanabe H, Ono M, Kimura H, Kagawa S, Nishii R, Fuchigami T, Haratake M, Nakayama M, Saji H. A dual fluorinated and iodinated radiotracer for PET and SPECT imaging of β-amyloid plaques in the brain. Bioorg Med Chem Lett 2011;21(21):6519-6522.
7. Divi MKP, Padakandla GR, Rao BN, Suresh DV; Google Patents, assignee. Process for the preparation of bazedoxifene acetate and intermediates thereof. U.S. patent 8,889,896. 2014.
8. Savjani KT, Gajjar AK, Savjani JK. Drug solubility: importance and enhancement techniques. ISRN pharm 2012;2012:1-10.
9. Mistry P, Stewart AJ, Dangerfield W, Okiji S, Liddle C, Bootle D, Plumb JA, Templeton D, Charlton P. In vitro and in vivo reversal of P-glycoprotein-mediated multidrug resistance by a novel potent modulator, XR9576. Cancer res 2001;61(2):749-758.
10. Kühnle M, Egger M, Müller C, Mahringer A, Bernhardt G, Fricker G, König B, Buschauer A. Potent and selective inhibitors of breast cancer resistance protein (ABCG2) derived from the p-glycoprotein (ABCB1) modulator tariquidar. J Med Chem 2009;52:1190-1197.
11. Obreque-Balboa JE, Sun Q, Bernhardt G, König B, Buschauer A. Flavonoid derivatives as selective ABCC1 modulators: synthesis and functional characterization. Eur J Med Chem 2016;109:124-133.
12. Burkhart C, Murray J, Isachenko N, Pajic M, Watt F, Flemming C, Smith J, Gurova K, Marshall G, Norris M. Reversan, a novel inhibitor of MRP1, increases the therapeutic index of conventional chemotherapeutic agents. Cancer Res 2008;68:3242-3242.
13. Burkhart CA, Watt F, Murray J, Pajic M, Prokvolit A, Xue C, Flemming C, Smith J, Purmal A, Isachenko N. Small molecule MRP1 inhibitor Reversan increases the therapeutic index of chemotherapy in mouse model of neuroblastoma. Cancer res 2009;69(16):6573.
14. Loukas YL, Vraka V, Gregoriadis G. Drugs, in cyclodextrins, in liposomes: a novel approach to the chemical stability of drugs sensitive to hydrolysis. Int J Pharm 1998;162(1):137-142.
15. Chaudhary A, Nagaich U, Gulati N, Sharma V, Khosa R, Partapur MU. Enhancement of solubilization and bioavailability of poorly soluble drugs by physical and chemical modifications: A recent review. J Adv Pharm Educ Res 2012;2(1):32-67.

16. Liversidge GG, Cundy KC. Particle size reduction for improvement of oral bioavailability of hydrophobic drugs: I. Absolute oral bioavailability of nanocrystalline danazol in beagle dogs. Int J Pharm 1995;125(1):91-97.
17. Tiwary AK. Modification of Crystal Habit and Its Role in Dosage Form Performance. Drug Dev Ind Pharm 2001;27(7):699-709.
18. Shiraki K, Takata N, Takano R, Hayashi Y, Terada K. Dissolution Improvement and the Mechanism of the Improvement from Cocrystallization of Poorly Water-soluble Compounds. Pharm Res 2008;25(11):2581-2592.
19. Leuner C, Dressman J. Improving drug solubility for oral delivery using solid dispersions. Eur J Pharm Biopharm 2000;50(1):47-60.
20. Tehler U, Fagerberg JH, Svensson R, Larhed M, Artursson P, Bergström CA. Optimizing solubility and permeability of a biopharmaceutics classification system (BCS) class 4 antibiotic drug using lipophilic fragments disturbing the crystal lattice. J Med Chem 2013;56(6):2690-2694.
21. Tommasini S, Raneri D, Ficarra R, Calabrò ML, Stancanelli R, Ficarra P. Improvement in solubility and dissolution rate of flavonoids by complexation with β-cyclodextrin. J Pharm Biomed Anal 2004;35(2):379-387.
22. Serajuddin A. Salt formation to improve drug solubility. Adv Drug Deliv Rev 2007;59(7):603-616.
23. Perrut M, Jung J, Leboeuf F. Enhancement of dissolution rate of poorly-soluble active ingredients by supercritical fluid processes: Part I: Micronization of neat particles. Int J Pharm 2005;288(1):3-10.
24. Milliken WJ, Leal LG. The influence of surfactant on the deformation and breakup of a viscous drop: The effect of surfactant solubility. J Colloid Interface Sci 1994;166(2):275-285.
25. Barreiro-Iglesias R, Bromberg L, Temchenko M, Hatton TA, Alvarez-Lorenzo C, Concheiro A. Pluronic-g-poly (acrylic acid) copolymers as novel excipients for site specific, sustained release tablets. Eur J Pharm Sci 2005;26(5):374-385.
26. Bernhardt G, Reile H, Birnböck H, Spruß T, Schönenberger H. Standardized kinetic microassay to quantify differential chemosensitivity on the basis of proliferative activity. J Cancer Res Clin Oncol 1992;118(1):35-43.
27. Glavinas H, Kis E, Pal A, Kovacs R, Jani M, Vagi E, Molnar E, Bánsághi S, Kele Z, Janáky T. ABCG2 (breast cancer resistance protein/mitoxantrone resistance-associated protein) ATPase assay: a useful tool to detect drug-transporter interactions. Drug Metab Dispos 2007;35(9):1533-1542.
28. Bakos E, Evers R, Szakács G, Tusnády GE, Welker E, Szabó K, de Haas M, van Deemter L, Borst P, Váradi A. Functional multidrug resistance protein (MRP1) lacking the N-terminal transmembrane domain. J Biol Chem 1998;273(48):32167-32175.
29. Evers R, Kool M, van Deemter L, Janssen H, Calafat J, Oomen L, Paulusma CC, Elferink RO, Baas F, Schinkel AH. Drug export activity of the human canalicular multispecific organic anion transporter in polarized kidney MDCK cells expressing cMOAT (MRP2) cDNA. J Clin Invest 1998;101(7):1310.
30. Kühnle M. Experimental therapy and detection of glioblastoma: investigation of nanoparticles, ABCG2 modulators and optical imaging of intracerebral xenografts [Doctoral thesis]. Regensburg: Regensburg University; 2010.

4 Resumen

El primer capítulo describe los moduladores específicos de la ABCG2 reportados hasta la fecha, La visión global puede facilitar el diseño racional de nuevos moduladores potentes y seguros. La proteína de resistencia al cáncer de mama (BCRP, ABCG2) es un miembro de la superfamilia de transportadores ATP-binding cassette (ABC) y fue descubierta recientemente. En la fisiología normal actúa como herramienta de desintoxicación en las barreras de los tejidos, pero en las células tumorales ABCG2 media la resistencia contra los fármacos citotóxicos estructuralmente no relacionados, resultando en resistencia a múltiples fármacos (MDR) y una quimioterapia ineficaz. La inhibición selectiva de ABCG2 podría ser una estrategia atractiva para eludir la resistencia a múltiples fármacos en el tratamiento contra el cáncer.

El segundo capítulo describe el diseño, síntesis y evaluación de la actividad inhibitoria de nuevas cetonas sobre la proteína de resistencia al cáncer de seno (ABCG2). La síntesis se lleva a cabo primero formando el enlace amida entre las acetofenonas y el ácido quináldico en presencia de trietilamina y cloruro de *p*-toluensulfonilo, seguido por una bromación en el carbono α a la cetona utilizando *N*-bromosuccinimida. El último paso es entonces una sustitución nucleofílica entre las tetrahidroisoquinolinas previamente sintetizadas y las cetonas bromadas para obtener el compuesto final. Esta serie fue activa sobre los transportadores ABC, especialmente sobre la ABCG2. El Compuesto **10c** fue comparable en potencia con la Fumitremorgina C y los compuestos **10e** y **10f** tuvieron los mayores efectos inhibitorios. Las cetonas sintetizadas fueron estables en EMEM después de 24 horas de incubación.

En el tercer capítulo se reporta la síntesis de una nueva serie de chalconas derivadas del tariquidar como moduladores de la proteína de resistencia al cáncer de seno (ABCG2). Compuestos reportados recientemente, como el UR-ME22-1 y el UR-COP78 fueron identificados como moduladores de la ABCG2 potentes y selectivos, pero bajo condiciones fisiológicas son hidrolizados por enzimas en el núcleo central. Para sustituir este fragmento lábil, se propone un reemplazo bioisostérico por una chalcona. La molécula final fue dividida en cuatro fragmentos para una fácil síntesis. El primer paso es obtener el enlace amida entre las aminoacetofenonas y el ácido quinaldico, adicionar las cadenas de etilen y trietilenglicol para mejorar la hidrofilicidad de los compuestos en las tetrahidroisoquinolinas y por último una condensación de Claisen-Schmidt. La chalcona **8d** fue la más potente de la serie con un potencial desarrollo futuro como modulador clínico de ABCG2.

5 Appendix: Chapter 2

a. Reagents and devices

Reagents and solvents

Reagents Commercial reagents were used as provided. Solvents were used in per analysis grade for reaction mixtures and industrial grade for chromatography.

Devices

Automated Flash chromatography

Purification by column chromatography was performed with a Biotage® Isolera™ Spektra One device. Silica gel 60 M (40-63 µM, Merck) for flash column chromatography was used.

Thin layer chromatography

Analytical TLC on silica gel coated alumina plates (MN TLC sheets ALUGRAM® Xtra SIL G/UV254) was used for monitoring reaction progress and product visualization was conducted with UV-light (254 and 366 nm), and staining with potassium permanganate or Ehrlich's reagent.3

Nuclear magnetic resonance spectroscopy

NMR spectra were recorded at room temperature on a Bruker Avance 9.4 Tesla (^{1}H: 400 MHz, ^{13}C: 101 MHz) spectrometer with a Nanobay console and a BBFOPlus broadband ATMA probe or a Bruker Avance 600 (^{1}H: 600.1 MHz, ^{13}C: 150 MHz) instrument. The chemical shifts were reported in δ [ppm] relative to tetramethylsilane as external standard according to IUPAC recommendations. The relative number of protons was determined by integration. Coupling constants J were reported in Hertz [Hz]. Abbreviations for the characterization of the signals: s=singlet, d=doublet, t=triplet, m=multiplet, dd=doublet of doublets, q=quartet.

Mass spectrometry

High resolution mass spectra were recorded with an Agilent Tech 6540 UHD Accurate Mass Q-TOF LC/MS spectrometer.

Infrared spectroscopy

IR-spectra were recorded with a spectrometer FTIR Nicolete iS 10 (Thermo Fisher Scientific). Scans of 50 readings were performed by spectrum; the data were recorded in units of transmitance. The accessory ATR (PIKE) was used with a diamond crystal and an incidence angle of 45 °; samples were analyzed with the software IRsolution.

Reversed phase high-performance liquid cromatography

Purification with preparative HPLC was performed on a system from Knauer (Berlin, Germany; 2x K-1800 pump, K-2001 detector @280 nm). Column: Nucleodur 100-5 C18 ec (250 × 21 mm, 5 µm, Macherey-Nagel, Düren, Germany). Solvents: millipore water (with 0.1 % (v/v) TFA) / acetonitrile (gradient grade). Flowrate: 15 mL/min at 26 °C. The products were collected manually, the acetonitrile was removed from the eluate under reduced pressure, and lyophilization furnished the corresponding TFA salts.

Analytical high-performance liquid cromatography

The purity of all final compounds (dissolved in DMSO) was determined by integration of the UV signal at 220 nm wavelength of an analytical HPLC (1220 Infinity LC System from Agilent) with a reverse phase Phenomenex Luna® 3µ C18(2) 100A column (150 × 2.0 mm, 100 Å) thermostatted at 40 °C. HPLC conditions were the following: solvent A = water (Millipore)/TFA (0.05% v/v), solvent B = MeCN (Merck, gradient grade); flow rate = 0.3 mL/min; injection volume 0.1 µL, elution with a gradient of 10% to 95% MeCN in 30 min.

a. Synthetic pathways

N-(3-(2-(6,7-dimethoxy-3,4-dihydroisoquinolin-2(1H)-yl)acetyl)phenyl)quinoline-2-carboxamide (176a)

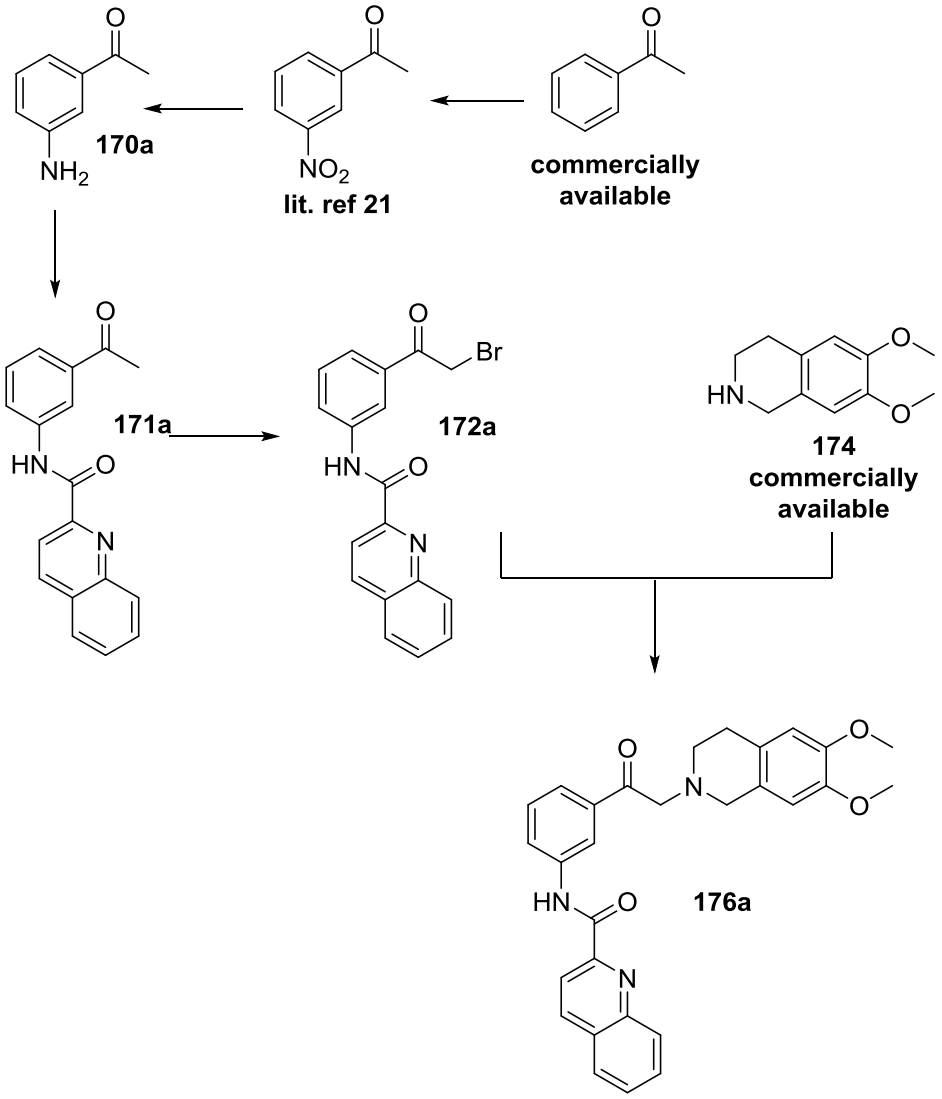

N-(3-(2-(6-methoxy-7-(2-methoxyethoxy)-3,4-dihydroisoquinolin-2(1H)-yl)acetyl)phenyl)quinoline-2-carboxamide (176b)

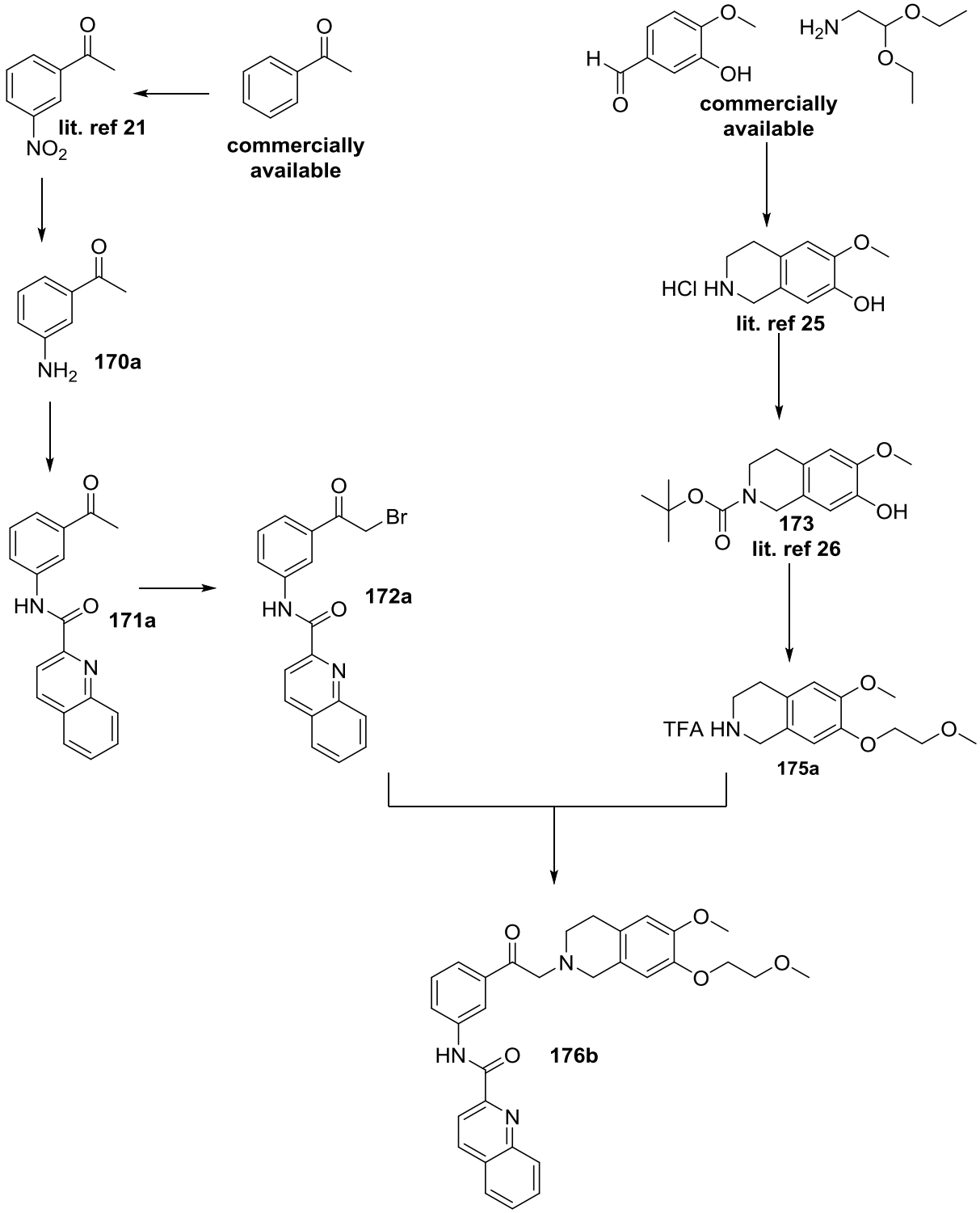

N-(3-(2-(6,7-bis(2-(2-(2-methoxyethoxy)ethoxy)ethoxy)-3,4-dihydroisoquinolin-2(1H)-yl)acetyl)phenyl)quinoline-2-carboxamide (176c)

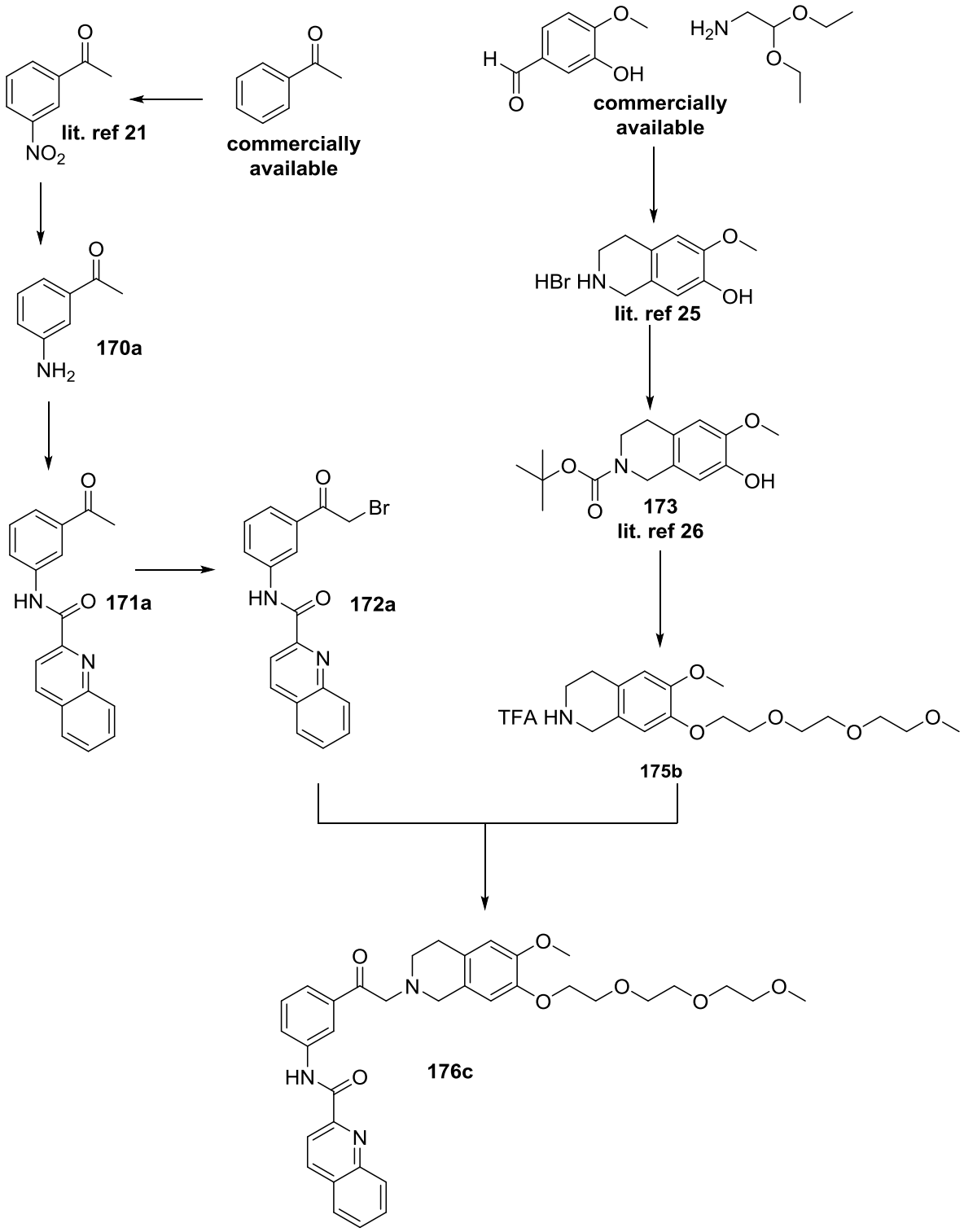

N-(5-(2-(6,7-dimethoxy-3,4-dihydroisoquinolin-2(1H)-yl)acetyl)-2-methylphenyl)quinoline-2-carboxamide (176d)

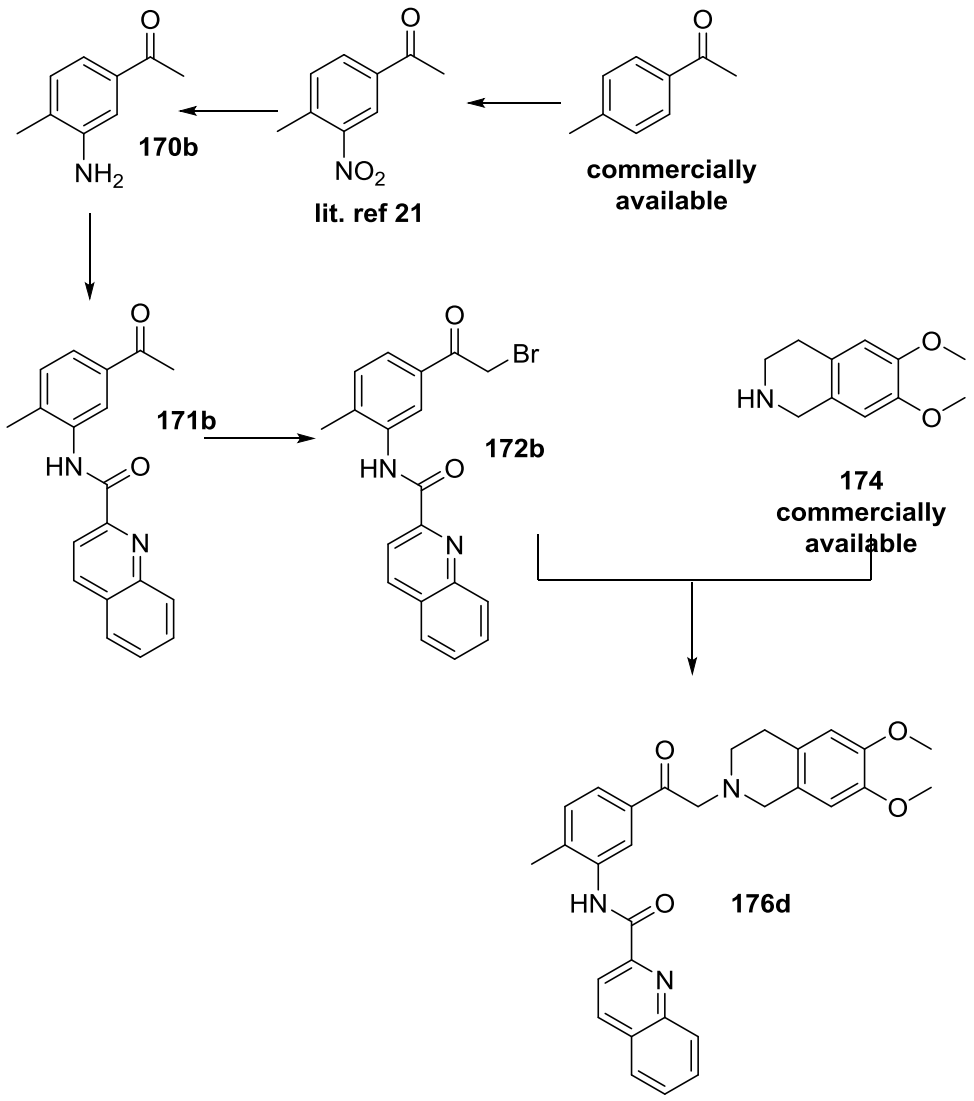

N-(3-(2-(6-methoxy-7-(2-methoxyethoxy)-3,4-dihydroisoquinolin-2(1H)-yl)acetyl)phenyl)quinoline-2-carboxamide (176e)

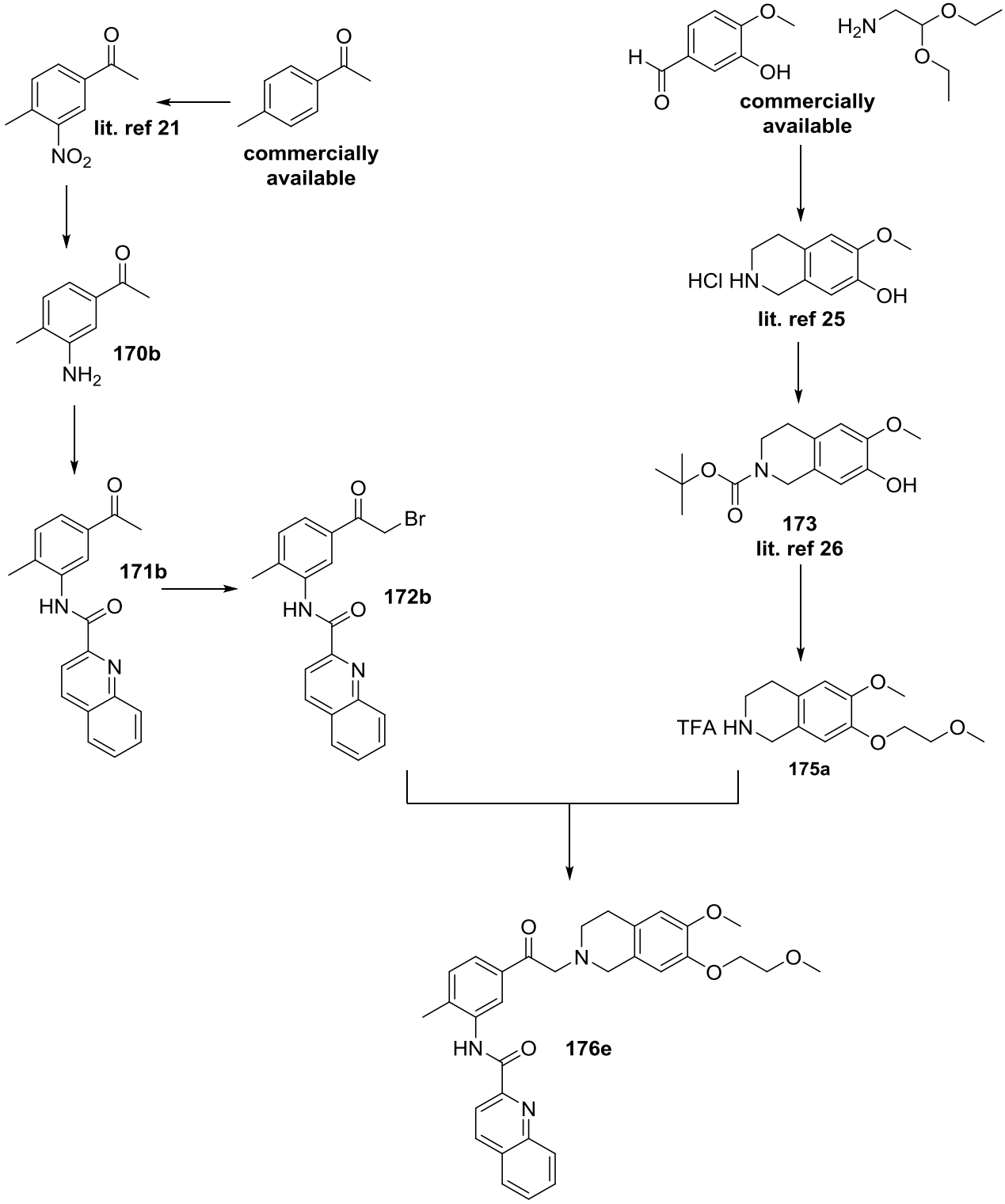

N-(5-(2-(6,7-bis(2-(2-(2-methoxyethoxy)ethoxy)ethoxy)-3,4-dihydroisoquinolin-2(1H)-yl)acetyl)-2-methylphenyl)quinoline-2-carboxamide (176f)

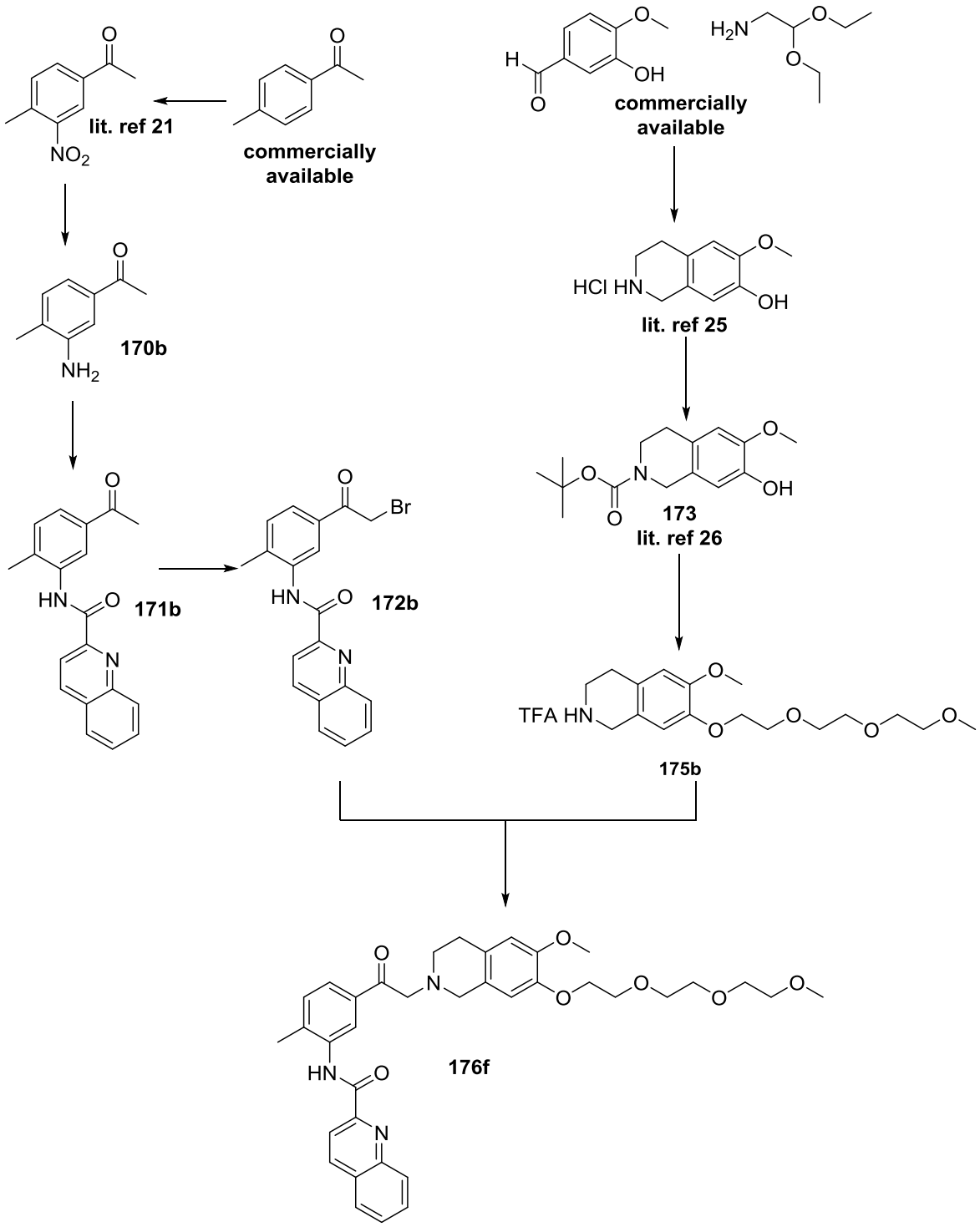

b. NMR spectra

N-(3-(2-bromoacetyl)phenyl)quinoline-2-carboxamide (172a)

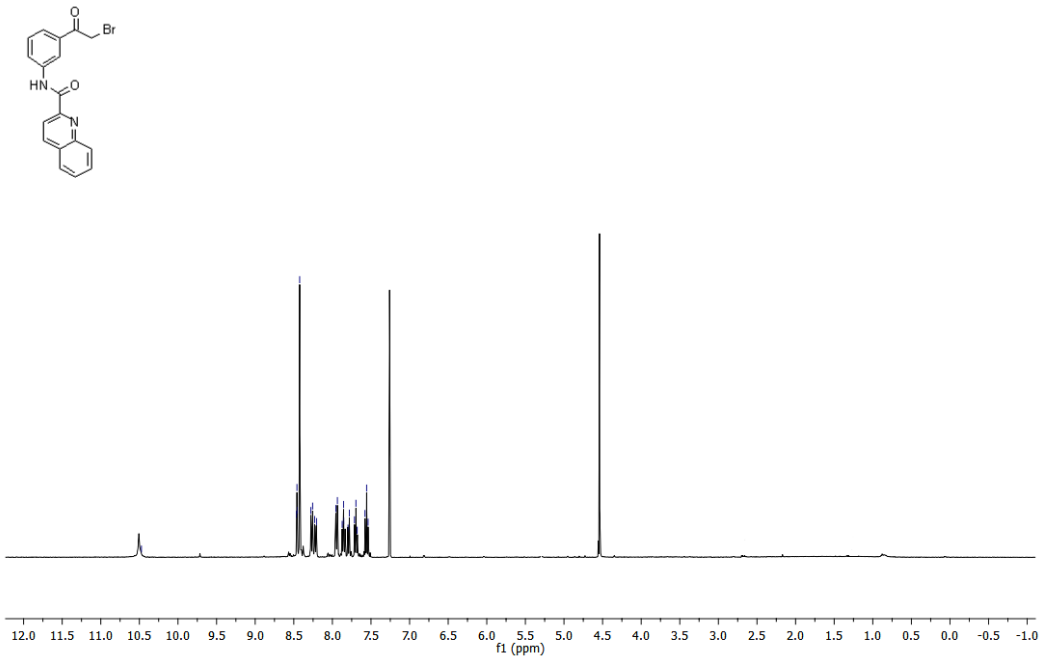

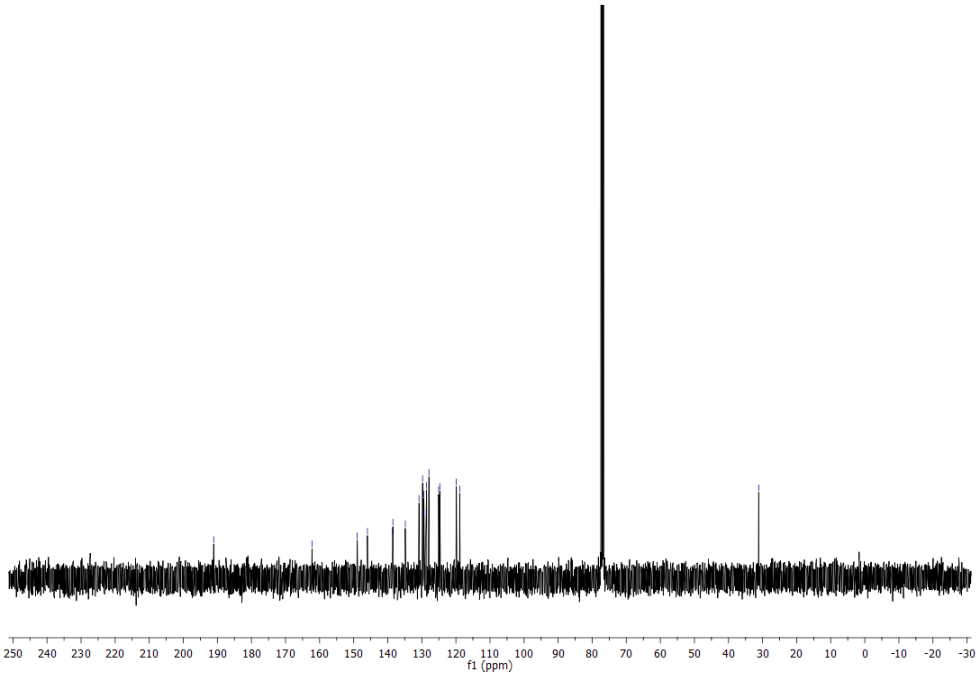

N-(5-(2-bromoacetyl)-2-methylphenyl)quinoline-2-carboxamide (172b)

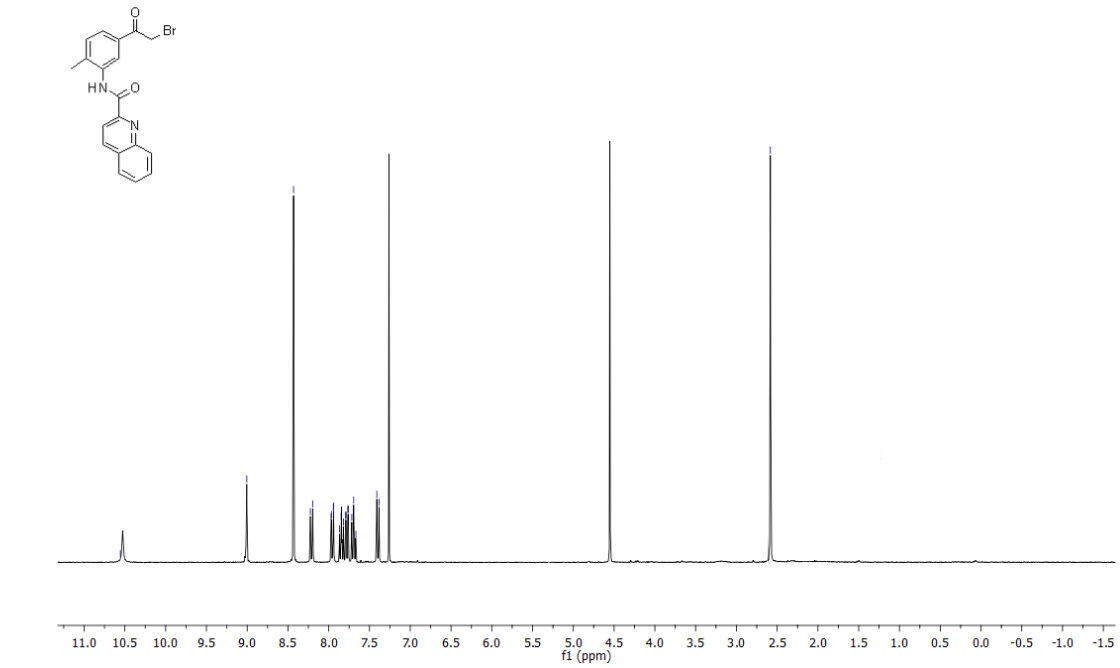

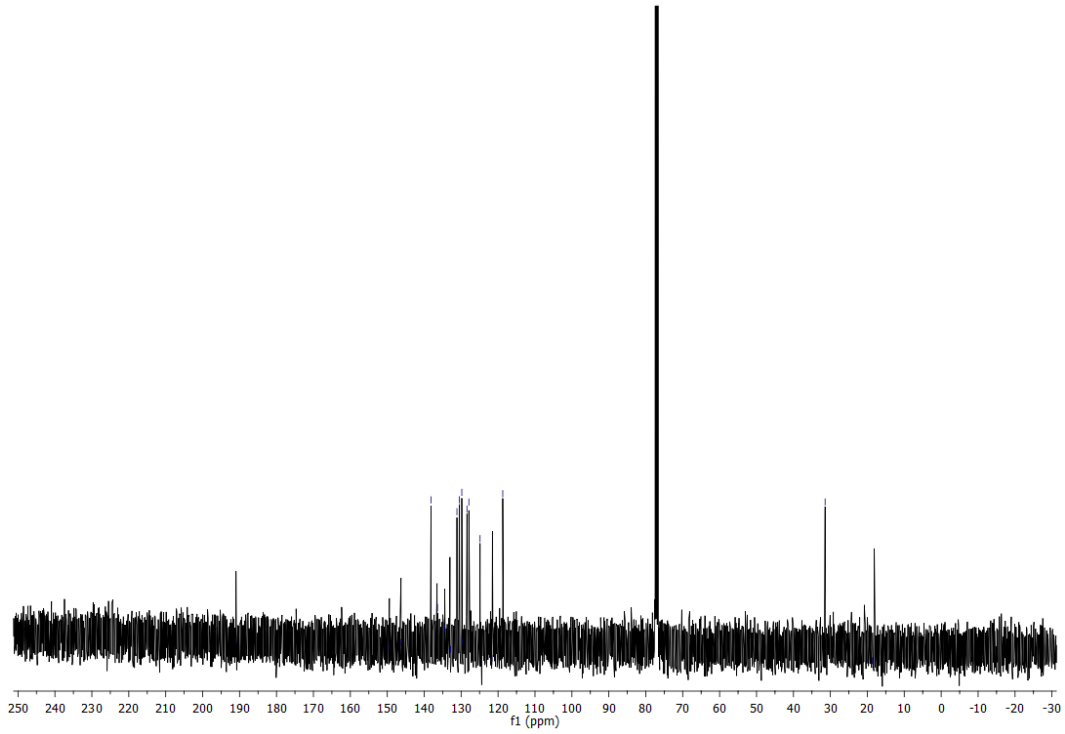

N-(3-(2-(6,7-dimethoxy-3,4-dihydroisoquinolin-2(1H)-yl)acetyl)phenyl)quinoline-2-carboxamide (176a)

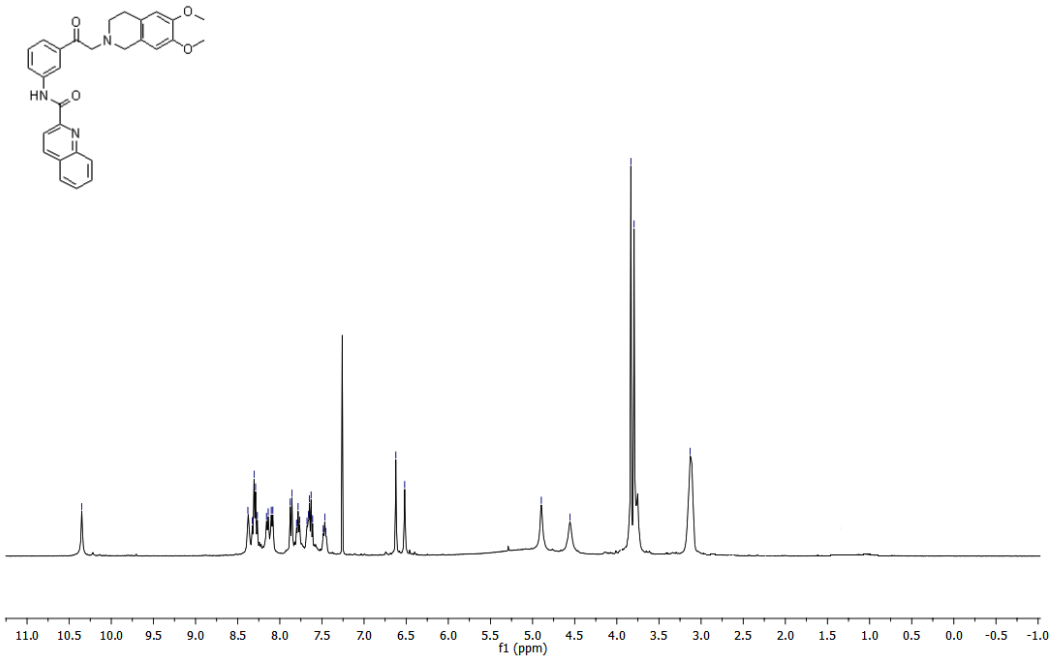

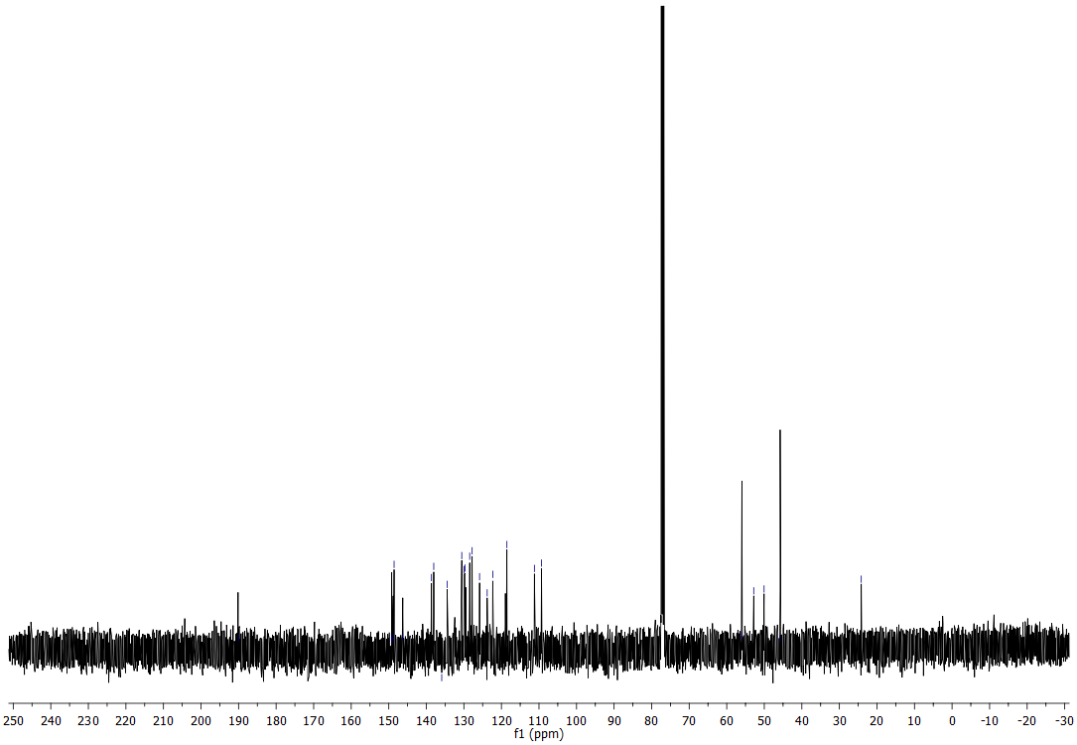

N-(3-(2-(6-methoxy-7-(2-methoxyethoxy)-3,4-dihydroisoquinolin-2(1H)-yl)acetyl)phenyl)quinoline-2-carboxamide (176b)

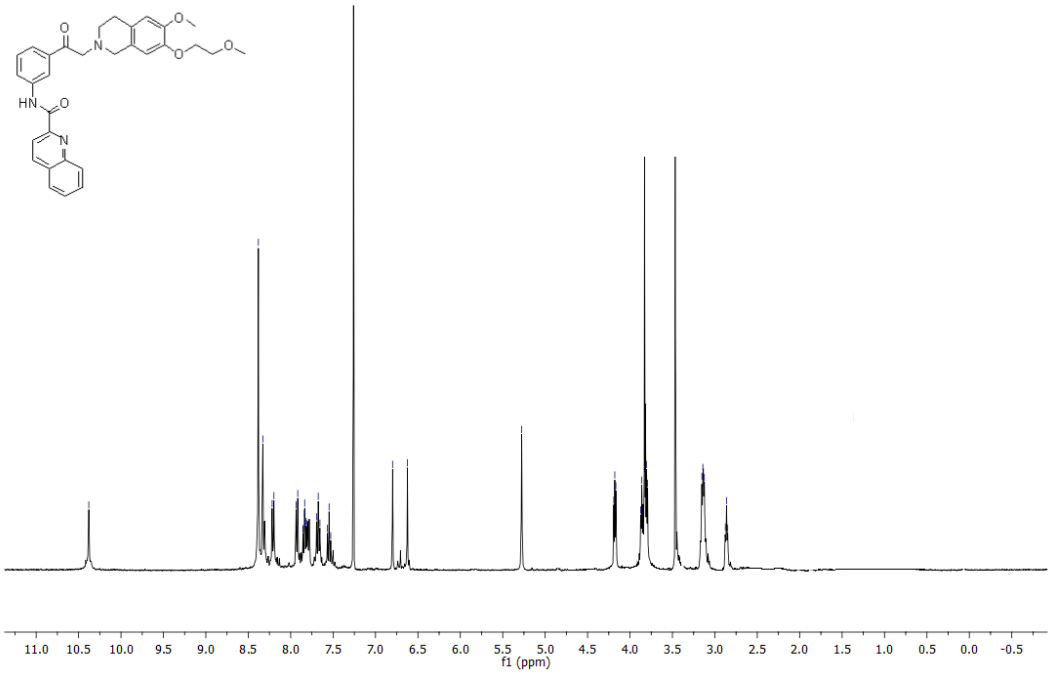

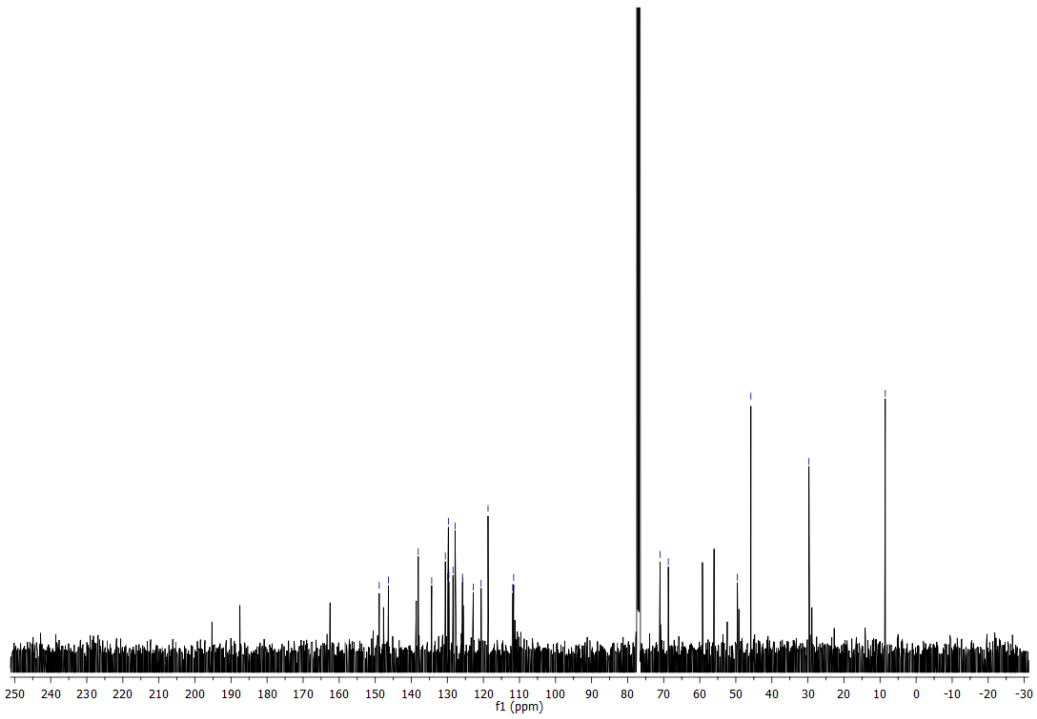

N-(3-(2-(6,7-bis(2-(2-(2-methoxyethoxy)ethoxy)ethoxy)-3,4-dihydroisoquinolin-2(1H)-yl)acetyl)phenyl)quinoline-2-carboxamide (176c)

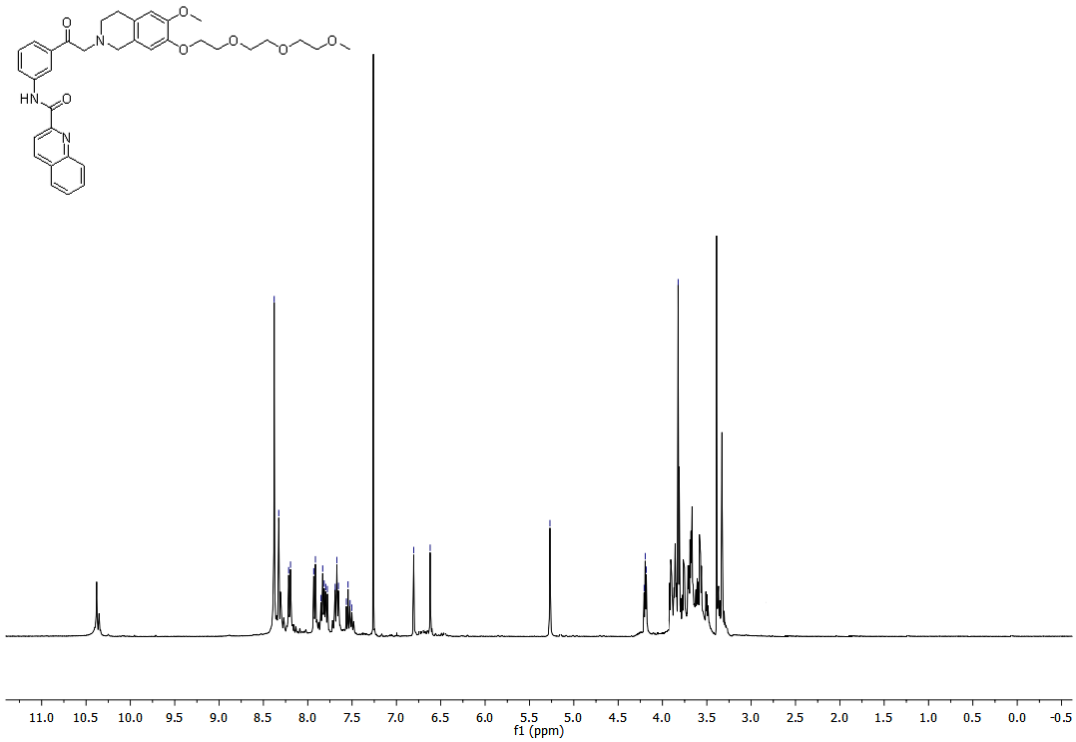

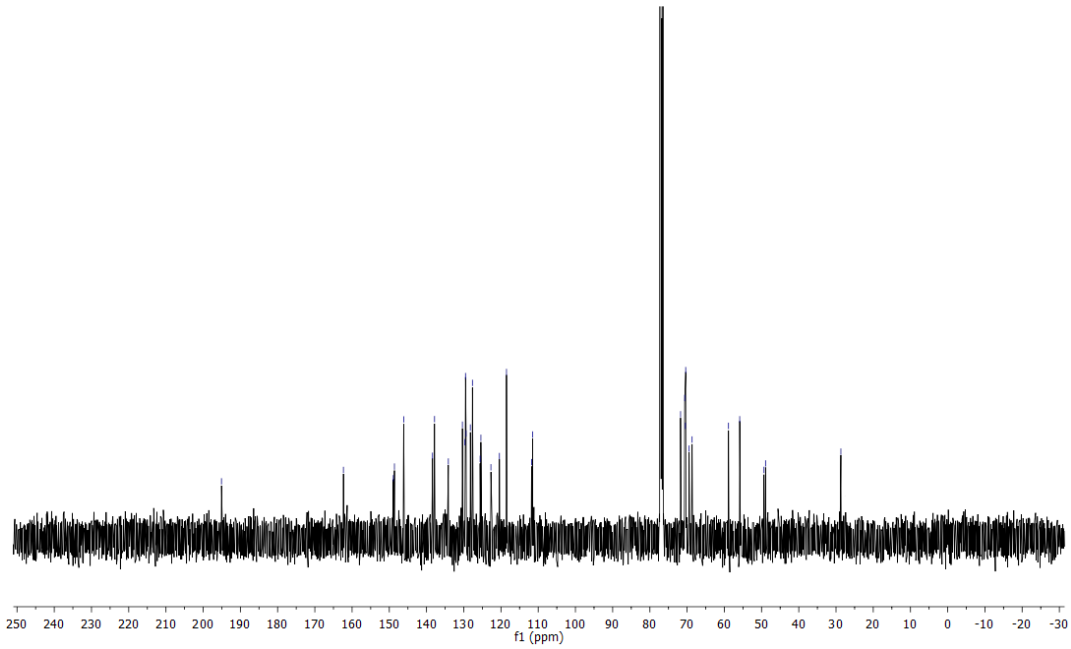

N-(5-(2-(6,7-dimethoxy-3,4-dihydroisoquinolin-2(1H)-yl)acetyl)-2-methylphenyl)quinoline-2-carboxamide (176d)

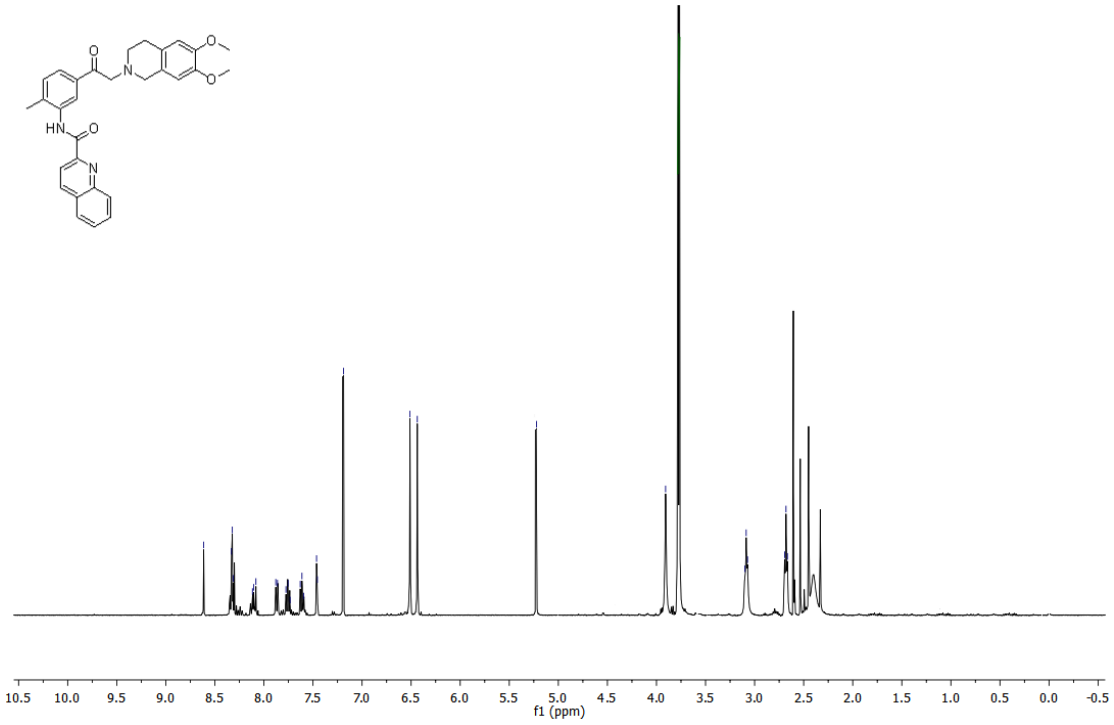

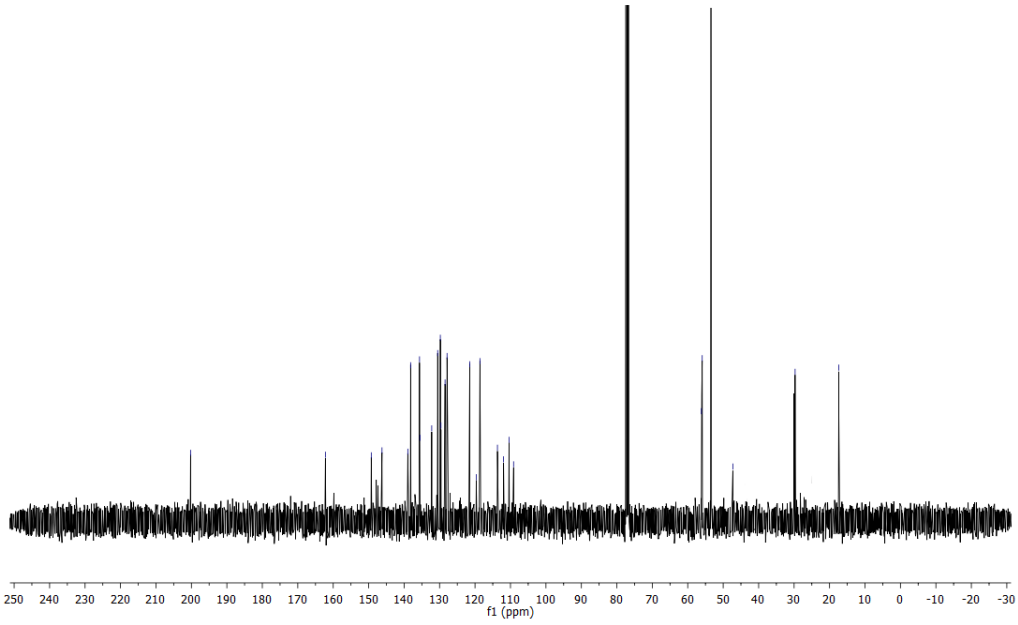

N-(3-(2-(6-methoxy-7-(2-methoxyethoxy)-3,4-dihydroisoquinolin-2(1H)-yl)acetyl)phenyl)quinoline-2-carboxamide (176e)

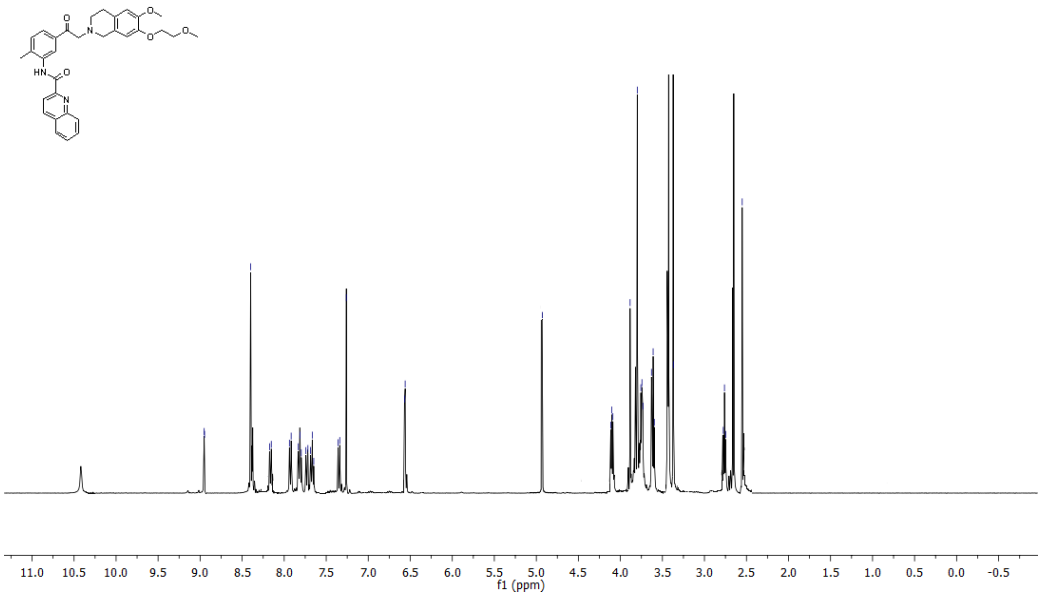

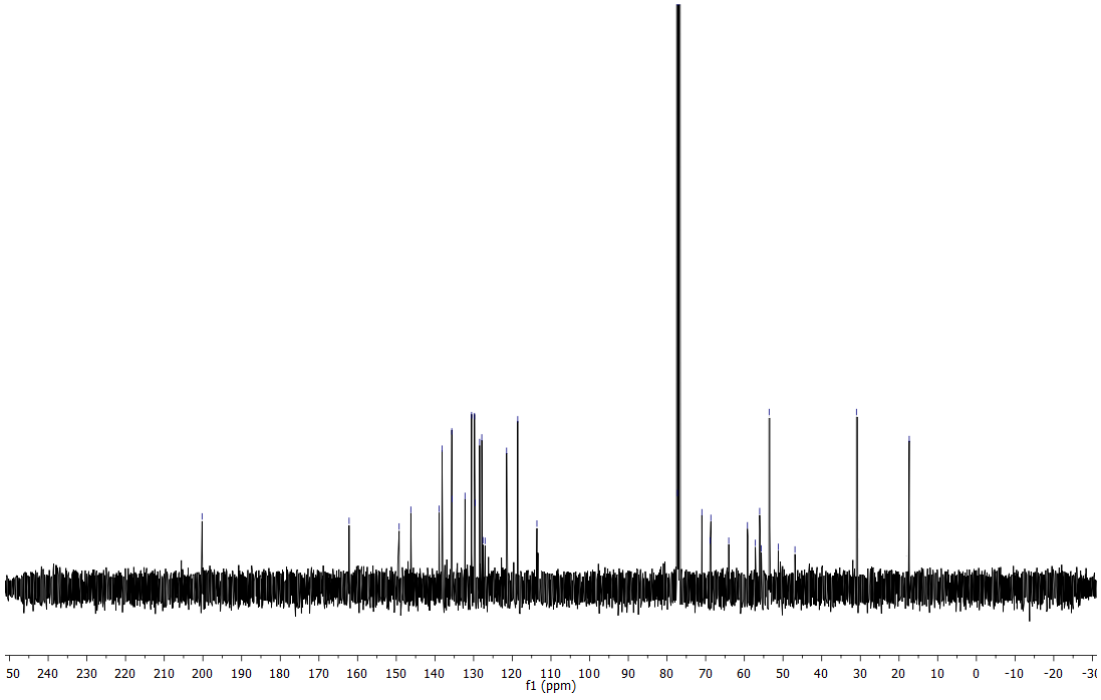

N-(5-(2-(6,7-bis(2-(2-(2-methoxyethoxy)ethoxy)ethoxy)-3,4-dihydroisoquinolin-2(1H)-yl)acetyl)-2-methylphenyl)quinoline-2-carboxamide (176f)

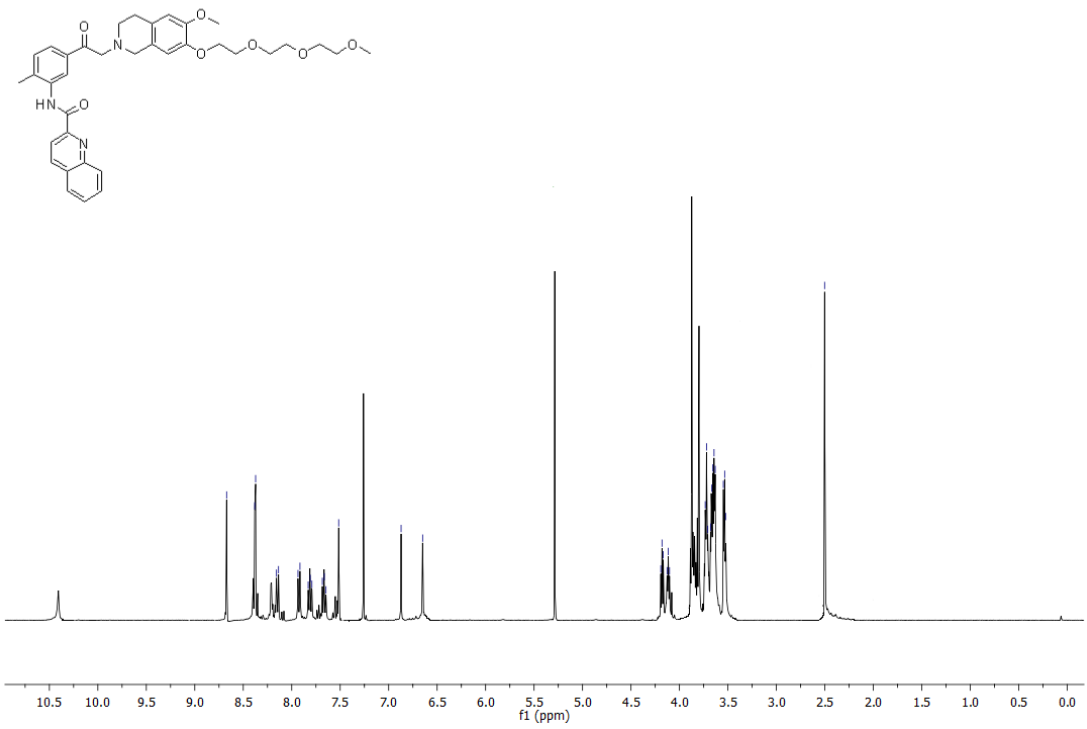

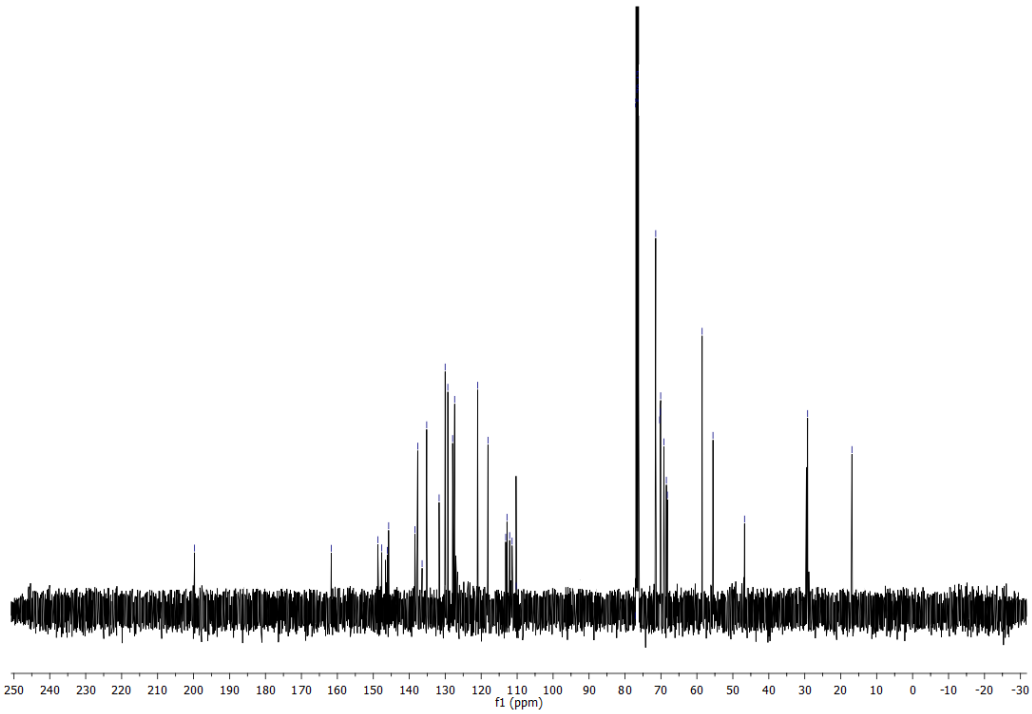

c. HPLC Analysis

Table 5-1 Purities of key compounds

Compound	Purity (%)	Retention time (min)
176a	95	14.069
176b	97	13.932
176c	95	13.885
176d	95	15.142
176e	97	15.004
176f	95	14.953

Compound **176a** in DMSO, 0.1 µL injected; Detector: 220 nm

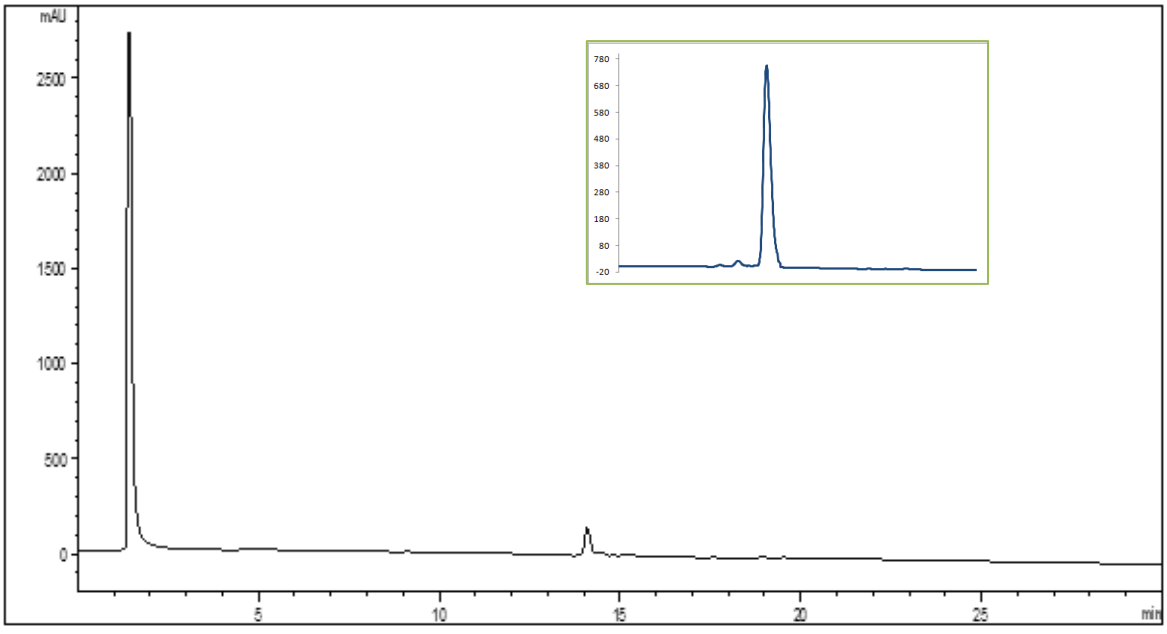

Compound **176b** in DMSO, 0.1 µL injected; Detector: 220 nm

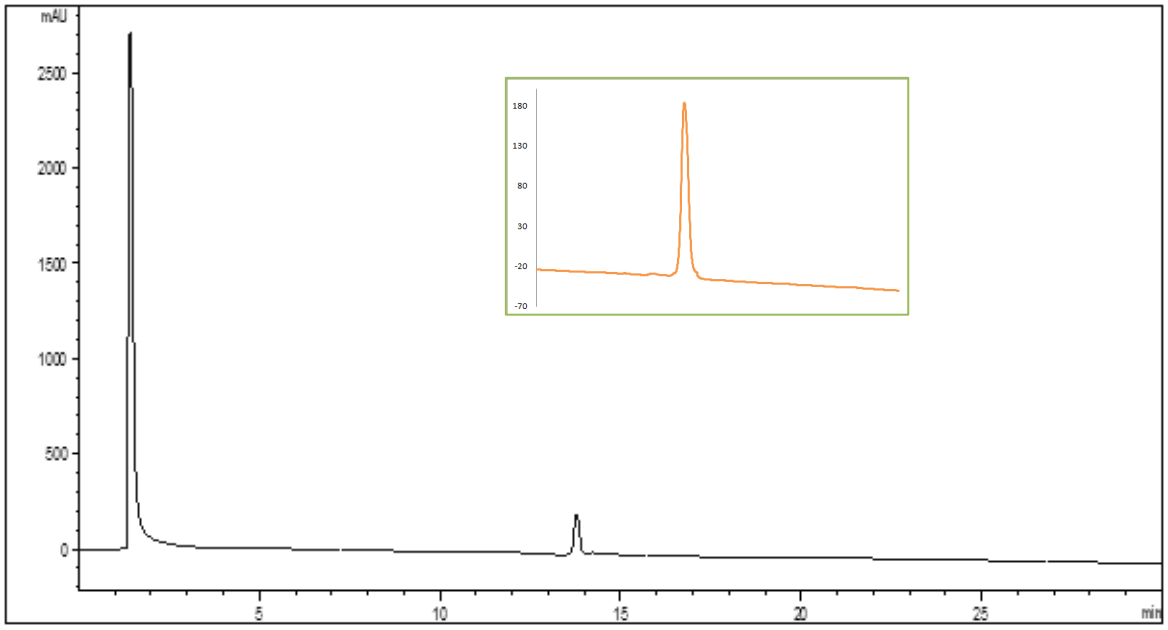

Compound **176c** in DMSO, 0.1 µL injected; Detector: 220 nm

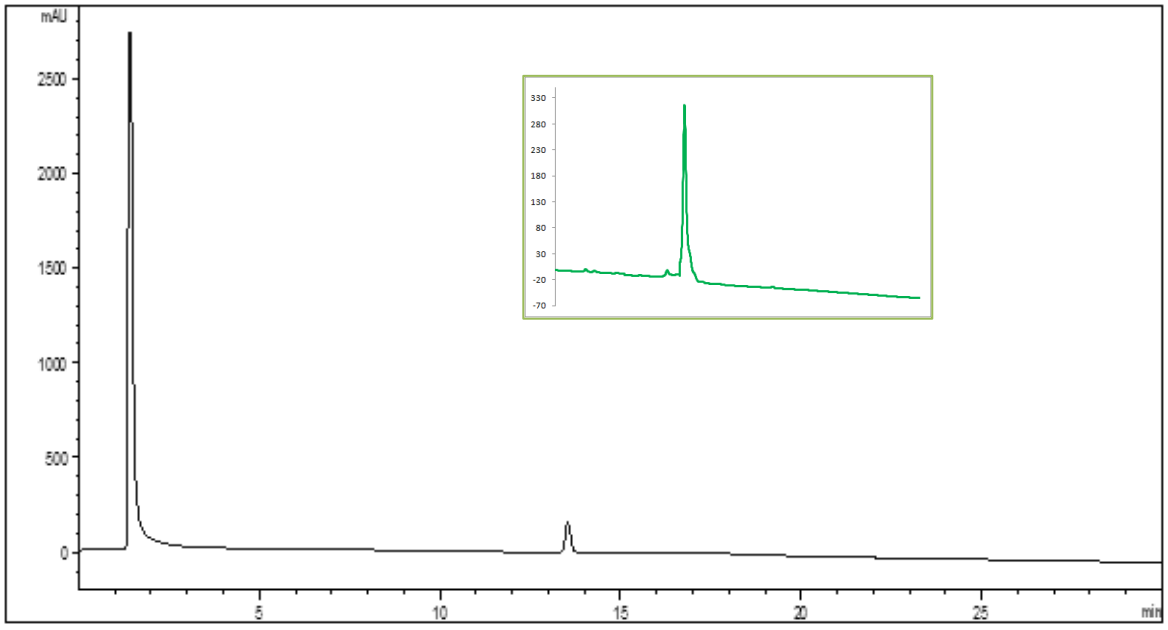

Compound **176d** in DMSO, 0.1 µL injected; Detector: 220 nm

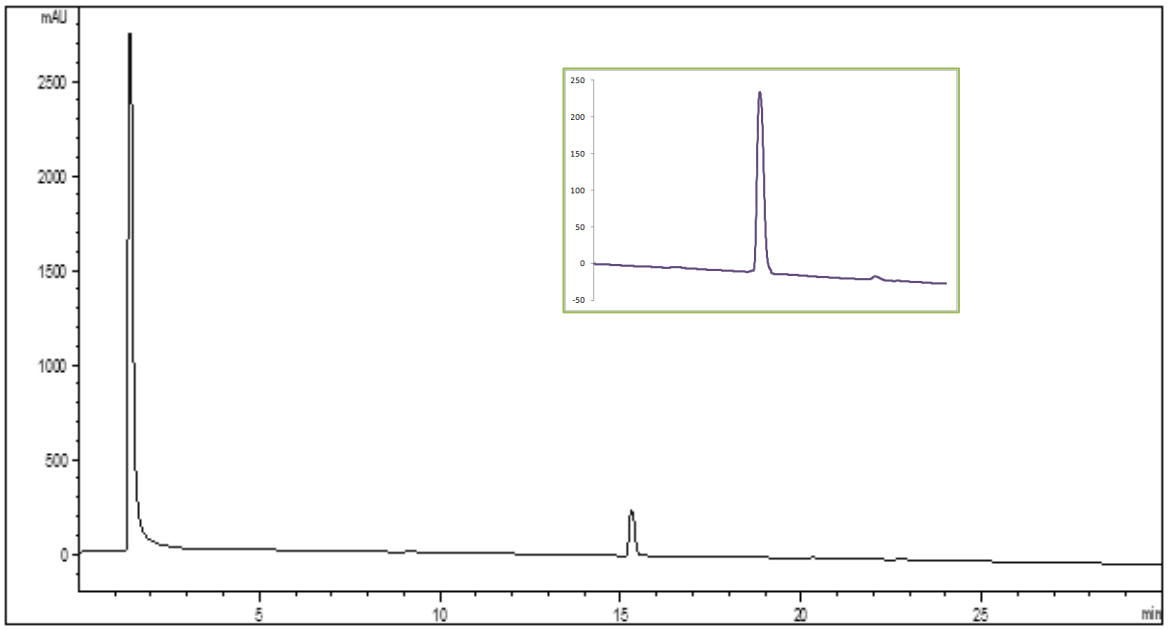

Compound **176e** in DMSO, 0.1 µL injected; Detector: 220 nm

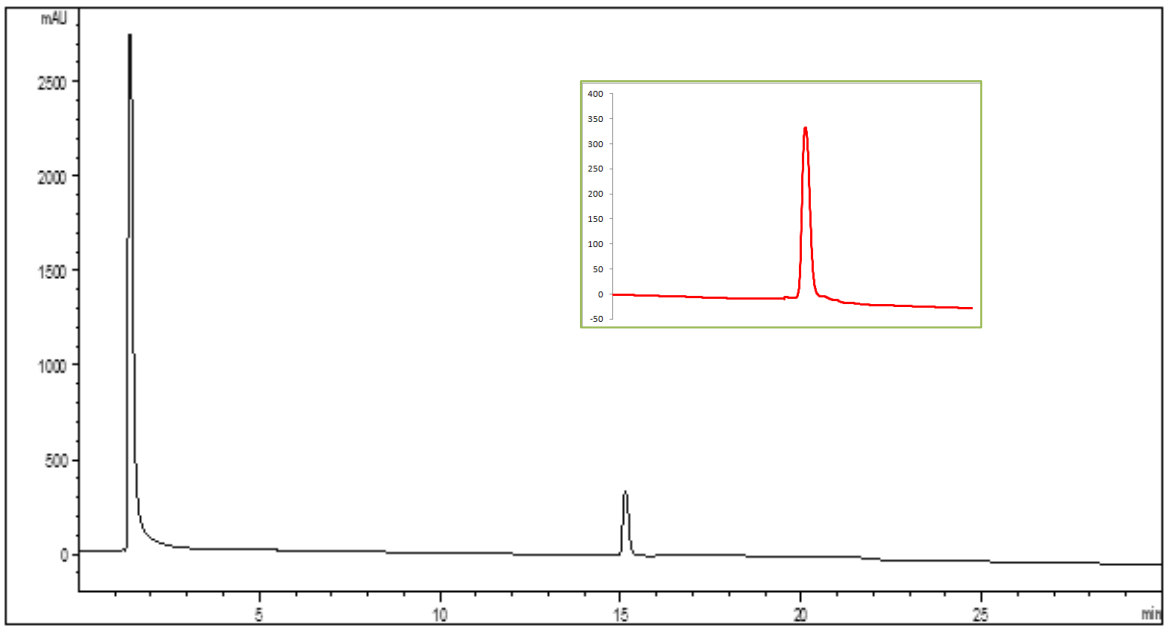

Compound **176f** in DMSO, 0.1 µL injected; Detector: 220 nm

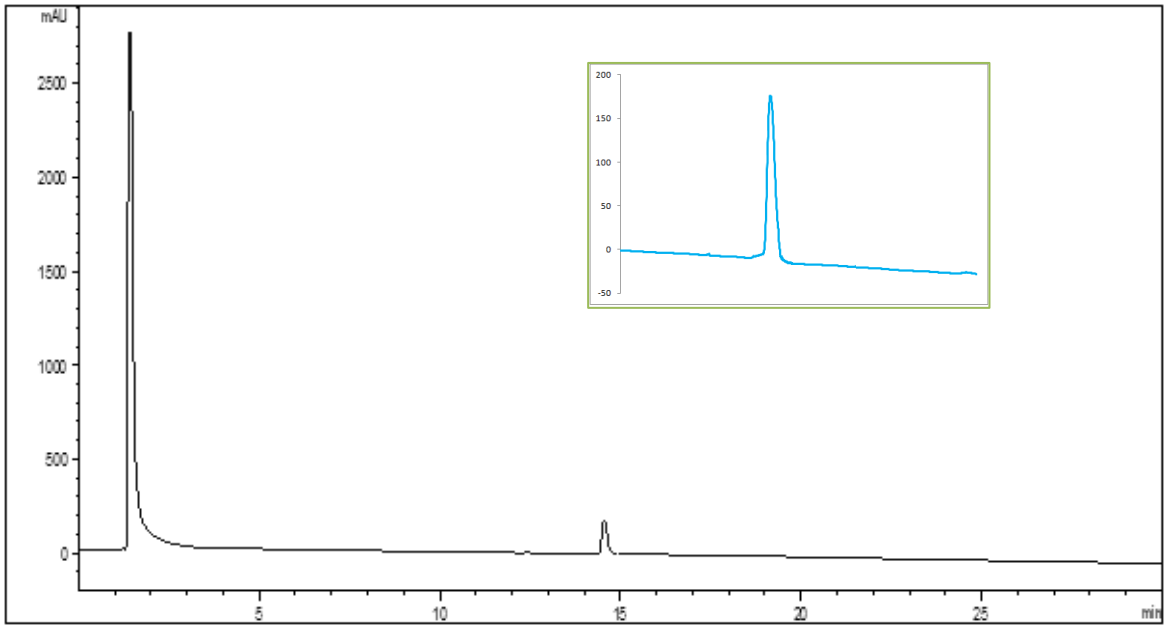

6 Appendix: Chapter 3

b. Synthetic pathways

(E)-N-(3-(3-(4-(2-(6,7-dimethoxy-3,4-dihydroisoquinolin-2(1H)-yl)ethoxy)phenyl)acryloyl)phenyl)quinoline-2-carboxamide (179a)

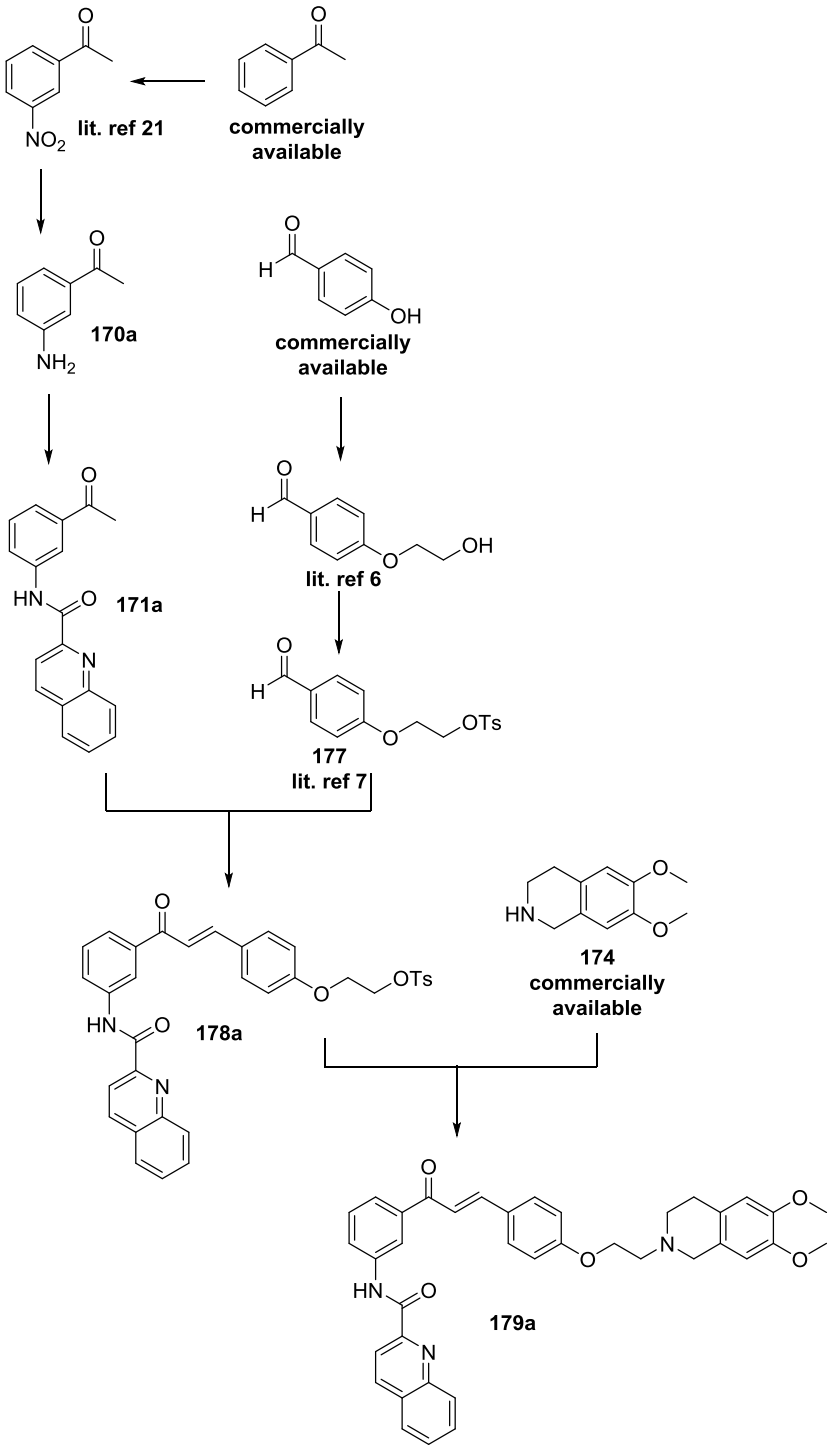

(E)-N-(3-(3-(4-(2-(6-methoxy-7-(2-methoxyethoxy)-3,4-dihydroisoquinolin-2(1H)-yl)ethoxy)phenyl)acryloyl)phenyl)quinoline-2-carboxamide (179b)

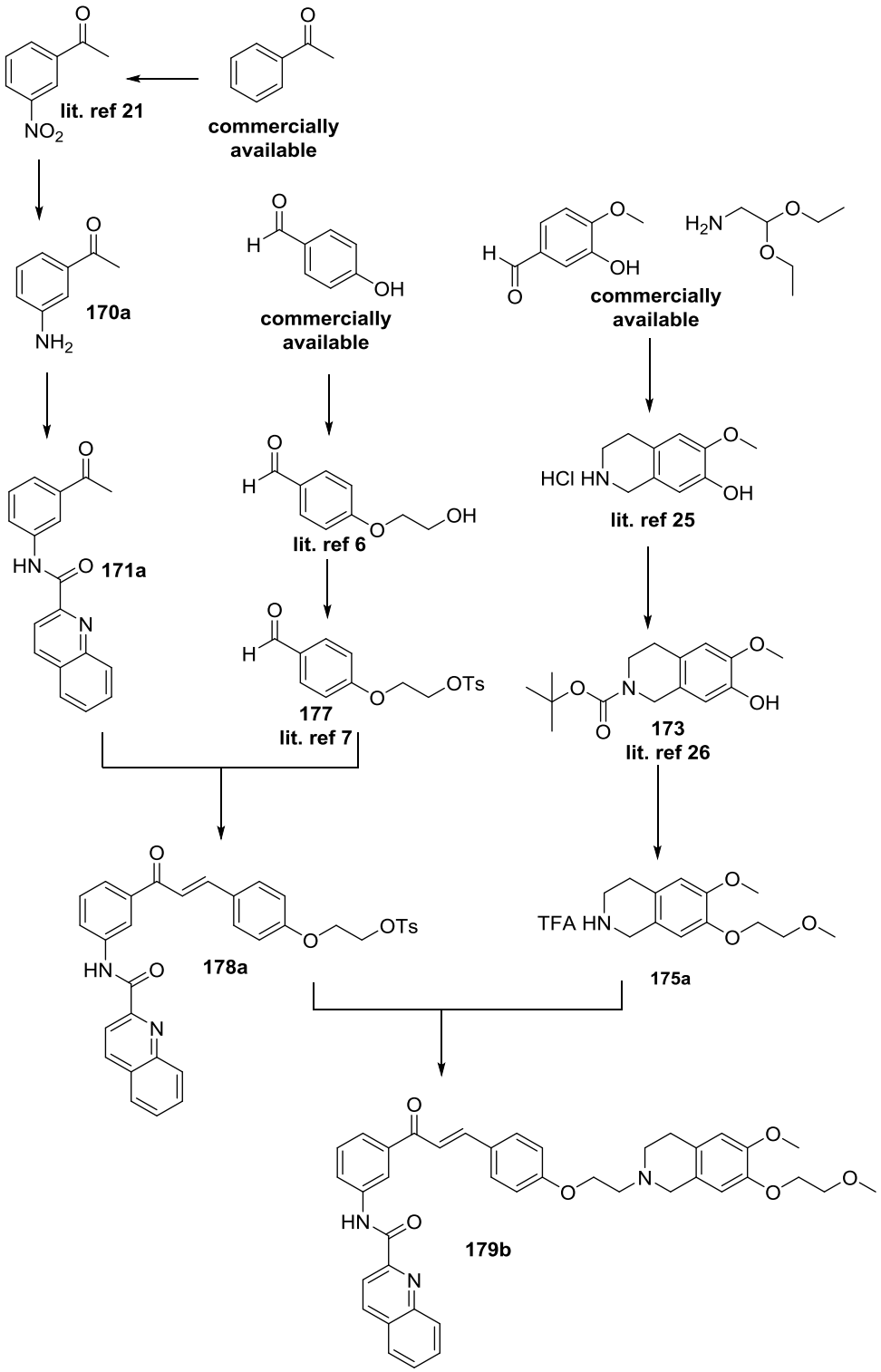

(E)-N-(3-(3-(4-(2-(6,7-bis(2-(2-(2-methoxyethoxy)ethoxy)ethoxy)-3,4-dihydroisoquinolin-2(1H)-yl)ethoxy)phenyl)acryloyl)phenyl)quinoline-2-carboxamide (179c)

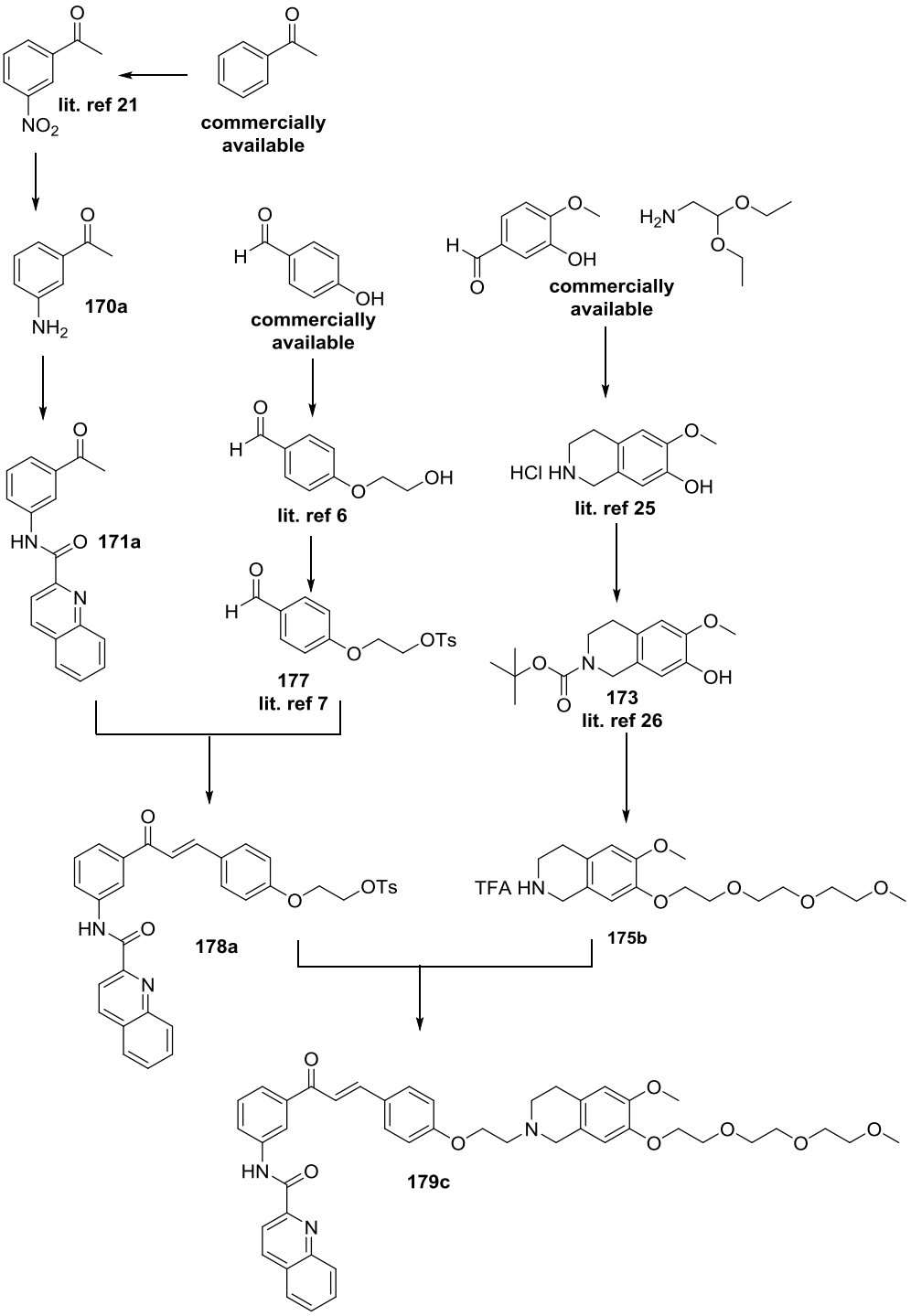

(E)-N-(5-(3-(4-(2-(6,7-dimethoxy-3,4-dihydroisoquinolin-2(1H)-yl)ethoxy)phenyl)acryloyl)-2-methylphenyl)quinoline-2-carboxamide (179d)

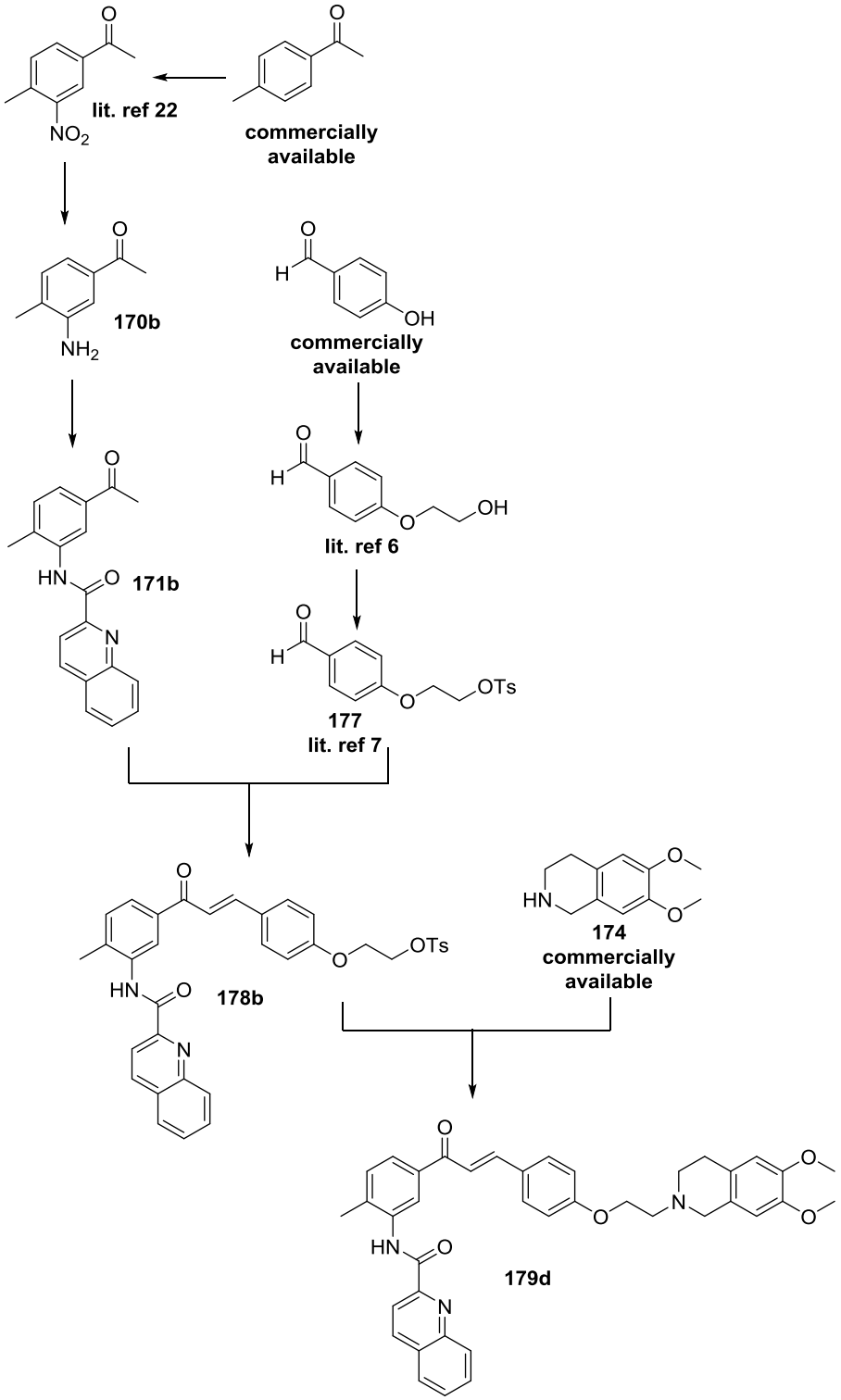

(E)-N-(5-(3-(4-(2-(6,7-bis(2-methoxyethoxy)-3,4-dihydroisoquinolin-2(1H)-yl)ethoxy)phenyl)acryloyl)-2-methylphenyl)quinoline-2-carboxamide (179e)

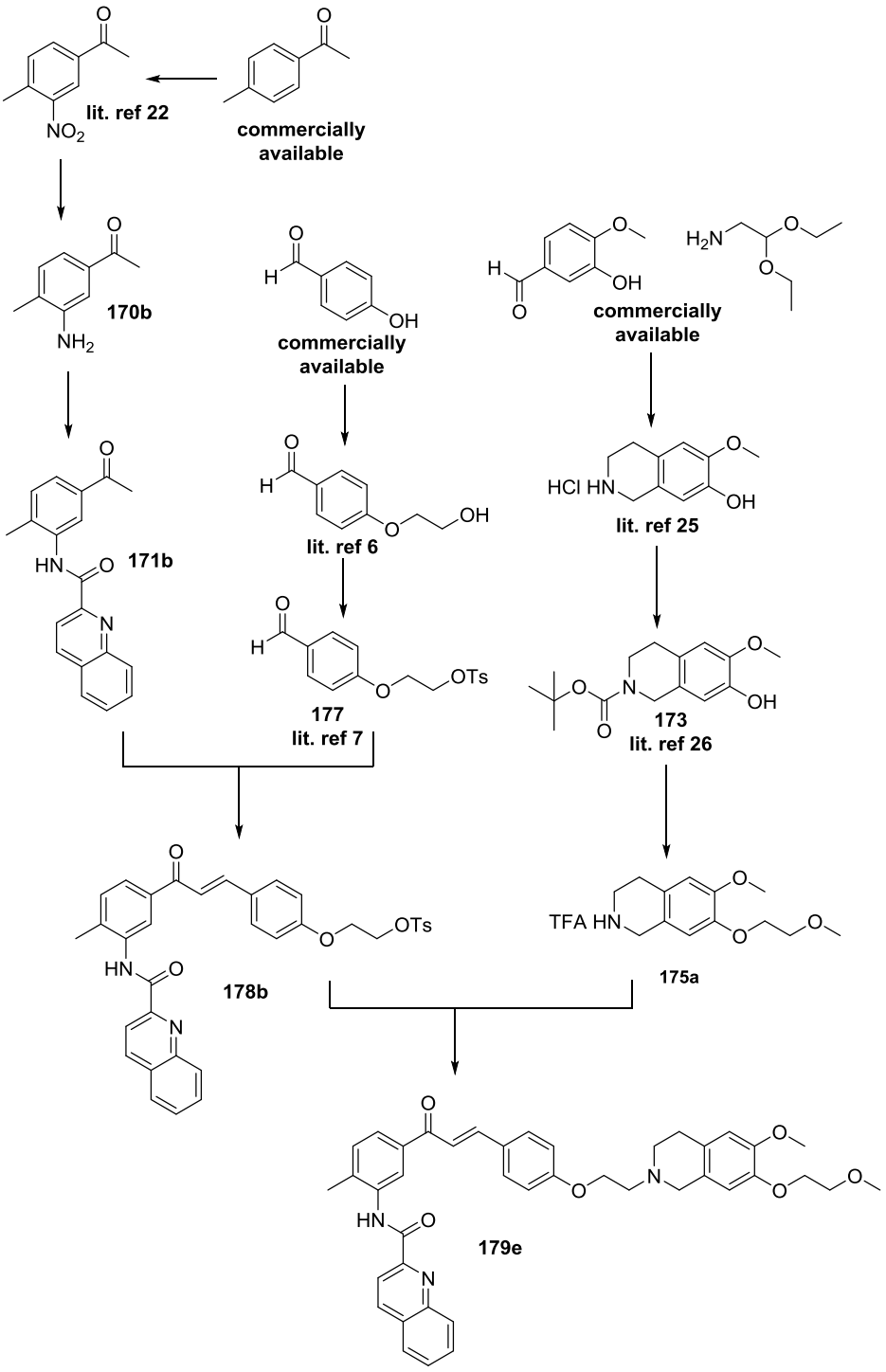

(E)-N-(5-(3-(4-(2-(6,7-bis(2-(2-(2-methoxyethoxy)ethoxy)ethoxy)-3,4-dihydroisoquinolin-2(1H)-yl)ethoxy)phenyl)acryloyl)-2-methylphenyl)quinoline-2-carboxamide (179f)

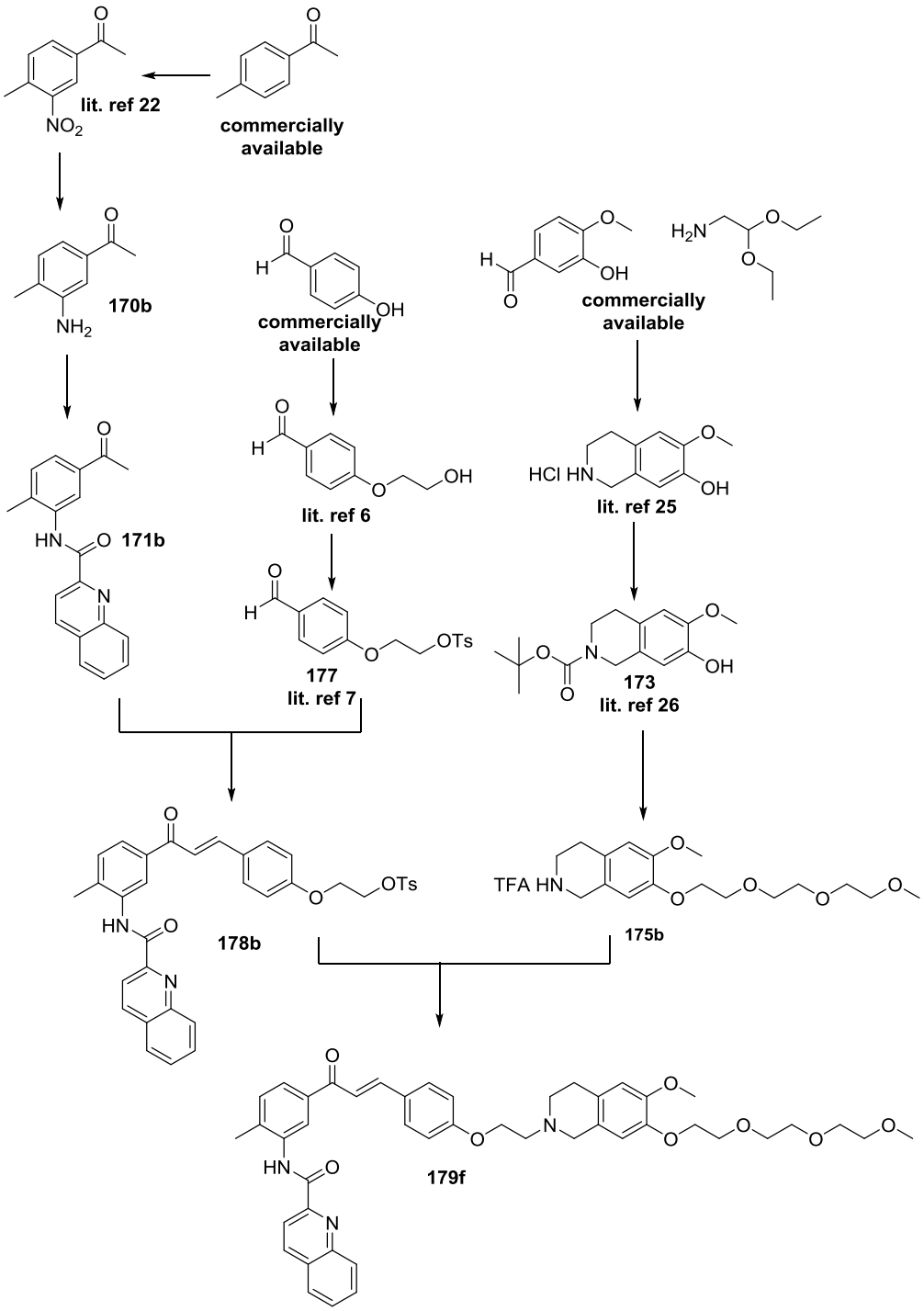

c. NMR spectra

N-(3-acetylphenyl)quinoline-2-carboxamide (171a)

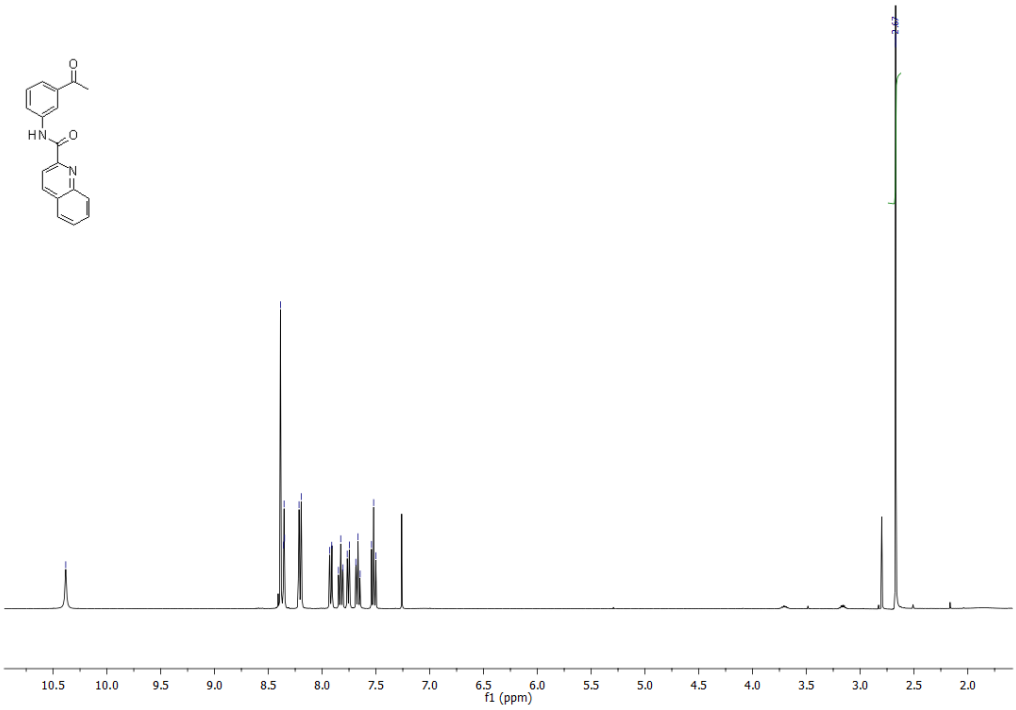

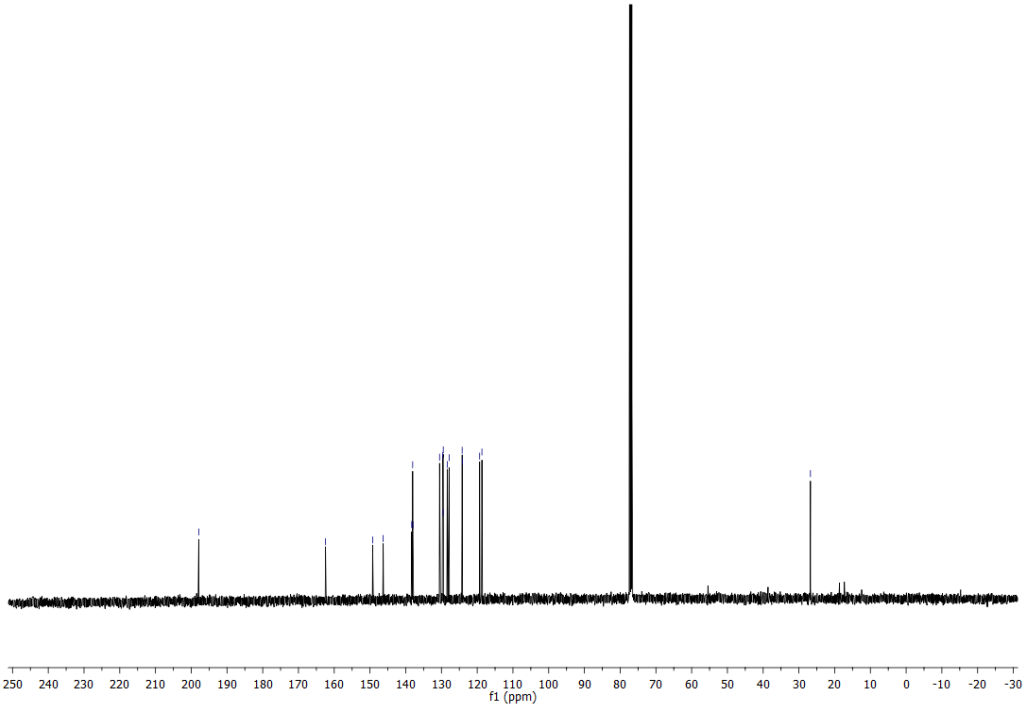

N-(5-acetyl-2-methylphenyl)quinoline-2-carboxamide (171b)

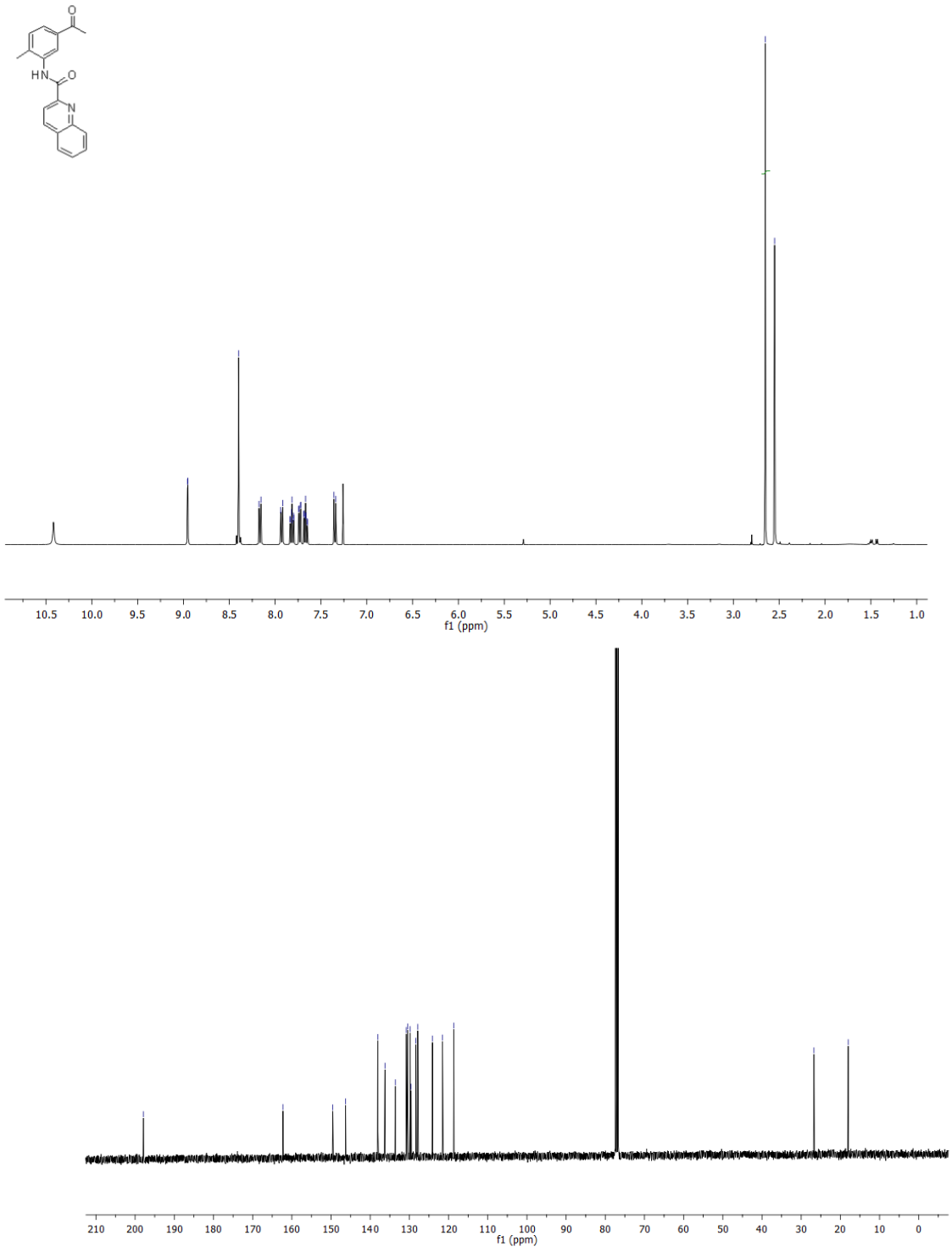

6-methoxy-7-(2-methoxyethoxy)-1,2,3,4-tetrahydroisoquinoline 2,2,2-Trifluoroacetate (175a)

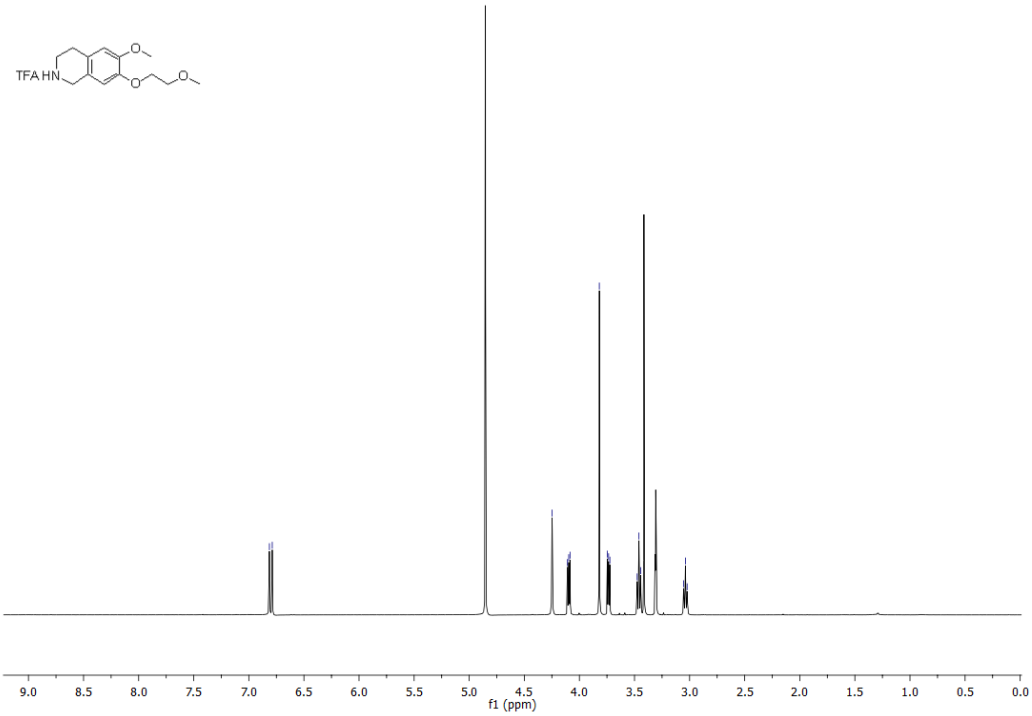

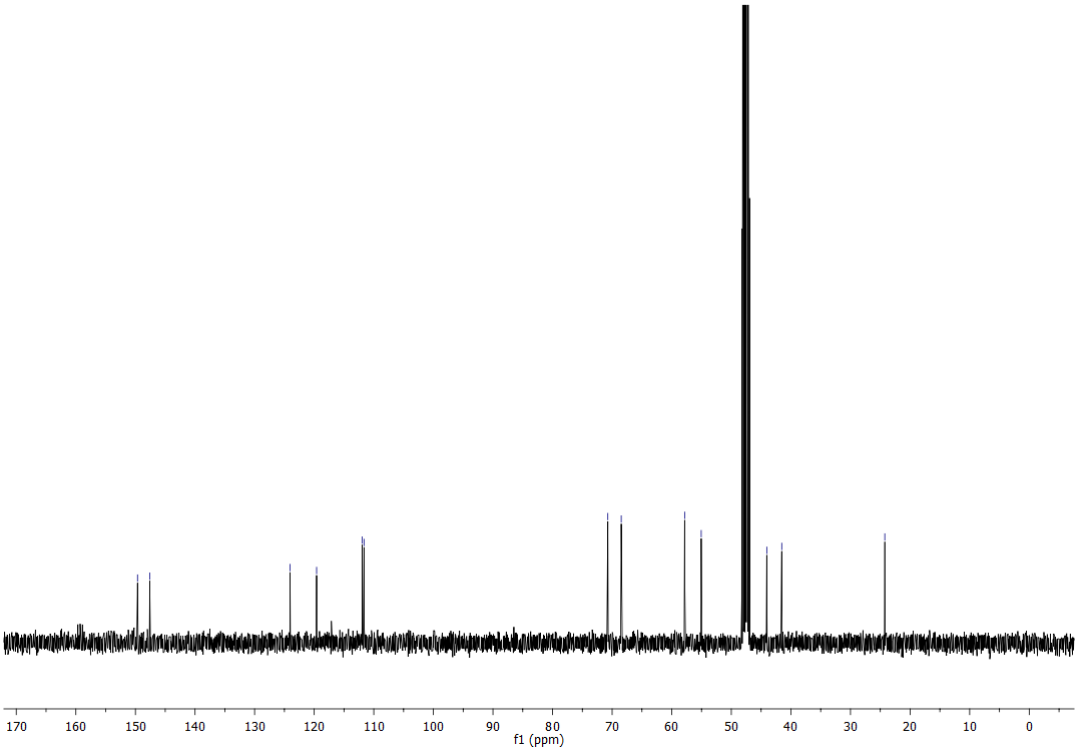

(E)-2-(4-(3-oxo-3-(3-(quinoline-2-carboxamido)phenyl)prop-1-en-1-yl)phenoxy)ethyl 4-methylbenzenesulfonate (178a)

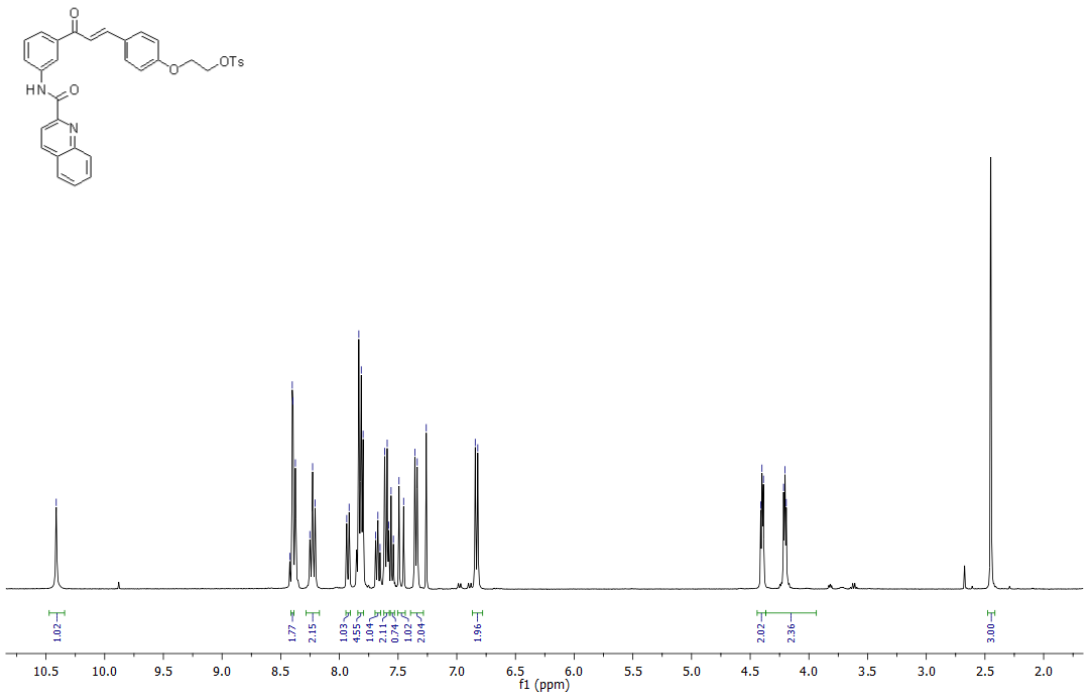

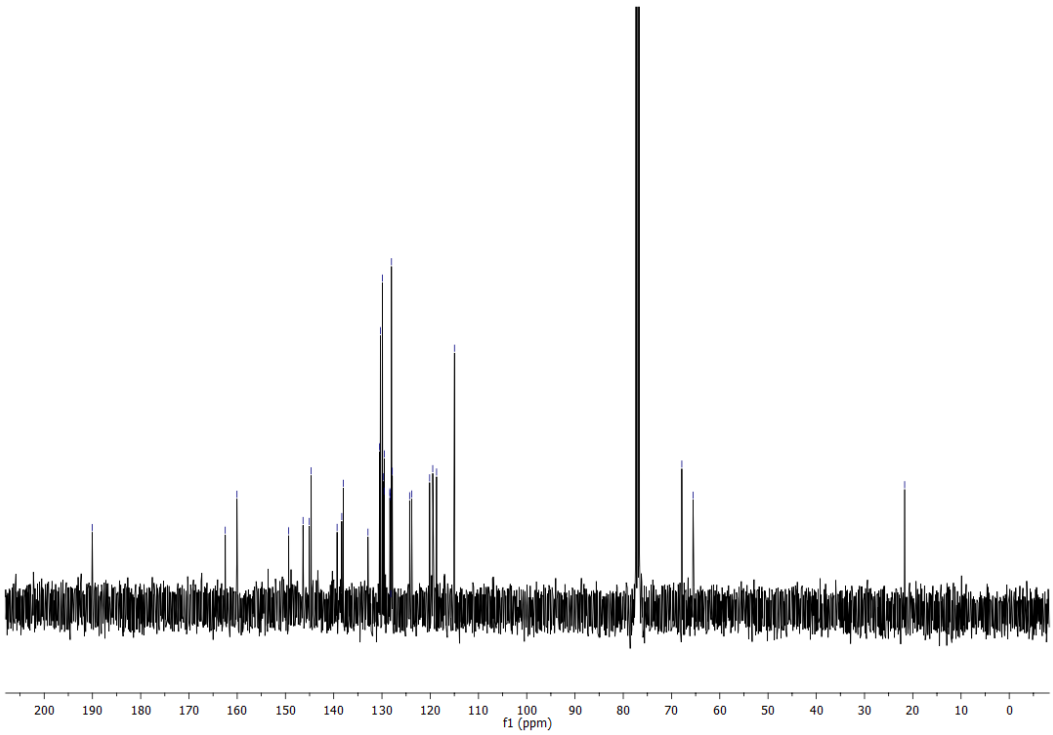

(E)-2-(4-(3-(4-methyl-3-(quinoline-2-carboxamido)phenyl)-3-oxoprop-1-en-1-yl)phenoxy)ethyl 4-methylbenzenesulfonate (178b)

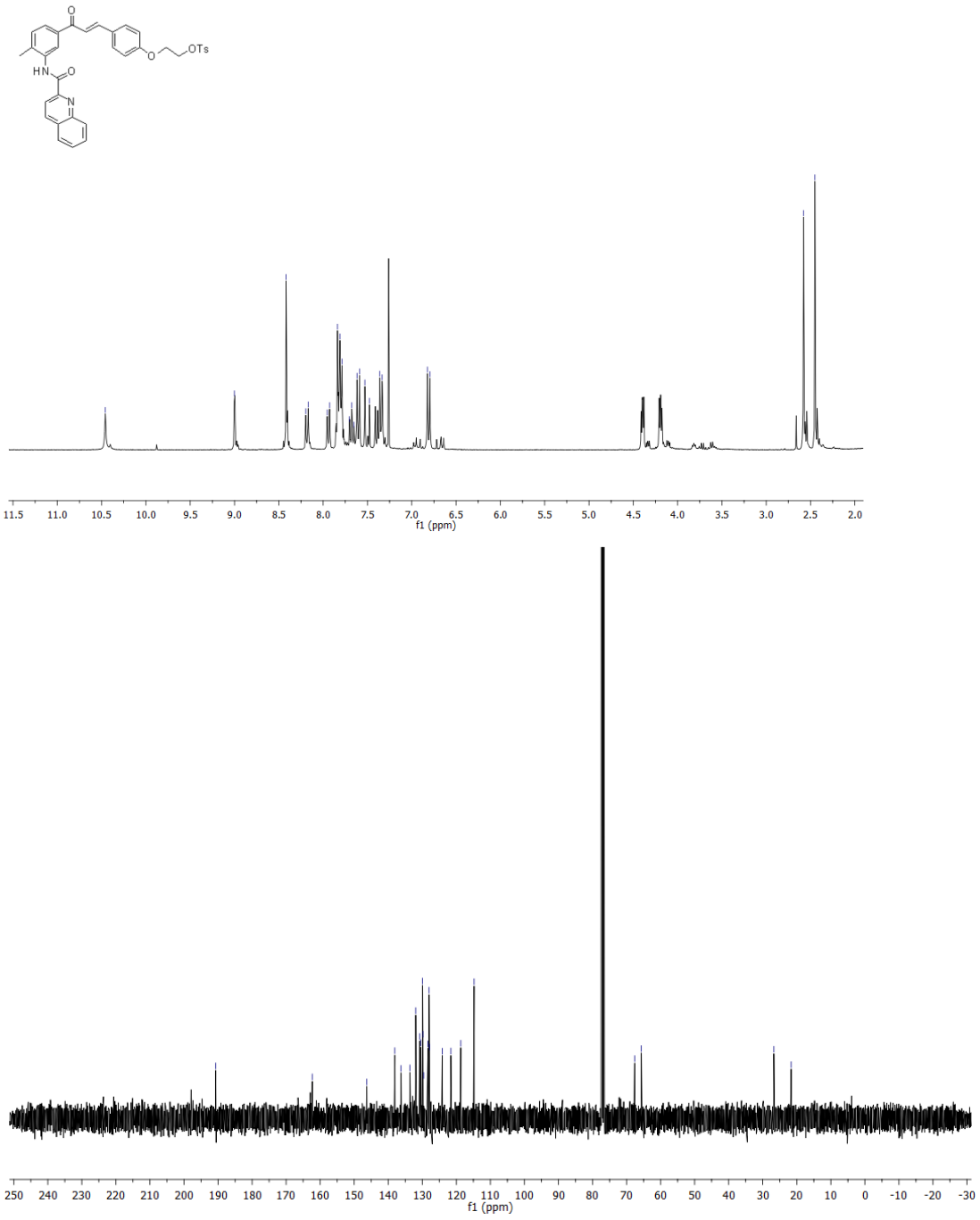

(E)-N-(3-(3-(4-(2-(6,7-dimethoxy-3,4-dihydroisoquinolin-2(1H)-yl)ethoxy)phenyl)acryloyl)phenyl)quinoline-2-carboxamide (179a)

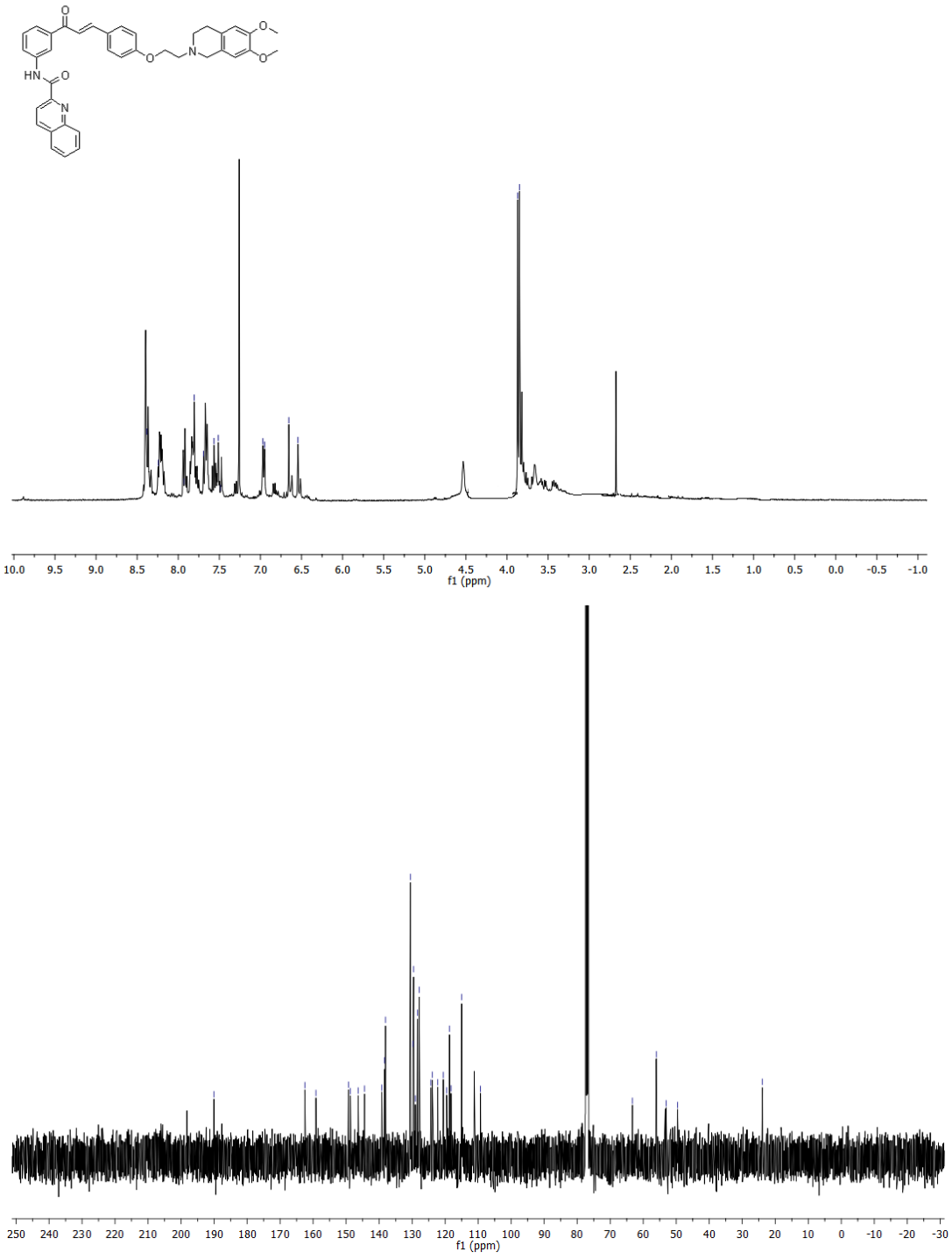

(E)-N-(3-(3-(4-(2-(6-methoxy-7-(2-methoxyethoxy)-3,4-dihydroisoquinolin-2(1H)-yl)ethoxy)phenyl)acryloyl)phenyl)quinoline-2-carboxamide (179b)

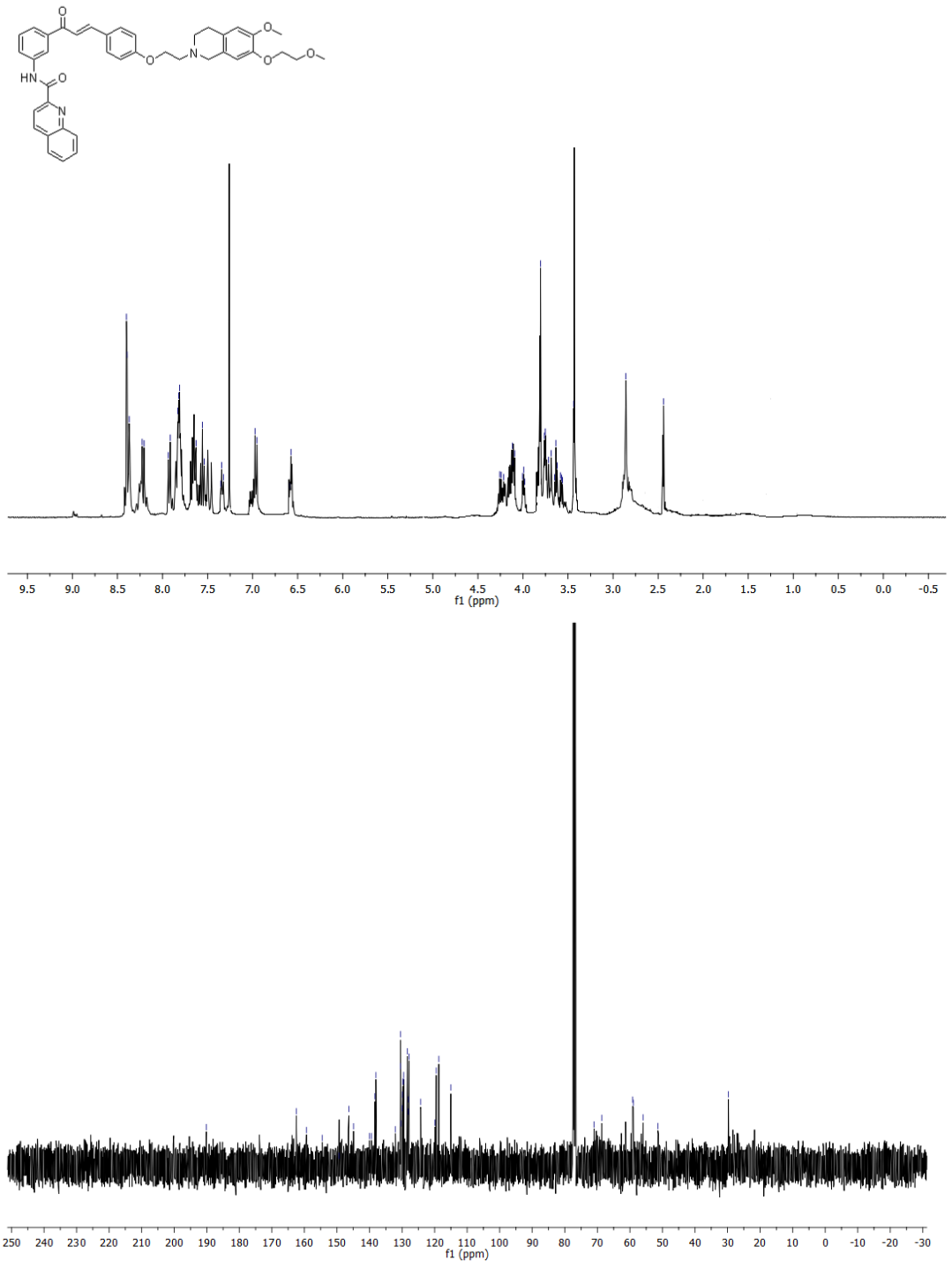

(E)-N-(3-(3-(4-(2-(6,7-bis(2-(2-(2-methoxyethoxy)ethoxy)ethoxy)-3,4-dihydroisoquinolin-2(1H)-yl)ethoxy)phenyl)acryloyl)phenyl)quinoline-2-carboxamide (179c)

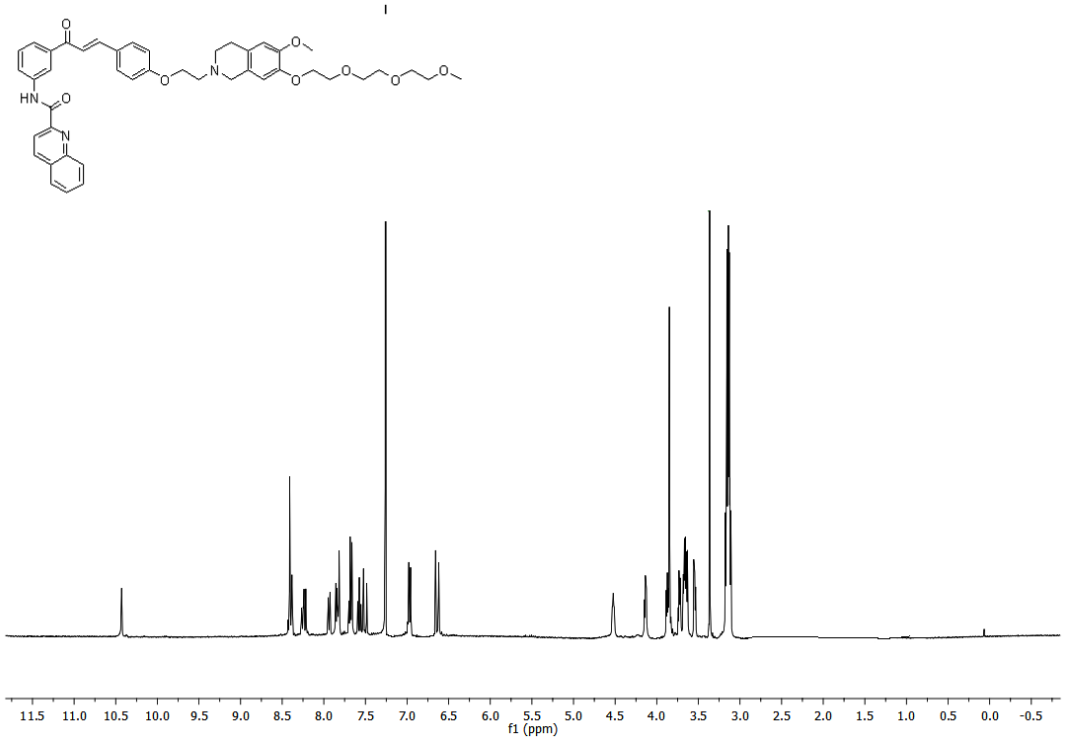

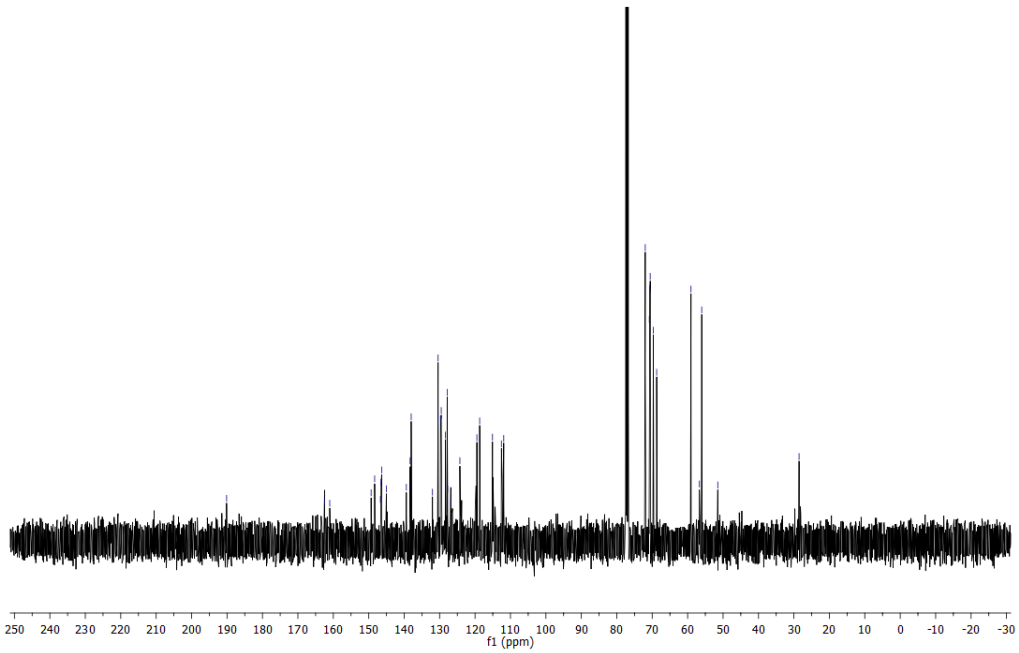

(E)-N-(5-(3-(4-(2-(6,7-dimethoxy-3,4-dihydroisoquinolin-2(1H)-yl)ethoxy)phenyl)acryloyl)-2-methylphenyl)quinoline-2-carboxamide (179d)

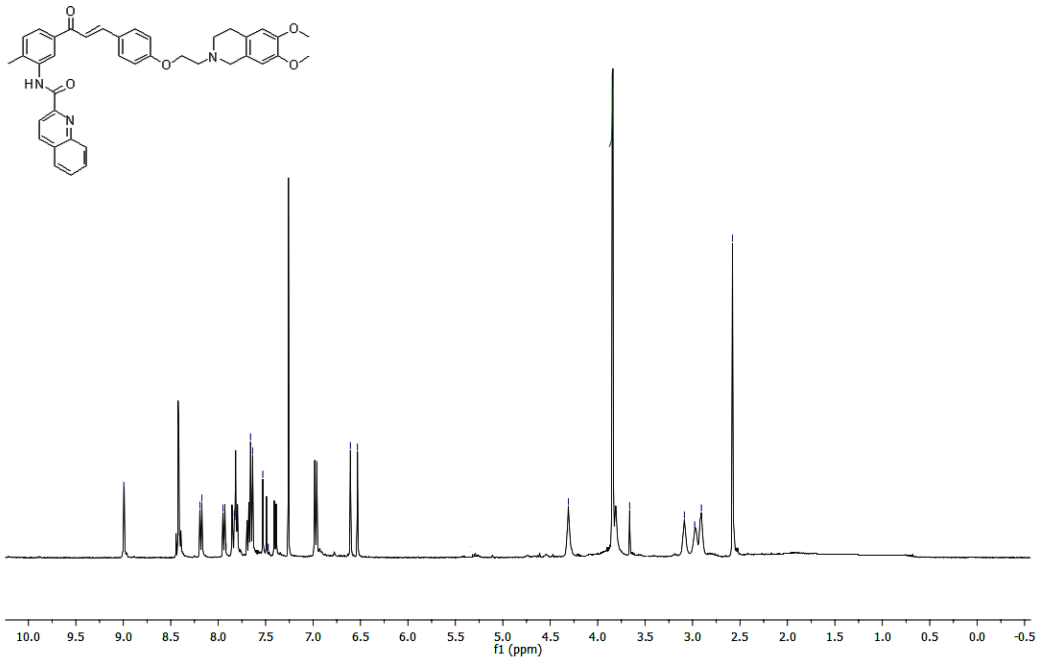

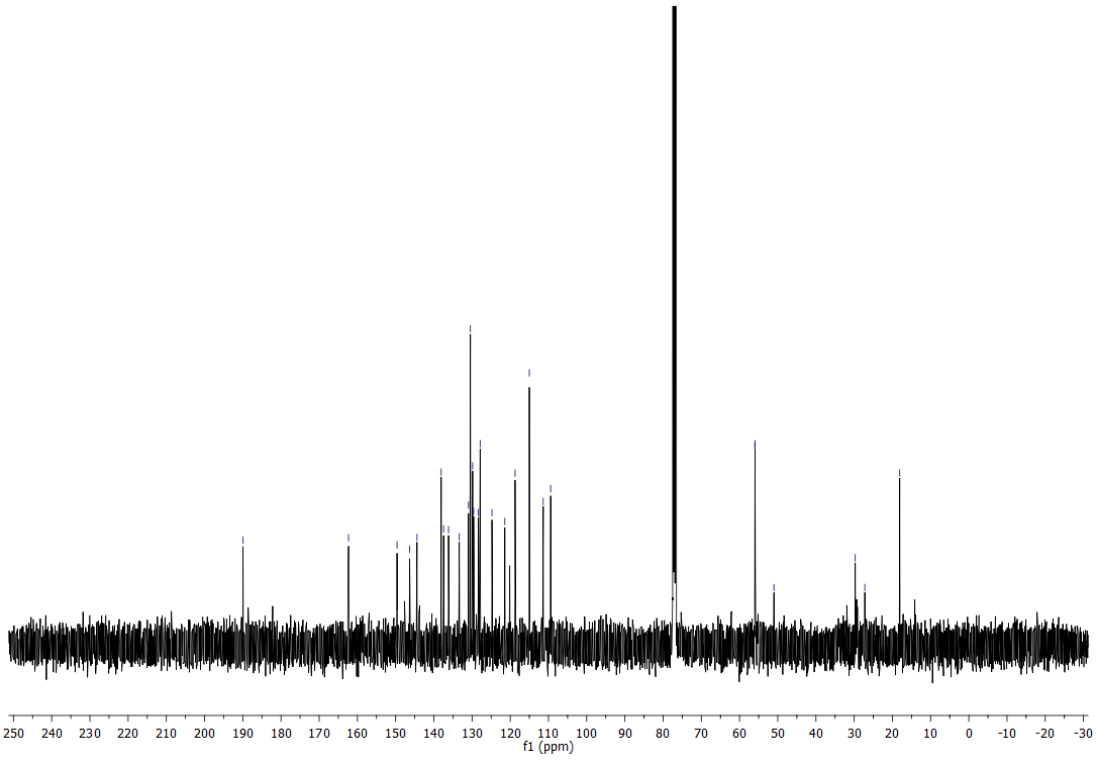

(E)-N-(5-(3-(4-(2-(6,7-bis(2-methoxyethoxy)-3,4-dihydroisoquinolin-2(1H)-yl)ethoxy)phenyl)acryloyl)-2-methylphenyl)quinoline-2-carboxamide (179e)

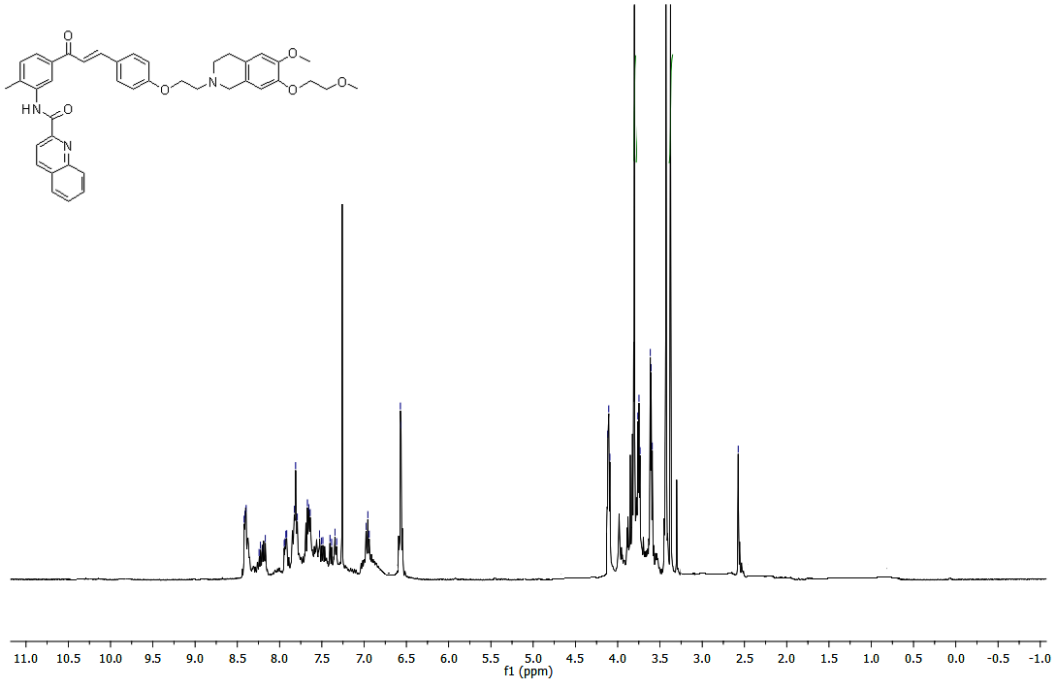

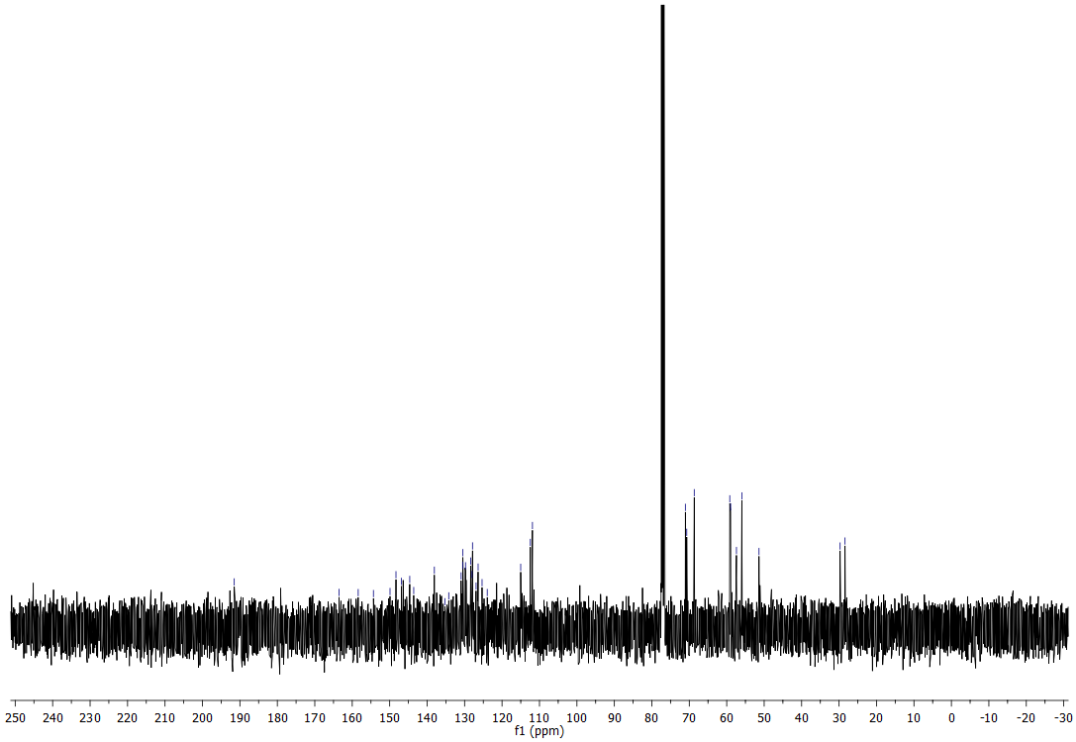

(E)-N-(5-(3-(4-(2-(6,7-bis(2-(2-(2-methoxyethoxy)ethoxy)ethoxy)-3,4-dihydroisoquinolin-2(1H)-yl)ethoxy)phenyl)acryloyl)-2-methylphenyl)quinoline-2-carboxamide (179f)

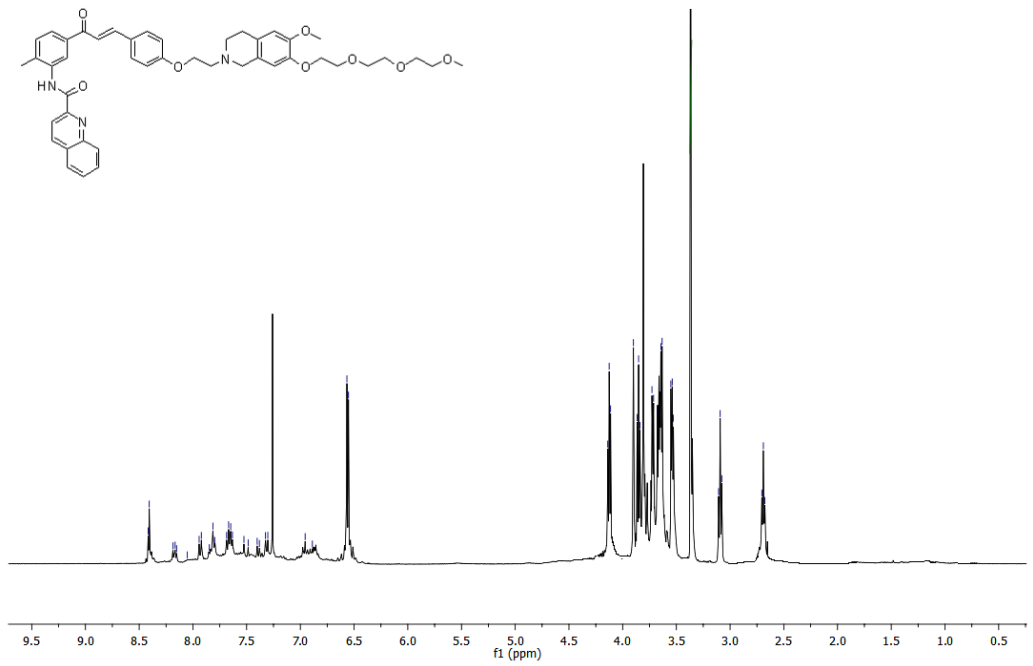

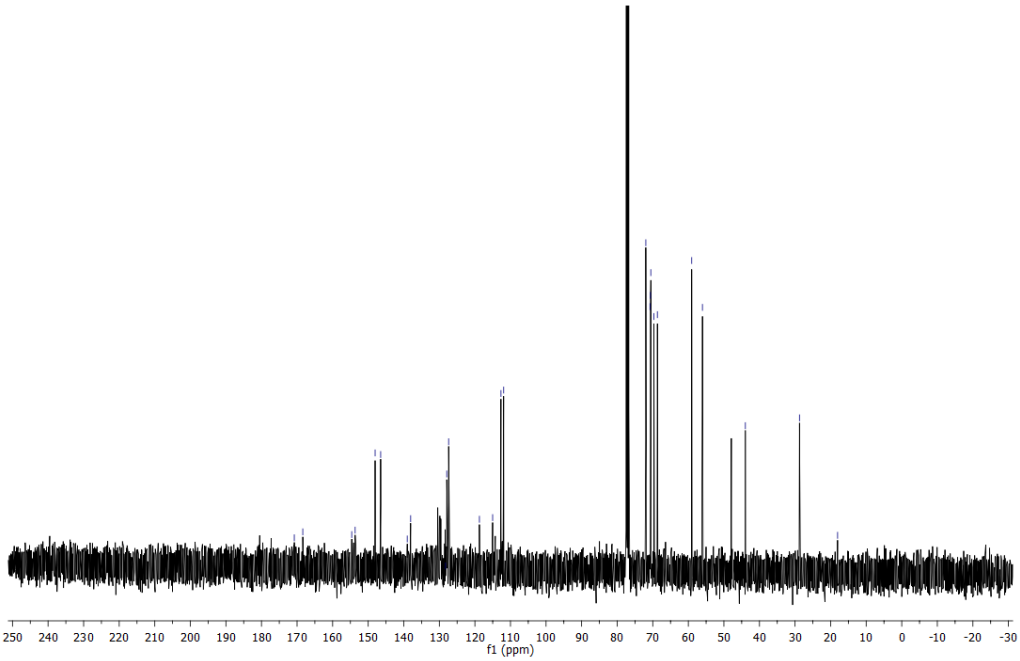

d. HPLC Analysis

Table 6-1 Purities of key compounds

Compound	Purity (%)	Retention time (min)
179a	96	16.698
179b	96	16.816
179c	97	16.781
179d	95	17.733
179e	96	17.425
179f	95	17.370

Compound **179a** in DMSO, 0.1 µL injected; Detector: 220 nm

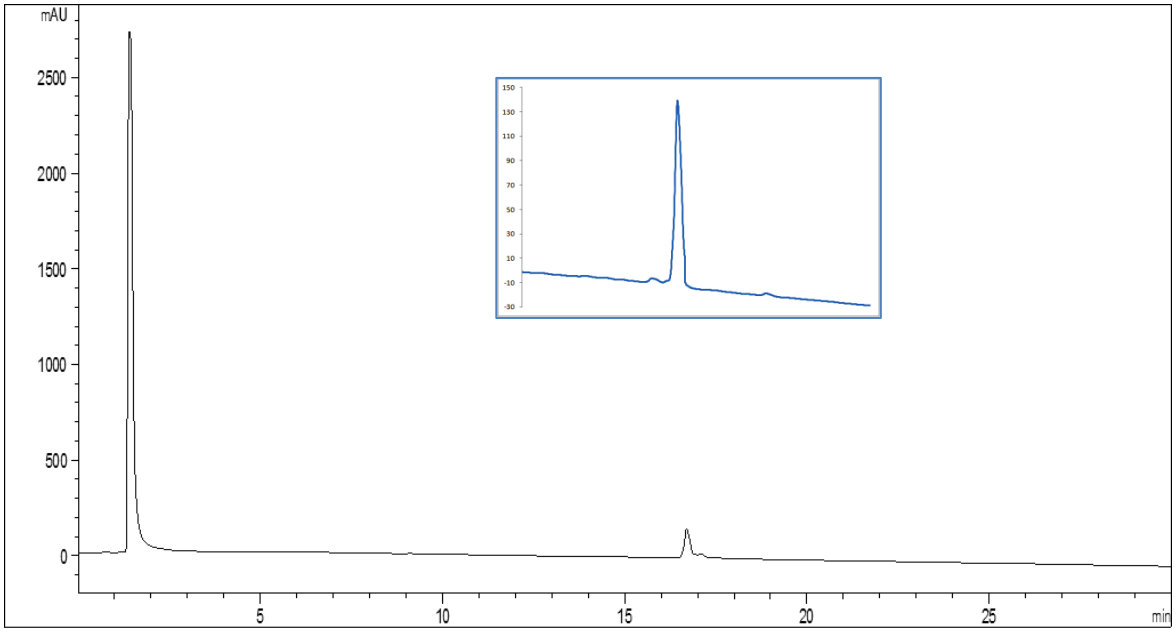

Compound **179b** in DMSO, 0.1 µL injected; Detector: 220 nm

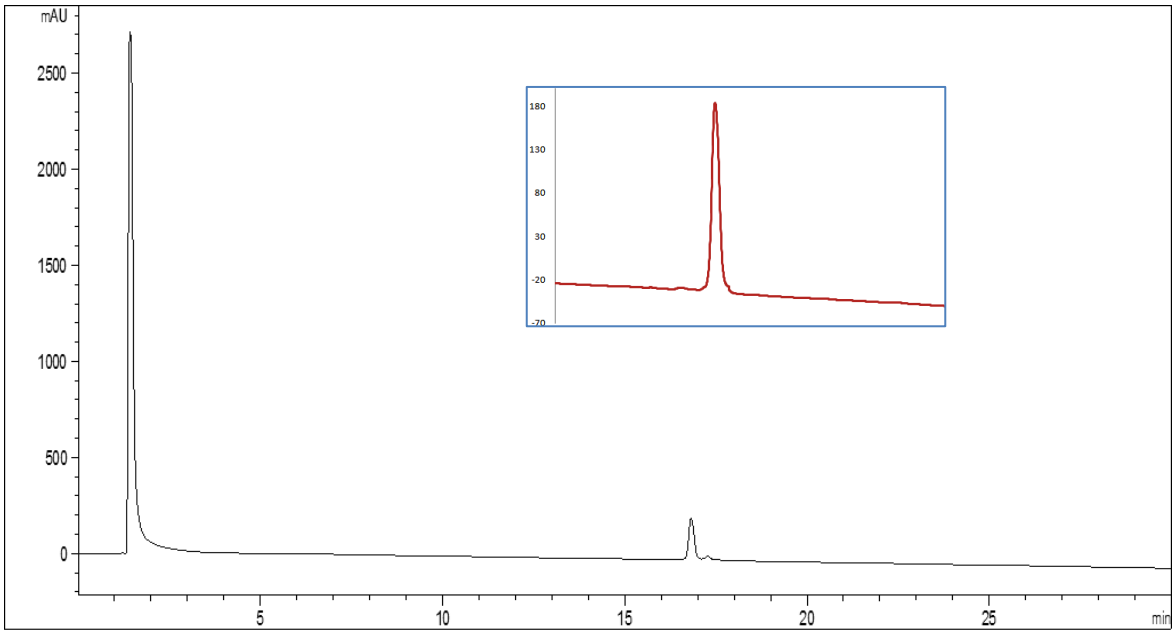

Compound **179c** in DMSO, 0.1 µL injected; Detector: 220 nm

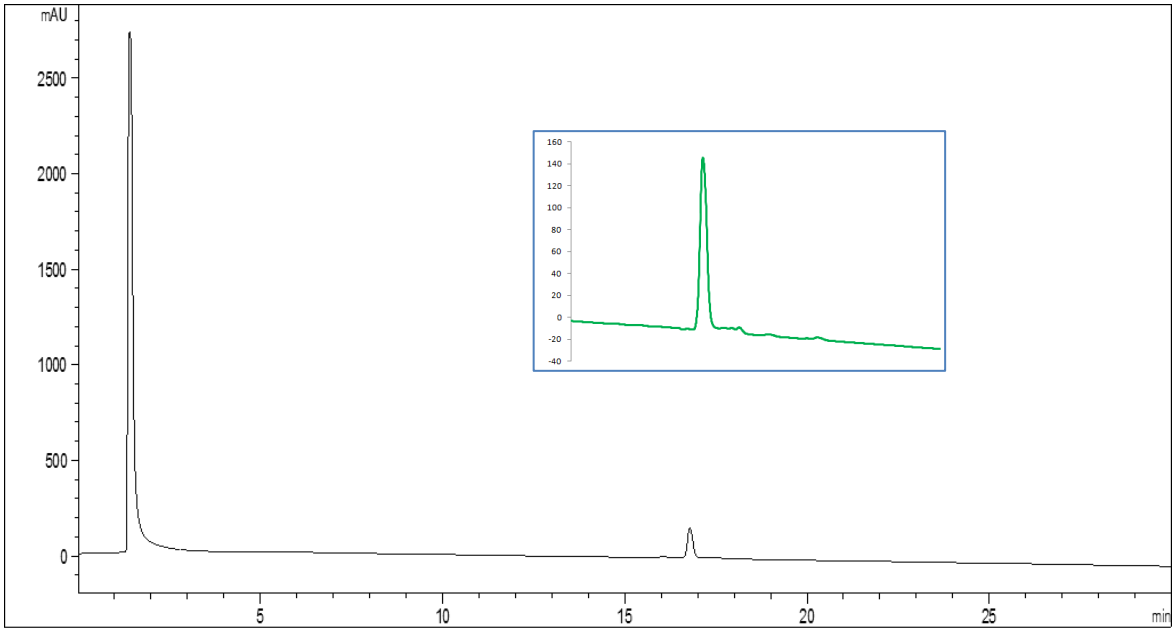

Compound **179d** in DMSO, 0.1 µL injected; Detector: 220 nm

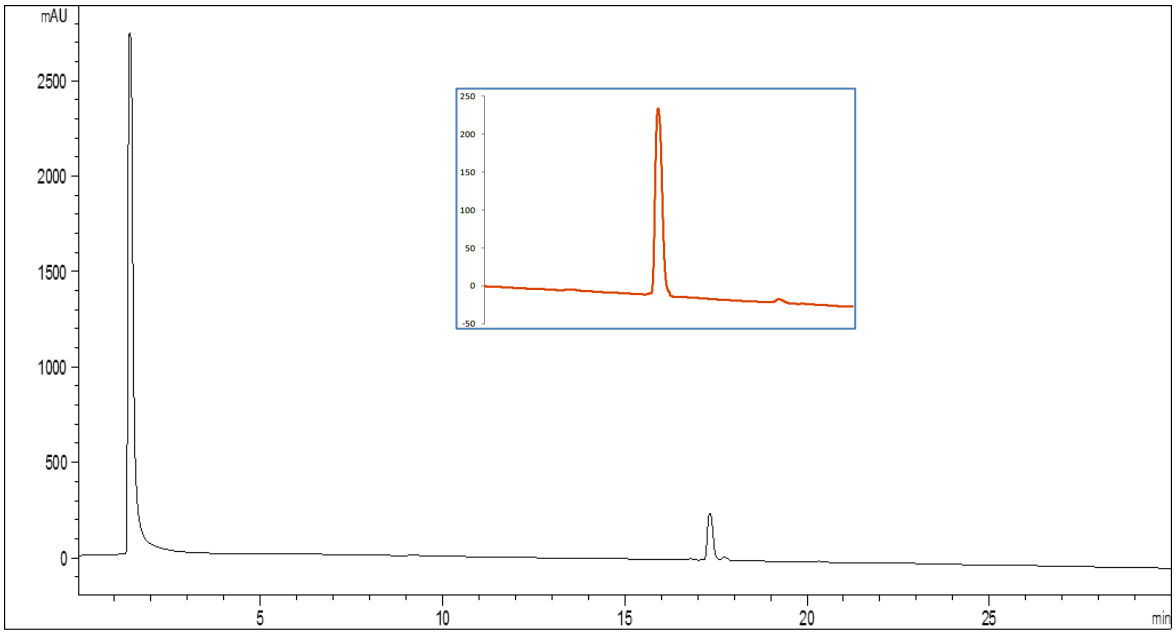

Compound **179e** in DMSO, 0.1 µL injected; Detector: 220 nm

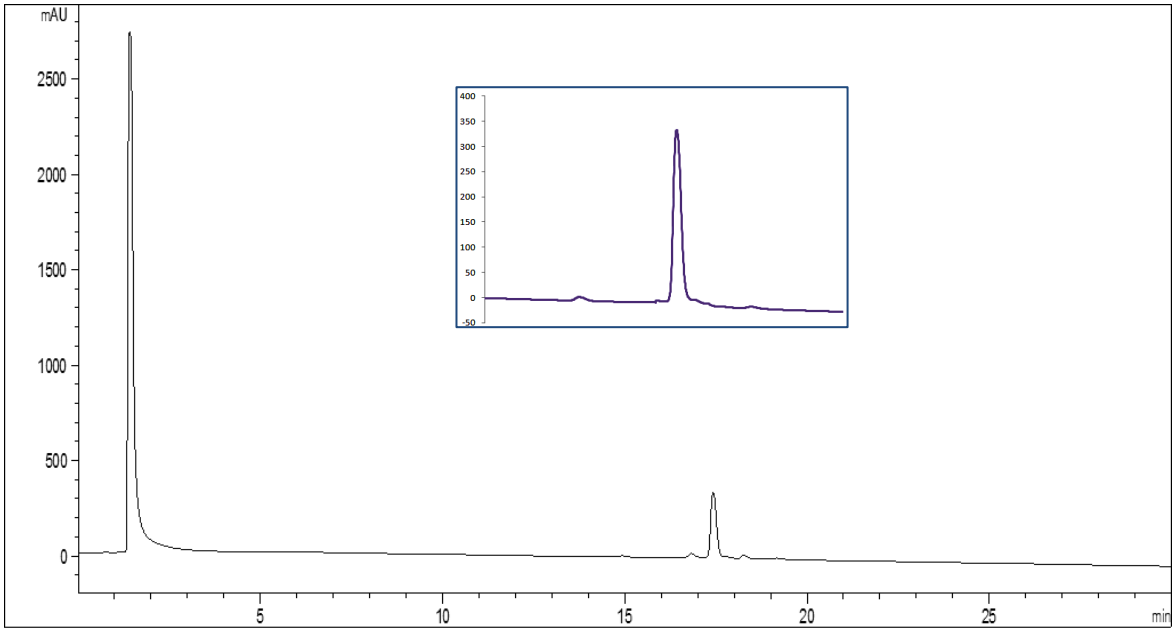

Compound **179f** in DMSO, 0.1 µL injected; Detector: 220 nm

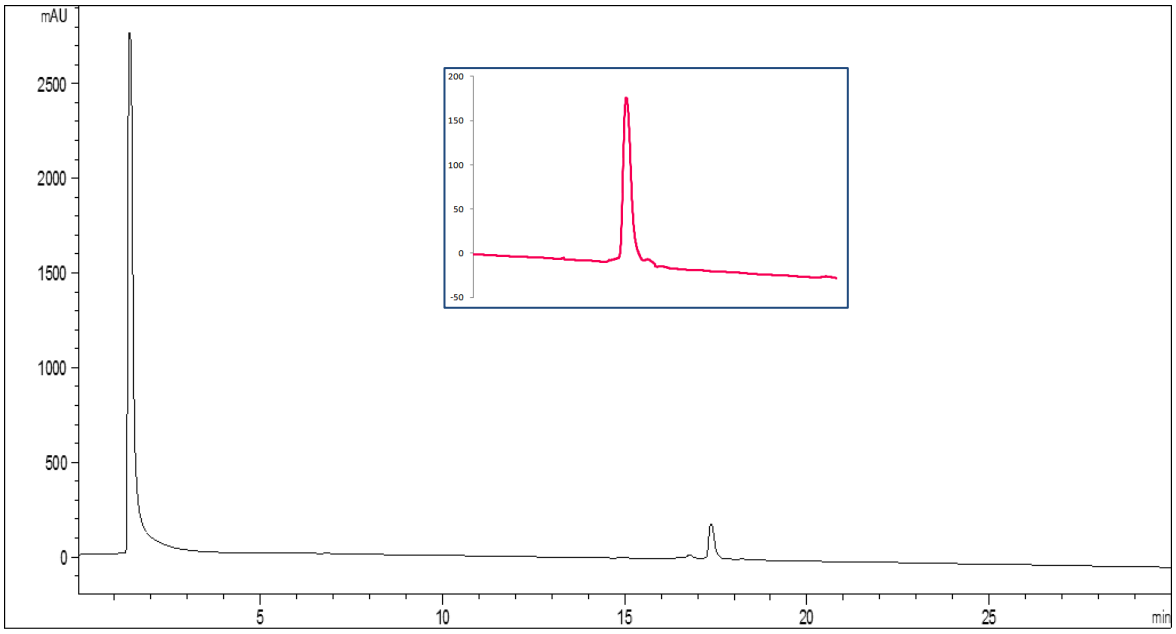

7 Publications, posters and conferences

- **Diana Peña-Solórzano**, Simone Alexandra Stark, Burkhard König, Cesar Augusto Sierra, and Cristian Ochoa-Puentes. ABCG2/BCRP: Specific and Non-Specific Inhibitors and Modulators. Medicinal Research Reviews, Doi: 10.1002/med.21428

- **Peña-Solórzano, D**; Scholler, M; Bernhardt, G; Buschauer, A; König, B; Sierra, C; Ochoa-Puentes, C. Synthesis and characterization of ABCG2 modulators combining chalcones and ketones with quinoline and isoquinoline moieties. In Revision

- **Diana Peña-Solórzano**, Burkhard König, Cesar A. Sierra and Cristian Ochoa-Puentes. Crystal Structure of three *N*-(3-Acetylphenyl)quinoline-2-carboxamides, Acta Cryst. (2017). E73, 804–808.

- **Diana Peña-Solórzano**, Burkhard König, Cesar A. Sierra and Cristian Ochoa-Puentes. Crystal Structure of *N*-(2-Benzoyl-5-ethynylphenyl)quinoline-2-carboxamide. Acta Cryst. (2017). E73, 602–605.

- 8 Summer School Medicinal Chemistry, R*egensburg University, Regensburg,* Germany, September 21-23, 2016. (Poster presentation)

- CIPSM: Scientific Oktoberfest, *Universidad técnica de Munich (TUM), Munich, Germany*, September 14-15, 2016

  2nd year of the Prague Summer School, *Advances in Drug Discovery Novel approaches in drug design and development, Prague, Czech Republic. August, 2015.*